THE ROLE OF FOXM1 IN PANCREATIC BETA CELL MASS REGENERATION AND EXPANSION

By

Amanda Ackermann Misfeldt

Dissertation

Submitted to the Faculty of the

Graduate School of Vanderbilt University

in partial fulfillment of the requirements

for the degree of

DOCTOR OF PHILOSOPHY

in

Molecular Physiology and Biophysics

December, 2008

Nashville, TN

Approved:

Professor Mark Magnuson, Chair

Professor Anna Means

Professor William Russell

Professor Roland Stein

Professor David Wasserman

ACKNOWLEDGEMENTS

If the best place to start is at the beginning, then I must first thank the Medical Scientist Training Program and its administration for granting me the opportunity to explore medicine and the basic sciences at a first-rate institution. Thank you to the Department of Molecular Physiology and Biophysics, the Program in Developmental Biology, and the Beta Cell Interest Group for providing strong training environments and faculty and for broadening my scientific scope.

Of course, I am grateful to my dissertation committee members Dr. Mark Magnuson, Dr. Anna Means, Dr. Bill Russell, Dr. Roland Stein, and Dr. David Wasserman for their suggestions and expertise with regard to my dissertation work. More than that, though, I appreciate their confidence in me and their guidance in making the most of my graduate school career. All of them have opened their laboratory and office doors to me for experiments and discussions that have been truly helpful.

So many people have been generous in their assistance in the experiments described in this dissertation, including: Dr. Robert H. Costa, Dr. Al Powers, Greg Poffenberger, Aramandla Radhika, Dr. Zhongyi Chen, Anastasia Golovin, Dr. Marcela Brissova, Rachel Reinert, Jeannelle Kantz, Leah Potter, Jennifer Plank, Dr. Shuangli Guo, Dr. Guoqiang Gu, Sui Wang, Dr. Kevin Niswender and his laboratory members, Dr. Richard O'Brien, Dr. Masa Shiota, Dr. Rob Carnahan, and Cassie Reid. Many thanks to the staff in the Hormone Assay and Analytical Services Core, the Islet Procurement and Analysis Core, the Microarray Shared Resource, the Molecular Biology Shared Resource, the Monoclonal Antibody Core, and the Mouse Metabolic Phenotyping Center.

There really is no way to appropriately thank the members of the Gannon lab, past and present, for their part in making it such a great place to work. I can't say that the people are the only thing that makes a lab, but I can say that they have been the most important to me. Thank you, Laura Wilding Crawford and Elizabeth Tweedie Ables, for being wonderful friends, first and foremost, and for setting the precedent that we have tried to maintain in the lab despite your departures…and by that I mean getting married and changing your last name, of course. Thank you, Peter Wiebe, for always being available to answer questions and for not backing down if I didn't agree with your response. Thank you to Hongjie Zhang, Venus Childress Roper, David Lowe, and Young Ah Oh for helping me with countless experiments. Gift Kopsombut and Xue Feng, you both are so incredible; thank you for all of your hard work and for keeping me young!

Jia Zhang, Renuka Menon, and Nik Patel, I am so glad that I got the chance to know you. Thank you for continuing to make lab an enjoyable workplace. Michelle Guney, Christine Pope, and Kathryn Henley, I will miss our discussions about science, reality TV, and everything in between. Thank you for being such great friends! Michelle, thank you for being my late-night lab partner and for making every conference and retreat ever so much more entertaining. Christine, thank you for understanding my OCD nature and not holding it against me. You are a tremendous asset to the lab. Kathryn, I am glad that someone with such spirit joined the lab. Good luck to all of you in your upcoming endeavors!

Certainly, my graduate school experience would not have been as valuable if Dr. Maureen Gannon had not been a part of it. Maureen is the sort of boss, colleague, and

friend that everyone wishes they had. Thank you, Maureen, for being all of those for me. Thank you for your never-ending support and encouragement. I am always impressed by your relentlessly positive attitude, and I hope that I will be able to take part of that with me. Thank you for encouraging all of your lab members to present their work, attend conferences, and pursue the goals from which others may discourage them. Foremost, thank you for being a great example to me of a principal investigator, leader, and mother. You are an inspiration to women in science.

To my family, thank you for always emphasizing the importance of education and hard work, and for encouraging me when things were more difficult than expected.

Saving the best for last, thank you to my husband Drew, without whom I am fairly certain I would not have endured these grueling years. Thank you for being a friend, confidant, and partner. Thank you for your love and support and your uncanny ability to know the answer to any question I ask, or at least to sound as if you do. Thank you for allowing three wonderful kitties to enter our home and our lives. I am glad that we have been able to share these experiences with each other, and I am looking forward to sharing many more in the years to come.

TABLE OF CONTENTS

LIST OF TABLES

LIST OF FIGURES

CHAPTER I

BACKGROUND AND SIGNIFICANCE

The number and functional capacity of an organism's pancreatic β-cells, in combination with peripheral insulin sensitivity, determine the ability of that organism to maintain glucose homeostasis. Because β cells are the only cell type in the body to secrete insulin in response to glucose, the size of this cell population, or β cell mass, is an important determinant of an organism's ability to regulate its blood glucose levels. Diabetes mellitus is characterized by either an absolute (Type I) or relative (Type II and gestational) insufficiency of insulin production by β cells. Existing treatments for diabetes primarily focus on replacing insulin and improving β cell function. However, increasing a patient's β cell mass could potentially improve or cure their condition. To this end, islet transplantation has been used to treat some patients with Type I diabetes, but limited supply and low yield of islets from donor pancreata, as well as graft failure, prevent widespread use of this therapy. Currently, efforts are being made to differentiate β cells from precursor populations and to expand β cells *in vitro* to generate an unlimited supply of β cells for transplantation. Theoretically, the same could be done *in vivo* to expand a patient's existing or transplanted β cell population. Thus, it is important to understand the molecular regulation of β cell mass development, maintenance, and expansion.

Pancreas Development

The pancreas originates from the foregut endoderm as ventral and dorsal buds beginning at embryonic day (e) 9.5 in the mouse, and the two buds later fuse at approximately e12.5 (Kim and MacDonald, 2002). The endodermal epithelium proliferates in response to various fibroblast growth factors (FGFs) produced by the adjacent mesenchyme (Bhushan *et al.*, 2001), undergoes branching morphogenesis, and differentiates into ductal, exocrine, and endocrine cells. Evagination and development of the ventral pancreatic bud is slightly delayed compared to that of the dorsal bud, and the ventral bud gives rise to fewer endocrine cells than does the dorsal bud (Spooner *et al.*, 1970). The ventral and dorsal buds also differ with regard to the signals they require for development. For example, the homeobox 9 (Hb9) transcription factor is required for formation of the dorsal, but not ventral, bud (Harrison *et al.*, 1999; Li *et al.*, 1999). Additionally, the LIM homeodomain protein islet 1 (Isl1) is specifically expressed in the mesenchyme surrounding the dorsal, but not ventral, bud at e9.0, as well as later in differentiated endocrine cells throughout the pancreas. *Isl1*$^{-/-}$ mice reveal that Isl1 is required specifically in the dorsal mesenchyme for formation of the dorsal pancreatic bud, and is required in the endoderm for differentiation of all endocrine cells (Ahlgren *et al.*, 1997).

Pancreatic progenitors within the foregut epithelium are marked by expression of pancreatic-duodenal homeobox 1 (Pdx1), which is induced at e8.5 in the posterior foregut endoderm and is expressed throughout the pancreatic epithelium at e9.5 (Guz *et al.*, 1995). Forkhead box A2 (FoxA2), previously called hepatic nuclear factor 3β (Hnf3β), can activate transcription of *Pdx1*, although there are many other upstream regulators of

Pdx1 (Melloul *et al.*, 2002; Gerrish *et al.*, 2004). Pdx1 is required for growth, rather than formation, of the pancreatic buds, as evidenced by *Pdx1*$^{-/-}$ mice in which both pancreatic buds initially form but then arrest at a very early stage of development, resulting in an apancreatic phenotype at birth (Jonsson *et al.*, 1994; Offield *et al.*, 1996). The same phenotype has been observed in a human infant with a homozygous inactivating point mutation of *PDX1* (Stoffers *et al.*, 1997b). Pdx1 expression is down-regulated in acinar and ductal cells beginning at approximately e13.0 but is maintained in differentiated endocrine cells and up-regulated specifically in β cells (Guz *et al.*, 1995). This expression pattern is maintained throughout life.

Pancreas transcription factor 1a (Ptf1a) is also expressed throughout the developing pancreas beginning at e9.5 and is required for growth of the pancreatic buds (Krapp *et al.*, 1998; Kawaguchi *et al.*, 2002). Ptf1a is later down-regulated in ductal and endocrine cells but is maintained in acinar cells throughout life, where it induces expression of Amylase and Elastase. *Ptf1a*$^{-/-}$ mice form a rudimentary dorsal pancreas that fails to grow or produce differentiated acinar tissue (Krapp *et al.*, 1998). Differentiated endocrine cells are present in these mice, although these cells are reduced in number and found scattered throughout the adjacent spleen. Furthermore, the cells that would otherwise have expressed Ptf1a and contributed to the pancreas become incorporated into the duodenum (Kawaguchi *et al.*, 2002).

β Cell Differentiation

No "master regulator" of β cell differentiation has been identified. Instead, the process of β cell differentiation is a complex pathway requiring the specification of

pancreas versus other endodermal organs, endocrine cells versus ductal or exocrine cells, and β cells versus non-β endocrine cells (Figure 1). Proper differentiation of β cells requires dynamic changes in transcription factor expression levels in appropriate sequences and within an appropriate timeline. Much of what is currently known regarding β cell differentiation has been discovered by studying endocrine cell differentiation *in vivo*, with the hope that these findings will aid attempts to differentiate β cells *in vitro*.

In Vivo β Cell Differentiation

The murine pancreas undergoes two waves of endocrine cell differentiation, the first of which gives rise to glucagon$^+$, insulin$^+$, and double-positive cells between e9.5 and e13.5. These cells appear to be a transient population, however, and lineage tracing studies show that they do not contribute to mature islets (Herrera, 2000). The second wave of endocrine differentiation begins at approximately e13.5 and yields endocrine cells that contribute to mature islets (Prasadan *et al.*, 2002). Second wave endocrine differentiation, unlike the first wave, relies on the transcription factors Pdx1 and Hnf6 (Offield *et al.*, 1996; Jacquemin *et al.*, 2000).

Differentiation of endocrine versus exocrine cells is regulated by the Notch signaling pathway (Apelqvist *et al.*, 1999; Jensen *et al.*, 2000). The pro-endocrine basic helix-loop-helix (bHLH) transcription factor neurogenin 3 (Ngn3), a downstream target of Hnf6 (Jacquemin *et al.*, 2000), induces expression of Notch ligands, which bind to Notch receptors on and activate the Notch pathway in adjacent cells (Heremans *et al.*, 2002). Downstream targets of the Notch pathway (e.g. Hairy/enhancer-of-split 1, Hes1)

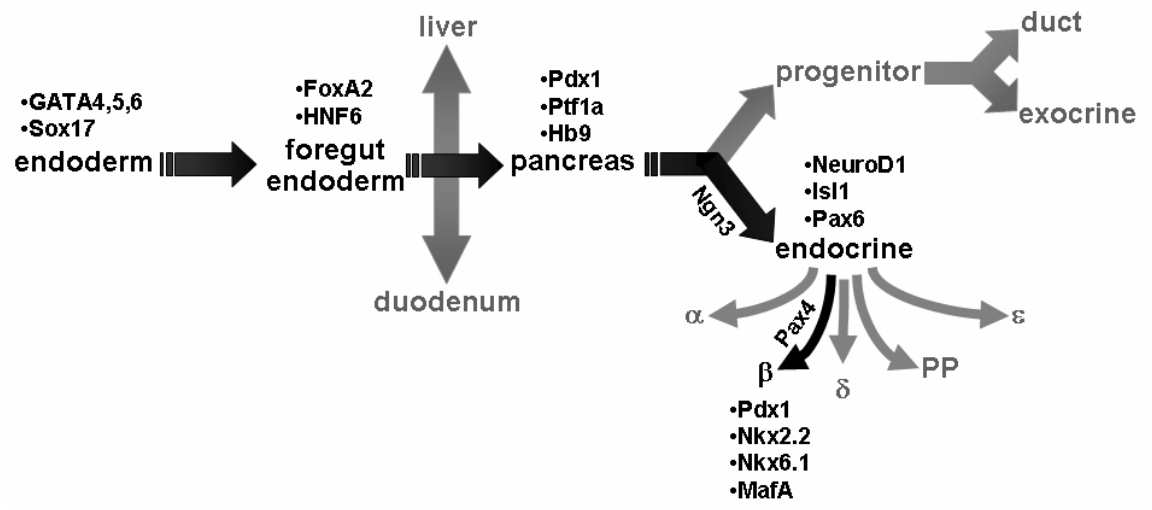

Figure 1. β cell differentiation from endoderm. During embryogenesis, the pancreas differentiates from foregut endoderm, which also gives rise to the liver and duodenum. Pancreatic progenitors are specified for an endocrine or non-endocrine fate, after which the non-endocrine progenitors differentiate into either duct or exocrine cells, while the endocrine progenitors differentiate into α, β, δ, PP, or ε cells. Transcription factors expressed in each of the cell populations preceding and including β cells are listed. Figure is from Ackermann and Gannon (2007).

repress *Ngn3* expression, which inhibits endocrine differentiation. Additionally, Hes1 represses the cell cycle inhibitor $p57^{Kip2}$, which maintains a proliferative pool of pancreatic progenitor cells within the embryonic ductal epithelium (Georgia *et al.*, 2006). Therefore, cells in which the Notch signaling pathway is activated maintain their proliferative capacity, while cells in which Notch signaling is not activated express Ngn3, exit the cell cycle, and differentiate into endocrine cells. Genetic mouse models of impaired Notch signaling, via deletion of Delta-like ligand 1 ($Dll1^{-/-}$), Recombination signal binding protein for immunoglobulin kappa J region ($Rbp\text{-}J\kappa^{-/-}$), or $Hes1^{-/-}$, exhibit increased endocrine cell differentiation at the expense of the pancreatic progenitor population (Apelqvist *et al.*, 1999; Jensen *et al.*, 2000).

Ngn3 is required for endocrine cell differentiation, as evidenced by $Ngn3^{-/-}$ mice, which lack all pancreatic endocrine cell types and die postnatally due to severe diabetes (Gradwohl *et al.*, 2000). Additionally, lineage tracing analysis revealed that all endocrine cells arise from $Ngn3^{+}$ cells (Gu *et al.*, 2002). Ngn3 induces expression of essential β cell transcription factors including neurogenic differentiation 1 (*Neurod1*), also known as *Beta2* (Huang *et al.*, 2000), and paired box gene 4 (*Pax4*) (Smith *et al.*, 2003), but is not itself expressed in hormone-producing cells. The bHLH transcription factor NeuroD1 induces expression of several endocrine genes, including Insulin, and its expression is maintained in mature endocrine cells (Naya *et al.*, 1995). $NeuroD1^{-/-}$ mice are diabetic due to severely reduced numbers of all endocrine cell types (Naya *et al.*, 1997), and humans with heterozygous mutations in *NEUROD1* suffer from a type of diabetes referred to as maturity-onset diabetes of the young type 6 (MODY6) (Kristinsson *et al.*, 2001). In contrast, ectopic expression of Ngn3 or NeuroD1 in the pancreatic epithelium

results in premature and expansive differentiation of endocrine cells, primarily glucagon-producing α cells, at the expense of the pancreatic progenitor pool, resulting in a hypoplastic pancreas (Apelqvist *et al.*, 1999; Schwitzgebel *et al.*, 2000).

The basic-leucine zipper (bZIP) transcription factor Musculoaponeurotic fibrosarcoma oncogene family protein B (MafB) is expressed in developing insulin$^+$ and glucagon$^+$ cells beginning during the first wave of endocrine cell differentiation, and then is subsequently down-regulated in β cells, concurrent with up-regulation of MafA in these cells (Artner *et al.*, 2006; Nishimura *et al.*, 2006). MafB can activate transcription of the *insulin* and *glucagon* genes, and is required for proper differentiation of α and β cells (Artner *et al.*, 2007). Loss of MafB (*Mafb*$^{-/-}$) results in impaired differentiation of α and β cells, but no change in total endocrine cell number and no alterations in endocrine cell lineage allocation, and insulin expression is delayed in these mice mice until the onset of MafA expression at e13.5.

Endocrine cells produced by the second wave of differentiation can first be identified at e13.5, forming endocrine cords adjacent to ducts (Pictet *et al.*, 1972). These cells delaminate from the ductal epithelium, differentiate, proliferate, and then cluster to form islets, which contain β cells, α cells, somatostatin-producing δ cells, pancreatic polypeptide-producing PP cells, and ghrelin-producing ε cells. Regulation of differentiation down each of these endocrine lineages from a Ngn3$^+$ cell is complex and still not completely understood. However, lineage tracing analyses have revealed that the β and α cell lineages diverge early, while β cells and PP cells may differentiate from the same lineage (Herrera, 2000). Additionally, β cells and δ cells share a requirement for Pax4, as *Pax4*$^{-/-}$ mice have increased numbers of α cells at the expense of β and δ cells

(Sosa-Pineda *et al.*, 1997). Pax4 is expressed in early insulin^{+}, but not glucagon^{+}, cells and is later restricted to mature β cells, but Pax4 alone is not sufficient to drive Ngn3^{+} cells toward either a β or δ cell fate (Grapin-Botton *et al.*, 2001). A putative antagonist of Pax4 is aristaless related homeobox (Arx), whose expression pattern and loss-of-function phenotype directly contrast with that of Pax4 (Collombat *et al.*, 2003). Arx is expressed in pancreatic progenitor cells beginning at e9.5 and is later restricted to mature α and δ cells. *Arx*$^{-/-}$ mice exhibit increased numbers of β and δ cells at the expense of α cells. Furthermore, Arx is up-regulated in *Pax4*$^{-/-}$ mice, while Pax4 is up-regulated in *Arx*$^{-/-}$ mice. Thus, Pax4 and Arx function in the differential specification of endocrine cell types.

Early broad expression of Pdx1 induces expression of the NK homeodomain transcription factors Nkx2.2 and Nkx6.1, but while Nkx2.2 expression becomes restricted to α, β, and PP cells (Sussel *et al.*, 1998), Nkx6.1 expression becomes tightly restricted to β cells (Sander *et al.*, 2000). *Nkx2.2*$^{-/-}$ mice reveal that Nkx2.2 is absolutely required for β cell differentiation and plays a lesser role in differentiation of α and PP cells (Sussel *et al.*, 1998), while *Nkx6.1*$^{-/-}$ mice have impaired but not complete loss of β cell differentiation (Sander *et al.*, 2000). Several pieces of evidence suggest that Nkx2.2 is upstream of Nkx6.1: initiation of expression of Nkx2.2 precedes that of Nkx6.1 (e9.5 versus e10.5, respectively); all Nkx6.1^{+} cells also express Nkx2.2, while not all Nkx2.2^{+} cells express Nkx6.1; *Nkx2.2*$^{-/-}$ mice lack expression of Nkx6.1; and *Nkx2.2*$^{-/-}$;*Nkx6.1*$^{-/-}$ mice exhibit a similar phenotype to *Nkx2.2*$^{-/-}$ mice.

In addition to its early role in pancreas development, Pdx1 plays a role in the terminal differentiation of β cells by inducing expression of Insulin, Glucose transporter 2

(*Glut2*), Glucokinase, and Islet amyloid polypeptide (*Iapp*) (Edlund, 2001), and Pdx1 is necessary for maintaining mature β cell function. MafA has also recently been identified as an important regulator of β cell function and a marker of mature β cells (Zhang C *et al.*, 2005; Nishimura *et al.*, 2006; Artner *et al.*, 2007). *MafA*$^{-/-}$ mice undergo normal pancreatic development but develop diabetes postnatally, associated with progressively impaired insulin secretion, abnormal islet morphology, and reduced expression of Insulin, Pdx1, NeuroD1, and Glut2. Additionally, insulin has been shown to be a direct transcriptional target of MafA (Kataoka *et al.*, 2002; Olbrot *et al.*, 2002; Matsuoka *et al.*, 2004; Artner *et al.*, 2008).

In Vitro β Cell Differentiation

As described above, β cell differentiation *in vivo* requires that expression of specific transcription factors be initiated, maintained, and repressed in a precise temporal and sequential manner, which is difficult to control in an *in vitro* setting. Furthermore, simply inducing insulin expression in a progenitor population does not equate with differentiating β cells because an important quality of mature β cells is their ability to sense blood glucose levels and appropriately respond by synthesizing and secreting proper amounts of insulin. These functions require expression of several transporter, receptor, and exocytosis proteins. To overcome these obstacles, many different approaches are being utilized to generate β cells, as shown in Figure 2: proliferation of existing β cells, differentiation of β cells from embryonic stem (ES) cells, differentiation of β cells from pancreatic progenitor cells (residing in pancreatic ductal epithelium), and

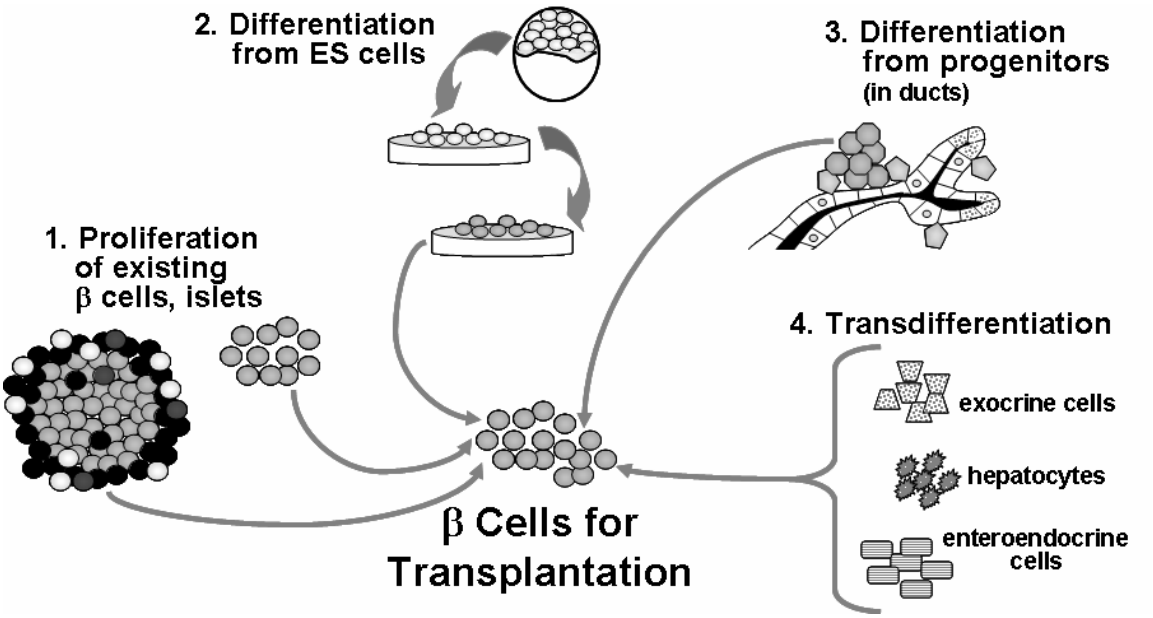

Figure 2. Sources of β cells for transplantation. A supply of β cells for transplantation may be derived by 1. inducing proliferation of existing β cells, either isolated or within islets; 2. by inducing differentiation of ES cells into β cells; 3. by inducing differentiation of isolated ductal epithelium into β cells or islets; and 4. by inducing transdifferentiation of related cell types, such as exocrine cells, hepatocytes, or intestinal enteroendocrine cells, into β cells. Figure is from Ackermann and Gannon (2007).

transdifferentiation of β cells from related cell types (e.g. pancreatic exocrine cells, hepatocytes, and intestinal enteroendocrine cells) (Bonner-Weir and Weir, 2005).

Although the prospect of deriving β cells from ES cells is intriguing, there has been much controversy in the field, and several early studies have since become cautionary tales. For example, initial reports claiming a 10-30% efficiency rate of differentiating β cells from ES cells failed to confirm *Insulin* mRNA expression, which was later observed in less than 0.00001% of cells (Rajagopal *et al.*, 2003). Improved results have been obtained by applying what has been learned about β cell differentiation *in vivo*. For example, transfection of ES cells with *Pax4*, and to a lesser extent *Pdx1*, results in increased differentiation of insulin-producing cells and increased expression of Isl1, Ngn3, Insulin, Iapp, and Glut2 (Blyszczuk *et al.*, 2003). Currently, the preferred method to produce β cells from ES cells is directed differentiation. Ku *et al*. showed that stepwise application of various growth factors known to influence β cell development (FGF, activin, betacellulin, exendin-4, and nicotinamide) induces 2.73% of ES cells to differentiate into insulin-producing cells (Ku *et al.*, 2004). D'Amour *et al*. developed a five-stage protocol to systematically induce differentiation of definitive endoderm, primitive gut tube, posterior foregut endoderm, pancreatic endoderm and endocrine precursors, and finally insulin-producing cells, along with the four other hormone-producing cell types (D'Amour *et al.*, 2006). This method induced 7-12% of ES cells to differentiate into insulin-producing cells, although these cells had limited glucose-stimulated insulin secretion. More recently, the same group optimized this protocol to differentiate ES cells to the fourth stage (pancreatic endoderm and endocrine precursors), which is characterized by expression of Pdx1, FoxA2, Hnf6, and Nkx6.1, and they then

implanted these cell aggregates into recipient mice (Kroon *et al.*, 2008). These grafts produced insulin within 44 days post-implantation, and by 90 days were producing as much insulin as did grafts of 3,000-5,000 adult human islets. Importantly, the ES cell-derived grafts appropriately secreted insulin in response to glucose but not in response to fasting or hypoglycemia. Additionally, these grafts were able to maintain glucose homeostasis in mice whose endogenous β cells were eliminated. Histological analysis of the grafts after 78 days revealed that hormone$^+$ cells formed islet-like clusters with relatively appropriate proportions of each cell type, no endocrine hormones were co-expressed within the same cell, and hormone$^+$ cells also expressed mature endocrine cell type-specific markers. Despite these encouraging results, grafts derived from ES cells have been shown in some cases to form teratomas after transplantation (Fujikawa *et al.*, 2005; Kroon *et al.*, 2008).

Isolation and culture of ductal epithelium from adult mouse pancreas also yielded insulin$^+$ cells, as well as islets, through islet producing stem cell (IPSC) and islet progenitor cell (IPC) intermediates (Ramiya *et al.*, 2000). Increased islet yield was obtained by culturing IPSCs with epidermal growth factor (EGF), hepatocyte growth factor (HGF), and nicotinamide. IPSCs can be maintained in culture long-term (>3 years) and can withstand freezing, and the islets derived from them can reverse streptozotocin (STZ)-induced diabetes in mice. Duct cells have also been isolated from humans, from the normally-discarded non-islet fraction of pancreatic tissue utilized for islet transplantation (Heremans *et al.*, 2002). Adenoviral infection of these cells with *Ngn3* or *Neurod1* results in differentiation into primarily insulin$^+$ cells (10-fold over that observed in control cells), although intracellular insulin content is relatively low. Similar

results were observed when immortalized ductal cell lines from mice or humans were transfected with *Ngn3* or *Neurod1* (Gasa *et al.*, 2004). However, whether or not the insulin$^+$ cells and islets that are derived from these various sources are fully differentiated and fully functioning is unknown.

Establishing an Organism's β Cell Mass

β cell mass is increased by β cell neogenesis (differentiation from precursor cells), β cell proliferation, and β cell hypertrophy (increased cell size), and is decreased by β cell death, primarily via apoptosis, and β cell atrophy (decreased cell size) (Figure 3A) (Ackermann and Gannon, 2007). From embryogenesis to adulthood, there is a net increase in β cell mass as the organism's size increases (Figure 3B), and the majority of new β cells are formed by replication (Meier *et al.*, 2008). β cell differentiation, as described above, gives rise to the initial β cells of an organism during embryogenesis, but there is much debate regarding whether and to what extent β cell neogenesis occurs in the postnatal and adult stages under normal circumstances. Lineage studies using DNA analog incorporation to assess sequential cell division showed that β cells in adult mice arise by uniform proliferation of pre-existing β cells, with no contributions from specialized populations of progenitor or stem cells (Teta *et al.*, 2007). However, β cell neogenesis has been reported in models of pancreatic injury in adult mice (Xu *et al.*, 2008; Bonner-Weir *et al.*, 2008).

β cell proliferation proceeds at a high rate (approximately 10% per day in mice) during late embryogenesis (Bernard-Kargar and Ktorza, 2001) but begins to decline postnatally (Scaglia *et al.*, 1997). During adulthood, β cells proliferate at a low rate that

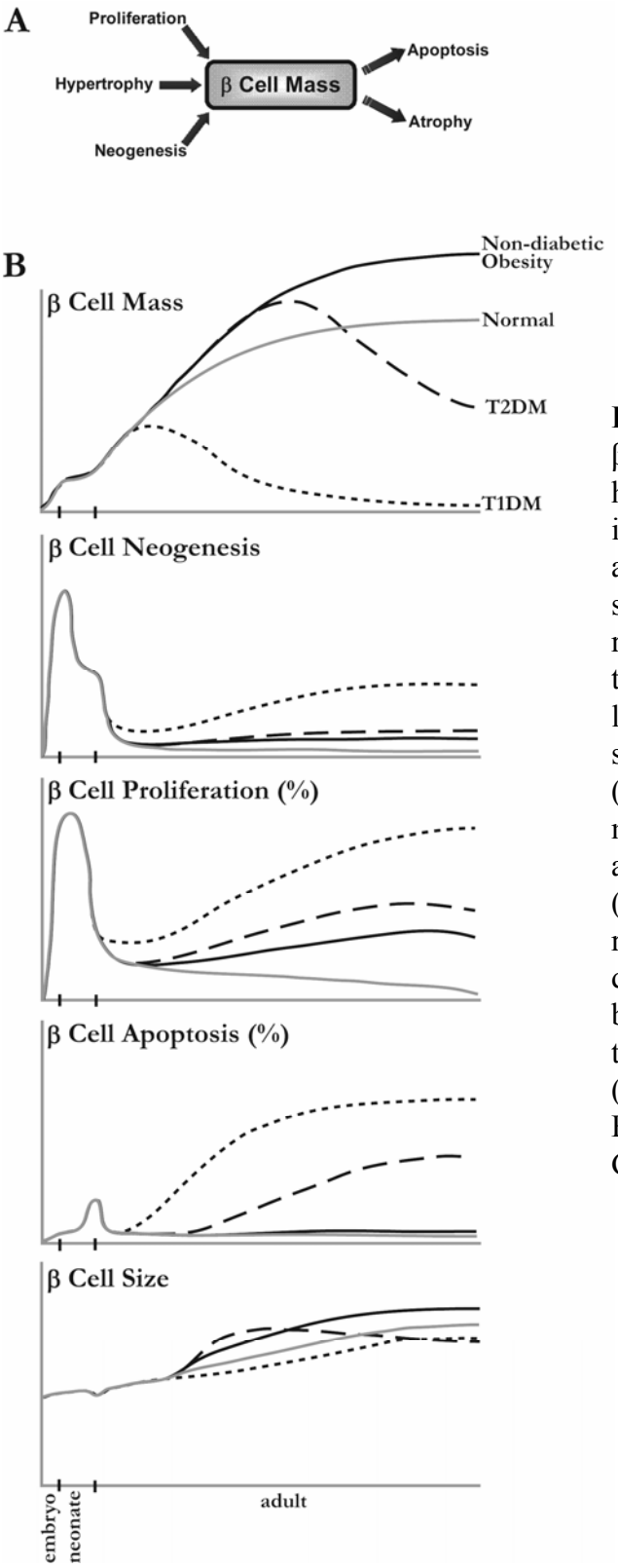

Figure 3. β cell mass dynamics. (A) β cell proliferation, neogenesis, and hypertrophy (enlarged cell size) increase β cell mass, while β cell apoptosis and atrophy (reduced cell size) decrease β cell mass. **(B)** Graphs represent approximate changes in these processes over the course of a lifetime in normal individuals (gray solid line), in non-diabetic obesity (black solid line), in Type II diabetes mellitus (T2DM; black dashed line), and in Type I diabetes mellitus (T1DM; black dotted line), based on rodent and human studies. Embryo denotes the period of time prior to birth. Neonate denotes the period of time between birth and weaning (approximately 3 weeks in the rodent). Figure is from Ackermann and Gannon (2007).

may gradually decline with age. Approximately 1-4% of β cells replicate per day in rats between 30 and 100 days old (Finegood *et al.*, 1995), while <1% of β cells replicate per day in mice at 1 year of age (Teta *et al.*, 2005). The differences observed in the rates of β cell proliferation at these timepoints is thought to be due to differences in the percentage of β cells that are able to be recruited to enter the cell cycle, rather than differences in cell cycle lengths. The mechanism by which more β cells are recruited to enter the cell cycle during embryonic versus postnatal and adult stages is currently unknown. However, evidence from several genetic mouse models indicates that the factors that regulate β cell proliferation during embryogenesis may differ from those that regulate β cell proliferation postnatally (Rane *et al.*, 1999; Georgia and Bhushan, 2004; Kushner *et al.*, 2005a; Georgia and Bhushan, 2006; Zhang H *et al.*, 2006). For example, global deletion of the cell cycle inhibitor $p27^{Kip1}$ (*p27*$^{Kip1-/-}$) increases β cell proliferation during embryogenesis and adulthood, but not during the early postnatal period, resulting in increased β cell mass at birth and throughout life (Georgia and Bhushan, 2006). In contrast, β cell-specific deletion of *Pdx1* (*Pdx1*$^{fl/-}$;*RIP-Cre*) impairs embryonic β cell proliferation and alters islet morphology with increased proportions of α and δ cells at the expense of β cells (Gannon *et al.*, 2008).

β cell apoptosis occurs at very low rates during embryogenesis, but there is evidence that a transient burst of β cell apoptosis occurs at weaning, which may be associated with islet remodeling and/or changes in β cell maturation (Scaglia *et al.*, 1997). During adulthood, β cell apoptosis again normally occurs at very low rates, although it modestly increases in mice fed a high-fat or high-fat/high-protein diet (Linn *et al.*, 1999). Average β cell size is fairly stable during the postnatal period (Scaglia *et al.*,

1997), but it increases with age during later adulthood (Montanya *et al.*, 2000) and with increased adiposity (Park *et al.*, 2007).

Proper development of an organism's β cell mass requires appropriate nutrition during embryogenesis. Poor maternal nutrition results in intrauterine growth retardation (IUGR), low birth weight, and underdeveloped β cell mass in newborn rats, which predisposes them to glucose intolerance and diabetes later in life (Breant *et al.*, 2006). When IUGR is caused by total caloric restriction, the reduction in β cell mass is due to reduced β cell differentiation, with decreased expression of Pdx1, Pax6, and Nkx6.1, rather than due to reduced β cell proliferation. These changes are associated with increased levels of glucocorticoids, which can independently reduce fetal β cell mass when exogenously administered to the mother. IUGR caused by protein restriction also results in under-developed β cell mass in newborn rats, but this is due to reduced β cell proliferation and increased β cell apoptosis, associated with reduced levels of insulin-like growth factors (IGFs) (Reusens and Remacle, 2006). IUGR initiated by surgical ligation of uterine arteries resulted in epigenetic modification of the *Pdx1* promoter, causing reduced islet Pdx1 expression in offspring at birth and during the neonatal period and absence of Pdx1 expression in the adult after diabetes onset (Park JH *et al.*, 2008). In contrast, maternal obesity and/or diabetes results in newborn macrosomia (large birth weight) and increased β cell mass associated with increased β cell proliferation, likely in response to maternal hyperglycemia. These offspring are also predisposed to obesity, insulin resistance, and diabetes, associated with early β cell exhaustion.

Maintaining an Organism's β Cell Mass

Although it was once thought that an organism was born with all of the β cells it would ever have, prevailing evidence now shows that new β cells can form throughout life. Several studies have revealed that the primary mechanism by which new β cells form during adulthood is via proliferation rather than neogenesis (Dor *et al.*, 2004; Georgia and Bhushan, 2004; Teta *et al.*, 2007). Thus, organisms born with reduced β cell mass, as discussed above, have fewer β cells available to enter the cell cycle later in life. Under normal circumstances during adulthood, β cells are a slowly-renewing population, with steady low levels of proliferation and apoptosis. However, β cell mass continuously expands over the lifespan of an organism (Montanya *et al.*, 2000), likely due to age-related increases in body weight and insulin resistance. In rats, β cells achieve this progressive increase in β cell mass by increasing their cell size, rather than increasing proliferation (Montanya *et al.*, 2000).

The ability of an organism to maintain its β cell mass during adulthood is paramount to maintaining glucose homeostasis and preventing diabetes. Table 1 summarizes the mouse models in which molecular regulators of postnatal β cell mass are perturbed, and many of these factors are key regulators of the cell cycle (Figure 4). Several genetic mouse models of cell cycle dysregulation impair postnatal β cell proliferation, and cause a progressive decline in β cell mass, associated with a progressive glucose intolerant and diabetic phenotype. For example, global inactivation of Cyclin-dependent kinase 4 in mice (*Cdk4*$^{-/-}$) specifically affects endocrine cells within the pancreas, causing diabetes by 2 months of age, and within the pituitary, causing reduced body size and infertility (Rane *et al.*, 1999). The diabetes observed in these mice

Table 1. Molecular Regulators of Postnatal β Cell Mass *in Vivo*

	Mouse Models	Effects	References
Transcription Factors			
Pdx1	*Pdx1*$^{+/-}$	↓ β cell mass, ↑ β cell apoptosis	(Johnson *et al.*, 2003)
	Pdx1$^{flox/flox}$;*Rip-Cre*	↓ β cell mass	(Ahlgren *et al.*, 1998)
Foxm1	*Foxm1*$^{flox/flox}$;*Pdx1*$^{4.3}$*-Cre*	↓ β cell mass, ↓ β cell proliferation, ↑-↓ β cell size, ↔ β cell apoptosis	(Zhang H *et al.*, 2006)
Cyclic AMP Response Element Binding Protein	*CBP*$^{S436A/+}$ Tg (↑ CREB activity)	↑ β cell mass, ↑ β cell proliferation, ↔ β cell size, ↔ β cell apoptosis	(Hussain *et al.*, 2006)
	HIP-ICER-Iγ Tg (↓ CREB activity)	↓ β cell mass, ↓ β cell proliferation, ↔ β cell apoptosis	(Inada *et al.*, 2004)
	Rip-dn*CREB* Tg	↓ β cell mass, ↑ β cell apoptosis	(Jhala *et al.*, 2003)
E2Fs	*E2F1*$^{-/-}$	↓ β cell mass, ↓ β cell proliferation, ↔ β cell apoptosis	(Fajas *et al.*, 2004)
	E2F1$^{-/-}$;*E2F2*$^{-/-}$	↓ β cell mass, ↑ β cell proliferation	(Iglesias *et al.*, 2004)
Nuclear Factor of Activated T Cells, cytoplasmic, calcineurin-dependent 1	*Rip-rtTA*;*NFATc1*^{nuc}	↑ β cell mass, ↑ β cell proliferation	(Heit *et al.*, 2006a)
Cell Cycle Proteins			
Cyclin-Dependent Kinases	*Cdk4*$^{R26C/R26C}$ Tg (↑ activity)	↑ β cell mass	(Rane *et al.*, 1999)
	Cdk4$^{-/-}$	↓ β cell mass	(Rane *et al.*, 1999)
Cyclins	*Rip-Cyclin D1* Tg	↑ β cell mass, ↑ β cell proliferation, ↔ β cell apoptosis	(Zhang X *et al.*, 2005)
	Cyclin D2$^{-/-}$	↓ β cell mass, ↓ β cell proliferation, ↔ β cell apoptosis	(Georgia and Bhushan, 2004; Kushner *et al.*, 2005a)
	Cyclin D1$^{+/-}$;*Cyclin D2*$^{-/-}$	↓ β cell mass, ↓ β cell proliferation, ↔ β cell apoptosis	(Kushner *et al.*, 2005a)
Cyclin-Dependent Kinase Inhibitors	*p16*^{INK4a} Tg	↓ β cell proliferation	(Krishnamurthy *et al.*, 2006)
	p16$^{INK4a-/-}$	↑ β cell proliferation	(Krishnamurthy *et al.*, 2006)
	p18$^{INK4c-/-}$	↑ β cell mass	(Pei *et al.*, 2004)
	p21$^{Cip1-/-}$	↔ β cell mass, ↔ β cell proliferation, ↔ β cell apoptosis	(Cozar-Castellano *et al.*, 2006b)
	Rip-p27^{Kip1} Tg	↓ β cell mass, ↓ β cell proliferation, ↔ β cell size	(Uchida *et al.*, 2005)
	p27$^{Kip1-/-}$	↑ β cell mass, ↑ β cell proliferation, ↔ β cell size	(Georgia and Bhushan, 2006)
Tumor Suppressors	*pRb*$^{flox/flox}$;*Rip-Cre*	↑ β cell mass, ↔ β cell proliferation, ↔ β cell size	(Vasavada *et al.*, 2007)
	pRb$^{+/-}$;*p53*$^{+/-}$	↑ β cell mass	(Williams *et al.*, 1994)
	pRb$^{+/-}$;*p53*$^{-/-}$	↑ β cell mass	(Williams *et al.*, 1994)
Growth Factors			
Lactogens	*Rip-PL1* Tg	↑ β cell mass, ↑ β cell proliferation, ↑ β cell size	(Vasavada *et al.*, 2000; Cozar-Castellano *et al.*, 2006c)
	PrlR$^{-/-}$	↓ β cell mass	(Freemark *et al.*, 2002)
Parathyroid Hormone-related Protein	*Rip-PTHrP* Tg	↑ β cell mass, ↔ β cell proliferation, ↔ β cell apoptosis, ↔ β cell size	(Porter *et al.*, 1998)
Growth Hormone	*GHR*$^{-/-}$	↓ β cell mass, ↓ β cell proliferation, ↓ β cell size	(Liu *et al.*, 2004)
Hepatocyte Growth Factor	*Rip-HGF* Tg	↑ β cell mass, ↑ β cell proliferation	(Garcia-Ocana *et al.*, 2000; Garcia-Ocana *et al.*, 2001; Cozar-Castellano *et al.*, 2006c)
	c-Met$^{flox/flox}$;*Rip-Cre*	↔ β cell mass, ↔ β cell proliferation	(Roccisana *et al.*, 2005)
Epidermal Growth Factor	*HIP-EGF* Tg	↑ β cell mass, ↑ β cell proliferation	(Krakowski *et al.*, 1999)
Keratinocyte Growth Factor	*HIP-KGF* Tg	↑ β cell mass, ↑ β cell proliferation	(Krakowski *et al.*, 1999)
Insulin, Insulin-like Growth Factors	*IR*$^{flox/flox}$;*Rip-Cre*	↓ β cell mass	(Otani *et al.*, 2004)
	Rip-IGF-I Tg	↔ β cell mass, ↑ β cell proliferation, ↔ β cell apoptosis, ↔ β cell neogenesis	(George *et al.*, 2002)
	IGF-I$^{flox/flox}$;*Pdx1*$^{4.3}$*-Cre*	↑ β cell mass, ↑ β cell size	(Lu *et al.*, 2004)
	IGF-IR$^{flox/flox}$;*Rip-Cre*	↔ β cell mass	(Kulkarni *et al.*, 2002)
	IGF-II Tg	↑ β cell mass, ↑ β cell proliferation, ↓ β cell apoptosis, ↔ β cell size	(Petrik *et al.*, 1999)
	Rip-IGF-II Tg	↑ β cell mass	(Devedjian *et al.*, 2000)
Fibroblast Growth Factors	*Pdx1-dnFGFR1c* Tg	↓ β cell mass, ↔ β cell apoptosis	(Hart *et al.*, 2000)
	Pdx1-dnFGFR2b Tg	↔ β cell mass	(Hart *et al.*, 2000)
Vascular Endothelial Growth Factors	*Rip-VEGF-A* Tg	↔ β cell mass	(Gannon *et al.*, 2002)
	VEGF-A$^{flox/flox}$;*Rip-Cre*	↔ β cell mass, ↑ β cell size	(Inoue *et al.*, 2002)
Incretins	*GLP-1R*$^{-/-}$	↔ β cell mass	(Ling *et al.*, 2001)
	GIPR$^{-/-}$	↑ β cell mass	(Pamir *et al.*, 2003)
Gastrin	*Rip-Gastrin* Tg	↔ β cell mass	(Wang *et al.*, 1993)
	Gastrin$^{-/-}$	↔ β cell mass, ↔ β cell proliferation	(Boushey *et al.*, 2003)
Cell Signaling Proteins			
Insulin Receptor Substrate	*Rip-Irs2* Tg	↑ β cell mass, ↔ β cell proliferation, ↔ β cell size	(Hennige *et al.*, 2003)
	Irs2$^{-/-}$	↓ β cell mass, ↑ β cell apoptosis	(Withers *et al.*, 1998; Withers *et al.*, 1999; Kubota *et al.*, 2000)
	Irs2$^{flox/flox}$;*Rip-Cre*	↓ β cell mass, ↓ β cell proliferation, ↔ β cell apoptosis	(Kubota *et al.*, 2004)
Protein Kinase B/Akt	*caAkt* Tg	↑ β cell mass, ↑ β cell proliferation, ↑ β cell size	(Fatrai *et al.*, 2006)
	Rip-caAkt Tg	↑ β cell mass, ↑ β cell proliferation, ↑ β cell size, ↑ β cell neogenesis	(Bernal-Mizrachi *et al.*, 2001)
	Rip-caAkt Tg	↑ β cell mass, ↑ β cell size, ↑ β cell apoptosis, ↔ β cell proliferation	(Tuttle *et al.*, 2001)
	Rip-kdAkt Tg	↔ β cell mass, ↔ β cell apoptosis, ↔ β cell size	(Bernal-Mizrachi *et al.*, 2004)
p70S6K	*p70*$^{S6K1-/-}$	↓ β cell mass, ↓ β cell size	(Pende *et al.*, 2000)
Phosphoinositide-Dependent Kinase	*PDK1*$^{flox/flox}$;*Rip-Cre*	↓ β cell mass, ↓ β cell proliferation, ↓ β cell size, ↑ β cell apoptosis	(Hashimoto *et al.*, 2006)
Others			
Menin	*Men1*$^{+/-}$	↑ β cell mass, ↑ β cell proliferation	(Karnik *et al.*, 2005)
	Men1$^{flox/flox}$;*Rip-Cre*	↑ β cell mass, ↑ β cell proliferation, ↔ β cell apoptosis	(Crabtree *et al.*, 2003)
S-phase kinase-associated protein 2	*Skp2*$^{-/-}$	↓ β cell mass, ↓ β cell proliferation, ↑ β cell size	(Zhong *et al.*, 2007)
Pkr-like ER Kinase	*PERK*$^{-/-}$	↓ β cell mass, ↓ β cell proliferation, ↔ β cell apoptosis, ↔ β cell neogenesis, ↔ β cell size	(Harding *et al.*, 2001; Zhang *et al.*, 2002; Zhang W *et al.*, 2006)
Phosphatase and Tensin homologue	*PTEN*$^{+/-}$	↓ β cell mass, ↓ β cell proliferation	(Kushner *et al.*, 2005b)
	PTEN$^{flox/flox}$;*Rip-Cre*	↑ β cell mass, ↑ β cell proliferation, ↓ β cell apoptosis, ↔ β cell size	(Stiles *et al.*, 2006)
Calcineurin b1	*Cnb1*$^{flox/flox}$;*Rip-Cre*	↓ β cell mass, ↓ β cell proliferation, ↔ β cell apoptosis	(Heit *et al.*, 2006a)

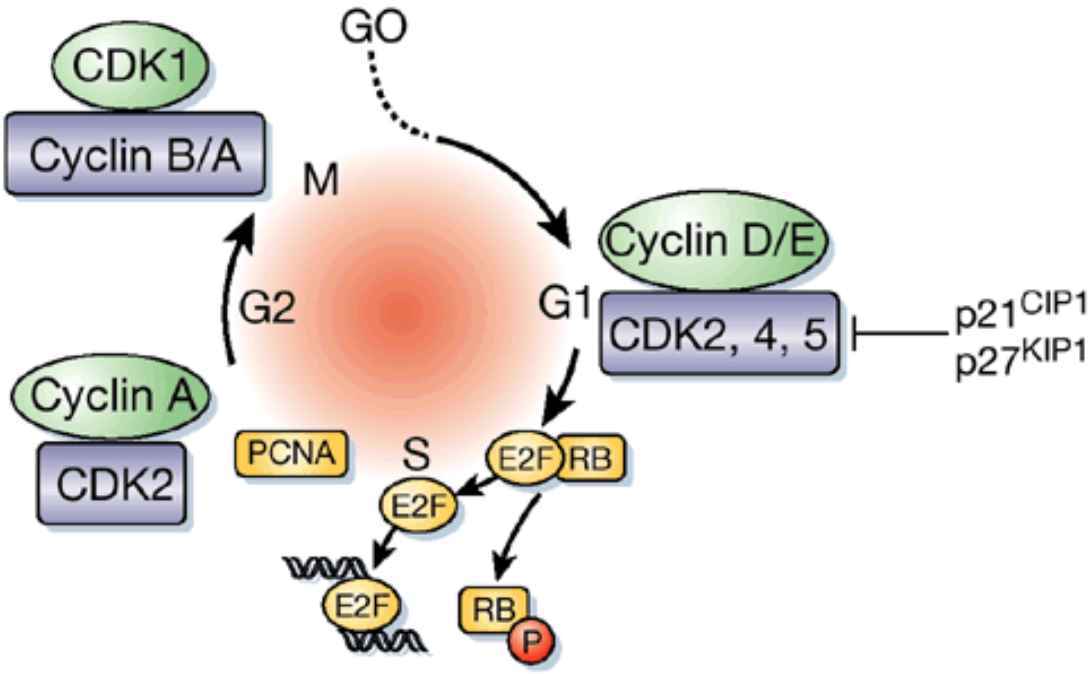

Figure 4. Cell cycle regulation. The G_1/S transition is controlled by Cdk2, 4, 5, or 6 bound to Cyclin D or E, which phosphorylates Rb, releasing the E2F transcription factor. Rb phosphorylation is maintained through the G_2/M transition by Cdk2 bound to Cyclin A and Cdk1 bound to Cyclin A or B. Figure is adapted from Dzau *et al*. (2002).

is associated with severely reduced β cell mass, although β cell mass is comparable to that of wild-type mice at postnatal days (P) 1 and 2. Progression from G_1 to S phase in the cell cycle requires phosphorylation of the Retinoblastoma protein (Rb) by Cdk4/6 complexed with a D Cyclin, which releases E2F allowing it to activate transcription of necessary cell cycle target genes. Thus, Cdk6 function is redundant with Cdk4; however, mouse β cells do not express detectable levels of Cdk6 (Martin *et al.*, 2003), making them uniquely susceptible to cell cycle perturbations caused by loss of Cdk4. In contrast, human islets express Cdk6 but not Cdk4 (Fiaschi-Taesch *et al.*, 2008). Similarly, global deletion of Cyclin D2 (*CyclinD2*$^{-/-}$), the predominant D Cyclin expressed in β cells, fails to stimulate adequate compensatory up-regulation of Cyclin D1 or D3 within islets and drastically impairs postnatal β cell proliferation (Georgia and Bhushan, 2004). *CyclinD2*$^{-/-}$ mice exhibit normal β cell mass at e17.5 but significantly reduced β cell mass postnatally, causing progressive glucose intolerance and diabetes.

Cdk inhibitor proteins (Cips, Kips, INKs) also play important roles in β cell proliferation. Transgenic over-expression of $p27^{Kip1}$ within β cells using the rat insulin promoter (*Rip-p27*^{Kip1}) impairs β cell proliferation, resulting in decreased β cell mass and diabetes in mice (Uchida *et al.*, 2005). In contrast, as mentioned before, global deletion of $p27^{Kip1}$ (*p27*$^{Kip1-/-}$) increases β cell proliferation under normal circumstances (Georgia and Bhushan, 2006). Loss of $p27^{Kip1}$ also increases β cell proliferation in genetic models of insulin resistance and diabetes (*Irs2*$^{-/-}$ or *db/db*) and restores glucose homeostasis in the latter model (Uchida *et al.*, 2005). β cell hyperplasia is also observed in humans with focal loss of heterozygosity of *p57*^{Kip2}, and these subjects suffer from hyperinsulinism of infancy (Kassem *et al.*, 2001). Additionally, mice that express a mutant Cdk4 that cannot

be bound and inhibited by $p16^{INK4a}$ (*Cdk4*$^{R24C/R24C}$) exhibit postnatal increases in β cell proliferation and β cell mass that improve glucose regulation (Rane *et al.*, 1999).

Our lab has recently found that FoxM1 also plays an important role in β cell proliferation (Zhang H *et al.*, 2006). FoxM1 is a transcription factor known to regulate expression levels of several cell cycle proteins. Pancreas-wide deletion of *Foxm1* using a Cre-lox strategy (*Foxm1*$^{flox/flox}$;*Pdx1*$^{5.5kb}$-*Cre*) in mice results in postnatal defects in β cell proliferation, which contribute to a postnatal deficiency in β cell mass and a progressive glucose intolerant and diabetic phenotype. However, β cell mass and islet morphology are normal at P1, despite inactivation of *Foxm1* early in embryogenesis. Increased nuclear $p27^{Kip1}$, which is an indirect target of FoxM1, and β cell senescence are associated with impaired β cell proliferation in these mice. Thus, FoxM1 is critical for maintaining β cell mass during adulthood by properly coordinating cell cycle progression.

One of FoxM1's transcriptional targets, S-phase kinase-associated protein 2 (Skp2), mediates degradation of $p21^{Cip1}$ and $p27^{Kip1}$ and has also been directly linked to β cell proliferation. *Skp2*$^{-/-}$ mice exhibit a phenotype similar to that observed in *Foxm1*$^{flox/flox}$;*Pdx1*$^{5.5kb}$-*Cre* mice, with reduced postnatal β cell mass, reduced β cell proliferation, progressive diabetes, β cell hypertrophy and polyploidy, and accumulation of nuclear $p27^{Kip1}$ in β cells (Zhong *et al.*, 2007). These effects of loss of Skp2 on β cells are attributed to increased nuclear $p27^{Kip1}$, as the metabolic and morphologic phenotypes are reversed in *Skp2*$^{-/-}$;*p27*$^{Kip1-/-}$ double knock-out mice.

Another regulator of cell cycle genes is the transcriptional coactivator Menin, encoded by *Men1*, mutation of which results in Multiple Endocrine Neoplasia type 1 (MEN1) in humans (Crabtree *et al.*, 2003). This syndrome is characterized by

hyperplasia of endocrine cell types primarily within the parathyroids, anterior pituitary, and pancreas, resulting in tumor formation, most commonly insulinomas composed of β cells. *Men1*$^{+/-}$ mice display a similar phenotype. β cell-specific deletion of *Men1* (*Men1*$^{flox/flox}$;*Rip-Cre*) also results in β cell hyperplasia, insulinomas, hyperinsulinemia, and hypoglycemia. Significantly increased β cell proliferation is observed, and this is associated with reduced levels of p18^{INK4c} and p27^{Kip1}, both of which are direct targets of Menin-mediated histone methylation (Karnik *et al.*, 2005). Furthermore, a MEN1-like phenotype is observed in *p18*$^{INK4c-/-}$;*p27*$^{Kip1-/-}$ mice (Franklin *et al.*, 2000). Other mouse models of impaired and enhanced β cell proliferation have been reviewed by (Cozar-Castellano *et al.*, 2006a) and (Heit *et al.*, 2006b).

Just as impaired β cell proliferation causes a net loss of β cells, increased β cell death can have the same effect. Inherent defects that make β cells more susceptible to apoptosis, for example, result in a negative balance of β cell turnover, as observed in *Pdx1*$^{+/-}$ mice, which exhibit normal β cell mass at 3 months of age but are unable to appropriately increase their β cell mass as they age (Johnson *et al.*, 2003). Haploinsufficiency of *Pdx1* makes β cells more susceptible to undergoing apoptosis, associated with reduced expression levels of the anti-apoptotic genes *Bcl*$_{XL}$ and *Bcl-2*. Increased β cell apoptosis results in insufficient β cell mass and progressive glucose intolerance. A more dramatic phenotype is observed in mice with adult-onset β cell-specific deletion of *Pdx1* (*Pdx1*$^{flox/flox}$;*Rip-Cre*) (Ahlgren *et al.*, 1998). These mice suffer from worsening glucose intolerance due to both progressive loss of β cell mass and impaired β cell function. Mutations of *PDX1* in humans result in similar phenotypes; a dominant-negative mutation of *PDX1* causes MODY4 (Stoffers *et al.*, 1997a), while a

heterozygous inactivating mutation of *PDX1* predisposes to late-onset Type 2 diabetes (Macfarlane *et al.*, 1999). Thus, Pdx1 is a critical regulator of β cell survival and maintenance of β cell mass and function during adulthood.

Dynamic Changes in an Organism's β Cell Mass

In addition to maintaining β cell mass under normal circumstances, as just discussed, an organism must also be able to alter its β cell mass in accordance with its requirements for insulin. In states of insulin resistance, such as pregnancy and obesity, β cell mass is known to increase (Rhodes, 2005) (Figure 3). In mice, such β cell mass expansion is accomplished primarily by increasing β cell proliferation (Karnik *et al.*, 2007), whereas β cell neogenesis humans accounts for β cell mass expansion (Butler *et al.*, 2003; Cao Minh *et al.*, 2008). Regardless of the mechanism, when compensatory β cell mass expansion is inadequate, diabetes ensues – gestational diabetes in the case of pregnancy, and Type II diabetes in the case of obesity. Although the majority of humans do not become diabetic in these circumstances, a significant portion of the population is predisposed to β cell failure, for currently unknown reasons. It is likely that factors that regulate β cell proliferation and neogenesis may play a role, although whether the factors that regulate β cell mass expansion are the same as those that regulate β cell mass maintenance is unclear. Recent genome-wide association studies have identified several polymorphisms in patients with Type II diabetes that correlate with disease risk (Sladek *et al.*, 2007; Zeggini *et al.*, 2008). Some of the identified loci include genes that play roles in cellular proliferation, such as *TCF7L2*, *HHEX*, *EXT2*, and *CDC123*. TCF7L2 and HHEX also play important roles in pancreas development, as do other identified loci

including *NOTCH2*. However, distinct functions of identified loci with regard to Type II diabetes are still unclear.

During pregnancy, rats exhibit over a 50% increase in β cell mass, which is accomplished primarily via an approximate 3-fold increase in β cell proliferation (Scaglia *et al.*, 1995). The chief stimuli of β cell proliferation during pregnancy are placental lactogens (PLs), although prolactin (Prl) and growth hormone (GH) also have similar effects on β cells and are also elevated during pregnancy. After delivery, β cell mass returns to normal levels within 10 days via increased β cell apoptosis, decreased β cell proliferation, and β cell atrophy.

To determine the direct role of PLs on β cell mass in non-pregnant animals, transgenic mice expressing PL1 within their β cells (*Rip-Pl1*) were developed (Cozar-Castellano *et al.*, 2006c). These mice exhibited hypoglycemia and improved glucose clearance due to hyperinsulinemia, which was associated with a doubling of β cell mass. This expansion of β cell mass was attributed to a 2-fold increase in β cell proliferation and a 20% increase in β cell size. Similar results were observed in transgenic mice expressing HGF within their β cells (*Rip-Hgf*) (Garcia-Ocana *et al.*, 2000; Garcia-Ocana *et al.*, 2001; Cozar-Castellano *et al.*, 2006c). These mice also exhibited a doubling of β cell mass, but the increase in β cell proliferation was not as significant as that in *Rip-Pl1* mice. Interestingly, islet number was significantly increased in *Rip-Hgf* mice but not in *Rip-Pl1* mice versus wild-type mice, suggesting that HGF may stimulate neogenesis.

In pregnant female mice, the negative cell cycle regulator Menin normally becomes down-regulated within islets, inversely correlated with β cell proliferation (Karnik *et al.*, 2007). β cell-specific over-expression of Menin using the Tet-on system

(*RIP-rtTA*, *TRE-Men1*) abrogates pregnancy-associated increases in β cell proliferation and β cell mass, associated with relatively increased levels of $p18^{INK4c}$ and $p27^{Kip1}$.

Diet-induced obesity results in insulin resistance and β cell mass expansion in humans and mice. The C57Bl/6 mouse strain is notoriously susceptible to these effects, exhibiting a 2.2-fold increase in β cell mass and proliferation after four months on a high-fat diet versus a control diet (Sone and Kagawa, 2005). However, these mice eventually become diabetic and lose their β cell mass due to increased β cell apoptosis and reduced β cell proliferation.

In genetic models of obesity and insulin resistance, there is also a compensatory expansion of β cell mass. For example, *db/db* mice, which lack a functional leptin receptor, exhibit a 2-fold increase in β cell mass by 8 weeks of age (Wang and Brubaker, 2002). This timepoint correlates with the onset of diabetes, which progresses from glucose intolerance that is first observed between 4-6 weeks of age. A similar rat model, the Zucker diabetic fatty (ZDF) rat (*fa*/*fa*), also has a homozygous mutation in the gene encoding the leptin receptor. ZDF rats exhibit increased β cell mass and increased β cell proliferation prior to the onset of diabetes, but increased β cell apoptosis prevents them from adequately expanding their β cell mass after the onset of diabetes, despite continued high rates of β cell proliferation (Pick *et al.*, 1998). This phenotype contrasts with what is observed in non-diabetic Zucker fatty (ZF) rats, which possess the same mutation as ZDF rats and also become obese and insulin resistant but do not develop diabetes due to sufficient β cell mass expansion via increased β cell proliferation, neogenesis, and hypertrophy (Pick *et al.*, 1998).

Another model of insufficient β cell mass expansion is the insulin receptor substrate 2 null mouse (*Irs2*$^{-/-}$) (Kubota *et al.*, 2004). Global inactivation of Irs2 results in severe insulin resistance, both centrally in the brain causing obesity, and peripherally, for which β cell mass expansion should be able to compensate. However, because β cells require Irs2 for proper proliferation and function, *Irs2*$^{-/-}$ mice are unable to expand their β cell mass, and they develop diabetes by 10 weeks of age. This phenotype is not observed in *Irs1*$^{-/-}$ mice, despite the fact that these mice exhibit similar insulin resistance, because Irs1 is not required for β cell mass expansion. Deletion of *Irs2* specifically within β cells and the hypothalamus (*Irs2*$^{flox/flox}$;*Rip-Cre*) causes central insulin resistance and obesity, with glucose intolerance developing at 8 weeks of age but without progression to diabetes, likely due to the lack of peripheral insulin resistance (Kubota *et al.*, 2004). These mice also exhibit reduced β cell proliferation and β cell mass at 8 weeks of age, although these impairments are not observed before the onset of insulin resistance (between 4 and 8 weeks). These experiments provide additional evidence that Irs2 is required for β cell mass expansion in response to insulin resistance. Furthermore, over expression of Irs2 in β cells (*Rip-Irs2*) is sufficient to prevent β cell failure in diet-induced obesity and streptozotocin-induced diabetic models (Hennige *et al.*, 2003).

Several downstream effectors of the insulin signaling pathway have been shown to play a role in β cell mass expansion in models of insulin resistance. For example, haploinsufficiency of FoxO1 (*Foxo1*$^{+/-}$) restores β cell mass and proliferation to nearly normal levels in *Irs2*$^{-/-}$ mice, possibly due to reduced FoxO1-mediated repression of *Pdx1* (Kitamura *et al.*, 2002). In contrast, expression of constitutively-nuclear FoxO1 prevents β cell mass expansion in two other models of insulin resistance (Okamoto *et al.*, 2006).

Therapeutic Implications

In understanding how β cell mass is developed, maintained, and manipulated, we seek to better understand diabetes etiology, identify new and optimal therapeutic targets, and develop new therapeutic techniques. Out of necessity, much of the work in this field has been and is being performed in lower mammals, and thus much of it must still be confirmed in humans. Furthermore, outside fields, such as gene therapy and immunology, must make substantial progress before some clinical interventions can be feasible. However, there remains great optimism regarding the future ability to manipulate β cell differentiation and proliferation *in vitro* to provide an unlimited supply of β cells for transplantation into patients with diabetes. Although studies in this area have revealed that it is difficult to achieve full differentiation and maturation of β cells, which is essential for clinical application, techniques are continuously being improved. Tumor formation, either from ES cell-derived cells or from induction of β cell proliferation which may induce transient de-differentiation, is another concern that must be considered. Ultimately, however, the processes of β cell differentiation and proliferation will likely one day be controlled *in vivo* as a means to treat or prevent diabetes.

Forkhead Box M1 (FoxM1)

Identification of FoxM1

FoxM1 is a member of the forkhead box family of transcription factors, so named for their relation to the *Drosophila melanogaster* gene *fork head* (*fkh*). Mutation of *fkh*

results in formation of ectopic head structures in place of the foregut and hindgut (Weigel *et al.*, 1989). The first mammalian homologue of *fkh* to be identified was Hepatocyte nuclear factor 3α (Hnf3α), which binds to and activates transcription of the liver-specific genes *Transthyretin* (*TTR*) and *α1-antitrypsin* (Costa *et al.*, 1989; Lai *et al.*, 1990). *Hnf3α* and *fkh* were found to share significant sequence similarity within their DNA binding domain, which was termed a "fork head domain" (Weigel and Jäckle, 1990). Two related mammalian gene products were then identified in the liver and were termed Hnf3β and Hnf3γ, the first evidence of a family of forkhead proteins (Lai *et al.*, 1990; Lai *et al.*, 1991). Structural analysis of Hnf3γ's forkhead domain bound to DNA revealed a variation on the helix-turn-helix motif, with three α-helices (H1-3), three β-sheets (S1-3), and two loops (W1-2) (Clark *et al.*, 1993) (Figure 5). As the loops resemble wings attached to a helical core, the DNA binding domain was termed a "winged-helix" domain.

Protein sequence comparisons revealed that *Drosophila* forkhead most closely resembles Hnf3β, with 91% identity (100/110 amino acids) within the DNA binding domain (Lai *et al.*, 1991). Expression pattern comparisons between the two proteins also revealed high similarity, suggesting that Hnf3β is the true mammalian orthologue of *Drosophila* forkhead (Monaghan *et al.*, 1993). Since this time, more than 100 forkhead family members have been identified in species ranging from yeast to humans (reviewed in Kaufman and Knochel 1996), and due to their diverse means of discovery a unified nomenclature was devised (Kaestner *et al.*, 2000). Currently, there are 44 murine forkhead family members, organized into 19 (A-S) phylogenetic subclasses (Tuteja and Kaestner, 2007a; Tuteja and Kaestner, 2007b; Montelius *et al.*, 2007).

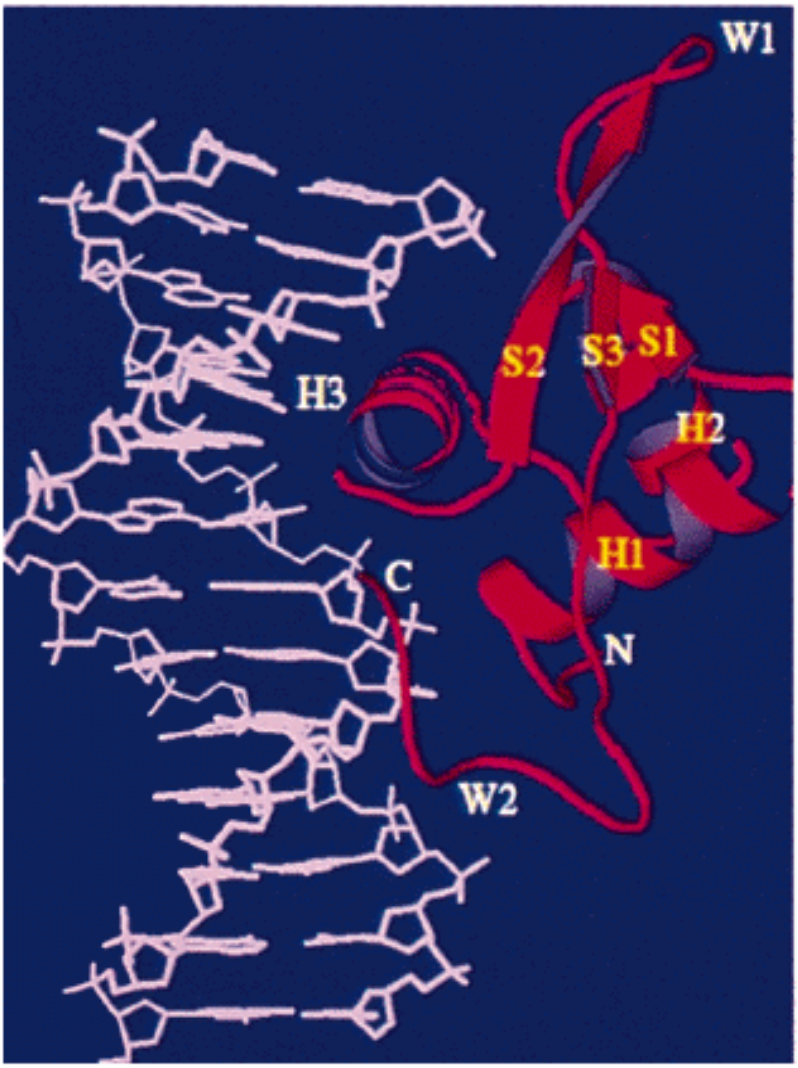

Figure 5. Winged-helix "forkhead" DNA binding domain structure. The characteristic forkhead DNA binding domain is a variation of the helix-turn-helix motif, with three α-helices (H1-3), three β-sheets (S1-3), and two loops (W1-2).

FoxM1 was originally identified as an M phase phosphoprotein (MPP) by its interaction with the Mitotic protein monoclonal 2 antibody MPM2 (Westendorf *et al.*, 1994). This antibody recognizes several phosphorylated epitopes, including F-phosphoT-P-L-Q. At that time, FoxM1 was referred to as MPP2. Soon thereafter, FoxM1 was simultaneously cloned by three groups looking for new forkhead family members, who assigned the names of Trident (Korver *et al.*, 1997a), Winged helix in INS-1 cells (WIN) (Yao *et al.*, 1997), and HNF3/forkhead homolog 11 (HFH11) (Ye *et al.*, 1997).

Trident was cloned from murine thymus and was found by northern blot analysis to be expressed broadly within the brain, heart, lung, liver, kidney, and limb of embryos but only within the thymus in 6 week old mice (Korver *et al.*, 1997a). Trident expression was also observed within multiple cell lines, and this expression was reduced upon serum starvation and stimulated upon serum return, coinciding with initiation of S phase. The DNA binding domain consensus site for Trident was identified as TAAACA.

WIN was cloned from the rat insulinoma cell line INS-1 and was found by northern blot analysis to be expressed in multiple rodent endocrine cell lines, as well as embryonic and neonatal, but not adult, pancreas and liver (Yao *et al.*, 1997). Evaluation of e12, e14, e18, neonatal, and adult whole pancreas revealed a progressive decline in WIN expression. Furthermore, WIN expression was detected within the testis and to a lesser extent the lung of adult mice, but not within brain, heart, liver, kidney, spleen, or skeletal muscle; and within the testis and thymus of adult humans, but not within stomach, intestine, pancreas, thyroid, adrenal cortex, adrenal medulla, or the human hepatoma cell line HepG2. Importantly, Yao *et al*. identified three splice variants of human WIN, which they termed classes a, b, and c (Figure 6), and they found that these

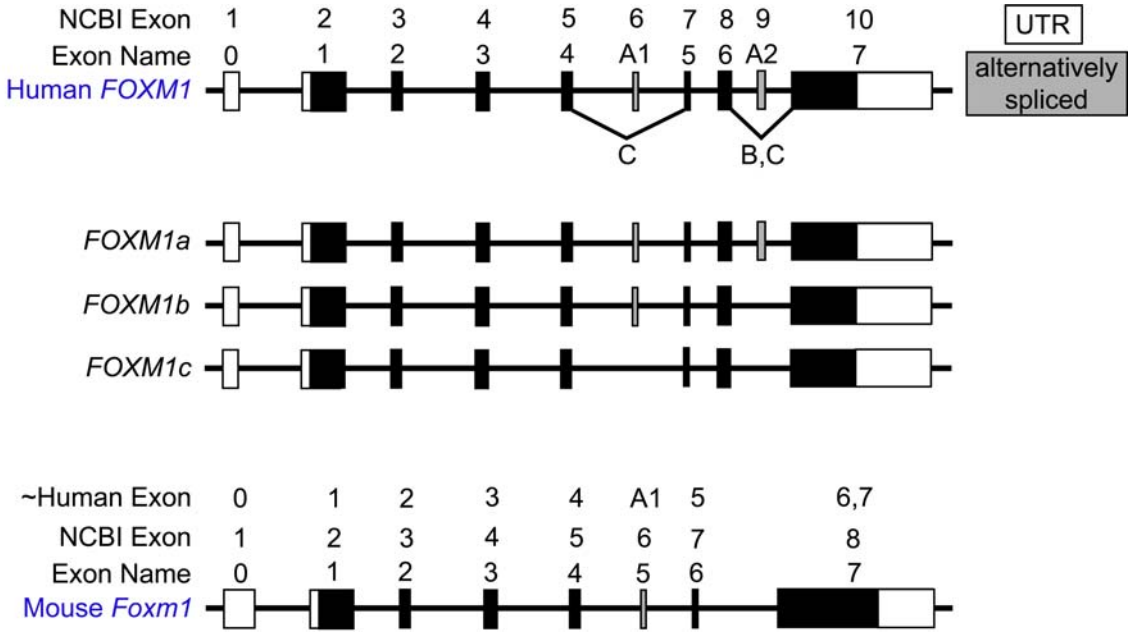

Figure 6. Human *FOXM1* and mouse *Foxm1* cDNA structures. *Foxm1* introns and exons are depicted in the diagram as lines and boxes, respectively. The human *FOXM1* cDNA contains two alternatively-spliced exons, producing three transcript variants. Although there exists conflicting variant nomenclature within the literature, the NCBI denotes these transcript variants as 1, 2, and 3, and we refer to them as *a*, *b*, and *c*, respectively, in accordance with Yao *et al*. (1997). Mouse *Foxm1* is most homologous to human *FOXM1b*.

variants were differentially expressed. Because these variants are derived by alternative splicing of two exons that encode portions of the DNA binding and transcription activation domains (Figure 7), it was suggested that they may have different transcriptional activities and targets. The consensus binding site for WIN was identified as AGATTGAGTA.

HFH11 was cloned from the human colon carcinoma cell line Caco-2, and it was found by northern blot analysis to be expressed in multiple human carcinoma cell lines including HeLa (cervical carcinoma), A549, and H441 (both pulmonary adenocarcinoma) (Ye *et al.*, 1997). Interestingly, HFH11 expression was observed within HepG2 cells, in contrast to observations made by the group that identified WIN (Yao *et al.*, 1997). Further northern blot analysis revealed that HFH11 was expressed at high levels in adult human thymus, testis, and intestine (small and large), and to a lesser extent in ovary, lung, heart, and placenta. Only two splice variants of HFH11 were identified by this group, and they were termed HFH11A and HFH11B. As HFH11A is the full-length transcript (encoding a 801-amino-acid protein), and HFH11B is missing two exons (encoding a 748-amino-acid protein), these variants are analogous to the human WIN class a and c variants (Yao *et al.*, 1997). The consensus binding site for HFH11 was identified as TACGTTGTTATTTGTTTTTTTCG.

FoxM1 Gene and Protein

FOXM1A has been shown to have little, if any, transcriptional activity, while FOXM1B and FOXM1C, along with murine FoxM1, which is most homologous to FOXM1B, are transcriptional activators (Ye *et al.*, 1997; Leung *et al.*, 2001; Ma *et al.*,

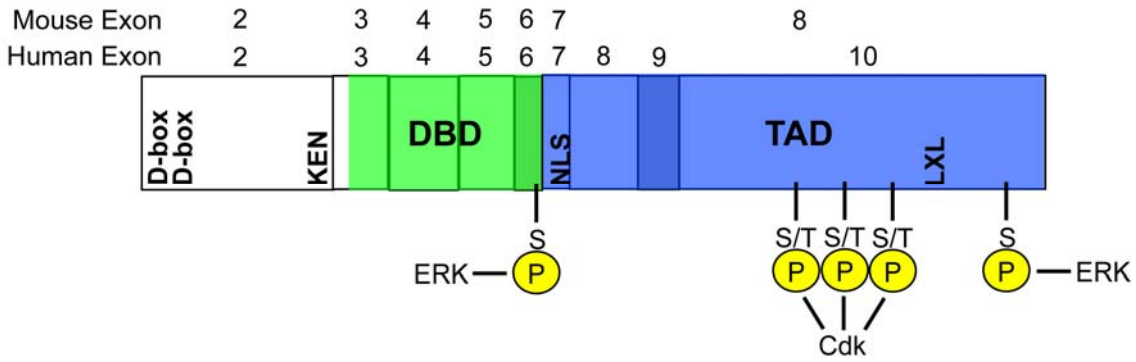

Figure 7. FoxM1 protein structure. This diagram depicts the domains and phosphorylation sites present within both mouse FoxM1 and human FOXM1, with the appropriate corresponding coding exons. The N-terminal domain is encoded by exon 2 and part of exon 3, and it contains two destruction boxes (D-box), as well as a KEN box, all of which are required for FoxM1 degradation. The DNA binding domain (DBD) is encoded by part of exon 3 and exons 4-6. As exon 6 is alternatively-spliced in humans, this may result in the transcript variants having different targets. The C-terminal transcription activation domain (TAD) is encoded by exons 7-10 (or 7 and 8 in the mouse). The presence of the alternatively-spliced exon 9 within transcript variant 1 (*FOXM1a*) accounts for the different activity observed in FOXM1A versus the B and C isoforms. FoxM1 is phosphorylated by ERK1/2 at a serine residue near the nuclear localization signal (NLS), as well as in the TAD near a protein interaction (LXL) sequence. Several Cdk phosphorylation sites are also located within the TAD.

2005). The lack of FOXM1A transcriptional activity is due to the presence of an additional exon (6 or A2) within the C-terminal transcription activation domain, which interferes with its activity (Ye *et al.*, 1997). Interestingly, FOXM1A is also expressed at much lower levels than are either FOXM1B or FOXM1C in many tissues (Yao *et al.*, 1997). Additionally, *FOXM1c* has been shown to be the predominant transcript found in human fibroblast cell lines (Ma *et al.*, 2005). Murine FoxM1 and human FOXM1B share 78% amino acid sequence identity and 86% sequence similarity.

FoxM1 is the only isoform within the M subclass of Fox proteins, and beyond the characteristic forkhead or winged-helix DNA binding domain, it does not share homology with other proteins. Based on amino acid sequence analysis, FoxM1 is most closely related to the P and O Fox subclasses, in both mouse and human (Figures 8, 9).

Transcriptional Regulation of *Foxm1*

Currently, little is known regarding transcriptional regulation of *Foxm1*. The same group that cloned Trident published the only *FOXM1* promoter analysis to date (Korver *et al.*, 1997b). This group reported that a 0.3 kb (-296 to +60 bp) fragment of the *FOXM1* promoter was activated during S-phase compared to G_0, and that fragments extending to -437 bp, -1411 bp, and -2436 bp upstream of the transcription start site also exhibited activation but to a lesser extent. Furthermore, they identified a putative E-box at -49 to -44 bp but did not find a TATA box. Teh *et al*. identified FOXM1 as a downstream target of Sonic hedgehog (SHH) and Gli1 signaling, and although a direct transcriptional link was not established, a putative Gli response element was identified at

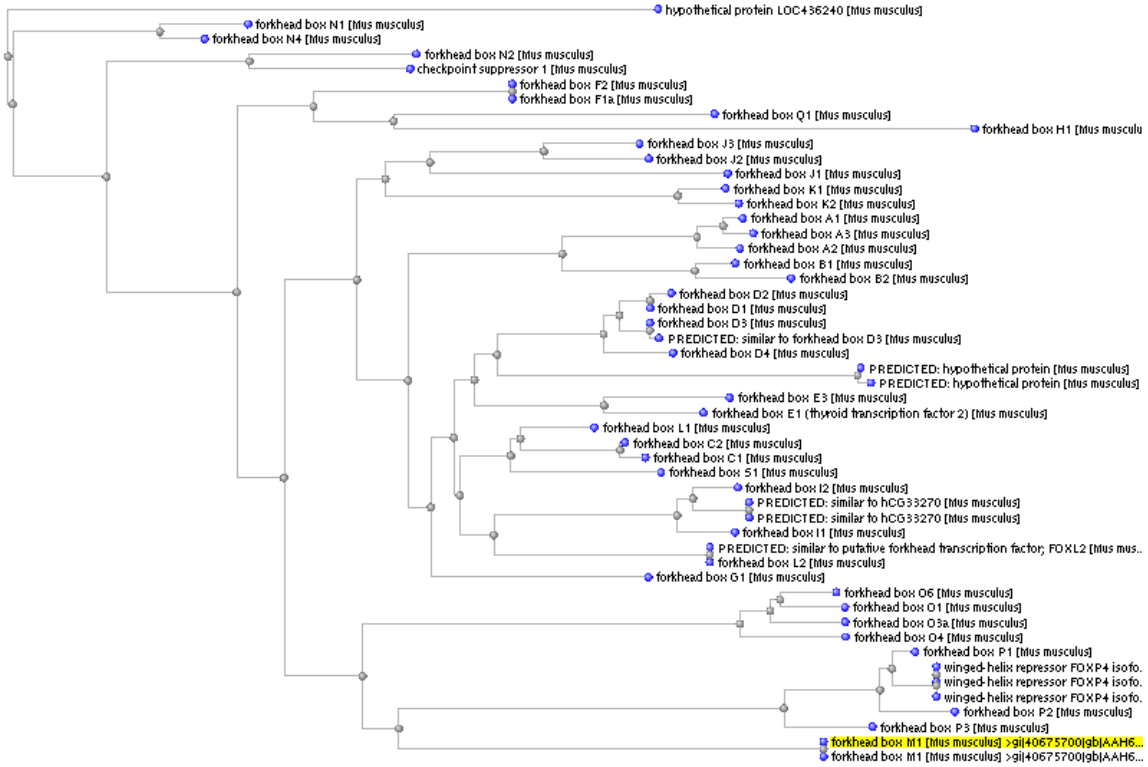

Figure 8. NCBI BLAST Tree for mouse FoxM1 protein. The basic local alignment search tool (BLAST) on the National Center for Biotechnology Information (NCBI) website was queried for the murine FoxM1 protein sequence (NP_032047.4) against the mouse refseq_protein database using pairwise alignment. The results are displayed in a rectangular arrangement, and they depict the relative sequence similarities between FoxM1 and other murine proteins. (rid7WT536TT012, performed on July 16, 2008)

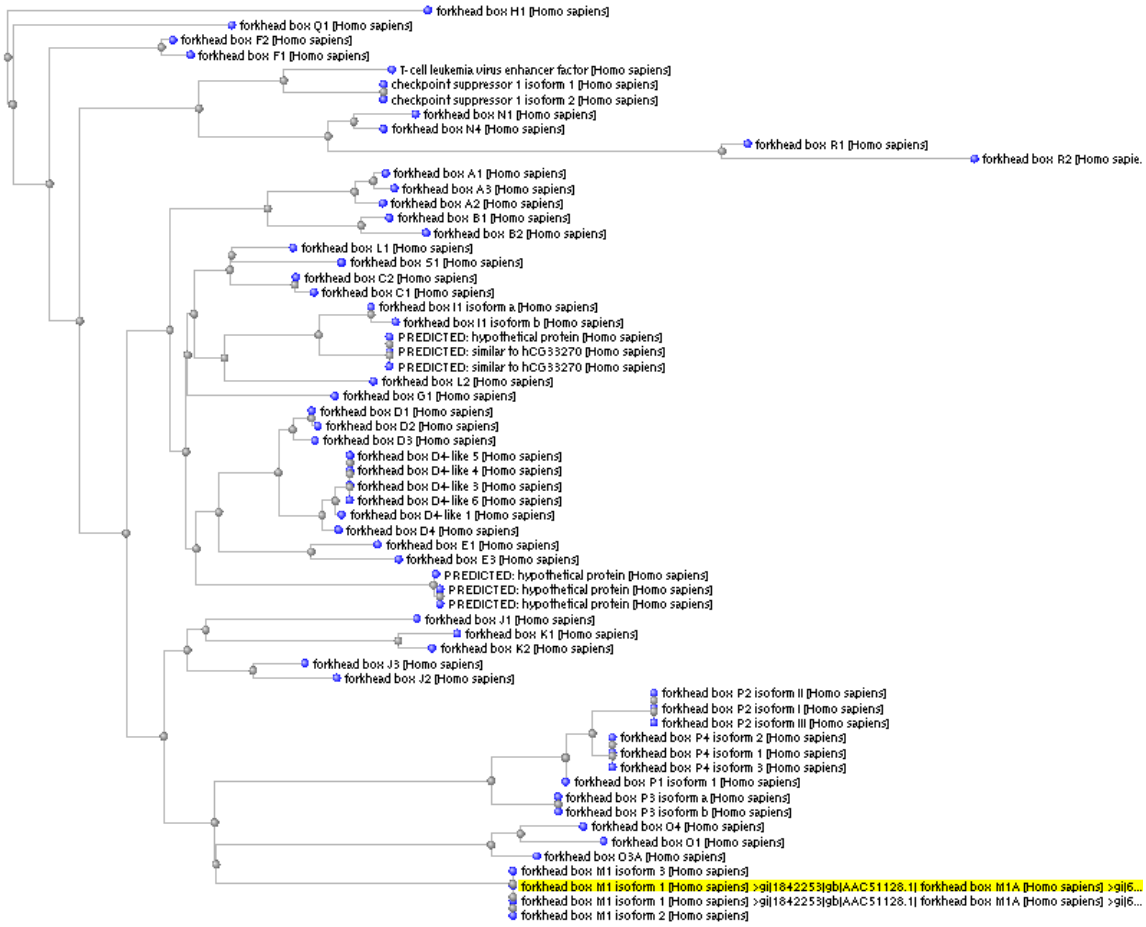

Figure 9. NCBI BLAST Tree for human FOXM1 protein. The BLAST tool on the NCBI website was queried for the human FOXM1 protein sequence (NP_973731) against the human refseq_protein database using pairwise alignment. The results are displayed in a rectangular arrangement, and they depict the relative sequence similarities between FOXM1 and other human proteins. (rid7WTMNA35015, performed on July 16, 2008)

-230 bp upstream of the transcription start site within the *FOXM1* promoter (Teh *et al.*, 2002).

Post-translational Regulation of FoxM1

FoxM1 is larger than most Fox proteins (predicted molecular weight is 83.3 kDa), and it contains unique domains and phosphorylation sites, primarily within the C-terminal transactivation domain, many of which have not yet been fully-characterized (Figure 7). These include multiple serine/threonine phosphorylation sites for Cdk/Cyclin complexes and Mitogen-activated protein kinases (MAPKs). A nuclear localization signal (NLS) is located near the DNA binding domain, and it has been shown that serine phosphorylation of FOXM1B by ERK1/2 near the NLS may mediate its nuclear localization and enhanced activity in response to MAPK signaling (Ma *et al.*, 2005). Importantly, activity of FOXM1C was not enhanced in response to MAPK signaling, as this isoform lacks the phosphorylation site due to alternative splicing of exon 6. An additional ERK1/2 serine phosphorylation site is located within the C terminus of FoxM1 near a Cdk/Cyclin complex interaction domain, and mutation of this residue impairs FoxM1 activity, possibly by interfering with this important protein-protein interaction. The domain by which FoxM1 interacts with Cdk/Cyclin complexes contains an LXL sequence, which is required for binding (Major *et al.*, 2004). Once bound to FoxM1, Cdks (specifically Cdk2 complexed with Cyclin E and Cdk1 complexed with Cyclin B) can phosphorylate specific serine/threonine residues within the transcription activation domain, which is required for recruitment of the p300/CREB-binding protein (CBP) transcriptional coactivators and for FoxM1 transcriptional activity. As Cdk2/Cyclin E are present during

the G_1/S transition and Cdk1/Cyclin B are present during the G_2/M transition (Dzau *et al.*, 2002), FoxM1 phosphorylation is maintained as the cell progresses through the cell cycle.

Interestingly, the Cdk inhibitor $p27^{Kip1}$ can be found in the Cdk/Cyclin/FoxM1 complex, where it indirectly inhibits FoxM1 transcriptional activity, likely by reducing Cdk-mediated phosphorylation of FoxM1 (Kalinichenko *et al.*, 2004). FoxM1 is also inhibited by the tumor suppressor $p19^{ARF}$, which binds to FoxM1 via a 19 amino acid sequence ($p19^{ARF26-44}$). Indeed, this peptide alone can inhibit FoxM1 activity both *in vitro* and *in vivo*, due at least in part to its ability to target FoxM1 to the nucleolus (Kalinichenko *et al.*, 2004; Gusarova *et al.*, 2007). In addition, FoxM1 has been shown to interact with the Rb protein, particularly during G_1, but hyper-phosphorylation of Rb disrupts this interaction (Major *et al.*, 2004), suggesting the FoxM1 may be negatively regulated by Rb. This hypothesis is supported by the finding that over-expression of the human papilloma virus type 16 E7 protein, which inhibits Rb and targets it for degradation in addition to binding to FoxM1 directly, enhanced FoxM1 activity in a reporter assay (Luscher-Firzlaff *et al.*, 1999).

FoxM1 is also negatively regulated by proteosome-mediated degradation (Park HJ *et al.*, 2008a). During late mitosis and early G_1, FoxM1 is found in a complex with the Anaphase-promoting complex/cyclosome (APC/C) E3 ubiquitin ligase and its adaptor Cdc20 homolog 1 (Cdh1). The N terminus of FoxM1 contains two "destruction" sequences (D-boxes; RXXL) and a KEN sequence (KEN box), which interact with Cdh1 and are required for FoxM1 degradation. Such negative regulation of FoxM1 is necessary in order to prevent inappropriate re-entry into S phase.

There is also evidence that the N terminus of FoxM1 acts as an auto-inhibitory domain by interacting with the C-terminal transactivation domain (Park HJ *et al.*, 2008b; Laoukili *et al.*, 2008). Deletion of the N terminal domain (amino acids 1-232) resulted in prolonged and increased transcriptional activity, even in the absence of MAPK signaling or Cdk/Cyclin complex binding. However, activated Cdk/Cyclin complexes disrupted the interaction between the N and C termini. These results suggest that phosphorylation of the C terminus by Cdk/Cyclin complexes releases the C-terminal transactivation domain from autoinhibition, providing a possible mechanism by which FoxM1 is kept inactive during initiation of the G_1/S transition.

FoxM1 Targets

Once within the nucleus and properly activated, FoxM1 drives transcription of various genes that coordinate the G_1/S and G_2/M transitions, as well as karyokinesis and cytokinesis (Figure 10) (Costa, 2005; Laoukili *et al.*, 2007). During the G_1/S transition, the pocket proteins Rb, p107, and p130 are phosphorylated by Cdk4 and Cdk6, both of which must bind D-type Cyclins in order to be active (Massague, 2004). Phosphorylation of the pocket proteins causes dissociation from the E2F transcription factor, allowing E2F to activate transcription of S phase-promoting genes, including *Cyclin E*. Cyclin E complexes with Cdk2, which is required for hyperphosphorylation of Rb. As mentioned before, Rb hyperphosphorylation disrupts its interaction with FoxM1, likely releasing FoxM1 from inhibition. In agreement with this theory, during the G_1/S transition, FoxM1 is required for transcription of Cell division cycle 25 homolog A (Cdc25A), which dephosphorylates and activates Cdk2 (Wang *et al.*, 2005). Cdk2 not only

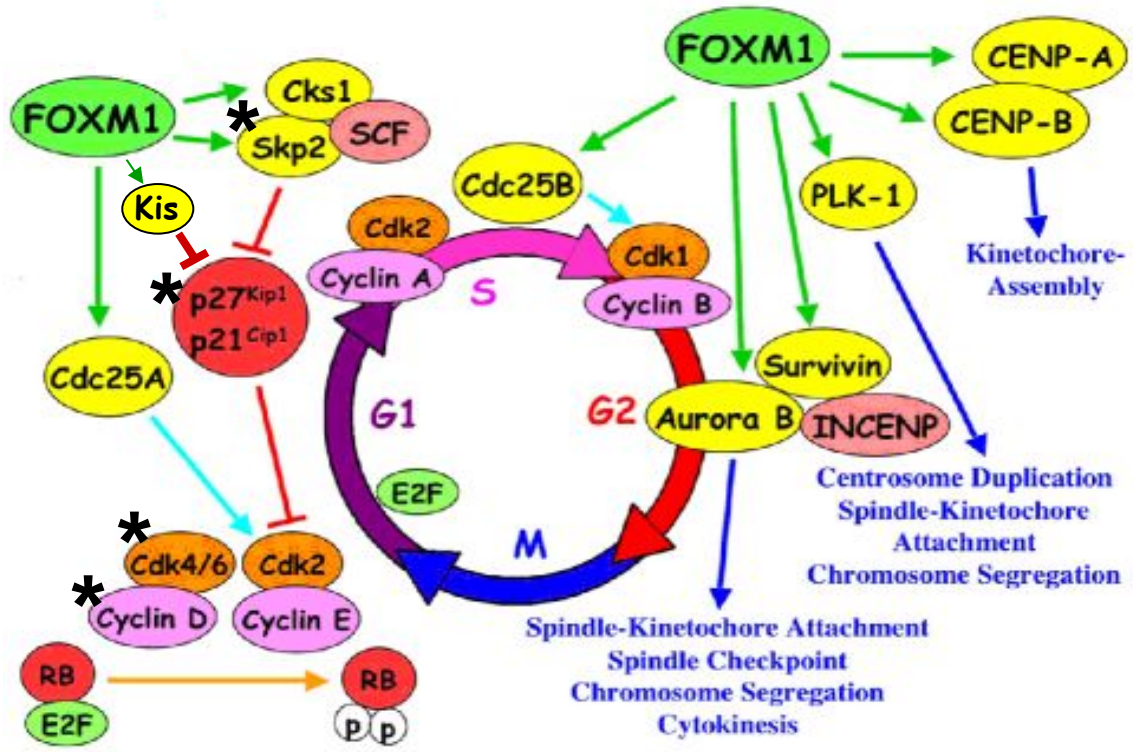

Figure 10. FoxM1 transcriptional targets are involved in cell cycle regulation. This diagram depicts key cell cycle regulators. Transcription factors, including FoxM1, are shown in green, Cyclins are shown in purple, Cdks are shown in orange, cell cycle inhibitors are shown in red, and FoxM1 transcriptional targets are shown in yellow. FoxM1 targets regulate the G_1/S transition, G_2/M transition, karyokinesis, and cyctokinesis. Proteins that have been shown to play an important role in β cell proliferation are designated with an asterisk (*) . Figure is adapted from Wang *et al.* (2005).

hyperphosphorylates Rb but also phosphorylates the Cdk inhibitor (CDKI) proteins $p21^{Cip1}$ and $p27^{Kip1}$, targeting them for recognition by the Skp1-Cullin1-F box (SCF) ubiquitin ligase complex, which initiates their proteosome-mediated degradation (Sheaff *et al.*, 1997; Carrano *et al.*, 1999; Montagnoli *et al.*, 1999; Bornstein *et al.*, 2003). The SCF ubiquitin ligase complex is composed of three proteins, two of which, Skp2 and Cdk subunit 1 (Cks1), confer substrate specificity to the SCF complex and are direct transcriptional targets of FoxM1 (Wang *et al.*, 2005). FoxM1 also indirectly regulates $p27^{Kip1}$ via direct transcriptional activation of Kinase interacting stathmin (Kis), a nuclear kinase that phosphorylates $p27^{Kip1}$ and promotes its nuclear export (Petrovic *et al.*, 2008). There is conflicting evidence regarding whether FoxM1 activates Cyclin D1 expression (Leung *et al.*, 2001; Wang *et al.*, 2001). Therefore, it is unclear whether initiation of the G_1/S transition involves FoxM1; however, progression into S phase does require FoxM1.

During the G_2/M transition, FoxM1 directly activates transcription of Cdc25B, which dephosphorylates and activates Cdk1 (Wang *et al.*, 2005). Cdk1 activity also depends on its binding to Cyclin B1, another direct transcriptional target of FoxM1 (Leung *et al.*, 2001; Wang *et al.*, 2005). The Cdk1/Cyclin B1 complex was previously referred to as the M-phase promoting factor (MPF) (Fung and Poon, 2005), and as discussed, this complex phosphorylates and activates FoxM1 (Major *et al.*, 2004), thus forming a positive feedback loop. FoxM1 also directly activates transcription of Polo-like kinase 1 (Plk1), Aurora B kinase, Centromere protein A (Cenp-A), Cenp-B, Cenp-F, and Survivin (Birc5) (Laoukili *et al.*, 2005; Wang *et al.*, 2005). Plk1 is necessary for centrosome duplication and, with Aurora B kinase, mediates attachment of the microtubule spindles to kinetochores (Barr *et al.*, 2004). Plk1 also phosphorylates and

activates Cdc25C, which dephosphorylates and activates Cdk1. Survivin regulates Aurora B kinase centromere localization, while Cenp-A, Cenp-B, and Cenp-F are involved in kinetochore assembly and chromosome segregation (Howman *et al.*, 2000; Laoukili *et al.*, 2005). FoxM1 also activates transcription of the proliferation-associated genes C-myc, C-fos, Hsp70, and Histone H2B/a (Wierstra and Alves, 2006; Wierstra and Alves, 2008).

Other transcriptional targets of FoxM1 that are not directly involved in cell cycle regulation include Estrogen receptor α (ERα) (Madureira *et al.*, 2006), Laminin α4 (Lama4) (Kim *et al.*, 2005), and c-Jun N-terminal kinase 1 (Jnk1) (Wang *et al.*, 2008a). Madureira *et al*. found that FOXM1 expression correlated with ERα expression in breast cancer cell lines and that FOXM1 activated the *ERα* promoter in reporter assays (Madureira *et al.*, 2006). In addition, they found that FOXM1 directly bound to forkhead response elements (FHREs) within the proximal region of the *ERα* promoter *in vivo*. Interestingly, FOXM1 was found to interact *in vivo* with FOXO3a, a previously-identified transcriptional activator of ERα. However, Laoukili *et al*. found that over-expression of FoxO3a could not rescue expression of Plk1, Cyclin B1, or Cenp-F in *Foxm1*$^{-/-}$ mouse embryonic fibroblasts (MEFs) (Laoukili *et al.*, 2005).

Kim *et al*. found that mice with a global deletion of FoxM1 (*Foxm1*$^{-/-}$) exhibit defects in development of the pulmonary vasculature (Kim *et al.*, 2005). They attributed these defects to, among other things, alterations in TGF-β signaling and laminin expression. In particular, they found that FoxM1 activated the *Lama4* promoter in reporter assays, identified two putative FoxM1 binding sites within the *Lama4* promoter, and determined that endogenous FoxM1 could bind to the *Lama4* promoter.

Wang *et al*. found that FoxM1 directly activates transcription of Jnk1 in the osteosarcoma cell line U2OS (Wang *et al.*, 2008a). Activation/phosphorylation of Jnk1 is associated with many cellular processes, including proliferation, due to the variety of transcription factors that it phosphorylates. Interestingly, Wang *et al*. found that over-expression of Jnk1 in *Foxm1*-depleted U2OS cells rescued the cells from G_1/S, but not G_2/M, blockade. Furthermore, they found that Jnk1 was required downstream of FoxM1 for anchorage-independent growth, migration, and invasion of U2OS cells *in vitro*, at least partially via expression of matrix metalloproteinases (MMPs) 2 and 9. Thus, FoxM1 may play roles in other cellular processes in addition to proliferation.

FoxM1 Null Mice

As previously discussed, FoxM1 is broadly expressed during embryogenesis and is restricted to tissues with high rates of cell turnover in the adult, in accordance with its role in regulating cell proliferation. Two groups have generated mice with global disruption of the *Foxm1* allele (Korver *et al.*, 1998; Krupczak-Hollis *et al.*, 2004). Korver *et al*. generated mice with targeted insertion of a *Phosphoglycerate kinase* (*PGK*)-*Neomycin resistance* (*Neo*) cassette into the fourth exon of *Foxm1* ($Foxm1^{Neo}$), which codes for the DNA binding domain (Figure 11A). In contrast, Krupczak-Hollis *et al*. generated mice with deletion of exons 4-8, which code for the DNA binding and transactivation domains (Figure 12A). These mice were generated by crossing mice with loxP sequences inserted into the third intron and the 3' UTR of the *Foxm1* locus to mice expressing a ubiquitous Cre recombinase (*E2A-Cre*). Cre-mediated recombination of the floxed *Foxm1* alleles within the germline allowed for propagation of a mouse line with a

A

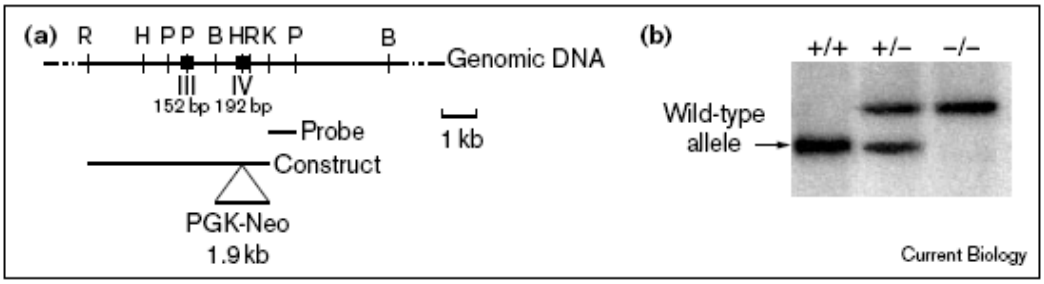

B

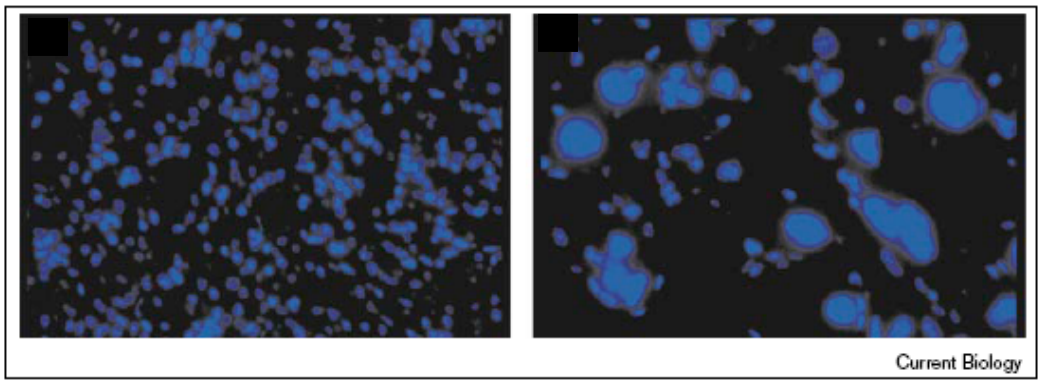

Figure 11. *Foxm1*$^{Neo/Neo}$ mice. (A) A FoxM1 hypomorph was generated by inserting a PGK-Neo cassette into exon 4, which codes for the DNA binding domain. **(B)** These mice exhibit variable neonatal lethality and polyploid hepatocytes and cardiomyocytes. A DAPI-labeled section from a neonatal *Foxm1*$^{Neo/+}$ heart is shown on the left, and from a *Foxm1*$^{Neo/Neo}$ heart on the right. Figure is adapted from Korver *et al*. (1998).

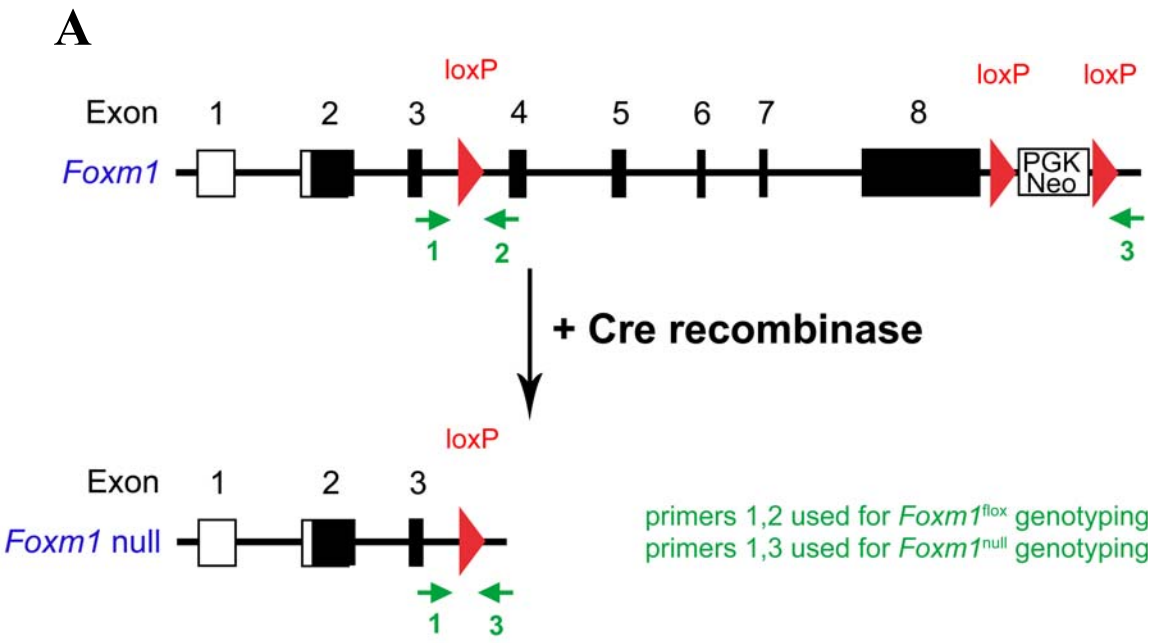

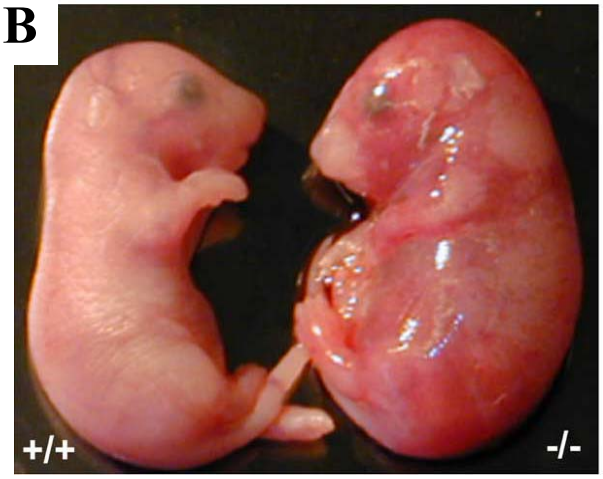

Figure 12. *Foxm1*$^{-/-}$ mice. (A) A *Foxm1*^{flox} allele was generated by inserting loxP sequences within the third intron and in the 3' untranslated region, flanking a PGK-Neo cassette. Deletion of the sequence between the loxP sites is accomplished by Cre recombinase driven by either a global (EIIA) or hepatoblast-specific (AFP) promoter. Deletion of the floxed region of *Foxm1* results in a null allele. **(B)** Global *Foxm1*$^{-/-}$ mice exhibit embryonic lethality with edema and hemorrhaging. Shown here are e17.5 embryos. Figure is adapted from Krupczsk-Hollis *et al*. (2004).

global functionally null *Foxm1* allele (*Foxm1*^{null}). Comparison of these two lines suggests that the *Foxm1*^{Neo} allele acts as a hypomorph, rather than as a true null.

Surprisingly, global deletion of *Foxm1* in mice (*Foxm1*$^{-/-}$) does not have catastrophic results, as gross embryological morphology is unaffected (Figure 12B) (Krupczak-Hollis *et al.*, 2004). However, *Foxm1* deletion does cause late embryonic lethality (between e13.5 and e18.5) due to hepatic and cardiac defects, with severe edema and hemorrhaging. These embryos exhibited significant reductions in hepatoblast proliferation and number, but gross liver size was unchanged due to hepatoblast hypertrophy. Part of the hypertrophic phenotype can be explained by the presence of polyploid hepatoblasts. Polyploid cardiomyocytes were also observed (Figure 11B) (Korver *et al.*, 1998), which was likely due to endoreduplication (DNA synthesis without subsequent cytokinesis) (Wonsey and Follettie, 2005). Furthermore, *Foxm1*$^{-/-}$ embryos displayed reduced proliferation of mesenchymal and vascular smooth muscle cells and defective vasculogenesis within the lungs due to impaired differentiation of mesenchymal cells into endothelial cells (Kim *et al.*, 2005), in addition to defects in development of intra-hepatic biliary ducts, hepatic vessels, hepatic sinusoids, and the gall bladder (Krupczak-Hollis *et al.*, 2004).

Consistent with the proliferation and polyploid phenotypes observed in *Foxm1*$^{-/-}$ embryos, MEFs collected from these embryos exhibited delayed entry into G_2, and those cells that did enter mitosis exhibited inappropriate chromosome segregation, resulting in frequent aneuploidy and mitotic failure (Laoukili *et al.*, 2005). These findings were associated with reduced expression of Cyclin A2, Cyclin B1, Cyclin B2, Plk1, Aurora B kinase, Cdc25B, and Cenp-F in *Foxm1*$^{-/-}$ MEFs compared to wild-type (WT) MEFs.

Mouse Models of Altered FoxM1 Expression in the Liver

Early deletion of *Foxm1* specifically within hepatoblasts using a Cre-lox system with an α-fetoprotein (Afp) enhancer driving Cre recombinase expression (*Foxm1*$^{flox/flox}$;*Afp-Cre*) yielded similar lethality as observed in global *Foxm1* null embryos, suggesting that the liver defects in the *Foxm1*$^{-/-}$ embryos were responsible for the lethal phenotype (Krupczak-Hollis *et al.*, 2004). Additionally, these embryos exhibited polyploid hepatoblasts and impaired development of intra-hepatic biliary ducts. However, hepatoblast proliferation and number were less-dramatically reduced in these embryos than in *Foxm1*$^{-/-}$ embryos, suggesting that *Foxm1* deletion is incomplete in the *Foxm1*$^{flox/flox}$;*Afp-Cre* mouse model. Thus, FoxM1 is necessary for proliferation of hepatoblasts, which are bipotential cells that can differentiate into hepatocytes or biliary epithelial cells.

FoxM1 is also required for proliferation of adult hepatocytes, evidenced by *Foxm1*$^{flox/flox}$;*Albumin-Cre* mice, which develop normally but exhibit significant reductions in hepatocyte proliferation and liver regeneration following partial hepatectomy (PHx) (Wang *et al.*, 2002a). These mice also displayed hepatocyte hypertrophy following PHx, which compensated for the reduced amounts of proliferation, resulting in regeneration of gross liver size similar to that of *Foxm1*$^{flox/flox}$ Control mice. These findings were associated with increased nuclear p21^{Cip1} expression, reduced expression of Cdc25A, Cdc25B, and Cyclin B1, and reduced hyperphosphorylation of Rb, but no changes in Cyclin D (*Ccnd*) or Cyclin E (*Ccne*) transcripts.

As FoxM1 is required for proliferation in some cell types and is highly-expressed in embryonic cells and most, if not all, cancer cell lines studied to date, several groups

have induced transgenic over-expression of *FOXM1* in order to study its role in aging and cellular transformation. Ye *et al*. found that transgenic liver-specific over-expression of *FOXM1c* (*TTR-FOXM1c*) accelerated hepatocyte proliferation following PHx (Ye *et al.*, 1999). However, the peak amount of hepatocyte proliferation was similar to that observed in WT, and hepatocyte proliferation under normal conditions was not affected by over-expression of *FOXM1c*, likely due to the fact that FOXM1 remained localized to the cytoplasm unless stimulated by PHx. These data are consistent with post-translational modification of FoxM1 being required for nuclear localization, and they suggest that the amount of endogenous FoxM1 limits the timeframe in which replication can occur, as increasing the expression of FoxM1 allowed for earlier nuclear localization and proliferation. Interestingly, Wang *et al*. found that over-expression of *FOXM1c*, either by transgenic (*TTR-FOXM1c*) or adenoviral (Ad-*FOXM1c*) means, reversed the normal age-related decrease in hepatocyte proliferation (Wang *et al.*, 2001; Wang *et al.*, 2002b). Using either means of FOXM1C over-expression, this group observed an increase in the absolute amount of proliferation in old (12 month old) mice following PHx to levels similar to those observed in young (2 month old) mice after the operation. Likewise, treatment with human GH (hGH), alone or in conjunction with PHx, induced FoxM1 expression and stimulated hepatocyte proliferation in old mice to levels comparable to those observed in young, untreated mice (Krupczak-Hollis *et al.*, 2003). Interestingly, even without the stimulus of PHx, treatment with hGH dramatically stimulated hepatocyte proliferation to a similar extent in young and old mice, in comparison to untreated mice. Importantly, such results were not observed in mice with hepatocyte-specific deletion of *Foxm1* (*Foxm1*$^{flox/flox}$;*Albumin-Cre*), indicating that

FoxM1 acts downstream of the GH signaling pathway to mediate hepatocyte proliferation.

Importantly, over-expression of FOXM1C within the liver (*TTR-FOXM1c*) was not found to be associated with hepatocellular carcinoma (HCC) progression, but was associated with increased proliferation of pre-neoplastic and early neoplastic lesions induced by diethylnitrosamine/phenobarbital (DEN/PB), resulting in increased size of these lesions (Kalinina *et al.*, 2003). However, FoxM1 was required for formation of hepatic adenomas and HCC, as *Foxm1*$^{flox/flox}$;*Albumin-Cre* mice exhibited no tumor formation, associated with reduced hepatocyte proliferation but increased hepatocyte size (hypertrophy), in response to DEN/PB treatment in comparison to *Foxm1*$^{flox/flox}$ Control mice. These results suggest that FoxM1 is necessary but not sufficient for initiation and progression of HCC (Kalinichenko *et al.*, 2004).

Mouse Models of Altered FoxM1 Expression in the Lung

FoxM1 has also been shown to play an important role within the lung. Kalinichenko *et al*. exposed transgenic mice that ubiquitously over-expressed FOXM1C driven by a fragment of the reverse orientation splice acceptor (Rosa) 26 promoter (*Rosa26-FOXM1c*) to butylated hydroxytoluene, a chemical known to induce lung injury that initiates within the epithelial population and then affects the endothelial and smooth muscle cells (Kalinichenko *et al.*, 2003). After exposure, these mice exhibited accelerated and enhanced proliferation of all of these cell types within the lungs in comparison to WT mice, and these changes were associated with earlier nuclear

localization of FoxM1, increased expression of Cyclin A2, Cyclin B1, Cyclin E, Cyclin F, and Cdk1, and decreased expression of $p21^{Cip1}$.

As discussed before, endothelial cell differentiation and smooth muscle cell proliferation were impaired within the lungs of global *Foxm1*$^{-/-}$ embryos (Kim *et al.*, 2005). However, these embryos died prior to the normal timepoint of completion of pulmonary vasculogenesis. Thus, mice with endothelial cell-specific deletion of *Foxm1* (*Foxm1*$^{flox/flox}$;*Tie2-Cre*) were used to study the role of FoxM1 in mature endothelial cells (Zhao *et al.*, 2006). These mice displayed no phenotype at baseline, indicating that FoxM1 is not required for normal endothelial cell turnover. However, when these mice were injected with lipopolysaccharide (LPS), a potent mediator of inflammation that induces microvascular injury within the lungs, they exhibited reduced endothelial cell proliferation, impaired endothelial barrier repair, increased vascular permeability, and increased mortality. These findings were associated with reduced expression of Cyclin B1 and Cdc25C, as well as increased expression of $p27^{Kip1}$. Additionally, LPS injection into WT mice resulted in a significant increase in *Foxm1* expression within the lungs, indicating that FoxM1 is normally up-regulated following microvascular injury and that this up-regulation is necessary for normal microvascular repair.

FoxM1 has also been shown to play an important role in lung tumorigenesis. In contrast to the results observed within the liver (Kalinina *et al.*, 2003), *Rosa26-FOXM1c* mice exposed to the tumor-inducing combination of 3-methylcholanthrene and butylated hydroxytoluene did exhibit enhanced lung adenoma progression compared to WT mice (Wang *et al.*, 2008b). The adenomas found within the lungs of *Rosa26-FOXM1c* mice were of greater number, size, and proliferative index than those found in WT mice after

the same treatment, and they developed more quickly. However, mice with an inducible global deletion of *Foxm1* driven by the Myxovirus (influenza virus) resistance 1 promoter (*Foxm1*$^{flox/flox}$;*Mx-Cre*), which is activated by exposure to Interferon (IFN) α, IFNβ, or double-stranded (ds) RNA, exhibited reduced number, size, and proliferative index of lung tumors after treatment with urethane than did *Foxm1*$^{flox/flox}$ Control mice after the same treatment (Kim *et al.*, 2006). Additionally, urethane treatment of *Foxm1*$^{flox/flox}$ Control mice stimulated expression FoxM1 within the pulmonary epithelium, whereas FoxM1 was undetectable in untreated *Foxm1*$^{flox/flox}$ Control pulmonary epithelium. Thus, FoxM1 expression levels clearly correlate with tumor burden in the lung.

Mouse Models of Altered FoxM1 Expression in the Colon

Similar to the lungs, FoxM1 expression levels within the colon also correlate with tumor burden. Over-expression of FOXM1C in *Rosa26-FOXM1c* mice exacerbated tumor development and progression in response to the carcinogen azoxymethane and dextran sodium sulfate (Yoshida *et al.*, 2007). These mice developed larger and more invasive tumors in greater number than those found in WT mice after the same treatment, associated with increased proliferation specifically within neoplastic lesions. Alternatively, mice with gut-specific deletion of *Foxm1* (*Foxm1*$^{flox/flox}$;*Villin-Cre*) exhibited reduced tumor development and growth after the same treatment versus *Foxm1*$^{flox/flox}$ Control mice. The neoplastic lesions that did develop in *Foxm1*$^{flox/flox}$;*Villin-Cre* mice exhibited reduced proliferation and never became invasive. Both mouse models (*Rosa26-FOXM1c* and *Foxm1*$^{flox/flox}$;*Villin-Cre*) exhibited alterations in expression of the FoxM1 targets Cyclin B1 and Survivin, as well as Cyclin A2.

Mouse Model of Altered FoxM1 Expression in the Prostate

Transgenic FOXM1C over-expression in *Rosa26-FOXM1c* mice also accelerated the progression of prostate carcinoma initiated in two mouse models of prostate cancer (Kalin *et al.*, 2006). Transgenic (Tg) adenocarcinoma of the mouse prostate (TRAMP) mice express the SV40 virus large T and small t tumor antigen oncoproteins in prostate epithelial cells, driven by the *Probasin* promoter. These proteins inactivate the tumor suppressors Rb and p53, resulting in hyperplasia, prostatic intraepithelial neoplasia, and invasive prostatic carcinoma. LADY mice express only the SV40 virus large T antigen oncoprotein driven by the same promoter and exhibit a similar progressive phenotype. Over-expression of FOXM1C on either the LADY or TRAMP background resulted in an increased propensity towards development of prostate carcinoma, as well as increased proliferation of prostatic cells within the carcinoma.

Mouse Models of Altered FoxM1 Expression in the Pancreas

One of the initial groups that identified FoxM1 (WIN) found it to be highly expressed in early embryonic pancreas, and to a progressively lesser extent in later embryonic and neonatal pancreas, with undetectable levels of expression in adult whole pancreas by northern blot analysis (Figure 13) (Yao *et al.*, 1997). Our laboratory utilized immunohistochemistry to confirm these results and to demonstrate that at all timepoints, FoxM1 is more abundant in endocrine than exocrine pancreatic cells (Figure 14A-C) (Zhang H *et al.*, 2006). Mice with a pancreas-wide deletion of *Foxm1* (*Foxm1*$^{flox/flox}$;*Pdx1*$^{5.5kb}$-*Cre*) exhibited normal pancreas development, but displayed postnatal effects of loss of FoxM1, including polyploidy of endocrine and exocrine cells,

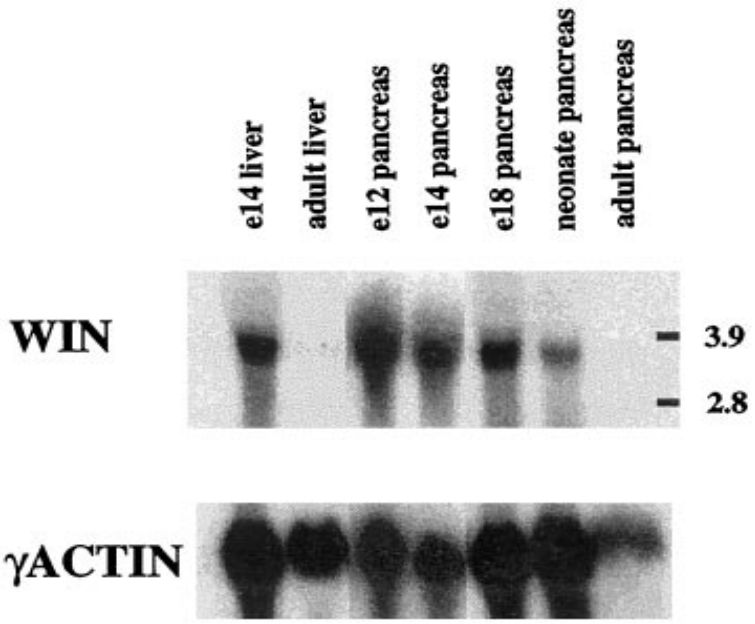

Figure 13. FoxM1 expression within the pancreas. Northern blot analysis shows that *Foxm1* (*WIN*) is expressed at high levels in embryonic liver and pancreas, but is expressed at a lower level in neonatal pancreas, and is undetectable in adult whole pancreas and liver. Figure is from Yao *et al.* (1997).

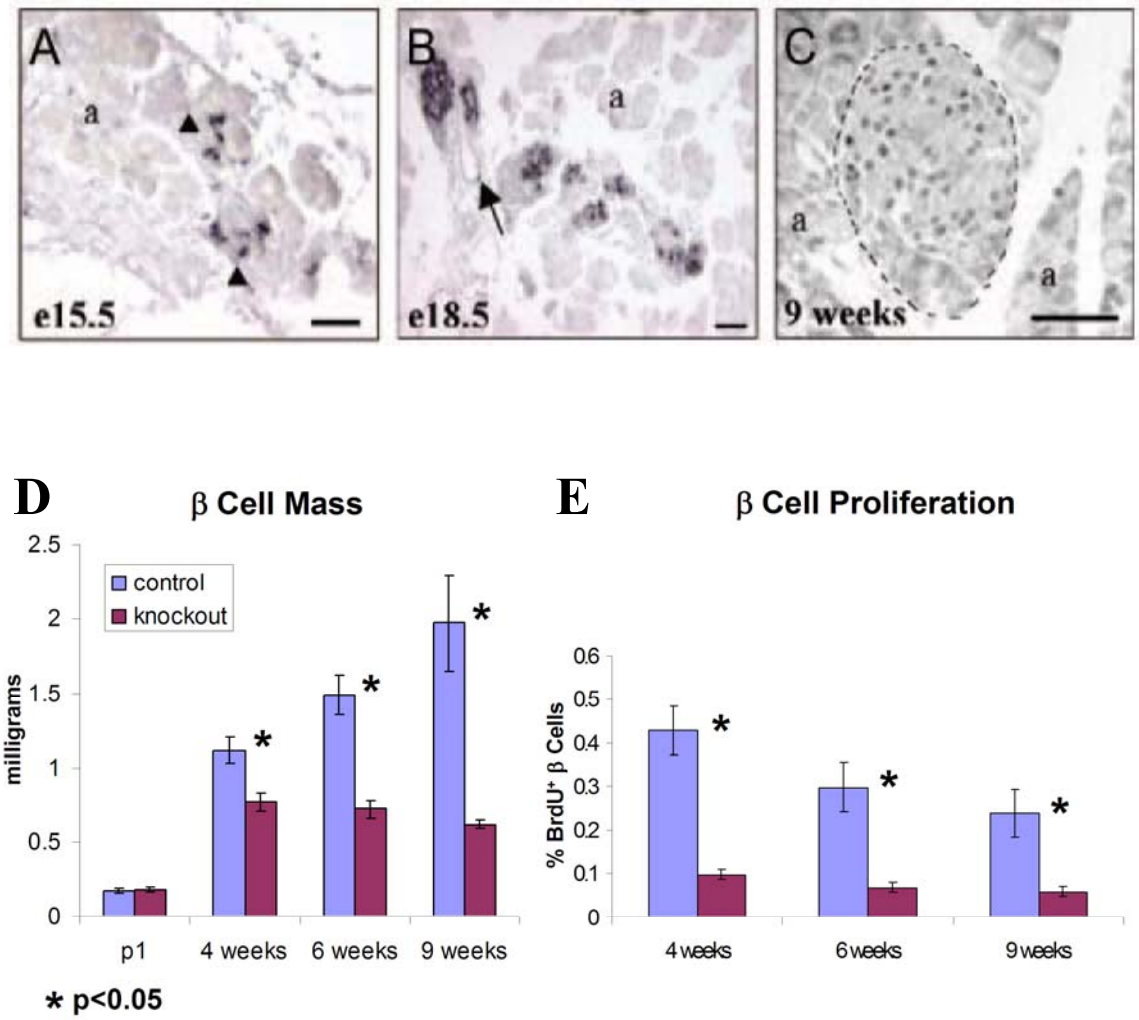

Figure 14. FoxM1 is highly expressed within the endocrine pancreas and is required for normal postnatal β cell growth and proliferation. FoxM1 protein is highly expressed within the endocrine cords (arrowheads) at e15.5 **(A)** and within the developing islets at e18.5 **(B)**. At these timepoints, FoxM1 is expressed to a lesser degree in acinar (a) and ductal (arrow) tissue. At 9 weeks of age **(C)**, FoxM1 is expressed at a low level in a subset of islet (outlined) cells, and to an even lesser extent in exocrine cells. Pancreas-wide deletion of *Foxm1* in *Foxm1*$^{flox/flox}$;*Pdx1*$^{5.5kb}$-*Cre* mice resulted in reduced growth of postnatal β cell mass **(D)** and reduced β cell proliferation **(E)** as early as 4 weeks of age. Pancreas and β cell mass development during embryogenesis were not impaired. Figure is adapted from Zhang *et al.* (2006).

reduced β cell mass (Figure 14D), reduced islet size, decreased pancreatic insulin content and reduced β cell proliferation (Figure 14E). These β cell effects were associated with increased nuclear $p27^{Kip1}$ and evidence of β cell senescence, and they resulted in a progressive diabetic phenotype specifically within male *Foxm1*$^{flox/flox}$;*Pdx1*$^{5.5kb}$-*Cre* mice. Thus, FoxM1 is required for normal postnatal growth of β cell mass and normal β cell turnover in the adult mouse.

Therapeutic Implications of FOXM1 Modification

As the above studies indicate, FoxM1 is involved in the processes of development, regeneration, aging, and tumorigenesis. Thus, it is a highly desirable target for clinical manipulation of these processes. However, these studies also highlight the importance of balancing FoxM1's beneficial and detrimental effects. Aberrantly high expression of FOXM1 is associated with many human cancers, including HCC (Okabe *et al.*, 2001), intrahepatic cholangiocarcinoma (Obama *et al.*, 2005), colorectal carcinoma (Douard *et al.*, 2006), basal cell carcinoma (Teh *et al.*, 2002), infiltrating ductal breast carcinoma (Wonsey and Follettie, 2005), and anaplastic astrocytoma and glioblastoma (van den Boom *et al.*, 2003; Liu *et al.*, 2006). A meta-analysis approach also identified FoxM1 as being up-regulated in tumors of the bladder, cervix, kidney, ovary, testis, pancreas, prostate, small intestine, stomach, trachea, and uterus (Pilarsky *et al.*, 2004). These data, combined with the findings that deletion of *Foxm1* protects mice against various forms of cancer formation and progression makes down-regulating FOXM1 expression and/or inhibiting its activity a potential treatment for multiple human cancers.

Three potentially therapeutic inhibitors of FoxM1 that have been identified are the $p19^{ARF26-44}$ peptide (Kalinichenko *et al.*, 2004; Gusarova *et al.*, 2007) and the thiazole antibiotics Siomycin A and thiostrepton (Radhakrishnan *et al.*, 2006; Gartel, 2007; Kwok *et al.*, 2008). Siomycin A and thiostrepton were identified using a high-throughput screen looking for agents that changed FoxM1 activity. In addition to inhibiting FoxM1 activity, these compounds also inhibited FoxM1 expression, as FoxM1 is involved in a positive autoregulatory loop. Importantly, both Siomycin A and thiostrepton specifically inhibited growth and stimulated apoptosis of cancer cell lines. $p19^{ARF}$ is an endogenous tumor suppressor, so named for its size (19 kDa) and the fact that it is encoded by an alternative reading frame within the *ARF/INK4a* locus that also encodes the CDKI $p16^{INK4a}$, reviewed in (Costa *et al.*, 2005). $p19^{ARF}$ is normally up-regulated in response to tumorigenic stimuli, and it functions to stabilize the p53 tumor suppressor and inhibit the functions of E2F, c-Myc, and FoxM1. However, $p19^{ARF}$ is silenced in many human cancers. Gusarova *et al*. successfully administered $p19^{ARF26-44}$ peptide, the portion required for its interaction with FoxM1, to mice with HCC and reduced their tumor burden, associated with reduced tumor cell proliferation, impaired angiogenesis, and increased tumor cell apoptosis (Gusarova *et al.*, 2007). As these effects were specific to HCC areas but not adjacent normal areas, this study indicates that whole-body administration of $p19^{ARF26-44}$ peptide can be used to specifically treat tumors. Additionally, these results highlight the two primary therapeutic effects of FoxM1 inhibitors: reducing proliferation of cancer cells and stimulating their apoptosis via mitotic catastrophe (Wonsey and Follettie, 2005).

Despite the concerns regarding tumorigenecity, up-regulation of FoxM1 expression or activity is of interest for enhancing tissue regeneration and preventing/reversing the aging process. In fact, FOXM1 is significantly down-regulated in a human disorder of premature aging termed Hutchinson-Gilford progeria (Ly *et al.*, 2000), and reduced FoxM1 expression with age has been described in multiple tissues. Over-expression of FoxM1 within the liver has been shown to reverse age-associated reductions in proliferation (Wang *et al.*, 2002a; Wang *et al.*, 2002b), and it is likely that FoxM1 would have such an effect in other tissues as well. However, because of the complexity of FoxM1's post-translational modifications that are required for both its nuclear localization and activation, it is clear that mere over-expression of FoxM1 is not sufficient to induce dramatic changes in cellular proliferation.

Overview and Aims of Dissertation

Previous studies in our laboratory showed that FoxM1 is highly expressed within pancreatic endocrine cells and is required for normal growth and maintenance of postnatal β cell mass via regulating postnatal β cell proliferation (Zhang H *et al.*, 2006). However, several questions remained, which this thesis sought to address. First, Zhang *et al*. showed that β cell mass at birth in *Foxm1*$^{flox/flox}$;*Pdx1*$^{5.5kb}$-*Cre* mice was comparable to that of *Foxm1*$^{flox/flox}$ Control mice (Zhang H *et al.*, 2006), but no analysis of β cell proliferation during embryogenesis was performed. Because other studies have shown that several of the factors that regulate β cell proliferation differ between embryonic and adult stages, it is possible that FoxM1 is not required during embryogenesis for β cell proliferation. Alternatively, FoxM1 could be required for embryonic β cell proliferation,

but neogenesis is able to compensate for this deficiency in *Foxm1*$^{flox/flox}$;*Pdx1*$^{5.5kb}$-*Cre* mice in order to generate a normal β cell mass by birth. Second, although Zhang *et al*. showed that *Foxm1*$^{flox/flox}$;*Pdx1*$^{5.5kb}$-*Cre* adult mice exhibited reduced β cell proliferation, it is unclear whether FoxM1 is absolutely required for β cell proliferation under all conditions, or whether only normal turnover of the β cell population relies on FoxM1. Third, because FoxM1 has been primarily described as a regulator of the cell cycle, Zhang *et al*. focused on analysis of β cell proliferation in *Foxm1*$^{flox/flox}$;*Pdx1*$^{5.5kb}$-*Cre* mice, but it is unclear whether the other processes that contribute to β cell mass are also affected by loss of FoxM1.

To address these questions, this thesis sought to determine whether FoxM1 regulated β cell proliferation and β cell mass during embryogenesis, following pancreatic injury, and in response to diet-induced obesity. Chapter II describes the methods used. Chapter III presents data regarding the role of FoxM1 in β cell proliferation, β cell size, and β cell neogenesis following 60% partial pancreatectomy (PPx) using *Foxm1*$^{flox/flox}$;*Pdx1*$^{5.5kb}$-*Cre* and *Rosa26-FOXM1c* mice. Chapter III also includes analyses of FoxM1's role in embryonic β cell proliferation. Chapter IV presents data regarding using a high-fat diet to induce β cell mass expansion, in order to assess the role of FoxM1 in this process. This chapter also describes preliminary studies of islet function in *Foxm1*$^{flox/flox}$;*Pdx1*$^{5.5kb}$-*Cre* mice. Chapter V presents an experimental design to assess β cell lineage labeling and β cell neogenesis following 60% PPx, as well as preliminary results regarding the use of tamoxifen in this system to activate the *Pdx1*^{PB}-*Cre*^{ERT2} fusion protein. Chapter VI describes the generation of a monoclonal

antibody against FoxM1. Conclusions, implications, and future directions for the studies described in this dissertation are presented in Chapter VII.

CHAPTER II

MATERIALS AND METHODS

Mice

Foxm1$^{flox/flox}$ mice on a mixed background (129SvJ, C57Bl/6) were generously provided by Dr. Robert H. Costa (University of Illinois at Chicago) and were described by (Wang *et al.*, 2002a). Briefly, loxP sequences were inserted within the third intron and the 3' untranslated region (UTR) of the *Foxm1* allele (Figure 12A). Thus, upon recombination by the P1 phage Cre recombinase protein, exons 4-8, which encode the DNA binding and transcription activation domains, will be deleted, yielding a null allele. Of note, a PGK-Neo cassette remains within the 3' UTR of the *Foxm1*^{flox} allele, flanked by an additional loxP sequence. Therefore, recombination can occur among 3 different loxP sequences, and complete recombination results in removal of exons 4-8 of *Foxm1* as well as the PGK-Neo cassette. For some experiments, *Foxm1*^{flox} mice were backcrossed for 8 generations to the C57Bl/6JBom strain (Taconic).

Pdx1$^{5.5kb}$*-Cre* mice (on a mixed ICR, CBA, C57Bl/6 background) were generously provided by Dr. Guoqiang Gu (Vanderbilt University) (Gu *et al.*, 2002). These mice express Cre recombinase driven by a 5.5 kb region of the *Pdx1* promoter (between the *Sal*I and *Sma*I restriction sites), which includes the endogenous *Pdx1* promoter (Figure 15A). This promoter region directs *Cre* expression throughout the endogenous *Pdx1* domain, including the antral stomach, rostral duodenum, and the entire pancreatic epithelium, as early as e10.5 (Gannon *et al.*, 2001; Stoffers *et al.*, 1999)

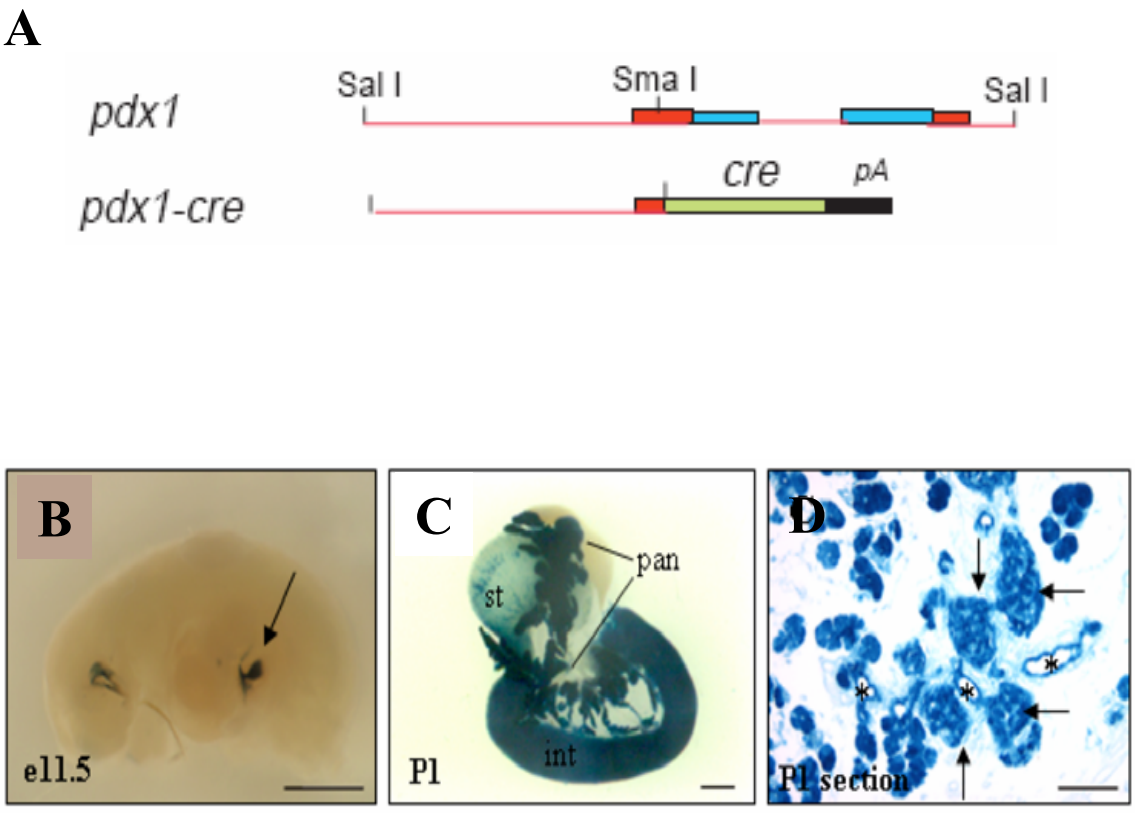

Figure 15. *Pdx1*$^{5.5kb}$*-Cre* transgene. *Pdx1*$^{5.5kb}$*-Cre* mice carry a transgene consisting of a 5.5 kb region of the *Pdx1* promoter, from the *Sal*I restriction site to the *Sma*I restriction site, placed upstream of the *Cre* coding sequence **(A)**. X-gal staining reveals that the *Pdx1*$^{5.5kb}$*-Cre* transgene mediates recombination of the Rosa26 reporter allele throughout the entire pancreatic epithelium as early as e11.5 **(B)** (arrow), as well as in the remainder of the endogenous Pdx1 expression domain, including the antral stomach and rostral duodenum **(C)** (pan = pancreas, st = stomach, int = intestine). All endodermally-derived cells within the pancreas underwent recombination **(D)** (arrows = islets, asterisks = ducts). Part A of the figure is from Gu *et al.* (2002). Parts B-D of the figure are from Zhang *et al*. (2006).

(Figure 15B-D). For some experiments, *Pdx1*$^{5.5kb}$-*Cre* mice were backcrossed for 8 generations to the C57Bl/6JBom strain (Taconic).

Pdx1^{PB}-*CreER*^{TM} mice (on a mixed B6CBAF1 background) were generated and characterized in collaboration with Dr. Chris Wright's laboratory (Vanderbilt University) (Zhang H *et al.*, 2005). These mice express a Cre recombinase-Estrogen Receptor (ER) hormone binding domain fusion protein driven by a 1 kb enhancer fragment of the *Pdx1* promoter (between the *Pst*I and *Bst*I restriction sites) and the *Hsp68* minimal promoter (Figure 16A). The hormone binding domain within this fusion protein construct has a point mutation (G525R) that makes it selective for binding to tamoxifen but not to endogenous estrogen (Littlewood *et al.*, 1995). The *Pdx1*^{PB} promoter drives expression of transgenes such as CreER^{TM} specifically within pancreatic endocrine cells as early as e11.5 (Gannon *et al.*, 2000; Gannon *et al.*, 2001; Zhang H *et al.*, 2005).

Rosa26-FOXM1c Tg mice (on a mixed FVB/N, C57Bl/6 background) were generously provided by Dr. Robert H. Costa (University of Illinois at Chicago) and were described (Kalinichenko *et al.*, 2003). These mice express a 2.7 kb region of the human *FOXM1c* cDNA (from the translation start site to the *HindIII* restriction site in the 3' UTR) driven by a -800 bp fragment of the *Rosa26* promoter (Figure 17). The construct used to generate these mice was modified from a transgene originally used for liver-specific over-expression of FOXM1C, in which a 2.7 kb region of *FOXM1c* cDNA was inserted into the second exon of a TTR minigene construct (Ye *et al.*, 1999). This construct contained a mutated *TTR* translation start site and a 3' SV40 polyadenylation sequence. Additionally, ~800 bp of the *FOXM1c* 3' UTR were deleted from this construct, which enhanced mRNA stability.

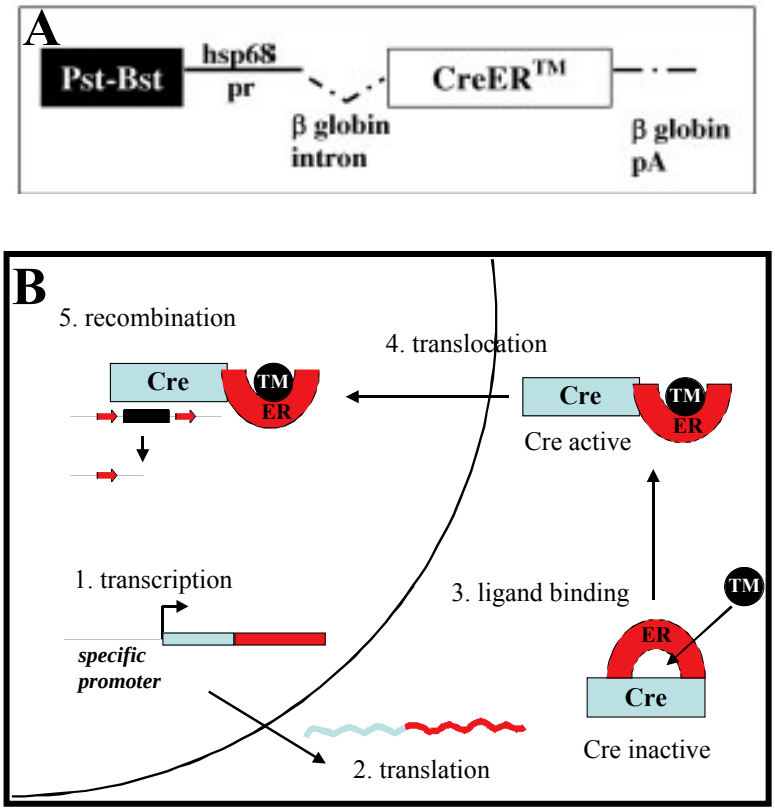

Figure 16. *Pdx1*^{PB}*-CreER*^{TM} transgene. *Pdx1*^{PB}*-CreER*^{TM} mice carry a transgene consisting of a 1 kb enhancer region of the *Pdx1* promoter, from the *Pst*I restriction site to the *Bst*I restriction site **(A)**. The CreER^{TM} fusion protein is sequestered in the cytoplasm until binding of tamoxifen stimulates its nuclear translocation, allowing for its recombinase activity **(B)**. Following tamoxifen injection, the *Pdx1*^{PB}*-CreER*^{TM} transgene mediates recombination of the *Rosa26* reporter allele specifically within islets **(C,D)**. Figure is adapted from Zhang *et al.* (2005).

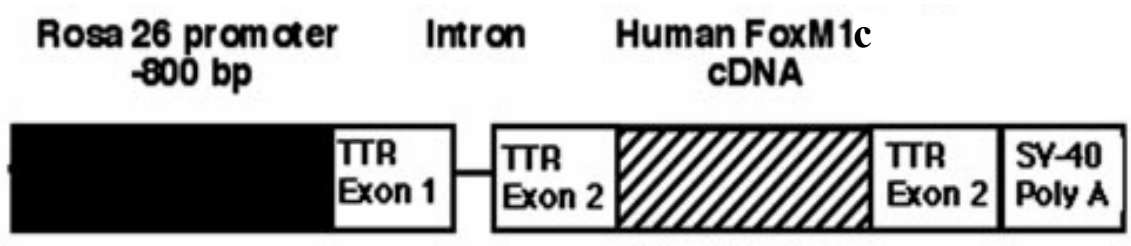

Figure 17. *Rosa26-FOXM1c* transgene. *Rosa26-FOXM1c* mice carry a transgene consisting of an 800 bp region of the *Rosa26* promoter driving expression of a TTR minigene with inserted *FOXM1c* cDNA. Figure is adapted from Kalinichenko *et al.* (2003).

Foxm1$^{+/-}$ mice (on a mixed 129SvJ, C57Bl/6 background) were provided by Dr. Robert H. Costa (University of Illinois at Chicago) and were described by (Krupczak-Hollis *et al.*, 2004). These mice were generated by crossing *Foxm1*$^{flox/flox}$ mice with *E2A-Cre* mice, which ubiquitously express Cre recombinase. Progeny with germline recombination of *Foxm1*^{flox} were propagated to generate a line of mice with a global null *Foxm1* allele (*Foxm1*$^{+/-}$).

Rosa26-LacZ reporter (R26R) mice on a C57Bl/6J background (B6.129S4-*Gt[ROSA]26Sor*^{tm1Sor}/J; The Jackson Laboratory) ubiquitously express β-galactosidase driven by the endogenous *Rosa26* promoter after Cre-mediated excision of a floxed stop cassette 5' of the *LacZ* gene (Soriano, 1999) (Figure 18).

LacZ/EGFP (Z/EG) reporter mice on a C57Bl/6J background (B6.Cg-Tg[CAG-Bgeo/GFP]21Lbe/J; The Jackson Laboratory) ubiquitously express β-galactosidase driven by a CMV enhancer/chicken β-actin promoter (Novak *et al.*, 2000) (Figure 19). Upon Cre-mediated excision of a floxed stop cassette between the *LacZ* and *EGFP* coding regions, enhanced green fluorescent protein (EGFP) is expressed in place of β-galactosidase.

For most studies, mice were fed mouse diet 5015 (LabDiet). For diet studies, mice were fed one of three diets: rodent diet 5001 (13.5% total kcal from fat, LabDiet), mouse diet 5015 (25.3% total kcal from fat, LabDiet), or high-fat/high-carbohydrate mouse diet F3282 (58.7% total kcal from fat, Bio-Serv) beginning at 4 weeks of age, after weaning, and continuing for 5-12 weeks. All mice received food and drink *ad libitum* and were on a 12 hour light-dark cycle. Z/EG mice on the C57Bl/6 background had reduced viability and required additional time prior to weaning. All mouse studies were

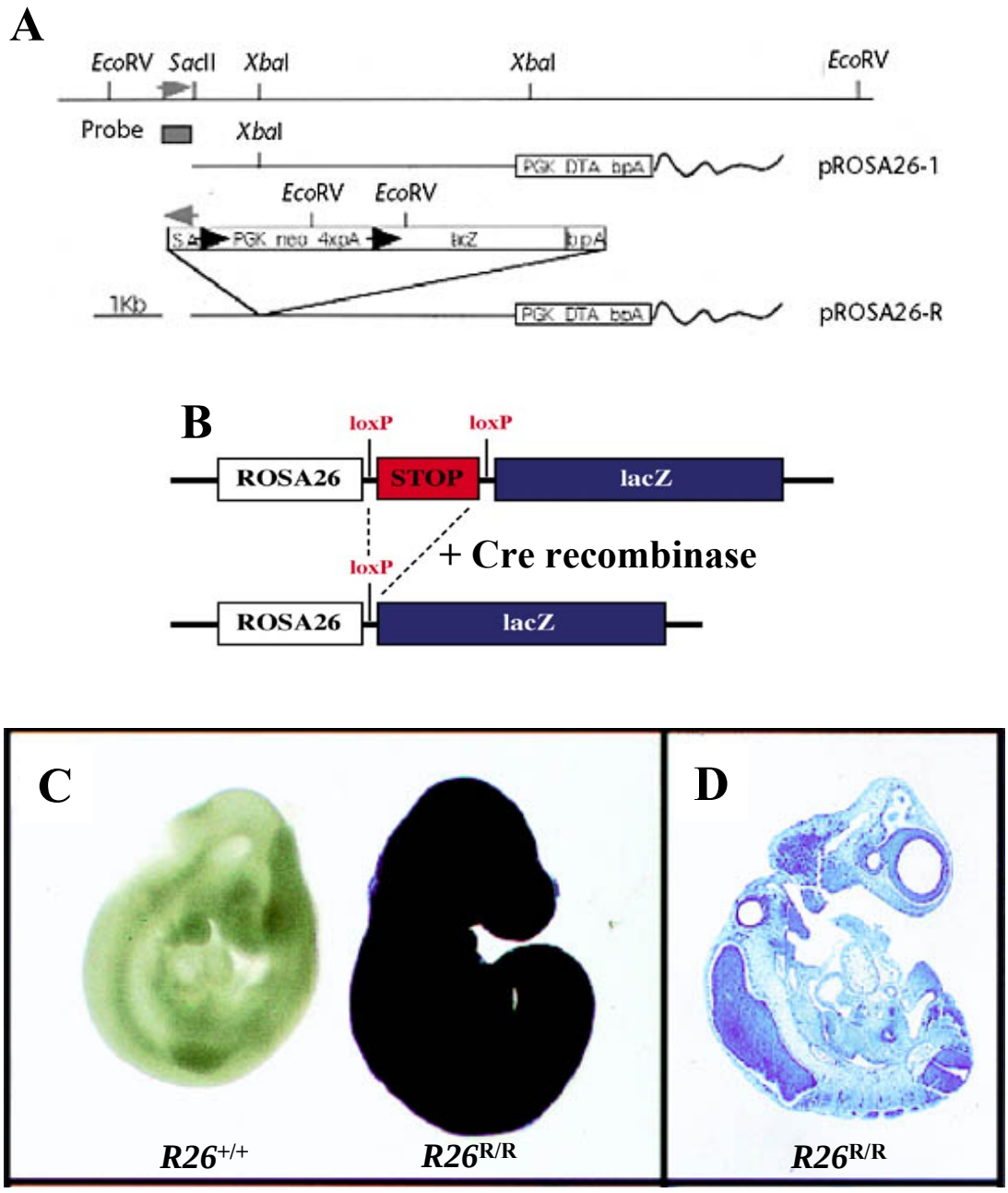

Figure 18. ***Rosa26-LacZ*** **reporter knock-in.** *R26*^{R} mice were generated by knock-in of a floxed stop cassette (*PGK-Neo-PolyA*) upstream of a *LacZ* coding sequence into the *Rosa26* locus **(A)**. Cre-mediated recombination of the *R26*^{R} allele removes the stop cassette **(B)**. The *Rosa26* promoter drives ubiquitous expression, and crossing *R26*^{R} mice with mice expressing a ubiquitous Cre (*E2A-Cre*) results in ubiquitous expression of *LacZ*, as evidenced by whole-body X-gal staining **(C,D)**. Parts A, C, and D of the figure are adapted from Soriano *et al*. (1999).

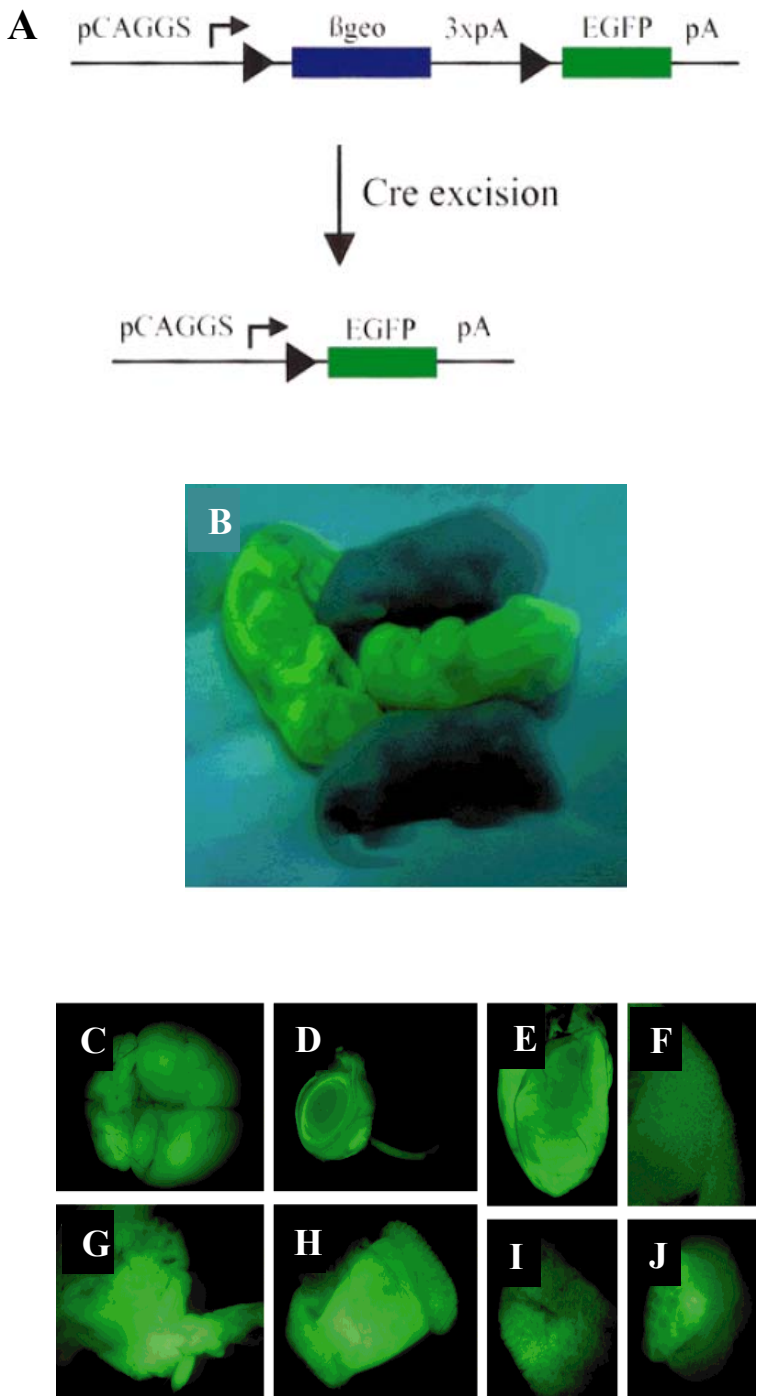

Figure 19. *Z/EG* mice. (A) The construct used to generate mice that express LacZ in the absence of Cre-mediated recombination, followed by expression of EGFP after recombination. **(B)** *Z/EG* mice ubiquitously express either LacZ or EGFP. Cre-mediated recombination of the *Z/EG* allele results in expression of EGFP in **(C)** brain, **(D)** eye, **(E)** heart, **(F)** lung, **(G)** pancreas, **(H)** intestine, **(I)** liver, and **(J)** ovary. Figure is adapted from Novak *et al*. (2000).

performed in accordance with the Vanderbilt Institutional Animal Care and Use Committee guidelines under the supervision of the Division of Animal Care.

For embryonic analyses, the morning of vaginal plug was considered e0.5.

DNA Extraction and Genotyping

DNA was extracted from ear-punch (adult mice), tail (late embryonic to adult mice), brain (embryos), yolk sac (embryos), or paraffinized tissue sections. Sections were deparaffinized in xylene and washed with 100% ethanol prior to extraction. All samples were digested overnight at 55°C in Lab Tissue Buffer 68.8 (35.2 mM Tris, 2.5 mM ethylenediaminetetraacetic acid [EDTA], 2.5 mM sodium citrate, 8.8 mM ammonium sulfate, 5% [v/v] Tween-20) with 0.3 mg/ml Proteinase K and 0.3 mg/ml RNase A. Samples were then digested at 37°C for 15 minutes and heat-inactivated at 95°C for 10 minutes. Undigested material was removed by centrifugation at high speed (16,000 x g) for 10 minutes, and the supernatant was stored at 4°C.

Genotyping for the *Foxm1*^{flox} allele was performed as described in (Zhang H *et al.*, 2006) using PCR with the following primers: *Foxm1*^{flox} forward 5'-TAG GAG ATA CAC TGT TAT AT-3' and *Foxm1*^{flox} reverse 5'-TGT GGG AAA ATG CTT ACA AAA G-3', which amplify a 180 bp product for wild-type *Foxm1* and a 230 bp product for *Foxm1*^{flox} due to insertion of a loxP sequence in the 3rd intron of *Foxm1* (Figure 10A). Each 10 µl PCR reaction included ~50-100 ng DNA, 250 nM of each primer, 2X FailSafe PCR PreMix C (Epicenter Technologies), and 0.5 U REDTaq DNA Polymerase (Sigma-Aldrich). The following reaction conditions were used for amplification: 92°C for 6 minutes (hot-start); 32 cycles of 92°C for 30 seconds (denature), 48°C for 30 seconds

(anneal), and 72°C for 1 minute (elongation); and 72°C for 6 minutes. PCR products were separated by 2% [w/v] agarose gel electrophoresis.

Genotyping for the *Foxm1*^{null} allele was performed as described in (Zhang H *et al.*, 2006) using PCR with the following primers: *Foxm1*^{null} forward 5'- TAG GAG ATA CAC TGT TAT AT-3' and *Foxm1*^{null} reverse 5'-CTC ATG TAG CAT AGA GGG CTG-3', which amplify a 510 bp product (Figure 10A). Primers for the internal control *IL-2* were also included: *IL-2* forward 5'-CTA GGC CAC AGA ATT GAA AGA TCT-3' and *IL-2* reverse 5'-GTA GGT GGA AAT TCT AGC ATC ATC C-3', which amplify a 324 bp product. Each 10 µl PCR reaction included ~50-100 ng DNA, 250 nM of each *Foxm1*^{null} primer, 125 nM of each *IL*-2 primer, 2X FailSafe PCR PreMix C (Epicenter Technologies), and 0.5 U REDTaq DNA Polymerase (Sigma-Aldrich). The following reaction conditions were used for amplification: 92°C for 6 minutes (hot-start); 30 cycles of 92°C for 30 seconds (denature), 56°C for 30 seconds (anneal), and 72°C for 1 minute (elongation); and 72°C for 6 minutes.

Genotyping for the *Cre* transgene was performed as described in (Gu *et al.*, 2002) using PCR with the following primers: *Cre* forward 5'-TGC CAC GAC CAA GTG ACA GC-3' and *Cre* reverse 5'-CCA GGT TAC GGA TAT AGT TCA TG-3', which amplify a 650 bp product. Primers for the internal control *IL-2* were also included. Each 10 µl PCR reaction included ~50-100 ng DNA, 250 nM of each *Cre* primer, 125 nM of each *IL*-2 primer, 10X PCR Buffer with 15 mM $MgCl_2$ (Applied Biosystems), 200 µM dNTP mix, and 0.5 U REDTaq DNA Polymerase (Sigma-Aldrich). The following reaction conditions were used for amplification: 92°C for 6 minutes (hot-start); 32 cycles

of 92°C for 30 seconds (denature), 58°C for 30 seconds (anneal), and 72°C for 1 minute (elongation); and 72°C for 6 minutes.

Genotyping for the *Rosa26-FOXM1c* transgene was performed as described in (Ye *et al.*, 1999) using PCR with the following primers: *Rosa26-FOXM1c* forward 5'-AAA GTC CTG GAT GCT GTC CGA G-3' and *Rosa26-FOXM1c* reverse 5'-CAG ACA TGA TAA GAT ACA TTG ATG-3', which amplify a 325 bp product. Each 10 µl PCR reaction included ~50-100 ng DNA, 250 nM of each primer, 10X PCR Buffer with 15 mM $MgCl_2$ (Applied Biosystems), 200 µM dNTP mix, and 0.5 U REDTaq DNA Polymerase (Sigma-Aldrich). The following reaction conditions were used for amplification: 92°C for 6 minutes (hot-start); 32 cycles of 92°C for 30 seconds (denature), 58°C for 30 seconds (anneal), and 72°C for 1 minute (elongation); and 72°C for 6 minutes.

Genotyping for the *Rosa26-LacZ* reporter knock-in (*R26R*) was performed using PCR with the following primers: *R26R* primer #1 5'-AAA GTC GCT CTG AGT TGT TAT-3', *R26R* primer #2 5'-GCG AAG AGT TTG TCC TCA ACC-3', and *R26R* primer #3 5'-GGA GCG GGA GAA ATG GAT ATG-3', which amplify a 500 bp product for the WT *R26* allele and a 250 bp product for the *R26R* allele. Each 10 µl PCR reaction included ~50-100 ng DNA, 400 nM of each primer, and 2X REDExtract-N-Amp PCR Ready Mix (Sigma-Aldrich). The following reaction conditions were used for amplification: 93°C for 2 minutes (hot-start); 40 cycles of 93°C for 30 seconds (denature), 58°C for 30 seconds (anneal), and 65°C for 1 minute (elongation); and 65°C for 5 minutes.

Genotyping for the *Z/EG* reporter transgene was performed using PCR with the following primers: *Z/EG* forward 5'-AAG TTC ATC TGC ACC ACC G-3' and reverse 5'-TCC TTG AAG AAG ATG GTG CG-3', which amplify a 173 bp product. Primers for the internal control *IL-2* were also included. Each 10 µl PCR reaction included ~50-100 ng DNA, 250 nM of each primer, 10X PCR Buffer with 15 mM $MgCl_2$ (Applied Biosystems), 200 µM dNTP mix, and 0.5 U REDTaq DNA Polymerase (Sigma-Aldrich). The following reaction conditions were used for amplification: 94°C for 1.5 minutes (hot-start); 35 cycles of 94°C for 30 seconds (denature), 60°C for 1 minute (anneal), and 72°C for 1 minute (elongation); and 72°C for 2 minutes.

Intraperitoneal Glucose Tolerance Test (IPGTT)

Mice were fasted overnight for 16 hours, after which their fasting blood glucose level was measured using blood obtained from the tail and a FreeStyle glucometer (Abbott Diabetes Care). The mice were then weighed, and 2 mg dextrose/g body weight (FisherBiotech) in sterile PBS, pH 7.4 (2.7 mM KCl, 14.7 mM KH_2PO_4, 136.9 mM NaCl, 8.1 mM $NaHPO_4 \cdot 7H_2O$) was injected intraperitoneally, and blood glucose levels were measured at 15, 30, 60, 90, and 120 minutes post-injection.

Intraperitoneal Insulin Tolerance Test (IPITT)

Mice were fasted in the morning for 6 hours, after which their fasting blood glucose level was measured using blood obtained from the tail and a FreeStyle glucometer (Abbott Diabetes Care). 0.75U/kg insulin (Novolin R, recombinant regular human insulin; Novo Nordisk) in 0.9% normal saline was injected intraperitoneally, and

blood glucose levels were measured at 15, 30, 60, 90, and 120 minutes post-injection. Percent of initial blood glucose was calculated for all time points.

Plasma and Pancreatic Insulin Content

For plasma insulin content, blood was collected at 0 and 30 minutes after glucose injection during an IPGTT from either the saphenous veins or retro-orbital plexus. For saphenous venous blood collection, the mouse was restrained, the distal-lateral portion of the leg was shaved, and the saphenous vein was punctured using a 25 5/8 G needle. Blood was collected into heparanized microvette tubes (Sarstedt), which were then placed on ice. For retro-orbital plexus blood collection, the mouse was anesthetized using isoflurane, the plexus was punctured using heparinized Natelson Blood Collecting Tubes (Fisher), and blood was then transferred to 1.5 ml tubes. All samples were centrifuged at 2,000 x g for 15 minutes at 4^{o}C, and the plasma supernatant was transferred and stored at -80^{o}C. At least 25 µl of each sample was analyzed for insulin content at the Hormone Assay and Analytical Services Core at Vanderbilt University by liquid-phase radioimmunoassay (RIA) using the Rat Insulin RIA Kit (Linco/Millipore). Plasma samples required longer incubation time with diluted antibody for increased sensitivity.

For pancreatic insulin content, pancreatic tissue was harvested from the mouse, weighed, homogenized in acid-alcohol (1 ml HCl in 110 ml 95% ethanol), and extracted in this solution for 3 days at 4^{o}C with agitation (Brissova *et al.*, 2002). The homogenate was then centrifuged at 800 x g for 30 minutes at 4^{o}C, and the supernatant was transferred and stored at -20^{o}C. Samples were analyzed for insulin content at the Hormone Assay and Analytical Services Core at Vanderbilt University by liquid-phase

RIA using the Rat Insulin RIA Kit (Linco/Millipore). Samples required dilution 1:1,000 in buffer prior to an analysis. Pancreatic insulin content was normalized to pancreas weight.

Body Fat Mass Analysis

Body composition analysis was performed in the Mouse Metabolic Phenotyping Center at Vanderbilt University with the Minispec mq7.5 (Bruker Instruments), which utilizes nuclear magnetic resonance (NMR) spectroscopy to assess percentage of body weight composed of fat, lean muscle, and free fluid.

60% Partial Pancreatectomy (PPx)

Mice were anesthetized using isoflurane. A midline abdominal incision allowed exteriorization of the splenic lobe of the pancreas (between the gastro-duodenal junction and the spleen). 60% PPx was performed by gently denuding the pancreatic tissue from the splenic lobe using cotton-tipped swabs soaked in 0.9% normal saline, leaving the main pancreatic duct and splenic artery intact. For Sham operations, the splenic lobe was isolated using cotton-tipped swabs and gently rubbed with a moistened gloved finger for 1 minute. Abdominal muscles were sutured using 5-0 vicryl (Ethicon), and the skin was stapled using 9.0 mm staples (Reflex Skin Closure Systems). Following the operation, 0.1 mg/kg buprenorphine-HCl in 0.9% normal saline was injected subcutaneously for analgesia, and 0.8 mg/ml bromo-deoxyuridine (BrdU; Sigma-Aldrich) was administered in the drinking water in a light-safe bottle and was replaced on the 4th day. Mice were sacrificed 1 week post-operation by cervical dislocation, and the splenic and duodenal

lobes of the pancreas were harvested and analyzed separately. One day prior to and 7 days after the operation, IPGTTs were performed.

Tamoxifen Injection

The shoulder and nape of the neck area were shaved, and then 8 mg of a 20 mg/ml solution of tamoxifen (Sigma-Aldrich) in filter-sterilized corn oil was injected subcutaneously. The injection site was glued with Vetbond tissue adhesive (3M) to prevent leakage. Mice were injected every other day for a total of one, two, or three injections. Control mice were injected with an equal volume of filter-sterilized corn oil.

Islet Isolation

All islet isolations were performed in the Islet Procurement and Analysis Core at Vanderbilt University. Mice were anesthetized via an intraperitoneal injection of 0.15 mg/g ketamine-HCl and 0.04 mg/g xylazine (Henry Schein), the abdominal cavity was exposed, and 3-4 ml of 0.6% collagenase P (Roche) in Hank's Balanced Salt Solution (HBSS) containing calcium and magnesium (Gibco) was injected into the common bile duct. The pancreas was then harvested and digested in 6.5 ml of the collagenase P solution for 4 minutes at 37^{o}C followed by 1.5 minutes at room temperature, with shaking. Islets were hand-picked using at least 4 passages to reach 98% purity.

Islet Perifusion

Islets were cultured overnight in Roswell Park Memorial Institute (RPMI) Media 1640 (Gibco) supplemented with 1% penicillin-streptomycin and 10% heat-inactivated FBS at 37°C in the presence of 5% CO_2. The following day, islets were collected and loaded into the perifusion column, and islet equivalent (IEQ) of each sample was measured based on islet number and size. Islets were perifused with perifusion media (Dulbecco's Modified Eagle's Medium [DMEM] supplemented with 4.7 mM 4-[2-hydroxyethyl]-1-piperazineethanesulfonic acid [HEPES], 38 mM $NaHCO_3$, 4.0 mM L-glutamine, 1.0 mM sodium pyruvate, 15.05 μM bovine serum albumin [BSA], and 0.0015% phenol red) + 5.6 mM glucose for 39 minutes (baseline) prior to sequential stimulation with the following secretagogues in perifusion media: 16.7 mM glucose, 100 μM isobutylmethylxanthine (IBMX) + 16.7 mM glucose, 300 μM tolbutamide, and 20 mM KCl. Each secretagogue was applied for 9 minutes, followed by 21 minutes of perifusion media + 5.6 mM glucose to return to baseline prior to subsequent stimulation. Perifusate was collected at a rate of 1 ml/min into 3 ml fractions. Insulin content in each fraction was measured using the Rat Insulin RIA Kit (Millipore/Linco) according to manufacturer's protocol.

RNA Isolation and Quantitative Real-Time RT-PCR (qRT-PCR)

RNA was extracted from freshly-isolated islets or transiently-transfected HeLa cells using the RNAqueous kit (Ambion) and DNase-treated using the TURBO DNA-free kit (Ambion). Concentrations of all samples, A_{260}/A_{280} ratios, and A_{260}/A_{230} ratios were assessed using the ND-1000 Spectrophotometer (NanoDrop). Islet RNA was analyzed by

the Microarray Shared Resource at Vanderbilt University, where RNA quality was further assessed using the 2100 Electrophoresis Bioanalyzer (Agilent).

For qRT-PCR, cDNA was generated from 20 ng of islet RNA using the Superscript III First-Strand Synthesis System for RT-PCR (Invitrogen). Real-time PCR was performed using the iQ5 Real-Time PCR Detection System (Bio-Rad) with iQ Real-Time SYBR Green PCR Supermix (Bio-Rad) and the following mouse primer sets: *Foxm1* forward 5'-CAC TTG GAT TGA GGA CCA CTT-3' and reverse 5'-GTC GTT TCT GCT GTG ATT CC-3', *Plk1* forward 5'-TTG TAG TTT TGG AGC TCT GTC G-3' and reverse 5'-AGT GCC TTC CTC CTC TTG TG-3', *Cenp-a* forward 5'-CAA GGA GGA GAC CCT CCA G-3' and reverse 5'-GTC TTC TGC GCA GTG TCT GA-3', *Birc5/Survivin* forward 5'-CCG ATG ACA ACC CGA TAG A-3' and reverse 5'-CAT CTG CTT CTT GAC AGT GAG G-3', *Ccnb1* forward 5'-TCT TGA CAA CGG TGA ATG GA-3' and reverse 5'-TCT TAG CCA GGT GCT GCA TA-3', *Ccna2* forward 5'-CTT GGC TGC ACC AAC AGT AA-3' and reverse 5'-CAA ACT CAG TTC TCC CAA AAA CA-3', *Skp2* forward 5'-GTA TGT TAG GGA ACC ATT TGC GAG-3' and reverse 5'-TTA GAA GGG CAC TTG GAA GAG TT-3', *Cks1* forward 5'-GAC CTC AAA GCC CTC GTG T-3' and reverse 5'-TGA AAC ATA AAT CCA TAA GTC ATC A-3', *Aurkb* forward 5'-CCC TAC GGC TCA AAG ACG-3' and reverse 5'-AGC AAG CGC AGA TGT CGT-3', *Cdc25b* forward 5'-CCC TTC CCT GTT TTC CTT TC-3' and reverse 5'-ACA CAC ACT CCT GCC ATA GG-3', *Ccnd2* forward 5'-CAC CGA CAA CTC TGT GAA GC-3' and reverse 5'-TCC ACT TCA GCT TAC CCA ACA-3', *Hprt1* (internal control) forward 5'-AGT CAA CGG GGG ACA TAA AA-3' and reverse 5'-TGC ATT GTT TTA CCA GTG TCA A-3'. The following human primers were also

used: *FoxM1* forward 5'-GGA GGA AAT GCC ACA CTT AGC G-3' and reverse 5'-TAG GAC TTC TTG GGT CTT GGG GTG-3'. Samples were assessed in duplicate, and results were quantitated using the comparative C_T method (Schmittgen and Livak, 2008) and normalized to control samples.

Custom TaqMan Low Density Arrays (Applied Biosystems) were designed to assess expression of 48 transcripts (Table 2). cDNA was generated from 40-50 ng of islet RNA using the High-Capacity cDNA Reverse Transcription Kit (Applied Biosystems). TaqMan-based qRT-PCR was performed according to manufacturer's instructions using a 7900HT Real-Time PCR System (Applied Biosystems). Samples were assessed in duplicate, and results were quantitated using the comparative C_T method and normalized to control samples.

Tissue Preparation and Histology

For paraffin embedding, tissue was fixed in 4% paraformaldehyde in PBS, pH 7.4 for 1-4 hours at 4°C, washed in PBS at 4°C, stored in 70% ethanol at 4°C, dehydrated in an ascending ethanol series at room temperature, cleared twice with xylene at room temperature, infiltrated with xylene:paraffin (1:1, v/v) and then 100% paraffin at 56°C, embedded in paraffin, and sectioned at 5 μm. Sections were then deparaffinized in xylene, rehydrated in a descending ethanol series, and washed in PBS.

For frozen embedding, tissue was fixed in 4% paraformaldehyde in PBS, pH 7.4 for 1-4 hours at 4°C, washed in PBS, partially dehydrated with 30% [w/v] sucrose overnight at 4°C, embedded in Tissue-Tek Optimal Cutting Temperature (OCT) compound (Sakura) on dry ice, and sectioned at 7 μm. Frozen blocks and sections were

Table 2. Transcripts assessed by Custom TaqMan Low Density Array. Hs indicates *homo sapiens*. Mm indicates *Mus musculus*. g1 indicates that primers may detect genomic DNA. m1 indicates that primers span an intron and will not detect genomic DNA. s1 indicates that transcript consists of only one exon and thus primers will detect genomic DNA. mH indicates that intron-spanning primers were designed to detect a transcript belonging to a family with high sequence homology. gH indicates that the primers were designed to detect a transcript belonging to a family with high sequence homology and may detect genomic DNA.

Common Name	Gene Symbol	Assay ID
18S	18s	Hs99999901_s1
Arx	Arx	Mm00545903_m1
Aurora B kinase	Aurkb	Mm01718146_g1
Survivin	Birc5	Mm00599749_m1
Cyclin A2	Ccna2	Mm00438064_m1
Cyclin B1	Ccnb1	Mm00838401_g1
Cyclin B2	Ccnb2	Mm00432351_m1
Cyclin D1	Ccnd1	Mm00432359_m1
Cyclin D2	Ccnd2	Mm00438071_m1
Cdc25A	Cdc25a	Mm00483162_m1
Cdc25B	Cdc25b	Mm00499136_m1
Cdk4	Cdk4	Mm00726334_s1
$p21^{Cip1}$	Cdkn1a	Mm00432448_m1
$p27^{Kip1}$	Cdkn1b	Mm00438167_g1
$p57^{Kip2}$	Cdkn1c	Mm00438170_m1
$p16^{INK4a}$	Cdkn2a	Mm00494449_m1
CenpA	Cenpa	Mm00483252_m1
Ctgf	Ctgf	Mm00515790_g1
Perk	Eif2ak3	Mm00438708_m1
FoxA2	Foxa2	Mm00839704_mH
FoxD3	Foxd3	Mm02384867_s1

Table 2 — continued

Common Name	Gene Symbol	Assay ID
FoxM1	Foxm1	Mm00514924_m1
FoxO1	Foxo1	Mm00490672_m1
Glucagon	Gcg	Mm00801712_m1
Hnf4a	Hnf4a	Mm00433964_m1
Insulin 1	Ins1	Mm01259683_g1
Insulin 2	Ins2	Mm00731595_gH
Isl1	Isl1	Mm00627860_m1
MafA	Mafa	Mm00845209_s1
MafB	Mafb	Mm00627481_s1
Men1	Men1	Mm00484963_m1
Myosin 5a	Myo5a	Mm00487823_m1
Neurogenin 3	Neurog3	Mm00437606_s1
Nkx2.2	Nkx2-2	Mm00839794_m1
Nkx6.1	Nkx6-1	Mm00454962_m1
Hnf6	Onecut1	Mm00839394_m1
Pax4	Pax4	Mm01159036_m1
Pax6	Pax6	Mm00443072_m1
Pdx1	Pdx1	Mm00435565_m1
Plk1	Plk1	Mm00440924_g1
Rab27a	Rab27a	Mm00469997_m1
Rab3a	Rab3a	Mm00725988_s1
Skp2	Skp2	Mm00449925_m1
Glut2	Slc2a2	Mm00446224_m1
Sox9	Sox9	Mm00448840_m1
Granuphilin	Sytl4	Mm00489110_m1
Munc13-1	Unc13b	Mm00498847_m1
Vamp2	Vamp2	Mm00494118_g1

stored at -80°C. Sections were then thawed at room temperature for 15-30 minutes, permeabilized in PBS with 0.1% (v/v) Triton-X-100 for 45 minutes or in PBS with 0.2% (v/v) Triton-X-100 for 10 minutes, and washed in PBS.

The following primary antibodies were incubated with 5% normal donkey serum (NDS) and 1% BSA in PBS at 4°C overnight: guinea pig anti-insulin (1:1,000; Linco), guinea pig anti-glucagon (1:1,000; Linco), rabbit anti-cytokeratin (1:1,000; DakoCytomation), rabbit anti-phospho-histone H3 (1:250; Upstate Cell Signaling Solutions), rabbit anti-Cre (1:10,000; Novagen), and chicken anti-β-galactosidase (1:1,000; AbCam). The rat anti-BrdU primary antibody (1:400; Accurate Chemical & Scientific) was incubated with 5% NDS and 1% BSA in PBS at room temperature overnight. The mouse anti-Neurogenin3 primary antibody (Ngn3; 1:100; Developmental Studies Hybridoma Bank, The University of Iowa) was incubated in 1% blocking solution (Invitrogen TSA Kit #2) at 4°C overnight. The anti-Cre and anti-β-galactosidase antibodies were used exclusively on cryosections.

The following secondary antibodies were incubated with 1% BSA in PBS for 1 hour at room temperature: peroxidase-conjugated donkey anti-guinea pig (1:250; Jackson Laboratories), Cy2-conjugated donkey anti-guinea pig, Cy2-conjugated donkey anti-rabbit, Cy3-conjugated donkey anti-guinea pig, Cy3-conjugated donkey anti-rabbit, Cy3-conjugated donkey anti-rat, Cy3-conjugated donkey anti-chicken (all 1:500; Jackson Laboratories). For Ngn3 labeling, peroxidase-conjugated goat anti-mouse seconday antibody (1:100; Invitrogen) was incubated in 1% blocking solution (Invitrogen) for 1 hour at room temperature.

Detection of cytokeratin required pre-treatment with 20 μg/ml Proteinase-K (DakoCytomation) in PBS for 5 minutes at room temperature. Detection of Ngn3 required slow-boil microwave antigen retrieval with Tris-EGTA (TEG) buffer, pH 9.0 (10 mM Tris, 500 μM ethylene glycol tetraacetic acid [EGTA]) and tyramide signal amplification with TSA Kit #2 (Invitrogen). Detection of phospho-histone H3 required microwave antigen retrieval at 1200 W in 10 mM sodium citrate, pH 6.5 for 4 minutes and permeabilization with 0.2% (v/v) Triton-X-100 in PBS for 10 minutes. Detection of BrdU required pre-treatment with 1.5 N HCl for 20 minutes at 37°C, sodium borate buffer (0.85% [w/v] boric acid, 0.15% [w/v] sodium borate) for 1 minute at room temperature, and 0.005 mg/ml trypsin (Sigma-Aldrich) with 0.005 mg/ml $CaCl_2$ in 0.5 M Tris-HCl, pH 7.5 for 3 minutes at 37°C.

For screening of mouse anti-FoxM1 sera (Vanderbilt Monoclonal Antibody Core) by immunohistochemistry (IHC), the HistoMouse-SP Kit (Zymed) was used according to manufacturer's protocol. Sera was incubated overnight at 4°C at dilutions ranging from 1:50 to 1:250 in PBS with 5% NDS and 1% BSA. The TSA Kit #2 (Invitrogen) was also used for screening, following manufacturer's protocol. In some cases, microwave antigen retrieval was performed with 10 mM sodium citrate, pH 6.5 or with TEG buffer, pH 9.0.

Coverslips were mounted with Permount (Fisher) for bright-field microscopy or with anti-fade mounting media (50% glycerol [v/v] and 2% N-propylgalate [w/v] in PBS, pH 7.4) for fluorescent microscopy. Nuclei were fluorescently labeled with 1.5 μg/ml 4',6'-diamidino-2-phenylindole (DAPI; Molecular Probes) in mounting media.

5-bromo-4-chloro-3-indolyl-B-D-galactoside (X-gal) staining was performed on paraformadehyde-fixed tissue or whole embryos. After washing with PBS, samples were permeabilized for 30 minutes at 4°C and again for 30 minutes at room temperature with permeabilization solution (2 mM $MgCl_2$, 0.01% [w/v] sodium deoxycholate, and 0.02% [v/v] NP-40 in PBS). Samples were then incubated overnight at room temperature in X-gal staining solution (0.1% [w/v] X-gal, 2 mM $MgCl_2$; 5 mM potassium ferricyanide; 5 mM potassium ferrocyanide; 20 mM Tris, pH 7.4).

In Situ Hybridization

Foxm1 probes were generated from a fragment of rat *Foxm1* cDNA (*Eco*RI-*Pst*I sub-clone, 500 bp) in the pGEM-1 vector, a generous gift from Robert H. Costa (University of Illinois at Chicago) (Ye *et al.*, 1997). The anti-sense probe was generated using SP6 RNA polymerase and *Eco*RI-digested plasmid DNA, while the sense probe was generated using T7 RNA polymerase and *Hind*III-digested plasmid DNA. Probes were labeled with non-radioactive digoxigenin-UTP (DIG) using the DIG RNA Labeling Kit (Roche) and purified using G-50 sephadex columns (Amersham). Labeling efficiency was determined by spot-testing according to instructions in the DIG RNA Labeling Kit.

Paraffin sections were deparaffinized in xylene, rehydrated in a descending ethanol series, and washed in PBS. Sections were then post-fixed in 4% paraformaldehyde in PBS, pH 7.4 for 20 minutes on ice, treated with 15 μg/ml Proteinase K in PBS for 7 minutes at room temperature, post-fixed again in 4% paraformaldehyde in PBS, pH 7.4 for 20 minutes on ice, and treated with acetylation

agent (86 mM triethanolamine, 26 mM acetic anhydride) for 10 minutes at room temperature. Tissue was then hybridized with an appropriate dilution of each probe in hybridization solution (40% [v/v] formamide, 20X SSC, 50X Denhardt's reagent [Fisher], 250 μg/ml heparin [Sigma], 1 mg/ml tRNA [Sigma]) at 65°C overnight. Slides were then washed in 5X SSC for 5 minutes at 60°C, 0.2X SSC for 1 hour at 60°C and then 5 minutes at room temperature, and maleic acid buffer, pH 7.5 (100 mM maleic acid, 150 mM NaCl, 175 mM NaOH) for 5 minutes at room temperature. Slides were then blocked in 1% blocking reagent (Roche) in maleic acid buffer for 1 hour at room temperature and incubated with anti-DIG primary antibody (1:5,000; Roche) in maleic acid buffer for 1 hour at room temperature. Slides were then washed two times for 15 minutes each in maleic acid buffer at room temperature and in Tris solution (100 mM Tris, pH 9.5; 100 mM NaCl, 5 mM $MgCl_2$) for 5 minutes at room temperature. Slides were then developed in detection buffer, pH 9.5 (2 mM Tris, 2 mM NaCl) with nitro blue tetrazolium/5-bromo-4-chloro-3-indolyl phosphate (NBT/BCIP) tablets (Roche) for 4 hours to overnight at room temperature, followed by serial washes in deionized H_2O and Tris-EDTA (TE) buffer, pH 8.0 (10 mM Tris-HCl, 1 mM EDTA) before mounting.

β Cell Mass Analysis

Sections 250 μm apart (3-15 sections per tissue sample, depending on tissue size) were incubated with anti-insulin primary antibody followed by peroxidase-conjugated anti-guinea pig secondary antibody, which was visualized using the DAB Peroxidase Substrate Kit (Vector Laboratories). Sections were counterstained with eosin, and a

digital image was created using a Nikon Coolscan 9000 and NikonScan v4.0.2. MetaMorph v6.1 software (Molecular Devices) was used to measure the total insulin$^+$ area and the total pancreatic area of each section. β cell mass was calculated by dividing the total insulin$^+$ area of all sections by the total pancreatic areas of all sections and multiplying this ratio by the pancreatic wet weight.

Proliferation Analyses

For adult β cell proliferation analyses, evenly-spaced sections (250-1250 μm apart, 2-8 sections per tissue sample, depending on tissue size) were labeled with anti-insulin and anti-BrdU primary antibodies and DAPI. Images of all insulin$^+$ cells on each section were captured at 400X magnification on an Olympus BX41 microscope with a digital camera using Magnafire (Optronics), and cells were counted using MetaMorph v6.1. Percent proliferating β cells was calculated by dividing the number of insulin/BrdU double-positive cells by the total number of insulin$^+$ cells. α cells were identified by glucagon labeling, and proliferation was measured in the same manner. Ductal cells were identified by cytokeratin labeling on sections 250-750 μm apart, and images were captured at 200X magnification. Acinar cells were identified by morphological characteristics on 200X images from sections 750 μm apart.

For embryonic β cell proliferation analyses sections 125 μm apart (6-9 sections per tissue sample) were labeled with anti-insulin and anti-phospho-histone H3 primary antibodies, and nuclei were labeled with DAPI in mounting media.

Islet Size, β cell Size, and β cell Nucleus Size Analyses

Using the same pictures analyzed for β cell proliferation, the cross-sectional area of each insulin$^+$ cell group was circumscribed and measured using MetaMorph. Average cross-sectional β cell size per islet was calculated by dividing the total area of the islet by the number of β cell nuclei within it. β cell nuclear size was measured by circumscribing the DAPI$^+$ cross-sectional area within insulin$^+$ cells.

β cell Apoptosis Analysis

Apoptotic β cells were identified on sections 750-1250 μm apart (2-4 sections per tissue sample) by terminal deoxynucleotidyl transferase-mediated dUTP nick-end-labeling (TUNEL) using the BD ApoAlert DNA Fragmentation Assay Kit (BD Biosciences-Clontech), followed by labeling with anti-insulin primary antibody and DAPI. Images of all insulin$^+$ cells on each section were captured at 400X magnification. Percentage of apoptotic β cells was calculated by dividing the number of insulin/TUNEL double-positive cells by the total number of insulin$^+$ cells.

R26^R Recombination Analysis

Evenly-spaced cryosections (2-3 sections per tissue sample, 250-750 μm apart, depending on tissue size) were labeled with anti-β-galactosidase and anti-insulin primary antibodies. Nuclei were labeled with DAPI in mounting media. Images of all insulin$^+$ cells on each section were captured at 400X magnification, and cells were counted using MetaMorph v6.1. The percent of recombined β cells was calculated by dividing the

number of β-galactosidase/insulin double-positive cells by the total number of insulin$^+$ cells.

Generation of an Anti-FoxM1 Monoclonal Antibody

Sub-cloning of *Foxm1* cDNA Fragments

Full-length murine *Foxm1* cDNA in pYX-Asc in DH5α *E. coli* was obtained from Open Biosystems (clone 6417436, accession number BC065067) (Figure 20). The DH5α *E. coli* were grown on Luria Broth (LB)-Ampicillin agar plates overnight at 37^{o}C, and isolated colonies were cultured overnight in Terrific Broth (TB; 1.2% [w/v] tryptone, 2.4% [w/v] yeast extract, 0.4% [v/v] glycerol, 17 mM KH_2PO_4, 72 mM K_2HPO_4) with 100 μg/ml Ampicillin at 37^{o}C with shaking at 225 rpm prior to plasmid purification.

Three fragments of the *Foxm1* cDNA were amplified by PCR, using primers that added a *Bam*HI restriction site and start (ATG) codon to the 5' end and a stop (TAG) codon and *Sal*I restriction site to the 3' end of each amplicon. The following primer sets were used: Fragment 1 forward 5'-GGA TCC ATG AGA ACC AGC CCC C-3' and reverse 5'-GTC GAC CTA CTC AGA CAC AGA GTC CTG-3', Fragment 2 forward 5'-GGA TCC ATG AAT CGC TAC TTG ACA TTG GAC C-3' and reverse 5'-GTC GAC CTA CTG AGG GCA GCT GAG-3', Fragment 3 forward 5'-GGA TCC ATG GAA GAG GGA GGA CCT TTC-3' and reverse 5'-GTC GAC CTA AGG GAT GAA CTG AGA CCA G-3'. Fragment 1 primers amplified a 714 bp product, consisting of bp 172-870 of the *Foxm1* cDNA (NM_008021). Fragment 2 primers amplified an 849 bp product, consisting of bp 1108-1938 of the *Foxm1* cDNA. Fragment 3 primers amplified

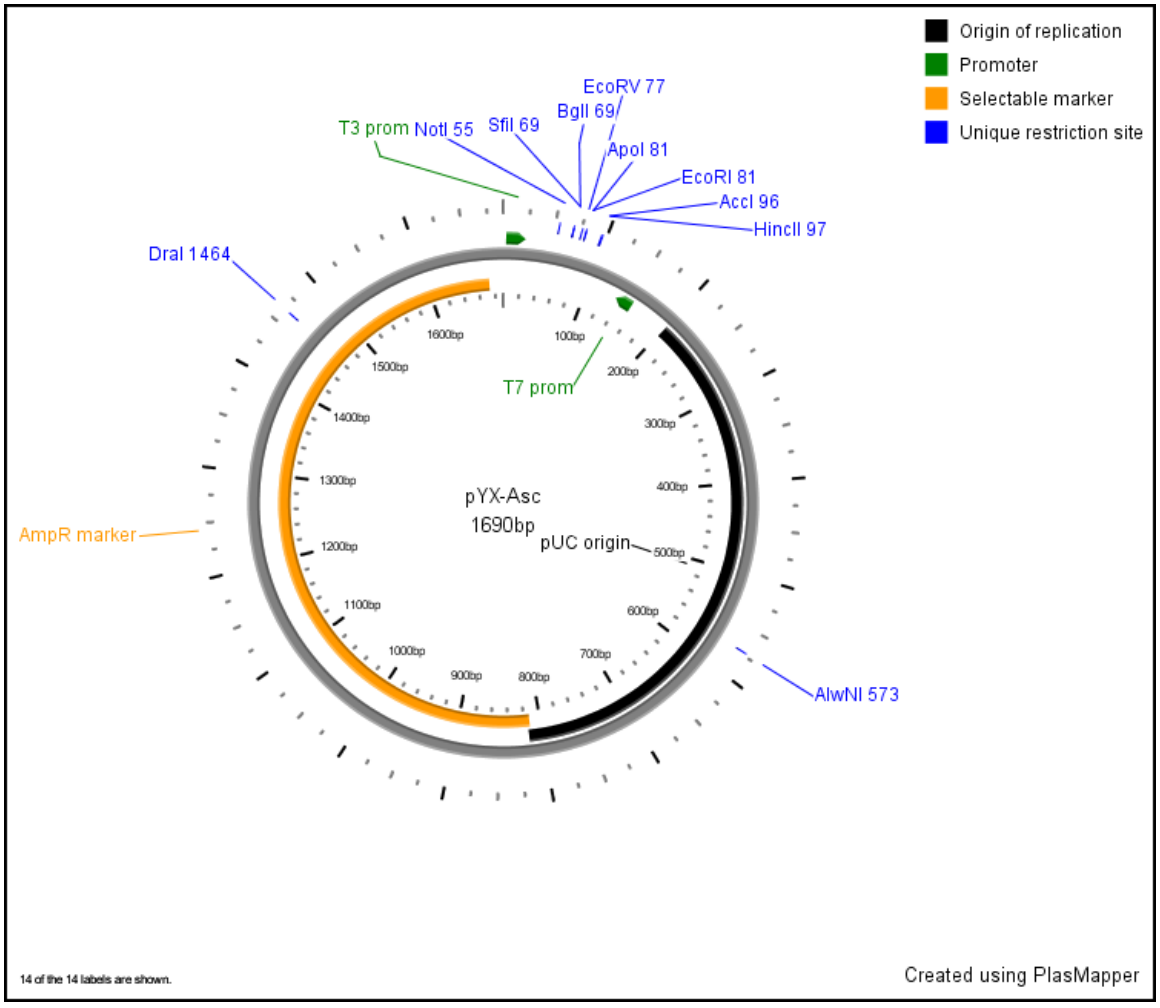

Figure 20. pYX-Asc vector. Murine *Foxm1* cDNA was obtained from OpenBiosystems in the pYX-Asc vector. Figure from OpenBiosystems website.

a 522 bp product, consisting of bp 1939-2445 of the *Foxm1* cDNA. Each 50 µl PCR reaction included 1 µg DNA, 200 nM of each primer, 10X PCR Buffer with 15 mM $MgCl_2$ (Takara), 400 µM dNTP mix, and 2.5 U Taq DNA Polymerase (Takara). The following conditions were used for amplification: 95°C for 2 minutes (hot-start); 30 cycles of 95°C for 30 seconds (denature), 61°C for 30 seconds (anneal), and 72°C for 1 minute (elongation); and 72°C for 10 minutes. PCR products were separated on a 0.8% [w/v] agarose gel with 50 ng/ml ethidium bromide and 1 mM guanosine and extracted using the QIAquick Gel Extraction Kit (Qiagen). DNA was stored at -20°C.

Each PCR-amplified *Foxm1* fragment was cloned into the pCR2.1-TOPO vector using the TOPO-TA Cloning Kit (Invitrogen) (Figure 21). Transformed OneShot TOP10 *E. coli* (Invitrogen) were grown overnight on LB-Ampicillin agar plates at 37°C. Isolated colonies were then cultured overnight in TB with 50 µg/ml Kanamycin at 37°C with shaking at 225 rpm prior to plasmid purification. Positive clones for each *Foxm1* fragment were identified by restriction digest with *Eco*RI followed by gel electrophoresis, which produced a vector band at 4 kb and *Foxm1* Fragment 1-, 2-, and 3-specific bands at 714, 849, and 522 bp, respectively. Clones were verified by sequencing using M13 reverse and T7 primers (Vanderbilt DNA Sequencing Facility).

Verified clones were cultured in TB with 50 µg/ml Ampicillin overnight at 37°C with shaking at 225 rpm prior to plasmid purification. Each *Foxm1* fragment was excised from pCR2.1-TOPO with *Bam*HI and *Sal*I, gel extracted, and sub-cloned into the maltose binding protein (MBP)-tagged expression vector pAT107b, provided by the Vanderbilt Monoclonal Antibody Core (Figure 22). Transformed DH5α *E. coli* were grown on LB-Kanamycin agar plates overnight at 37°C, and isolated colonies were cultured in TB

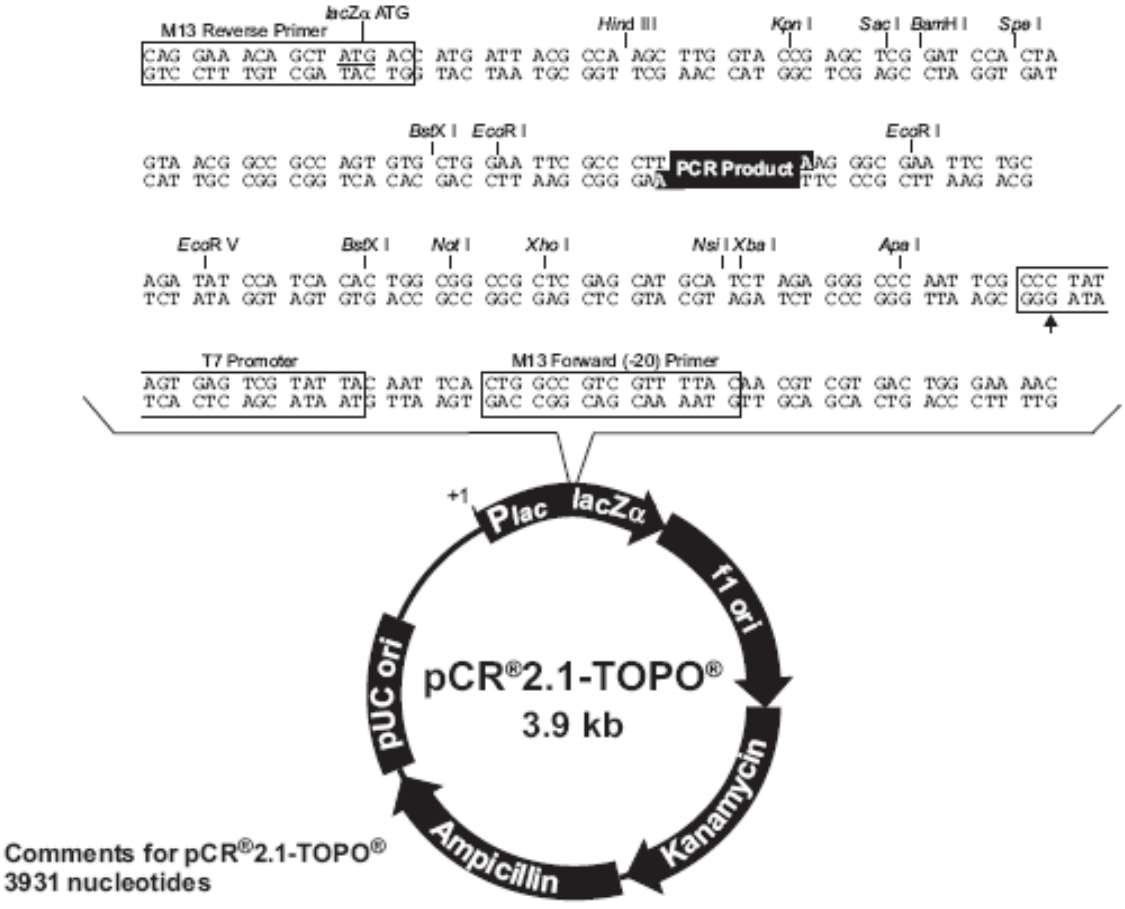

Comments for pCR®2.1-TOPO®
3931 nucleotides

*Lac*Zα fragment: bases 1-547
M13 reverse priming site: bases 205-221
Multiple cloning site: bases 234-357
T7 promoter/priming site: bases 364-383
M13 Forward (-20) priming site: bases 391-406
f1 origin: bases 548-985
Kanamycin resistance ORF: bases 1319-2113
Ampicillin resistance ORF: bases 2131-2991
pUC origin: bases 3136-3809

Figure 21. pCR-TOPO2.1 vector. Murine *Foxm1* cDNA fragments generated by PCR were sub-cloned into the pCR-TOPO2.1 vector and then excised using restriction digest with *Eco*RI. Figure from Invitrogen website.

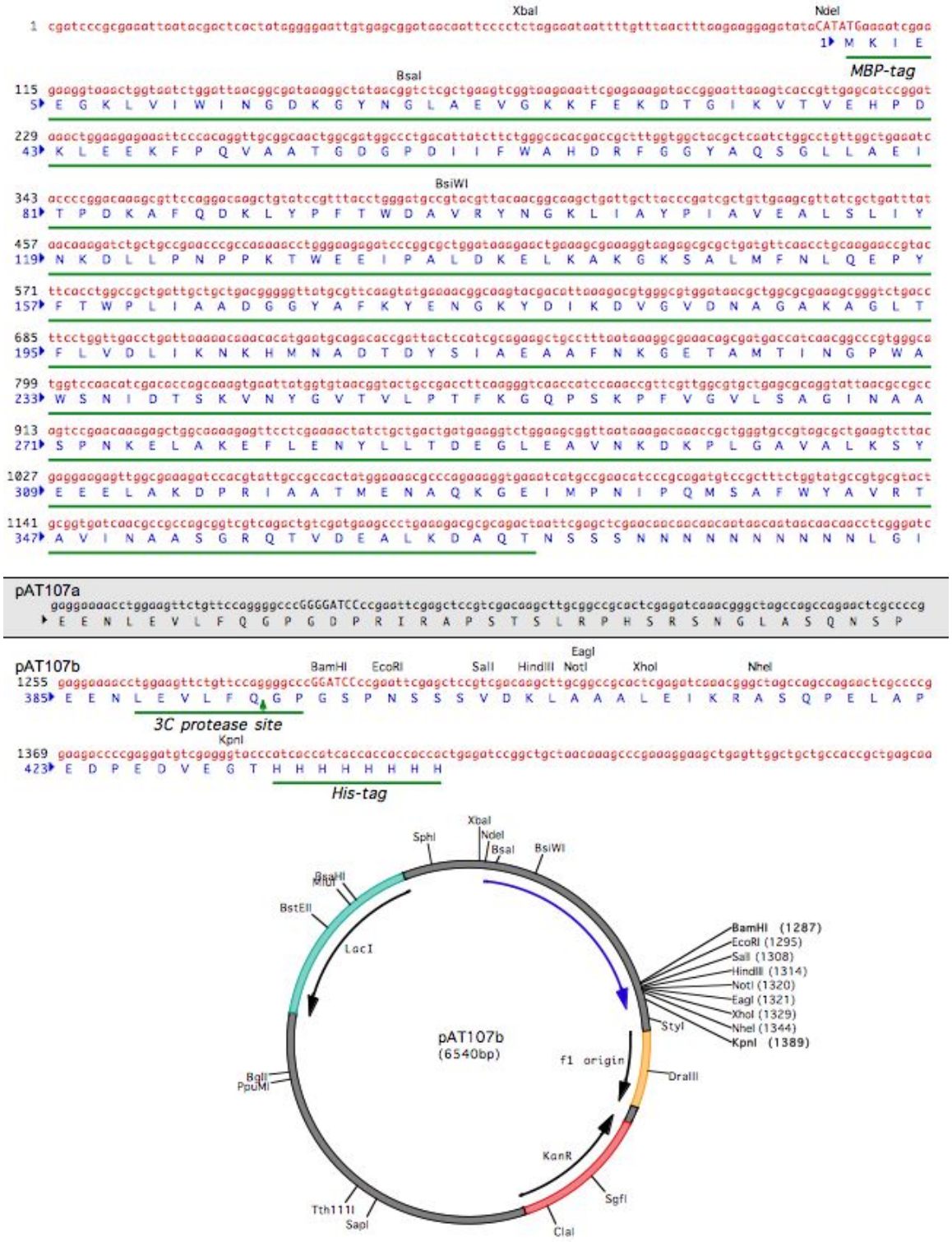

Figure 22. pAT107b vector. Murine *Foxm1* cDNA fragments were sub-cloned into the multiple cloning site of the pAT107b expression vector, via ligation at the *Eco*RI and *Not*I restriction sites. The pAT107b vector adds an MBP tag and an 8X polyhistidine tag to each cDNA clone, which can be cleaved by digestion with 3C protease.

with 50 μg/ml Kanamycin overnight at 37°C with shaking at 225 rpm prior to plasmid purification. Positive clones for each *Foxm1* fragment were identified by restriction digest with *Bam*HI and *Not*I followed by gel electrophoresis, which produced a vector band at 6.5 kb and *Foxm1* Fragment 1-, 2-, and 3-specific bands at 722, 857, and 529 bp, respectively. Putative *Foxm1* Fragment 1 clones were verified by restriction digest with *Sal*I and *Eco*RV, which produced bands of 6780 and 452 bp. Putative *Foxm1* Fragment 2 clones were verified by restriction digest with *BamH*I and *Pvu*II, which produced bands at 6528 and 831 bp. Putative *Foxm1* Fragment 3 clones were verified by restriction digest with *Sal*I and *Pst*I, which produced bands of 6869 and 168 bp.

Verified clones were used to transform BL21 CodonPlus (DE3)-RIPL *E. coli* (Stratagene), which were then grown on LB-Kanamycin agar plates overnight at 37°C.

Plasmid Purification

Plasmid mini-preps were performed on 1 ml overnight cultures. Cultures were pelleted by centrifugation at 1,000 x g for 1 minute, resuspended/lysed in 100 μl Alkaline Lysis Solution I (50 mM glucose; 25 mM Tris-HCl, pH 8.0; 10 mM EDTA, pH 8.0), and mixed with 200 μl of Alkaline Lysis Solution II (0.2 N NaOH, 1% [w/v] sodium dodecyl sulfate [SDS]). Then 150 μl Alkaline Lysis Solution III (3 M potassium acetate, 11.5% [v/v] glacial acetic acid) was added to each sample, and samples were vortexed. Lysate was cleared by centrifugation at high speed (16,000 x g) for 10 minutes, and then transferred to 900 μl of 95% ethanol. Precipitated DNA was pelleted by centrifugation at high speed (16,000 x g) for 5 minutes, washed with cold 70% ethanol, and resuspended in

55 µl TE buffer with 200 ng/µl RNase A. For sequencing, plasmid mini-preps were performed using the Plasmid Mini Kit (Qiagen) according to manufacturer's protocol.

Plasmid maxi-preps were performed using the Plasmid Maxi Kit (Qiagen) according to manufacturer's protocol. DNA was resuspended in 100 µl TE buffer with 200 ng/µl RNase A.

Spectrophotometry

DNA concentration was measured by optical density (OD) absorption at 260 nm (A_{260}) using a SmartSpec 3000 spectrophotometer (Bio-Rad) and a quartz cuvette. A conversion factor of 50 µg/ml dsDNA per absorption unit (AU) was used. Nuclease-free water was used as a blank and to dilute the samples appropriately to attain A_{260} between 0.1 and 1.5 for accuracy.

Bacterial growth was determined by OD absorption at 600 nm (A_{600}) using a SmartSpec 3000 spectrophotometer (Bio-Rad) and disposable polystyrene cuvettes. A conversion factor of 5×10^8 cells/ml per AU was used. LB (1% [w/v] tryptone, 0.5% [w/v] yeast extract, 171 mM NaCl) was used as a blank and to dilute the cultures appropriately to attain A_{600} between 0.1 and 1.5 for accuracy.

Restriction Digests

Restriction enzymes were obtained from New England Biolabs and used according to the manufacturer's instructions. Restriction digests were performed in 20 µl reactions using 10 µg DNA, 2 µl each restriction enzyme (4 U per µg DNA),

2 µl appropriate 10X buffer, 0.2 µl BSA if necessary, and nuclease-free H_2O. Reactions were incubated at 37°C for 2 hours to overnight.

DNA Ligation

Ligations of insert and vector were performed using the Quick Ligation Kit (New England Biolabs). Each ligation step consisted of two control reactions (vector alone, insert alone) and two ligation reactions (1:1 [v/v] vector:insert, 1:7 [v/v] vector:insert). Each 20 µl reaction contained 1 µl Quick Ligase, 10 µl 2X Quick Ligase Buffer, appropriate volume of vector and insert, and nuclease-free H_2O. Reactions were incubated at room temperature for 5 minutes and chilled on ice prior to use. Ligation products were stored at -20°C.

Bacterial Transformation

DH5α *E. coli* were transformed by adding 2 µl purified plasmid or 10 µl ligation products to 100 µl cells in 14 ml round-bottom tubes (Falcon) on ice, mixing gently, incubating on ice for 2 minutes, incubating at 42°C for 1 minute, and incubating again on ice for 2 minutes. Transformed cells were then spread onto LB agar plates with appropriate antibiotic.

OneShot TOP10 *E. coli* were transformed according to manufacturer's protocol (Invitrogen). Transformed cells were then spread onto LB agar plates with appropriate antibiotic.

BL21 CodonPlus (DE3)-RIPL *E. coli* were transformed according to manufacturer's protocol (Stratagene). 200 µl transformed cells were then spread onto LB agar plates with appropriate antibiotic.

Induction of Recombinant FoxM1 Expression in Bacteria

Transformed BL21 CodonPlus (DE3)-RIPL *E. coli* were cultured in LB with 50 µg/ml Kanamycin and 50 µg/ml Chloramphenicol overnight at 37°C with shaking at 225 rpm. The cultures were then diluted to an OD A_{600} of 0.1-0.2 AU with LB with 50 µg/ml Kanamycin and 50 µg/ml Chloramphenicol and cultured at 37°C with shaking at 225 rpm until the OD A_{600} reached ~0.5 AU. Bacteria were induced to express recombinant FoxM1 by adding isopropyl-β-D-thiogalactopyranoside (IPTG) to a final concentration of 1 mM and culturing for 2-6 hours with shaking at 225 rpm at 37°C, 32°C, 29°C, or 25°C.

Small samples of each culture prior to and after induction were collected, centrifuged at high speed (16,000 x g) for 2 minutes to remove media, and resuspended in protein gel sample buffer (50 mM Tris, pH 6.8; 1% [w/v] SDS; 5% [w/v] sucrose; 0.004% [w/v] bromophenol blue; 120 mM β-mercaptoethanol) for SDS-polyacrylamide gel electrophoresis (PAGE) analysis. Bacteria (pellets and resuspended) were stored at -20°C.

Purification of Recombinant FoxM1 Antigen

Bacterial cultures induced to express recombinant FoxM1 were centrifuged at 5,000 x g for 10 minutes at 4°C to remove media. Cells were resuspended/lysed in

Bacterial Protein Extraction Reagent (B-PER; Pierce Biotechnology) with NaCl (final concentration 150 mM), EDTA (final concentration 2 mM), and 2.5% (v/v) Protease Inhibitor Cocktail (Sigma-Aldrich) for use with bacterial cell extracts (Sigma-Aldrich), vortexed, and mixed for 10 minutes at 4°C. The insoluble fraction was pelleted by centrifugation at 15,000 x g for 15 minutes at 4°C. Soluble and insoluble fractions were stored at -20°C.

FoxM1 fragment-MBP fusion proteins were purified from soluble lysate by binding to Amylose Resin (New England Biolabs) and eluting with Maltose Monohydrate (Supelco). The amylose resin was prepared for binding by brief centrifugation at low speed to remove the ethanol in which it was stored, washed twice with 2 volumes of column buffer (20 mM Tris-HCl, pH 7.4; 150 mM NaCl; 2 mM EDTA; 0.1% [v/v] NP-40), resuspended in 1 volume of column buffer, and stored at 4°C. Soluble lysate was mixed 20:1 with prepared amylose resin at 4°C for 1 hour, then briefly centrifuged at <6,000 x g, and the unbound fraction was removed. Pelleted bound resin was washed five times with 2 volumes of column buffer. MBP-bound proteins were eluted by resuspending pellet in 10 mM maltose in column buffer, mixing for 10 minutes at 4°C, and centrifuging briefly at <6,000 x g. The eluted fraction was removed and stored at -20°C.

Small samples of crude lysate, insoluble fraction, soluble fraction, unbound fraction, bound fraction, eluted fraction, and non-eluted fraction were collected, mixed with 2X protein gel sample buffer for SDS-PAGE analysis of induction and purification efficiencies, and stored at -20°C.

Mice in Vanderbilt Monoclonal Antibody Core

Balb/c and A/J mice were injected with purified MBP-tagged FoxM1 fragments. A total of 50 μg of FoxM1 Fragment 1-MBP and Fragment 3-MBP were mixed with sterile PBS in a final volume of 100 μl. Two injections of 50 μl each were injected per mouse, one subcutaneous and the other intraperitoneal. Mice were injected approximately once every 30 days. Prior to the initial injection and two weeks after the second and consecutive boosts, blood was collected from either the tail vein or the retro-orbital plexus. Serum was collected after coagulation and centrifugation. Enzyme-linked immunosorbent assay (ELISA) was performed by the Monoclonal Antibody Core to assess sera reactivity with MBP, Fragment 1-MBP, and Fragment 3-MBP.

Transient Transfection of Mammalian Cells

Full-length murine *Foxm1* cDNA was sub-cloned from the pYX-Asc vector to the pcDNA3.1^{+} vector by digestion with *Eco*RI and *Not*I. DH5α *E. coli* were transformed with ligation products and grown on LB-Ampicillin agar plates overnight at 37^{o}C. Isolated colonies were cultured in TB with 200 μg/ml Ampicillin overnight at 37^{o}C prior to plasmid purification. Positive clones were identified by restriction digest with *Eco*RI and *Not*I, which produced bands of 5,428 and 4,390 bp; restriction digest with *Eco*RV, which produced bands of 9,938 and 420 bp; and restriction digest with *Nhe*I, which produced bands of 7,279 and 2,539 bp. Clones were verified by sequencing using T7 primer (Vanderbilt DNA Sequencing Facility).

Verified clones were used to transiently transfect HeLa cells, generously provided by Shuangli Guo, Post-Doctoral Fellow in Dr. Roland Stein's laboratory (Vanderbilt

University). 4 μg plasmid prep was complexed with Lipofectamine Reagent (Invitrogen) by mixing 1:4 (w/v) DNA:Lipofectamine in Opti-MEM I Reduced Serum Medium (Invitrogen) and incubating for 30 minutes at room temperature. Negative controls lacked DNA. HeLa cells were transfected at ~50% confluence, after washing twice with Dulbecco's PBS and incubating for 10-15 minutes with Opti-MEM at 37°C. DNA:Lipofectamine complexes in Opti-MEM were incubated with cells for 5 hours at 37°C, then growth medium was added, and the cells were incubated for 20 hours at 37°C prior to RNA and protein extraction.

Protein Extraction

Total protein was extracted from mouse tissue (embryonic liver, embryonic heart and lungs, embryonic whole body, or adult islets). Tissue was homogenized in lysis buffer (20 mM HEPES, 400 mM NaCl, 752 μM spermidine, 250 μM EDTA, 2 mM EGTA, 1% [v/v] NP-40, 25% [v/v] glycerol, 2 mM dithiothreitol [DTT], 1 mM phenylmethylsulphonyl fluoride [PMSF], 0.04% [v/v] protease inhibitor cocktail), then centrifuged at high speed (16,000 x g) for 10 minutes at 4°C. Supernatant was stored at -80°C.

Nuclear and cytoplasmic protein fractions were extracted from transfected HeLa cells. Cells were incubated with lysis buffer (100 mM Tris-HCl, pH 8.0; 0.5% [v/v] NP-40) for 5 minutes on ice with vortexing, then centrifuged at high speed (16,000 x g) at 4°C for 5 minutes. The supernatant (cytoplasmic fraction) was collected and stored at -80°C. The pellet was resuspended in nuclear extraction buffer (20 mM HEPES, pH 7.5; 400 mM NaCl; 1 mM DTT; 2 mM Na_3VO_4; 1 mM EDTA;

1 mM EGTA, pH 8.0; 1 mM PMSF), incubated for 20 minutes on ice with vortexing, then centrifuged at high speed (16,000 x g) at 4°C for 5 minutes. The supernatant (nuclear fraction) was collected and stored at -80°C.

Protein Quantification

Extracted protein samples were quantitated using the DC Protein Assay Kit (Bio-Rad). Samples and BSA standards were assessed in duplicate using a microplate reader to measure A_{750}.

SDS-PAGE, Western Immunoblotting

Protein samples were mixed with 4X NuPAGE LDS Sample Buffer (Invitrogen), boiled at 95-100°C for 5 minutes, chilled, and subjected to denaturing electrophoresis on NuPAGE Novex 4-12% Bis-Tris Mini Gels using 3-morpholinopropanesulfonic acid, 3-(N-morpholino) propanesulfonic acid (MOPS) SDS Running Buffer, and the Xcell SureLock Mini cell electrophoresis system (all from Invitrogen) according to manufacturer's protocol. SeeBlue Plus2 Pre-Stained Standard (Invitrogen) was used as a molecular weight marker.

For analysis of recombinant protein induction and purification, gels were stained with Bio-Safe Coomassie G250 Stain (Bio-Rad) according to manufacturer's protocol.

For western immunoblotting, protein was transferred from gel to Hybond-P polyvinylidene difluoride (PVDF) membrane (Amersham) using the Xcell II Blot Module (Invitrogen), following manufacturer's protocol. Membranes were then blocked in 5% [w/v] non-fat milk in Tris-buffered saline, pH 7.4 (TBS; 20 mM Tris, 137 mM NaCl)

for 1 hour at room temperature and incubated with primary antibody in 3% [w/v] non-fat milk overnight at 4^{o}C, washed for 30 minutes in TBS with 0.1% (v/v) Tween 20 (TBS-T) at room temperature, and incubated with species-specific peroxidase-conjugated secondary antibody in 3% non-fat milk for 1 hour at room temperature. Following 30 minutes to 1 hour of washing in TBS-T, antibody detection was performed using ECL Western Blotting Detection Reagents (Amersham) and BioMax or X-Omat scientific imaging film (Kodak).

Primary antibodies used for western immunoblotting included: rabbit anti-FoxM1 (1:1,000; a gift from Robert H. Costa [University of Illinois at Chicago]) (Wang *et al.*, 2005), rabbit anti-MPP2 (C-20) (1:200; Santa Cruz Biotechnology), mouse anti-FoxM1 sera (1:1,000; Vanderbilt Monoclonal Antibody Core). Secondary antibodies included: peroxidase-conjugated goat anti-mouse IgG (1:5,000; Promega) and peroxidase-conjugated goat anti-rabbit IgG (1:5,000; Promega).

Statistical Analyses

Data were analyzed by unpaired t-test, one-way ANOVA with Bonferroni's post-tests, or two-way ANOVA with Bonferroni's post-tests, as appropriate, using GraphPad Prism v5.01. $P<0.05$ was considered significant. Specific analyses performed and sample sizes are included in the figure legends.

CHAPTER III

INVESTIGATING THE ROLE OF FOXM1 IN β CELL REGENERATION AND EXPANSION FOLLOWING 60% PARTIAL PANCREATECTOMY

Introduction

As type I and type II diabetes result from an absolute or relative deficiency in β cell number, respectively, understanding how β cell number is determined and can be manipulated may lead to new therapeutic options. While transplantation of cadaveric islets remains promising, additional sources of islets or β cells are required to make this treatment more widely available (Shapiro *et al.*, 2006). Diabetic patients would also benefit from *in vivo* manipulation of their β cell population. Although β cells proliferate slowly after birth (Finegood *et al.*, 1995), increased β cell proliferation can be stimulated under various conditions, including obesity, pregnancy, injury, and growth factor over-expression. In adult rodents and humans, β cell replication is the primary mechanism by which new β cells are formed (Dor *et al.*, 2004; Teta *et al.*, 2007; Meier *et al.*, 2008), and there is much debate regarding whether and how new β cells arise *de novo* in the adult. However, a recent study in mice has conclusively shown that new β cells are generated from facultative adult progenitor cells (neogenesis) in response to pancreatic injury, in a manner reminiscent of embryonic endocrine cell differentiation (Xu *et al.*, 2008). Additionally, lineage tracing studies using the duct marker carbonic anhydrase II (CAII) showed that duct ligation stimulates differentiation of both acinar and endocrine cells from duct cells in adult mice, similar to what occurs during development (Bonner-Weir *et al.*, 2008). Furthermore, patients with type I diabetes exhibit evidence for continued β

cell production in the face of immune destruction (Meier *et al.*, 2005; Meier *et al.*, 2006), providing support for the ability of human β cells to regenerate.

Partial pancreatectomy (PPx) has been used by several groups as a method of pancreatic injury that stimulates regeneration (Bonner-Weir *et al.*, 1983; Leahy *et al.*, 1988; De Leon *et al.*, 2003; Lee *et al.*, 2006; Peshavaria *et al.*, 2006; Joglekar *et al.*, 2007; Teta *et al.*, 2007). However, there are important differences in the actual techniques used in these studies, with tissue removal ranging from 50-90% and the process of tissue removal being either excision (including removal of the main pancreatic duct and splenic artery) or denuding (leaving the main pancreatic duct and splenic artery relatively intact). Although it is difficult to directly compare results among such studies, it seems that the greater amount of tissue removed creates a stronger stimulus for regeneration, and that denuding the tissue results in more *de novo* differentiation than is observed following pure excision of tissue, although both techniques stimulate proliferation. Additionally, removal of 90% of pancreatic tissue results in hyperglycemia (Bonner-Weir *et al.*, 1983; Sharma *et al.*, 1999), which is an independent stimulus for β cell proliferation, while 60% PPx does not induce hyperglycemia (Leahy *et al.*, 1988; Peshavaria *et al.*, 2006). This study aimed to determine FoxM1's role in β cell proliferation and regeneration under normoglycemic conditions using 60% PPx, in which tissue from the splenic lobe of the pancreas is denuded from the main pancreatic duct and splenic artery.

FoxM1 is an important regulator of postnatal β cell proliferation, but loss of FoxM1 in *Foxm1*$^{flox/flox}$*;Pdx1*$^{5.5kb}$*-Cre* (FoxM1$^{\Delta panc}$) mice does not affect embryonic pancreas or β cell development (Zhang H *et al.*, 2006). These outcomes mirror those

reported for widespread deletion of other cell cycle regulators (Cdk4, Cyclin D), with postnatal endocrine cell-specific effects causing diabetes (Rane *et al.*, 1999; Georgia and Bhushan, 2004; Kushner *et al.*, 2005a). Female FoxM1$^{\Delta panc}$ mice remain glucose tolerant despite significantly reduced β cell mass and thus are the focus of this study, allowing for analysis of β cell proliferation and regeneration without the confounding effects of hyperglycemia.

To determine whether FoxM1 is required for new β cell formation during regeneration, 60% PPx was performed on adult female FoxM1$^{\Delta panc}$ mice and Control (*Foxm1*$^{flox/flox}$) littermates (Figure 23A,B). Importantly, *Foxm1* and some of its transcriptional targets were up-regulated within islets following PPx during the period of peak regeneration, and endocrine cell proliferation and regeneration of β cell mass following PPx were specifically impaired in FoxM1$^{\Delta panc}$ mice. Furthermore, loss of FoxM1 did not impair islet neogenesis but did impair islet growth after PPx.

Results

60% PPx up-regulated *Foxm1* and select targets within islets while maintaining normoglycemia.

FoxM1 mRNA and protein are relatively low in adult islets (Figure 24A) (Zhang H *et al.*, 2006), but it was unknown whether up-regulation occurs upon stimulation of endocrine cell proliferation. Indeed, *Foxm1* expression was up-regulated 2-fold in Control islets 6 days after PPx versus Sham (Figure 24B), suggesting that FoxM1 plays a role in the regenerative response of endocrine cells. Importantly, *Foxm1* up-regulation

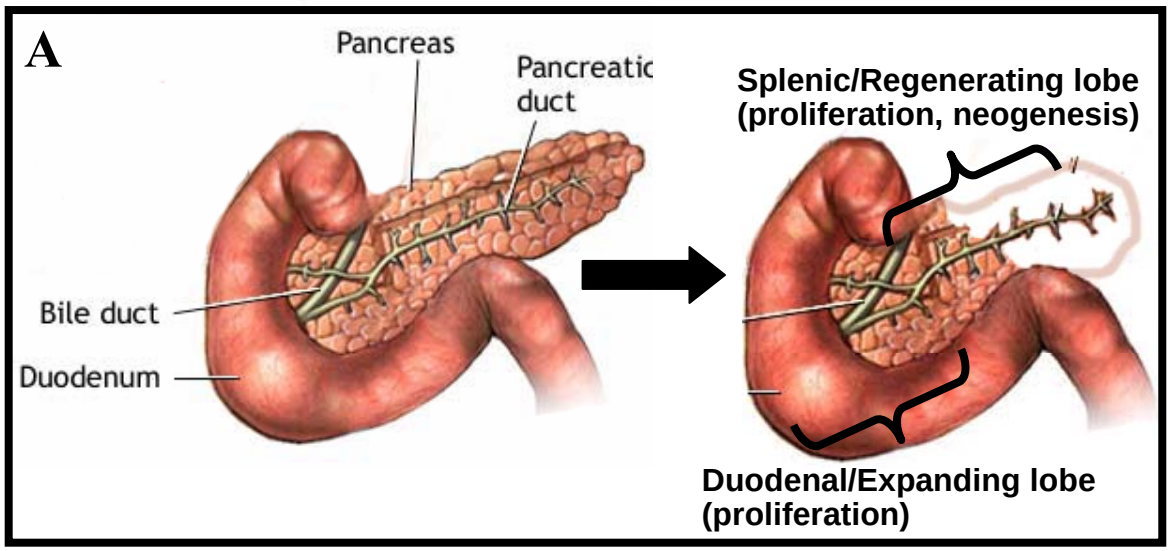

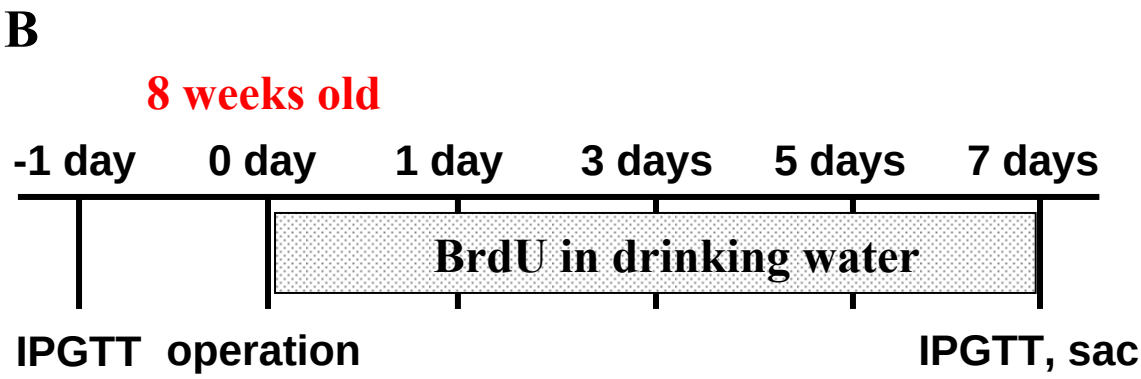

Figure 23. 60% partial pancreatectomy (PPx). (A) Exocrine and endocrine tissue were removed from the splenic lobe of the pancreas, leaving the main pancreatic duct intact. The splenic (regenerating) and duodenal (expanding) lobes were analyzed separately. It was expected that the regenerating lobe would undergo both proliferation and neogenesis, while the expanding lobe would undergo only proliferation. **(B)** Eight week old female mice underwent either a PPx or a Sham operation, in which no tissue was removed. One day prior to the operation, IPGTT was performed. Mice recovered for one week, during which they were given BrdU in the drinking water. After 7 days, IPGTT was performed again, and the mice were sacrificed for tissue harvest.

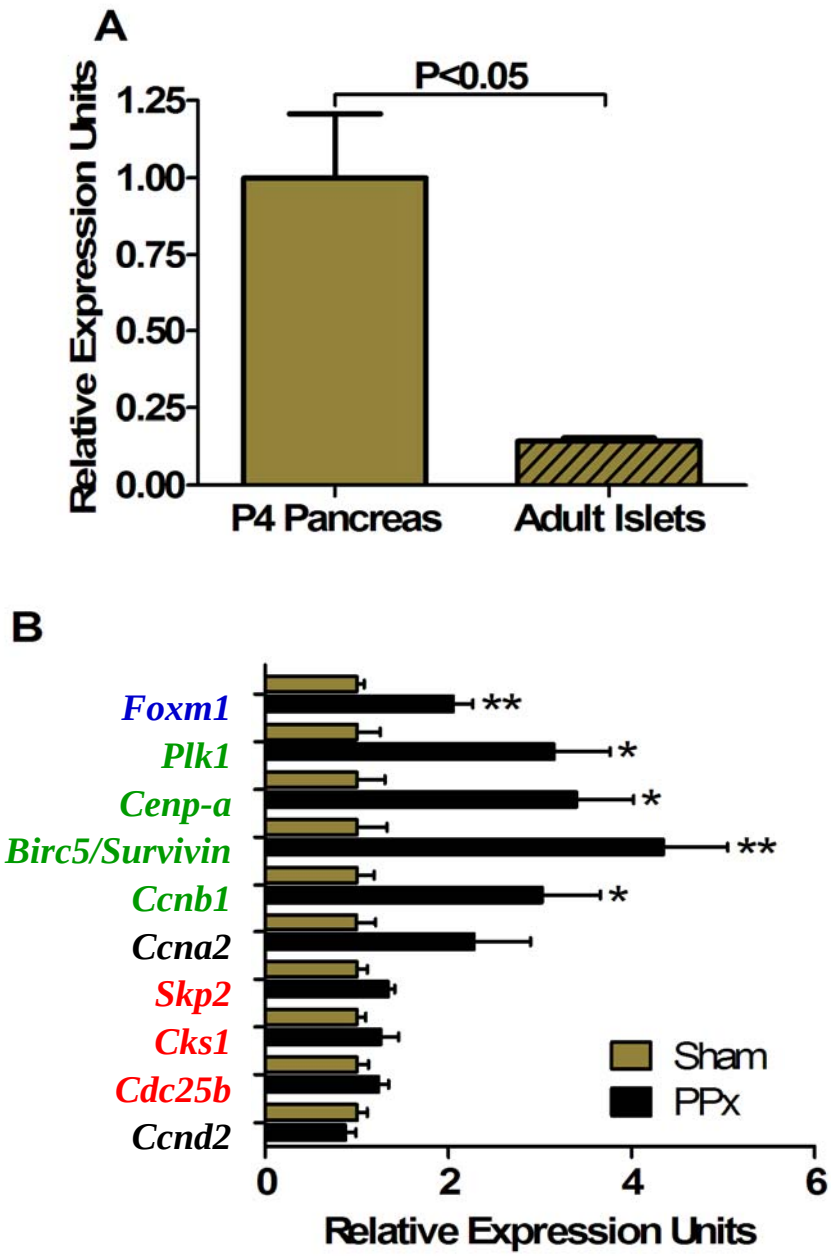

Figure 24. Expression of *Foxm1* and targets in Control islets. **(A)** qRT-PCR revealed that *Foxm1* expression was relatively low in adult islets, compared to postnatal day 4 (P4) whole pancreas. **(B)** After 60% PPx, expression of *Foxm1* (blue) and several of its targets (green) were up-regulated within islets compared to after a Sham operation. Other FoxM1 targets were not up-regulated after PPx (red), nor were cell cycle regulators that are not FoxM1 targets (black). Results were normalized to *Hprt1* levels and then to control samples. Error bars represent SEM. Unpaired t-test with Welch's correction was used in A, and with no corrections in B, to measure significance. *P<0.05, **P<0.01. n=3-4 per group in A, 4-6 per group in B.

corresponded with the peak of β cell proliferation following PPx (Peshavaria *et al.*, 2006).

Other transcripts of interest were then screened for differences in expression after 60% PPx versus Sham, using Custom TaqMan Low-Density Arrays. Although preliminary, these screens revealed that many transcripts were up-regulated within islets following PPx, most notably *Aurkb*, *Birc5/Survivin*, *Ccna2*, *Ccnb1*, *Ccnb2*, *Cenp-a*, *Plk1*, and *Sox9* (Figure 25). Other transcripts, including *Cdc25b*, *Ctgf*, *Nkx2.2*, and *Skp2* were up-regulated to a similar extent as was *Foxm1*. qRT-PCR was used to validate these findings, and this analysis confirmed that several of FoxM1's known transcriptional targets were up-regulated, including *Plk1, Cenp-a*, *Birc5/Survivin*, and *Ccnb1* (Figure 24B). Other targets, including *Skp2*, *Cks1*, and *Cdc25b*, displayed a trend of up-regulation following PPx versus Sham but were not significantly altered. A similar trend was observed for *Ccna2* but not for *Ccnd2*, both of which have been linked to β cell proliferation (Georgia and Bhushan, 2004; Inada *et al.*, 2005; Kushner *et al.*, 2005a), but neither of which is a known FoxM1 target.

To determine whether FoxM1 is necessary for endocrine cell regeneration following pancreatic injury, FoxM1$^{\Delta panc}$ and Control female littermates underwent PPx or Sham operation at 8 weeks of age. In agreement with previous reports showing that 60% PPx does not induce hyperglycemia (Leahy *et al.*, 1988; Peshavaria *et al.*, 2006), IPGTTs performed 7 days following 60% PPx or Sham confirmed that Control and FoxM1$^{\Delta panc}$ female mice remained glucose tolerant, although there was a trend toward slightly higher glucose levels in both genotypes after PPx versus Sham (Figure 26A,B).

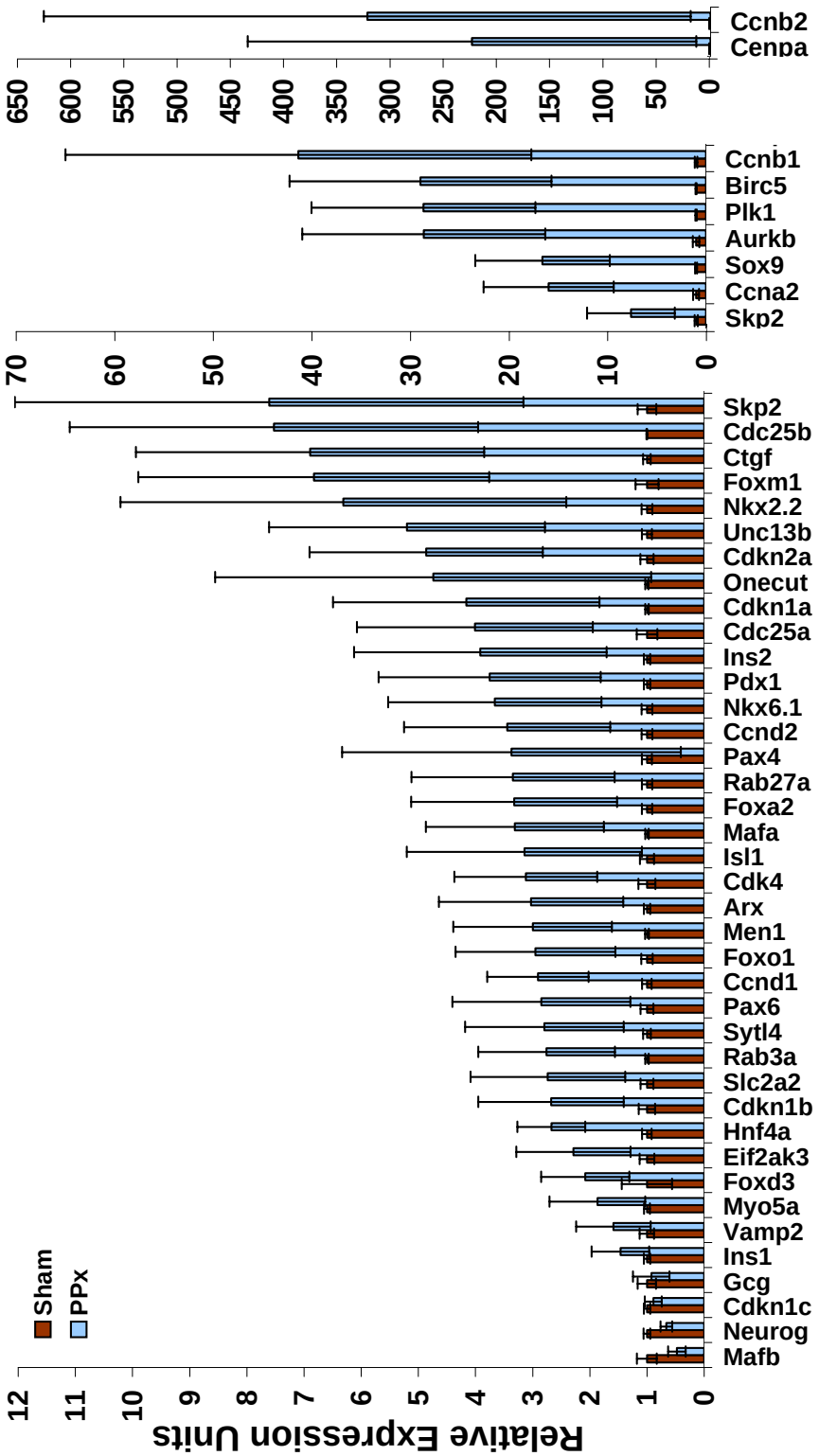

Figure 25. Analysis of transcript expression in Control islets after 60% PPx or Sham operation using Custom TaqMan Low Density Arrays. Error bars represent SEM. n=2 Sham, 3 PPx.

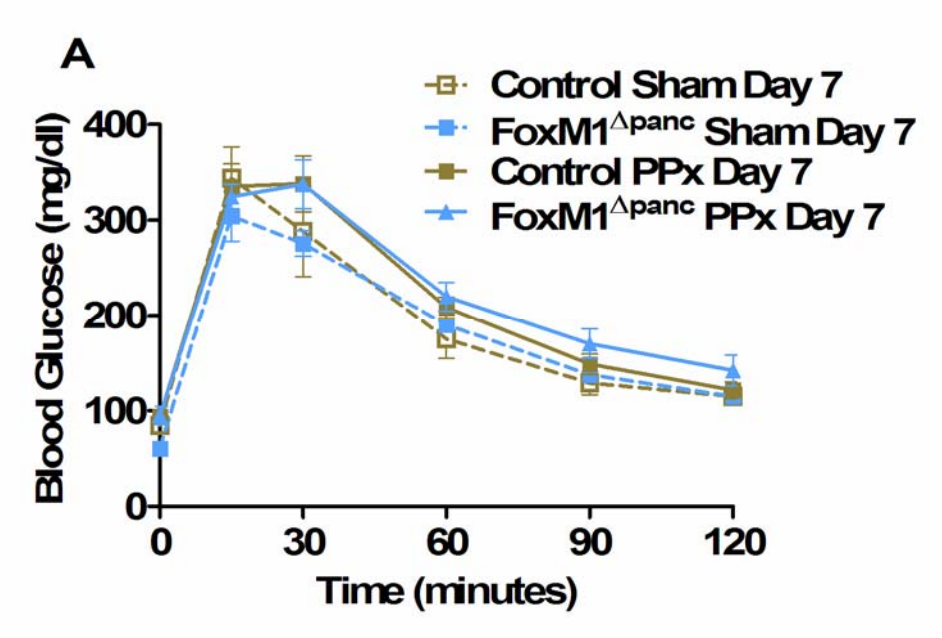

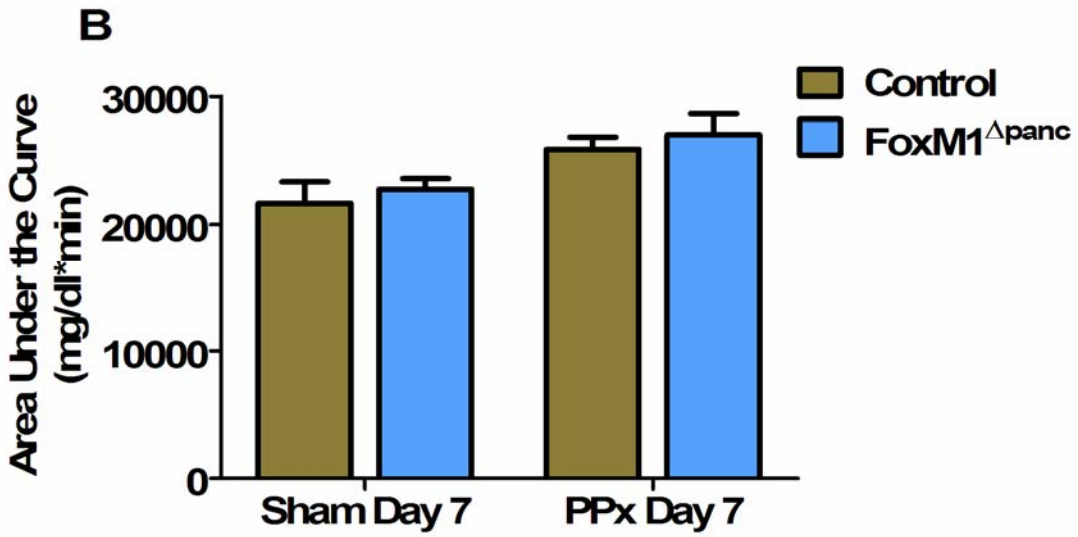

Figure 26. Glucose tolerance was maintained in Control and FoxM1$^{\Delta panc}$ mice following 60% PPx. (A) IPGTTs were performed in FoxM1$^{\Delta panc}$ and Control female mice 1 week after 60% PPx or a Sham operation. **(B)** Area under the curve (AUC) for glucose was calculated based on blood glucose levels during IPGTT in FoxM1$^{\Delta panc}$ and Control female mice 1 week after 60% PPx or a Sham operation. Error bars represent SEM. Two-way ANOVA with Bonferroni's post-tests was used to measure significance. n=5-7 per group.

Regeneration of β cell mass within the splenic lobe was specifically impaired in FoxM1$^{\Delta panc}$ mice.

Similar to FoxM1$^{\Delta panc}$ male mice (Zhang H *et al.*, 2006), FoxM1$^{\Delta panc}$ female mice also exhibited ~40% reduced β cell mass at 9 weeks of age compared to littermate Controls (1.07 mg versus 1.62 mg), although FoxM1$^{\Delta panc}$ female mice remained normoglycemic. This ~40% reduction in β cell mass was unchanged after a Sham operation (Figure 27A), but was specifically due to a reduction in β cell mass within the splenic, not duodenal, pancreatic lobe (Figure 27C,E). Furthermore, the reduction in β cell mass was specific to the endocrine compartment of the pancreas, as neither total pancreatic weight nor weights of the individual lobes was different between Control and FoxM1$^{\Delta panc}$ mice (Figure 27B,D,F). There was also no significant difference in total pancreatic area on sections (data not shown). Consistent with previous findings (Spooner *et al.*, 1970), a significant majority of β cell mass was located within the splenic lobe of Control mice after a Sham operation versus the duodenal lobe (Figure 27C,E) ($P<0.01$).

PPx effectively eliminated most of the tissue from the splenic lobe, although a relatively small amount of acinar and endocrine tissue remained attached to the main pancreatic duct after the procedure (Figure 27D, 28A,C). Within 7 days, a significant and equivalent amount of tissue regenerated in both FoxM1$^{\Delta panc}$ and Control mice (Figure 27D, 28B,D), suggesting that overall pancreas regeneration during this time period was not impaired by *Foxm1* deletion. β cell mass regeneration within the splenic lobe, however, was impaired in FoxM1$^{\Delta panc}$ mice, as β cell mass in these mice did not significantly increase within 7 days following PPx, in contrast to Control littermates (Figure 27C). There were no significant alterations in tissue weight or β cell mass within the duodenal lobe of Control or FoxM1$^{\Delta panc}$ mice following 60% PPx (Figure 27E,F).

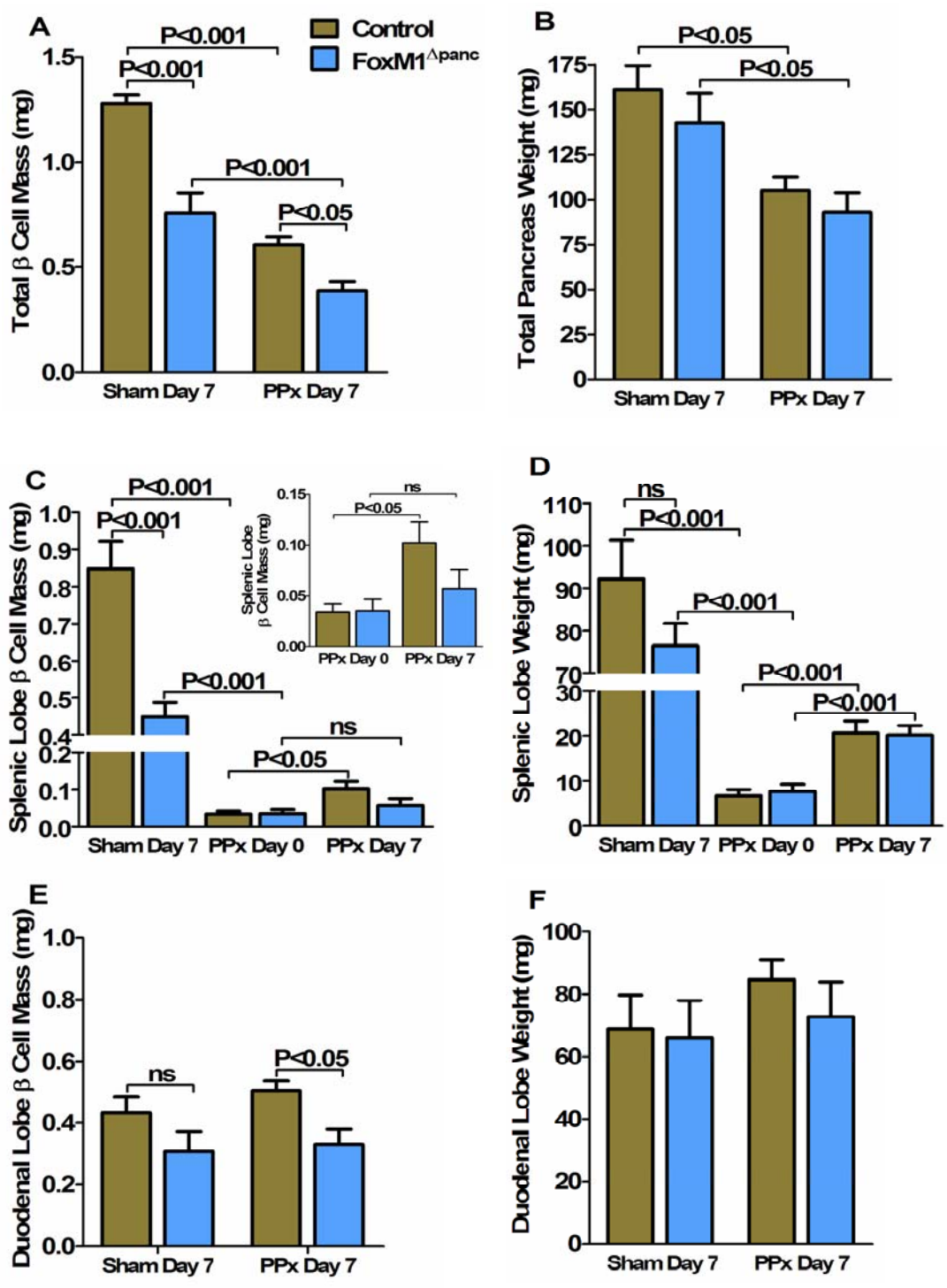

Figure 27. β cell mass and pancreas weight in Control and FoxM1$^{\Delta panc}$ mice after 60% PPx or a Sham operation. **(A)** Total β cell mass and **(B)** pancreas weight. **(C)** Splenic lobe β cell mass and **(D)** weight. **(E)** Duodenal lobe β cell mass and **(F)** weight. Error bars represent SEM. Two-way ANOVA with Bonferroni's post-tests was used to measure significance. ns=not significant. n=4-6 per group.

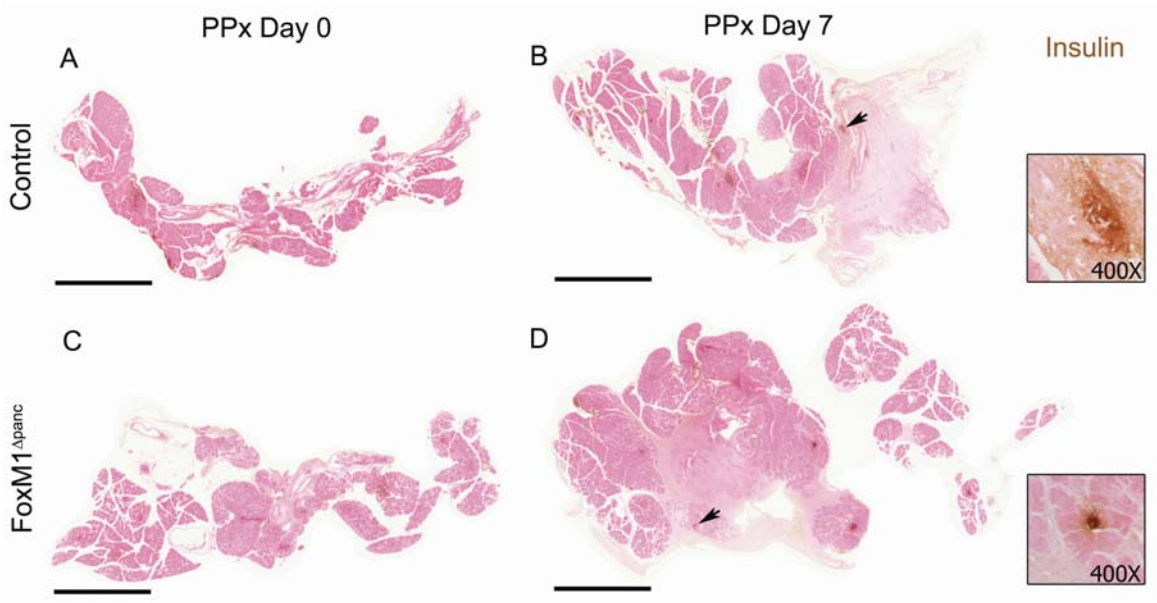

Figure 28. Regeneration of the splenic lobe was observed within 7 days after 60% PPx in Control and FoxM1$^{\Delta panc}$ mice. Sections through the splenic lobe of Control **(A, B)** and FoxM1$^{\Delta panc}$ pancreata **(C, D)** at either Day 0 **(A, C)** or Day 7 **(B, D)** following PPx were labeled with anti-insulin antibody (brown) and counterstained with eosin. The majority, but not all, of the endocrine and exocrine tissue was removed by the PPx operation, and an increased amount of tissue was observed 7 days later in both groups of mice. Larger islets were observed in Control mice than in FoxM1$^{\Delta panc}$ mice, and in both groups of mice there was evidence of islet neogenesis within newly-differentiating portions of the splenic lobe (arrowheads, insets). Scale bar = 1 mm.

β cell proliferation was reduced in FoxM1$^{\Delta panc}$ mice compared to Controls after 60% PPx.

Because β cells are replenished primarily by self-replication (Dor *et al.*, 2004), and FoxM1 is important for postnatal β cell proliferation (Zhang H *et al.*, 2006), it seemed likely that reduced β cell proliferation contributed to the impaired β cell mass regeneration observed in FoxM1$^{\Delta panc}$ mice. Indeed, PPx dramatically stimulated β cell proliferation in both pancreatic lobes of Control mice, and these effects were significantly blunted in FoxM1$^{\Delta panc}$ mice (Figure 29A-F). Moreover, β cell proliferation within the duodenal lobe of FoxM1$^{\Delta panc}$ mice did not significantly increase after PPx.

β cell proliferation in the splenic lobe of FoxM1$^{\Delta panc}$ mice did increase significantly following PPx versus Sham, despite *Foxm1* deletion (Figure 29E), due to increased proliferation of β cells within small endocrine cell clusters (8 or fewer insulin^{+} cells) and definitive islets (9 or more insulin^{+} cells) (Figure 30A,C). However, β cell proliferation within definitive islets was significantly reduced in FoxM1$^{\Delta panc}$ versus Control mice (Figure 30C). Because there was no significant impairment in β cell proliferation in small endocrine cell clusters in FoxM1$^{\Delta panc}$ mice, we hypothesized that these represented newly-formed β cells that did not require FoxM1 for proliferation. This hypothesis was supported by the finding that embryonic β cell proliferation did not require FoxM1 (Figure 31A,B). Additionally, proliferation of β cells within small endocrine cell clusters after PPx was specifically stimulated in the regenerating splenic lobe (Figure 30A), but not duodenal lobe (Figure 30B). These data suggest that just as perinatal β cells can proliferate in the absence of FoxM1, newly-differentiated β cells in the adult can undergo several rounds of FoxM1-independent replication prior to switching to FoxM1-dependent proliferation.

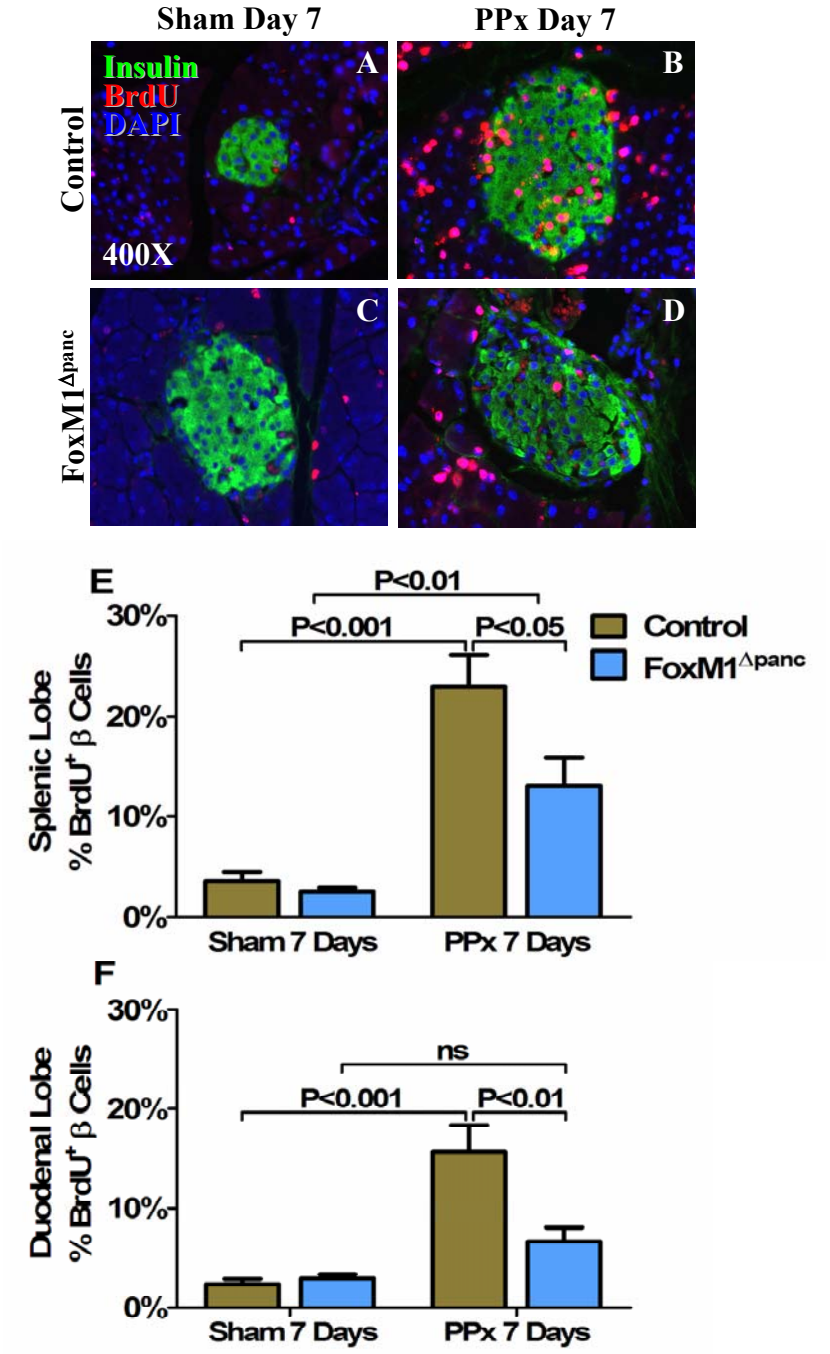

Figure 29. β cell proliferation was reduced in FoxM1$^{\Delta panc}$ mice after 60% PPx. Low levels of β cell proliferation were observed in the splenic lobes of Control **(A)** and FoxM1$^{\Delta panc}$ **(C)** mice after a Sham operation. PPx enhanced BrdU incorporation into all pancreatic cell types within the splenic lobe of Control mice **(B)**, but incorporation into endocrine cells was reduced in FoxM1$^{\Delta panc}$ mice **(D)**. β cell proliferation was quantified for both the splenic **(E)** and duodenal **(F)** pancreatic lobes. Error bars represent SEM. Two-way ANOVA with Bonferroni's post-tests was used to measure significance. ns=not significant. n=4-5 per group

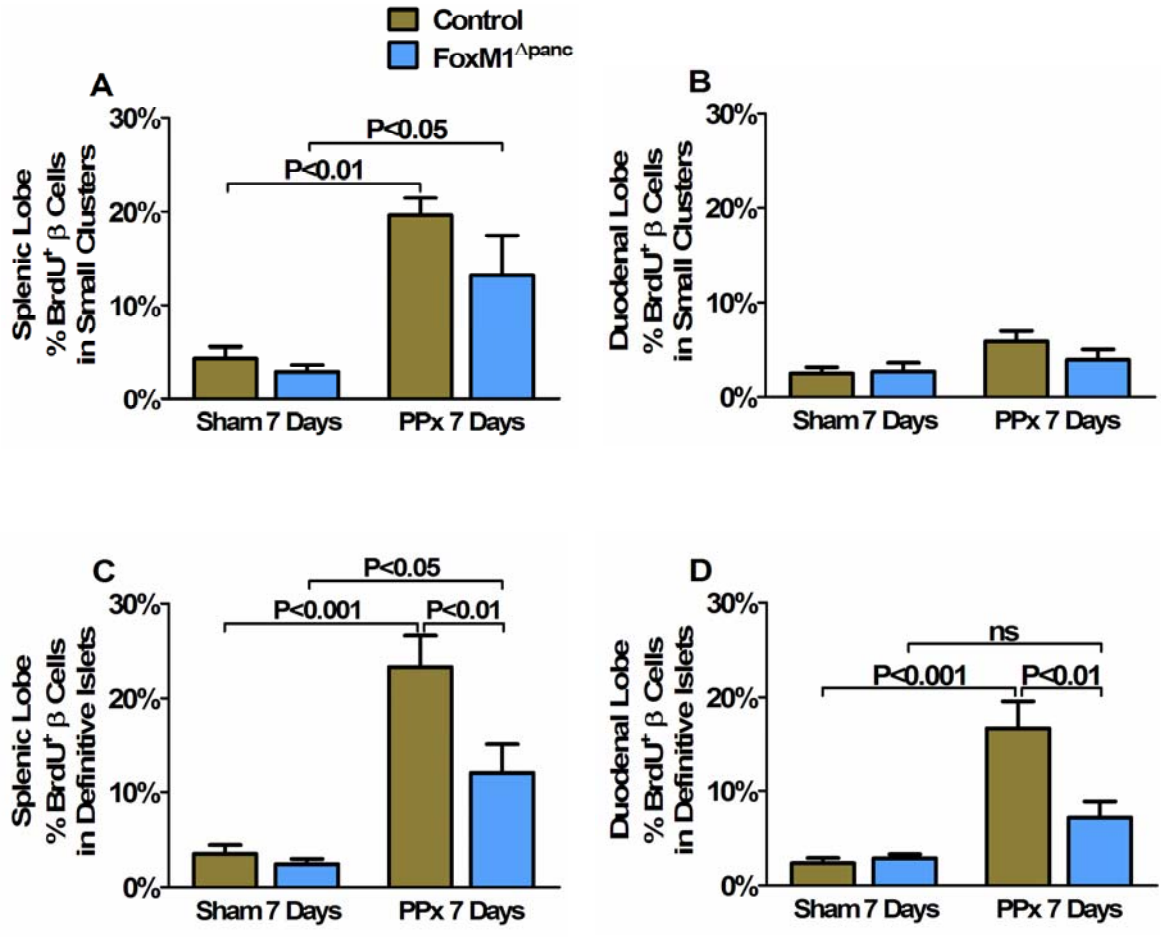

Figure 30. β cell proliferation was only reduced in definitive islets, but not small endocrine cell clusters, in FoxM1$^{\Delta panc}$ versus Control mice after 60% PPx. β cell proliferation within small endocrine cell clusters (≤8 β cells) after PPx versus Sham was similarly enhanced in the splenic lobes of FoxM1$^{\Delta panc}$ and Control mice **(A)**, but was not significantly altered in the duodenal lobes **(B)**. β cell proliferation within definitive islets (≥9 β cells) after PPx was enhanced in the splenic lobe of Control mice, and this effect was partially inhibited in FoxM1$^{\Delta panc}$ mice **(C)**. PPx also significantly stimulated β cell proliferation within definitive islets in the duodenal lobe of Control, but not FoxM1$^{\Delta panc}$, mice **(D)**. Error bars represent SEM. Two-way ANOVA with Bonferroni's post-tests was used to measure significance. ns=not significant. n=4-5 per group

Table 3. Summary of β cell proliferation results for Control and FoxM1$^{\Delta panc}$ mice after Sham versus PPx.

	β Cell Proliferation in Clusters	**β Cell Proliferation in Islets**
Control PPx vs. Sham		
Splenic Lobe	↑	↑
Duodenal Lobe	↔	↑
FoxM1$^{\Delta panc}$ PPx vs. Sham		
Splenic Lobe	↑	↑
Duodenal Lobe	↔	↔
FoxM1$^{\Delta panc}$ Sham vs. Control Sham		
Splenic Lobe	↔	↔
Duodenal Lobe	↔	↔
FoxM1$^{\Delta panc}$ PPx vs. Control PPx		
Splenic Lobe	↔	↓
Duodenal Lobe	↔	↓

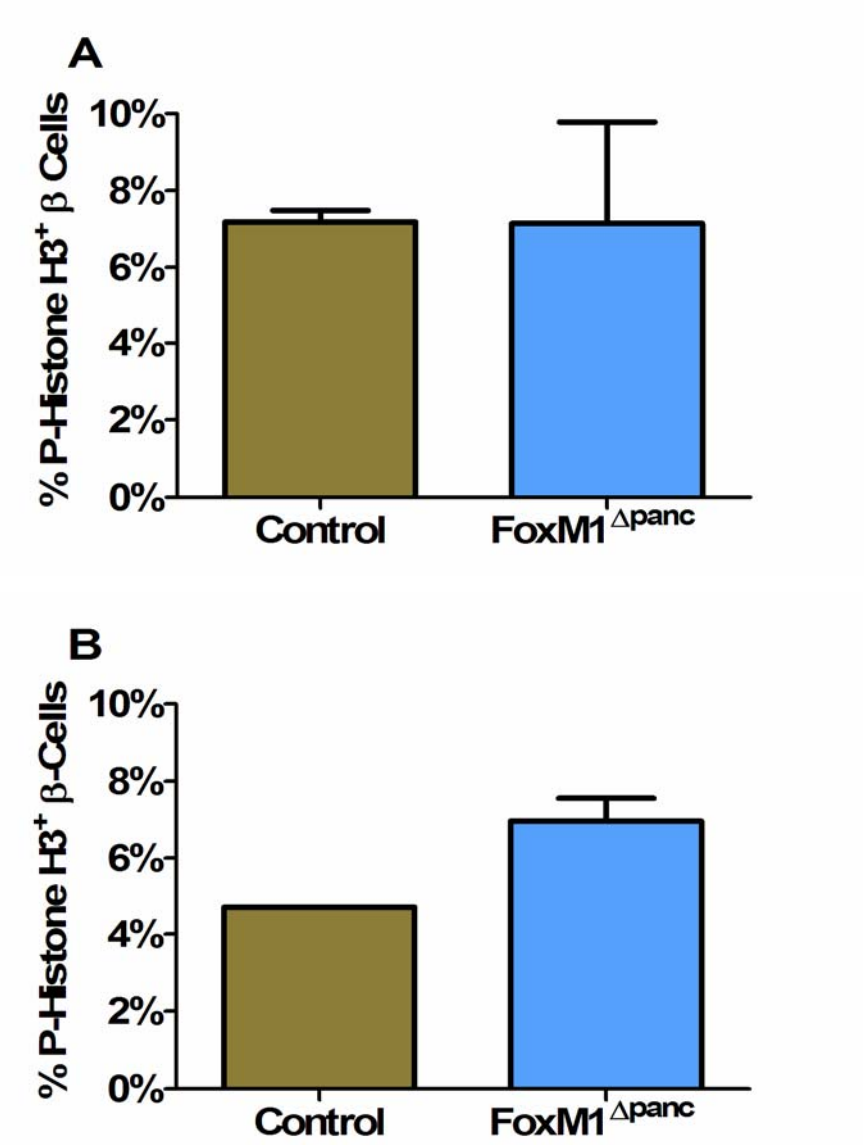

Figure 31. β cell proliferation was unaffected in FoxM1$^{\Delta panc}$ embryos versus Control littermates. Phospho-histone H3 labeling at e17.5 **(A)** and e18.5 **(B)** was used to measure β cell proliferation. Error bars represent SEM. Unpaired t-test was used to measure significance. n=2-3 per group.

PPx stimulated β cell proliferation within definitive islets of Control mice to the same extent (7-fold) in both the splenic and duodenal lobes versus Sham (Figure 30C,D). In contrast, proliferation in the splenic lobe of FoxM1$^{\Delta panc}$ mice increased only 5-fold, while the increase within the duodenal lobe was not significant, suggesting that proliferation of pre-existing β cells was impaired in the absence of FoxM1. The increased BrdU incorporation within definitive islets in the splenic lobe of FoxM1$^{\Delta panc}$ mice 7 days after PPx versus Sham (Figure 30C) may represent proliferation that occurred at an earlier stage of new islet development. These results are summarized in Table 3.

Similar to the results observed for the β cell population, α cell proliferation was also stimulated by PPx in Control mice, and this effect was significantly blunted in FoxM1$^{\Delta panc}$ mice (Figure 32A). In contrast, acinar (Figure 32B) and ductal cell (Figure 32C) proliferation were not impaired in FoxM1$^{\Delta panc}$ mice compared to Control mice after PPx. In fact, acinar proliferation was enhanced in FoxM1$^{\Delta panc}$ mice, perhaps in part as a compensatory mechanism due to reduced islet regeneration. However, no differences in gross splenic lobe weight nor acinar cell number were apparent between the two genotypes (Figure 27D and data not shown). These results indicate that FoxM1 is specifically required for endocrine cell proliferation in the pancreas following PPx.

FoxM1$^{\Delta panc}$ mice exhibited increased β cell and nucleus size compared to Controls.

Sham-operated FoxM1$^{\Delta panc}$ mice exhibited larger average β cell size in both pancreatic lobes (Figure 33A,B) versus Control littermates, due in part to increased β cell nucleus size (Figure 33C,D). However, enlarged nuclei alone could not account for the

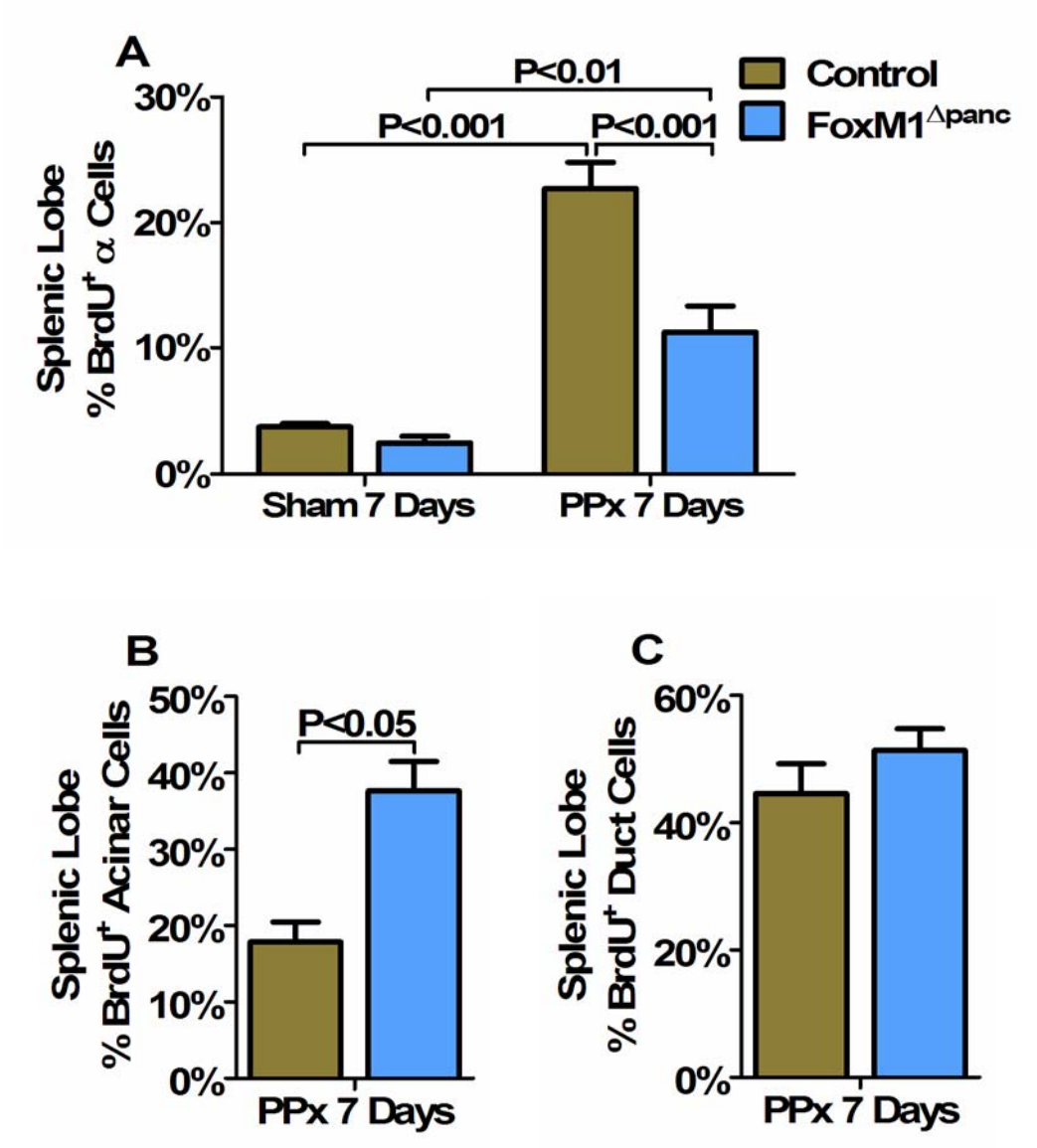

Figure 32. α cell proliferation was reduced in FoxM1$^{\Delta panc}$ mice after 60% PPx, but acinar and ductal cell proliferation were not impaired. BrdU incorporation into α cells **(A)**, acinar cells **(B)**, and duct cells **(C)** was measured in Control and FoxM1$^{\Delta panc}$ mice after PPx or Sham. Error bars represent SEM. Two-way ANOVA with Bonferroni's post-tests was used to measure significance. n=3-5 per group

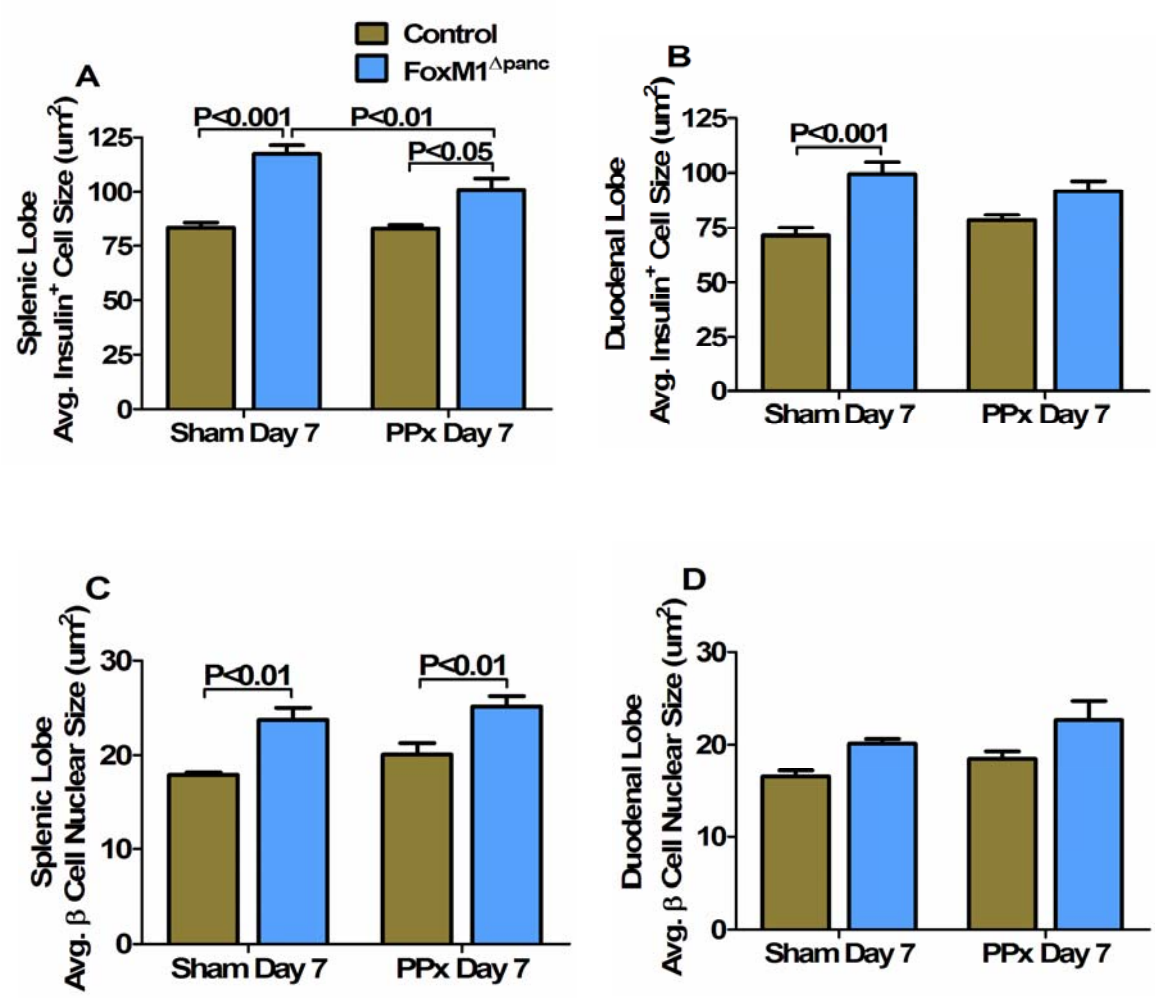

Figure 33. FoxM1$^{\Delta panc}$ mice exhibited increased β cell and nucleus size. After a Sham operation, FoxM1$^{\Delta panc}$ mice exhibited increased β cell size in both the splenic **(A)** and duodenal **(B)** pancreatic lobes. Increased β cell size was also observed after PPx in the splenic lobe of FoxM1$^{\Delta panc}$ mice versus Controls but was significantly reduced compared to after a Sham operation. The average β cell size in Control pancreata was unchanged by PPx. FoxM1$^{\Delta panc}$ mice also exhibited increased β cell nucleus size in the splenic **(C)** but not duodenal **(D)** lobe, which was unchanged by PPx. Error bars represent SEM. Two-way ANOVA with Bonferroni's post-tests was used to measure significance. n=4-5 per group.

total increase in β cell size observed. Thus, cellular hypertrophy also contributed, likely as a compensatory measure due to reduced β cell number. Although PPx did not alter β cell size in Control mice, average β cell size was significantly reduced specifically within the splenic lobe of FoxM1$^{\Delta panc}$ mice after PPx, likely due to new β cell formation.

Islet size in FoxM1$^{\Delta panc}$ mice was reduced compared to Control mice following 60% PPx.

Although PPx reduced total β cell number within the splenic lobe, islets present within this lobe 7 days after PPx were of the same average size as after a Sham operation in Control mice (Figure 34A). However, FoxM1$^{\Delta panc}$ islets were significantly smaller 7 days after PPx compared to Sham. There was also a trend for the average islet size within the duodenal lobe of Control mice to increase following PPx versus Sham, but no islet expansion was observed in the duodenal lobe of FoxM1$^{\Delta panc}$ mice (Figure 34B). These data suggest that *Foxm1* deletion impairs islet growth after PPx. Of note, islets within the splenic lobe of Control mice after Sham operation were approximately twice as large as islets within the duodenal lobe ($P<0.05$), which may be due to a greater proportion of small endocrine cell clusters versus definitive islets normally found in the duodenal versus splenic lobe ($P<0.05$) (Figure 34C,D). Interestingly, after PPx FoxM1$^{\Delta panc}$ mice exhibited an increased proportion of small endocrine cell clusters versus definitive islets within their splenic lobe in comparison to Control mice (Figure 34C), which likely contributed to their reduced average islet size. No differences were observed in the proportion of small endocrine cell clusters between Control and FoxM1$^{\Delta panc}$ mice after Sham operation or within the duodenal lobe under any condition (Figure 34D). These data are consistent with the hypothesis that new insulin^{+} cell

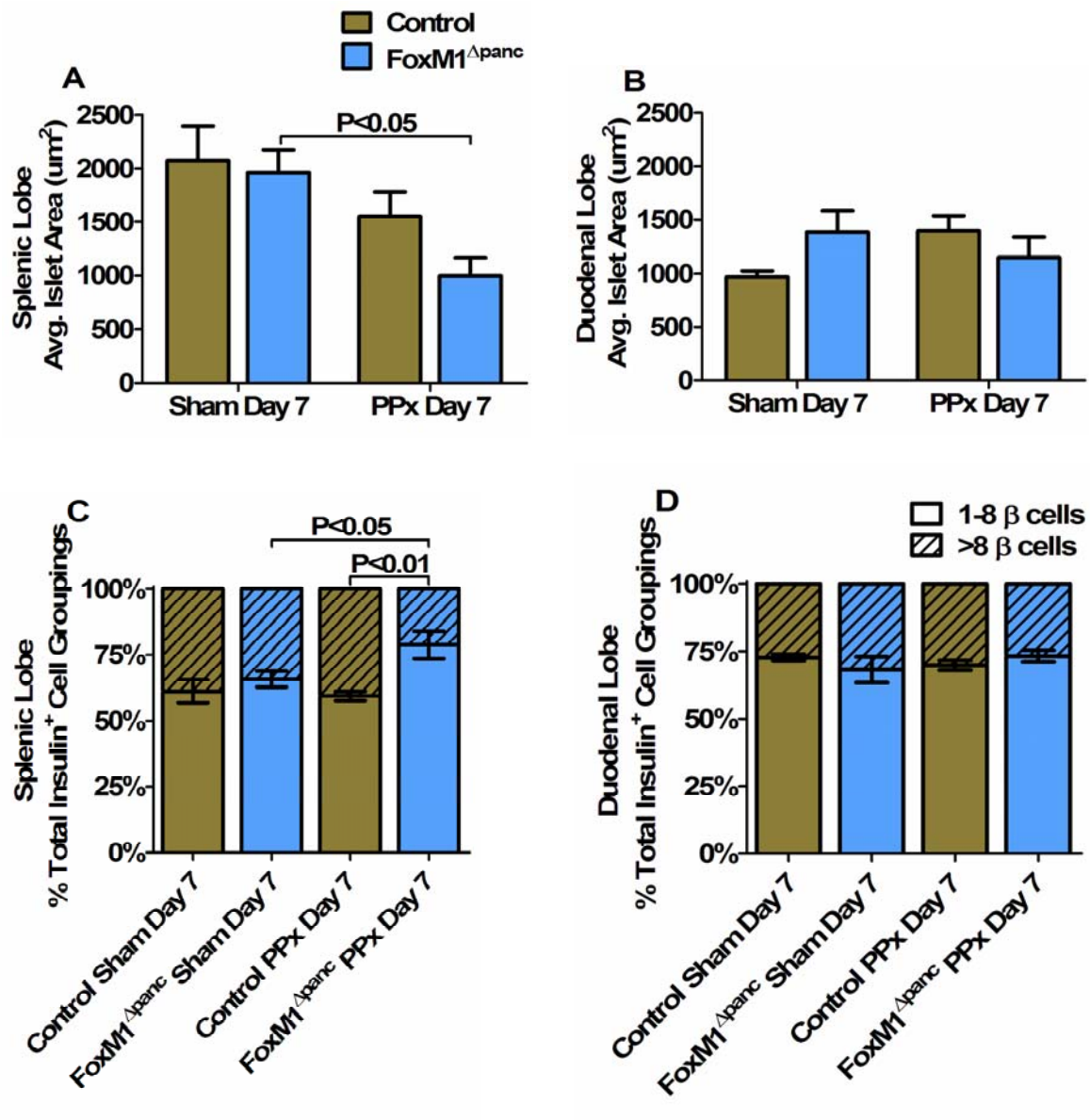

Figure 34. FoxM1$^{\Delta panc}$ mice exhibited impaired islet growth after 60% PPx. There was no significant difference in average islet size between Control and FoxM1$^{\Delta panc}$ mice after a Sham operation or PPx in either the splenic **(A)** or duodenal **(B)** pancreatic lobes. Following PPx, the average islet size in the splenic lobe of Control pancreata was similar to that observed in Sham-operated mice, but FoxM1$^{\Delta panc}$ islets were significantly reduced in size. Within the duodenal lobe, Control mice trended toward increased average islet size after PPx, but no increase was observed in FoxM1$^{\Delta panc}$ mice. **(C)** FoxM1$^{\Delta panc}$ mice specifically exhibited an increased proportion of small insulin^{+} cell clusters (1-8 β cells) within the splenic lobe after PPx, but **(D)** no differences were observed within the duodenal lobe. Error bars represent SEM. Two-way ANOVA with Bonferroni's post-tests was used to measure significance. n=4-5 per group

clusters form in the splenic/regenerating lobes after PPx, and that subsequent growth of these clusters is impaired by loss of FoxM1.

β cell neogenesis following 60% PPx was not impaired in FoxM1$^{\Delta panc}$ mice.

Islet density was significantly less in the splenic lobe of FoxM1$^{\Delta panc}$ mice versus Controls after a Sham operation (Figure 35A), but no differences were observed in the duodenal lobe between the two genotypes (Figure 35B). Interestingly, the density of insulin^{+} cell groupings in the splenic lobe of both FoxM1$^{\Delta panc}$ and Control mice trended toward an increase 7 days after PPx versus Day 0 (Figure 35A), and insulin^{+} cells were observed within foci of regeneration in the splenic lobes of both groups of mice (Figure 28B,D). However, islet density in the duodenal lobe was unchanged by PPx in either genotype. These data suggest that generation of new insulin^{+} cell groups, or neogenesis, occurs specifically in the splenic lobe after PPx and is not impaired in FoxM1$^{\Delta panc}$ mice. In support of these findings, Ngn3, a marker of endocrine progenitor cells (Gradwohl *et al.*, 2000), was observed in ductal epithelial cells in both Control (Figure 35C) and FoxM1$^{\Delta panc}$ (Figure 35D) mice following PPx. Importantly, Ngn3 expression was only observed in ductules within the regenerating portion of the splenic lobe, but not within differentiated pancreas tissue. Furthermore, no difference in the number of Ngn3^{+} ductal epithelial cells was detected between Control and FoxM1$^{\Delta panc}$ mice following PPx.

***FOXM1c* over-expression did not enhance β cell mass regeneration following 60% PPx.**

To determine whether FoxM1 over-expression affects pancreas and β cell regeneration following PPx, *Rosa26-FOXM1c* Tg mice were used, which constitutively

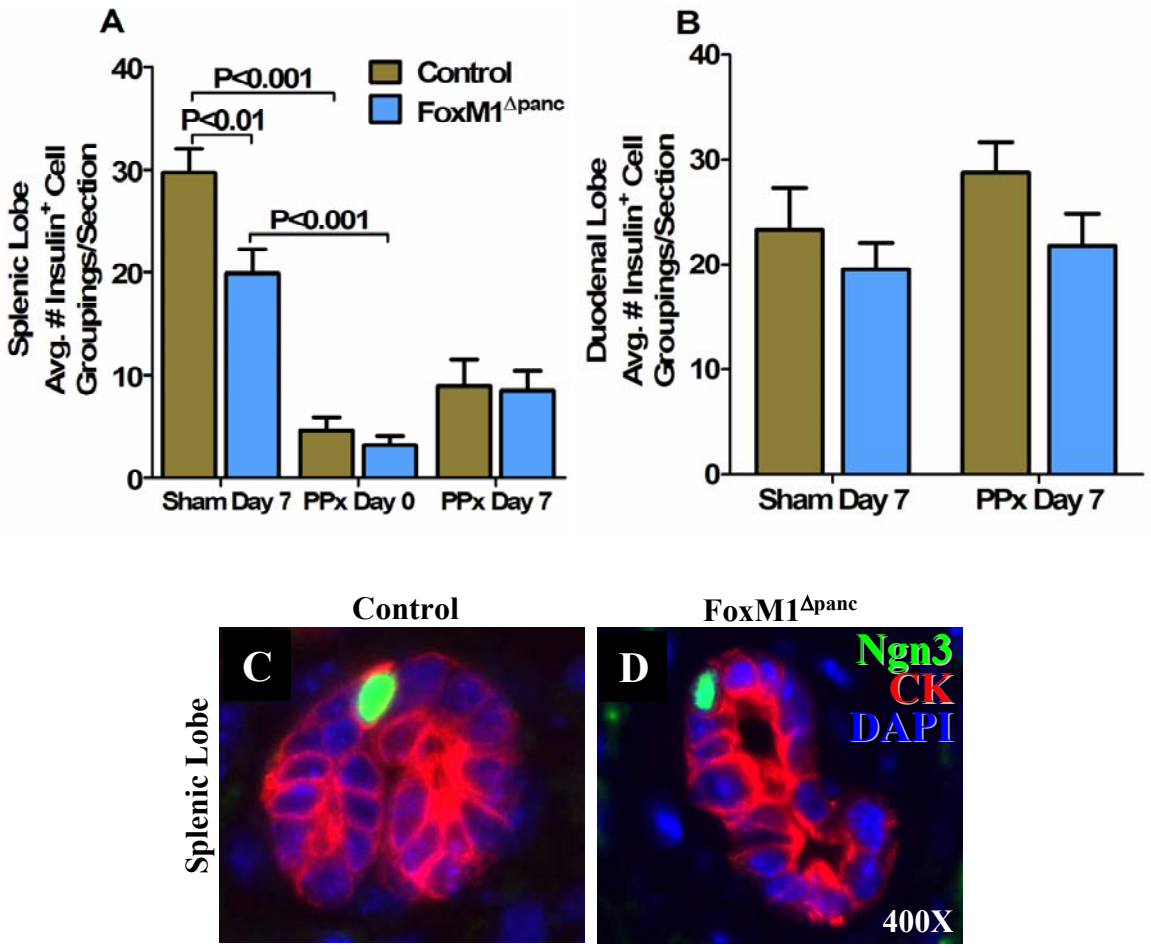

Figure 35. FoxM1$^{\Delta panc}$ mice did not exhibit impaired β cell neogenesis after 60% PPx. **(A)** The number of insulin^{+} cell groupings per section (islet density) was reduced within the splenic lobe of FoxM1$^{\Delta panc}$ mice compared to Control littermates after a Sham operation, but at Day 0 and Day 7 following PPx, the number of insulin^{+} cell groupings per section was equivalent between FoxM1$^{\Delta panc}$ and Control mice. 7 days after PPx, there was a trend in both groups of mice to show increased numbers of insulin^{+} cell groupings per section within the splenic lobe compared to Day 0. **(B)** No differences in islet density were observed between any groups of mice in the duodenal lobe. **(C)** Ngn3 expression was detected only after PPx within cytokeratin^{+} (CK^{+}) ductal epithelial cells located within foci of regeneration in the splenic lobes of both Control and **(D)** FoxM1$^{\Delta panc}$ mice. Error bars represent SEM. Two-way ANOVA with Bonferroni's post-tests was used to measure significance. n=4-5 per group.

and ubiquitously over-express human *FOXM1c* (Kalinichenko *et al.*, 2003). Despite *FOXM1c* over-expression within islets (Figure 36A), Tg mice exhibited no significant differences in glucose tolerance (Figure 36B) nor β cell mass following PPx (Figure 37A) compared to wild-type (WT) littermates. Furthermore, no differences in pancreatic tissue weight (Figure 375B), average islet size (Figure 37C), or islet density (Figure 37D) were observed between Tg and WT mice in either lobe. Preliminary analyses also revealed no obvious differences in β cell proliferation within the splenic/regenerating lobe of Tg and WT mice after PPx (Figure 37E). Additionally, no significant changes in transcript levels of the FoxM1 targets *Plk1* or *Cenp-a*, or of the cell cycle regulator *Ccnd2*, were observed in *Rosa26-FOXM1c* Tg versus Control islets (data not shown).

Discussion

FoxM1 is highly expressed within pancreatic endocrine cells during embryogenesis and is down-regulated with age (Figure 14A-C) (Zhang H *et al.*, 2006), corresponding with reduced β cell proliferation. Our laboratory previously showed that mice with *Foxm1* deleted throughout the pancreatic epithelium ($FoxM1^{\Delta panc}$) exhibit impaired growth and maintenance of postnatal β cell mass secondary to reduced postnatal β cell proliferation, associated with increased nuclear-localized $p27^{Kip1}$ and premature cellular senescence (Zhang H *et al.*, 2006). Several of FoxM1's direct transcriptional targets inhibit $p27^{Kip1}$ by promoting its ubiquitination and subsequent degradation (Skp2, Cks1) (Wang *et al.*, 2005) or its nuclear export (KIS) (Petrovic *et al.*, 2008). The study presented here showed that $FoxM1^{\Delta panc}$ mice have impaired β cell mass regeneration

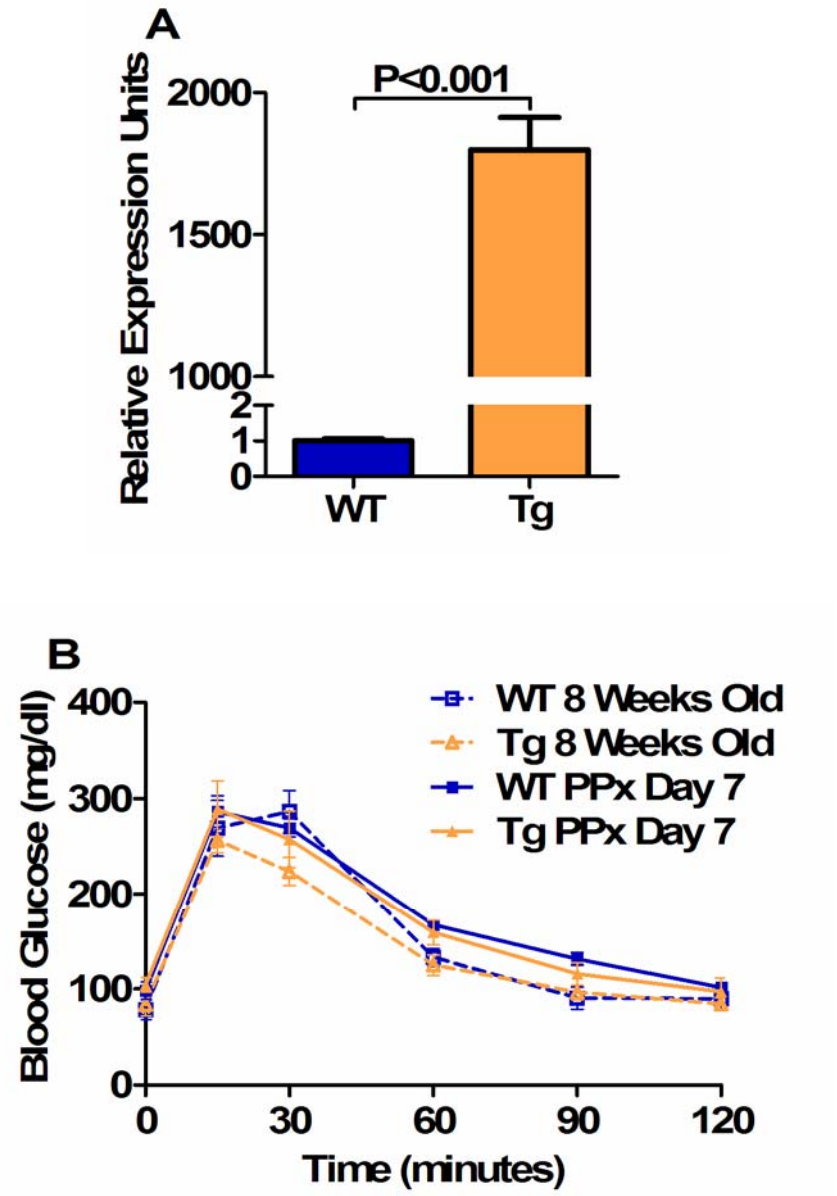

Figure 36. Over-expression of FOXM1C had no effect on glucose tolerance. (A) Real-time qRT-PCR with primers specific to human *FOXM1c* was performed on RNA extracted from isolated islets from 9 week old WT and *Rosa26-FOXM1c* Tg mice. **(B)** Tg mice did not display any significant differences in glucose tolerance after a sham operation or PPx. Error bars represent SEM. Unpaired t-test was used to measure significance for A. Two-way ANOVA with Bonferroni's post-tests was used to measure significance for B. n=2-3 WT, 4-5 Tg.

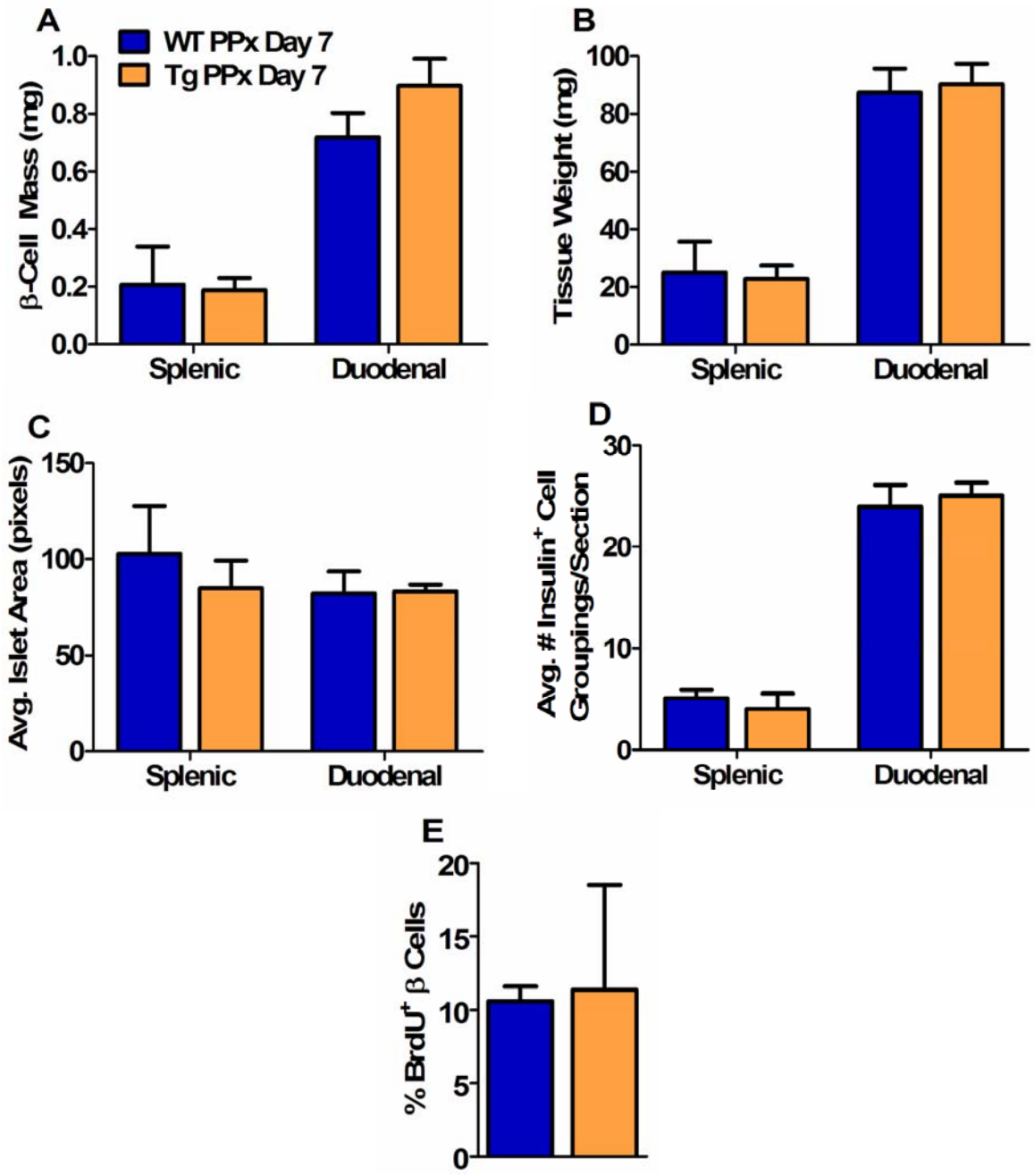

Figure 37. Over-expression of FOXM1C had no effect on β cell regeneration after 60% PPx. No differences were observed in β cell mass **(A)**, pancreas weight **(B)**, average islet size **(C)**, or average number of insulin$^+$ cell groupings per section (islet density) **(D)** after PPx in either the splenic or duodenal pancreatic lobes of *Rosa-FOXM1c* Tg mice compared to WT littermates. Islet size and number were obtained from the same images used to measure β cell mass. **(E)** β cell proliferation in the splenic lobe after PPx was also similar between *Rosa-FOXM1c* Tg and WT mice. Error bars represent standard error of the mean (SEM). Unpaired t-test was used to measure significance. n=2-3 WT, 4-5 Tg for A-D. n=2 per group for E.

following PPx, due to reduced β cell proliferation, but there was no evidence that neogenesis was affected by loss of FoxM1.

60% PPx is a normoglycemic pancreatic injury model that stimulates regeneration by (1) differentiation and proliferation and (2) hyperplasia of pre-existing tissue. This study revealed that *Foxm1* and some of its targets were up-regulated within islets following PPx during a period of enhanced α and β cell proliferation, leading to the hypothesis that FoxM1 is required for injury-stimulated endocrine cell proliferation. Indeed, FoxM1$^{\Delta panc}$ mice exhibited impaired α and β cell proliferation and impaired β cell mass regeneration following PPx. PPx stimulated β cell proliferation in both the splenic (regenerating) and duodenal (expanding) lobes of Control mice, but not in the duodenal lobe of FoxM1$^{\Delta panc}$ mice. Thus, hyperplasia of pre-existing β cells after injury requires FoxM1.

Interestingly, PPx-stimulated β cell proliferation was blunted but not completely inhibited within the splenic lobe of FoxM1$^{\Delta panc}$ mice, due at least in part to impaired proliferation of β cells in definitive islets, but not small endocrine cell clusters, in the absence of FoxM1. Of course, small clusters of insulin^{+} cells are not necessarily newly-formed, as a certain amount of such clusters are normally present in the adult pancreas. Furthermore, because islet size and insulin^{+} cell number were quantified using two-dimensional histology, it is possible that some of the clusters included in these analyses were in fact the edges of larger islets. However, because Control and FoxM1$^{\Delta panc}$ mice were analyzed in a similar manner, it is unlikely that this method skewed the data based on genotype, although comparisons between Sham, Day 0, and Day 7 may have been

affected. To avoid this caveat, three-dimensional analyses of re-constituted confocal z-stacks could be used to more accurately determine cluster and islet size.

The proliferation data presented here suggest that another pathway(s), which may mimic that utilized during embryonic pancreas development, compensates for loss of FoxM1 during regeneration, as FoxM1 was also not required for embryonic β cell proliferation. Thus, pre-existing β cells seemingly exhibit a stronger requirement for FoxM1 than do new β cells formed by neogenesis. Although it is currently unclear which factors are required for β cell proliferation during embryogenesis and following islet neogenesis, this study supports the hypothesis that neogenesis in the adult is similar to embryonic β cell development, both with regard to re-expression of Ngn3 and initial FoxM1-independent proliferation.

Because BrdU was administered over 7 days, this study may have under-estimated the effects of *Foxm1* deletion on endocrine cell proliferation. Previous studies have shown that *Foxm1*$^{-/-}$ cells can undergo multiple rounds of DNA synthesis without karyo- or cytokinesis (endoreduplication), resulting in polyploid nuclei (Krupczak-Hollis *et al.*, 2004). Evidence of polyploid β cells and exocrine cells were observed in FoxM1$^{\Delta panc}$ mice, and these cells would have been counted as proliferating cells in this study, but would not have actually resulted in increased cell number. This phenomenon could partially explain the increased BrdU incorporation in β cells without significant β cell mass regeneration within the splenic lobe of FoxM1$^{\Delta panc}$ mice after PPx compared to Sham, although it most likely would not be restricted to one lobe. Labeling with phospho-histone H3 may yield different results, as this protein is specifically phosphorylated during mitosis (Dai *et al.*, 2005), and such labeling would be a useful

addition to these experiments. However, it may be necessary to analyze phospho-histone H3 labeling at multiple time points following PPx, as the time course of stimulated β cell proliferation may vary between Control FoxM1$^{\Delta panc}$ mice.

Additionally, incomplete *Foxm1* recombination could have resulted in mosaic expression, allowing some β cells to continue proliferating in FoxM1$^{\Delta panc}$ mice. However, this is unlikely because *Pdx1*$^{5.5kb}$-*Cre* was previously shown to recombine the *Rosa26-LacZ* reporter allele within all endodermally-derived pancreatic cells and to yield a significant reduction in FoxM1 protein by e15.5 (Zhang H *et al.*, 2006). Additionally, *Foxm1* transcripts were significantly reduced in FoxM1$^{\Delta panc}$ neonatal pancreas (Figure 38A) and even more dramatically in adult islets (Figure 38B). These tissues contain non-endodermally-derived mesenchymal, endothelial, and neuronal cells, which would not undergo *Foxm1* recombination, and thus likely account for remaining transcript expression. Verification of FoxM1 protein expression, or the lack thereof, could not be performed because antibodies to detect FoxM1 protein in mouse tissue do not currently exist.

Proliferation of α and β cells, but not acinar or ductal cells, was reduced in FoxM1$^{\Delta panc}$ mice versus Control littermates following PPx, suggesting that FoxM1 is required specifically within endocrine cells. These data concur with other studies showing that endocrine cells are particularly susceptible to perturbations in cell cycle regulation (Georgia and Bhushan, 2004; Kushner *et al.*, 2005a; Mettus and Rane, 2003; Rane *et al.*, 1999). The current study utilized qRT-PCR on islet RNA to assess changes in *Foxm1* expression following PPx. Lack of an anti-FoxM1 antibody precludes precise identification of the cell population(s) in which FoxM1 expression or localization

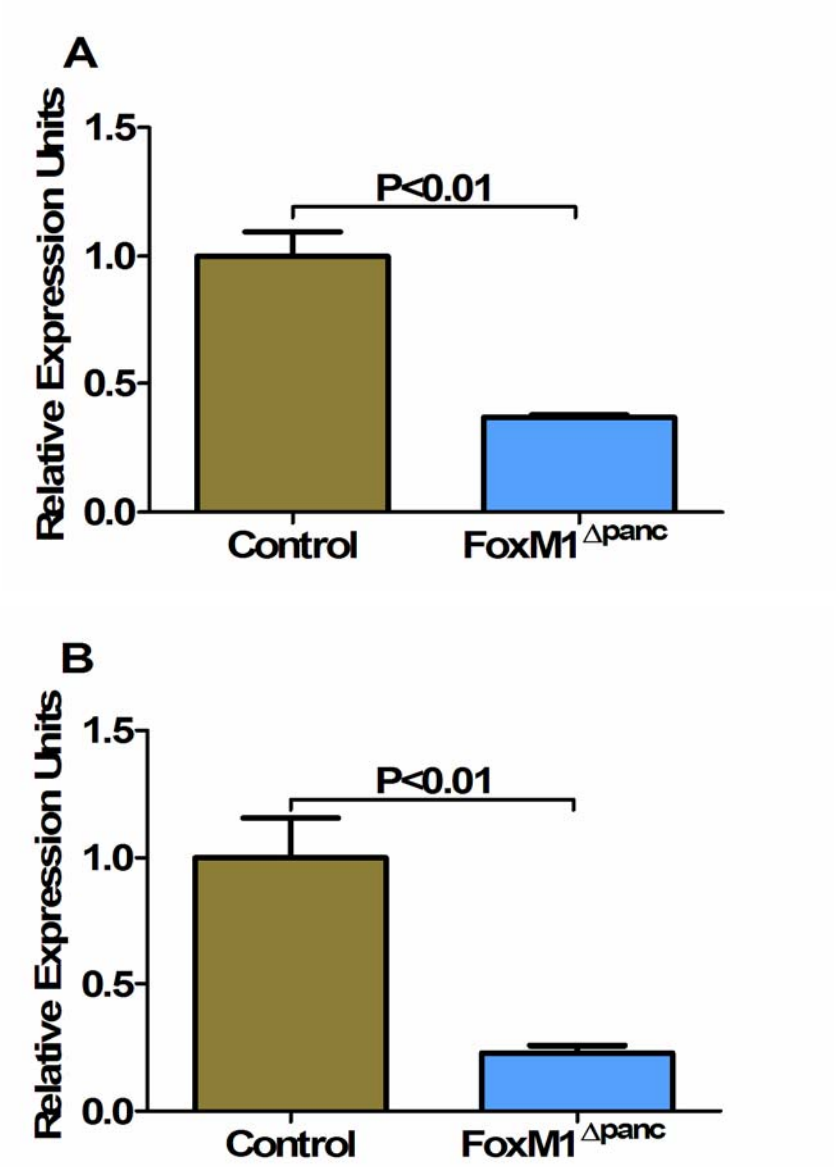

Figure 38. ***Foxm1*** **transcript levels were dramatically reduced in FoxM1$^{\Delta panc}$ mice versus Control littermates.** Real-time qRT-PCR was performed on RNA isolated from postnatal day 4 FoxM1$^{\Delta panc}$ and Control pancreata **(A)** and from isolated islets from 9 week old mice **(B)**. *Foxm1* transcript levels were reduced by 63% in postnatal day 4 FoxM1$^{\Delta panc}$ pancreata and by 77% in adult FoxM1$^{\Delta panc}$ islets. Error bars represent SEM. Unpaired t-test with Welch's correction was used to measure significance. n=3-5 per group.

changes with time and after PPx. Such studies will in the future allow for better understanding of cell type-specific requirements for FoxM1 and may help to explain the differing effects of FoxM1 absence that were observed between endocrine and exocrine cells following PPx. However, the expression analyses described here identified several potentially important regulators of pancreatic endocrine cell proliferation and regeneration that are themselves regulated by FoxM1 (*Plk1, Cenp-a*, *Birc5/Survivin*, *Ccnb1*).

This study also presented evidence of β cell neogenesis following 60% PPx, including $Ngn3^{+}$ duct cells, $insulin^{+}$ cells within regenerating tissue, and increased islet density. Although each finding alone is not sufficient to support neogenesis, all pieces of data together strongly indicate the occurrence of neogenesis. Importantly, these findings were equivalent between Control and $FoxM1^{\Delta panc}$ mice, revealing that β cell neogenesis in the adult mouse does not require FoxM1. Because neither β cell mass at birth (Zhang H *et al.*, 2006) nor embryonic β cell proliferation were altered in $FoxM1^{\Delta panc}$ mice, it is clear that β cell neogenesis during development also does not require FoxM1. Peshavaria *et al*. (Peshavaria *et al.*, 2006) showed increased small endocrine cell clusters by 2 days post-PPx, which normalized by 7 days. Although the definition of "cluster" in that work was based on $insulin^{+}$ area, while here "cluster" was defined by number of $insulin^{+}$ cells (in order to avoid confounding effects of β cell size on cluster area), the data presented here are consistent the findings of Peshavaria *et al*., as Control mice at 7 days post-PPx exhibited a normal proportion of small endocrine cell clusters. However, $FoxM1^{\Delta panc}$ mice had an increased proportion of small endocrine cell clusters at 7 days post-PPx, indicating that formation of these clusters is not impaired in the absence of FoxM1, but

significant growth is. These data support the hypothesis that initial proliferation of newly-differentiated β cells does not require FoxM1, but that these cells later switch to a FoxM1-dependent state. Unfortunately, current technology precludes real-time monitoring of β cell proliferation and islet growth. However, this study highlights the importance of β cell proliferation as a mechanism of β cell mass regeneration, as neogenesis, without adequate proliferation, was not sufficient to regenerate a significant amount of β cell mass in FoxM1$^{\Delta panc}$ mice after 60% PPx.

As β cell regeneration after partial duct ligation mimics embryonic β cell differentiation with Ngn3 re-expression (Xu *et al.*, 2008), it is not surprising that similar processes occur following 60% PPx, although perhaps to a lesser extent. In comparison to results published for ductal ligation (Xu *et al.*, 2008), relatively few ductule cells were found to express Ngn3 at 7 days after PPx (0-3 positive cells per 200X field of view). However, analysis at an earlier timepoint, such as 1-2 days after PPx when there is a significant increase in small insulin^{+} cell clusters (Peshavaria *et al.*, 2006), would likely reveal more Ngn3^{+} cells, as Ngn3 expression is transient in endocrine progenitors.

This is the first study to show Ngn3 re-expression following PPx, in contrast to several previous studies that concluded that after PPx, neogenesis and Ngn3 re-expression did not occur. However, the partial pancreatectomy procedures used in these studies were performed in a manner that likely precluded true regeneration. Lee *et al*. performed 50% PPx, in which the entire splenic lobe and pancreatic duct were surgically excised, and they reported no re-expression of Ngn3 in the remaining tissue by immunohistochemistry and *Ngn3-EGFP* knock-in analyses (Lee *et al.*, 2006). As we only observed Ngn3 expression in foci of regeneration within the splenic lobe after 60%

PPx, these results are not surprising. The data presented here and by others (Bonner-Weir *et al.*, 1993; Sharma *et al.*, 1999) reveal the importance of leaving the main pancreatic duct and splenic artery in order to stimulate differentiation of new pancreas tissue. Teta *et al*. also utilized 50% PPx, in conjunction with sequential thymidine analog labeling to assess proliferation, and they concluded that no specialized progenitors gave rise to new β cells in the adult because individual β cells only rarely incorporated more than one thymidine analog after PPx (Teta *et al.*, 2007). Again, complete removal of the splenic lobe and main pancreatic duct likely precluded differentiation of new pancreas tissue in this model. Furthermore, our results do not indicate that newly-formed β cells (in small clusters) undergo more proliferation than do pre-existing β cells (in definitive islets) in Control mice after 60% PPx. Dor *et al*. performed 60-70% PPx in a manner similar to that described here, but they did not analyze the splenic and duodenal lobes separately (Dor *et al.*, 2004). Based on β cell lineage labeling results, in which β cells were labeled with a heritable marker prior to PPx and no significant dilution of this label was observed after PPx, they concluded that neogenesis did not give rise to new β cells. Because the splenic lobe comprises only a small percentage of total pancreas weight and β cell mass after PPx (~20% after 7 days), and because the contribution of neogenesis and regeneration to new β cell formation is relatively small following PPx, it would be unlikely to detect any significant changes in the β cell lineage label using this technique without analyzing the splenic and duodenal lobes separately. The current study removed tissue from the splenic lobe, leaving the main pancreatic duct intact. This lobe was analyzed separately, and only specific foci of regeneration within the splenic lobe exhibited evidence of neogenesis. In contrast, the duodenal lobe, which was the sole or

primary source of tissue analyzed in the aforementioned studies, exhibited significant hyperplasia with no evidence of neogenesis after 60% PPx, in agreement with these other published works. Thus, this study does not contradict but adds to the current knowledge regarding the potential for pancreas regeneration and β cell neogenesis.

FOXM1C over-expression did not affect β cell regeneration following PPx, which could have been due to differences in activity between human FOXM1C and murine FoxM1, although both are transactivators. *Rosa26-FOXM1c* Tg mice were used for these experiments because mice over-expressing murine *Foxm1* or the more closely-related human *FOXM1b* have not yet been generated. However, these results suggest that over-expression of FoxM1 is not sufficient to elevate β cell proliferation, emphasizing that the β cell cell cycle is under tight negative regulatory control, even after injury. As reviewed (Cozar-Castellano *et al.*, 2006a), β cells express all of the cell cycle "brakes" studied thus far, but only some "accelerators". Thus, it may be more difficult than initially anticipated to stimulate β cell proliferation *in vivo* or *in vitro* as a therapeutic option for diabetic patients. Because FoxM1 positively regulates cell cycle accelerators and negatively regulates cell cycle brakes, it is of particular interest. However, because over-expression of FOXM1C did not seem up-regulate target genes in mouse islets *in vivo*, FoxM1 may not be a limiting factor for β cell proliferation. Alternatively, it may be necessary to directly activate FoxM1 in addition to over-expressing it in order to stimulate β cell proliferation. Thus, better understanding of post-translational and inhibitory regulators of FoxM1 will be essential for successful manipulation of FoxM1 activity in β cells.

CHAPTER IV

INVESTIGATING THE ROLE OF FOXM1 IN β CELL HYPERPLASIA IN RESPONSE TO DIET-INDUCED OBESITY

Introduction

Obesity is a primary risk factor for developing Type II diabetes (Staff, 2007), and it has been well-characterized that increased adiposity leads to insulin resistance, as reviewed in (Kahn *et al.*, 2006). Insulin resistance is known to stimulate β cell compensation via enhanced insulin secretory function and expansion of β cell mass in order to produce more insulin in an attempt to maintain normoglycemia. Genetic mouse models of insulin resistance have been generated by deletion of the insulin receptor (IR) (Okada *et al.*, 2007; Cohen *et al.*, 2007), Irs1 (Tamemoto *et al.*, 1994; Araki *et al.*, 1994), or Irs2 (Withers *et al.*, 1998; Kubota *et al.*, 2000; Kubota *et al.*, 2004). Spontaneous mutations in the genes encoding leptin (*ob*/*ob*) (Lindstrom, 2007) or the leptin receptor (*db*/*db*) (Chen *et al.*, 1996) also resulted in obesity and insulin resistance. Additionally, mouse models of diet-induced obesity have been shown to exhibit insulin resistance. In particular, high-fat diets cause the most dramatic effects on body weight and insulin resistance, and the C57Bl/6 mouse strain is most susceptible to these effects (Collins *et al.*, 2004).

In rodents, β cell mass expansion in response to insulin resistance occurs primarily via increased proliferation (Zhong *et al.*, 2007) and secondarily via β cell hypertrophy (Lingohr *et al.*, 2002). C57Bl/6 mice fed a high-fat diet exhibit 2.2-fold increases in β cell mass and proliferation within four months compared to mice fed a

control diet (Sone and Kagawa, 2005). Rodent studies have shown that both hyperglycemia and hyperlipidemia stimulate β cell proliferation, both under acute and chronic conditions (Bonner-Weir *et al.*, 1989; Steil *et al.*, 2001). Furthermore, hyperinsulinemia stimulated by peripheral insulin resistance can act through the insulin/IGF-1 receptor on β cells to stimulate proliferation and promote survival (Bernal-Mizrachi *et al.*, 2001). Additionally, incretins, such as glucagon-like peptide 1 (GLP-1) and gastric inhibitory peptide (GIP), which are secreted by intestinal cells after feeding, can promote β cell proliferation and survival (Drucker, 2006). All of these stimuli also enhance β cell insulin secretory function. However, chronic exposure to these stimuli eventually results in β cell failure, characterized by apoptosis and senescence, reduced proliferation and β cell mass, and diabetes.

In contrast, obese humans undergo only an approximate 50% expansion of β cell mass compared to lean individuals (Butler *et al.*, 2003). Such expansion is primarily due to β cell neogenesis, with β cell proliferation being difficult to observe under any condition, which is consistent with the low replicative capacity of human versus rodent β cells, as discussed in (Butler *et al.*, 2007). Although Type II diabetes in humans progresses in a similar manner as in obese rodents (Rhodes, 2000), the majority of obese humans do not develop Type II diabetes (Mokdad *et al.*, 2001; Kahn *et al.*, 2006) suggesting that diet alone is not responsible, and that primary β cell dysfunction may play a role in pre-disposing some people to developing the disease. Type II diabetes, although a complex multifactorial disorder, is subject to high genetic risk and has been linked to several gene mutations, some of which likely affect β cell function (Permutt *et al.*, 2005; Sladek *et al.*, 2007; The Wellcome Trust Case Control Consortium, 2007). Thus,

identification of factors that play a role in regulating β cell mass expansion may give some insight into the pathogenesis of Type II diabetes, as well as provide putative therapeutic targets.

While FoxM1 has been identified as an important regulator of β cell proliferation and β cell mass growth after weaning in mice under normal conditions (Zhang H *et al.*, 2006), it was unknown whether FoxM1 was similarly required for β cell proliferation and β cell mass expansion stimulated by diet-induced obesity and insulin resistance. To address this question, FoxM1$^{\Delta panc}$ mice were placed on a high-fat/high-carbohydrate diet, and their physiological and islet responses were analyzed in comparison to Control littermates and to mice on a chow diet with moderate fat content (Figure 39).

In response to the high-fat diet, FoxM1$^{\Delta panc}$ female mice became obese to the same extent as did Control female littermates. Both Control and FoxM1$^{\Delta panc}$ mice on the high-fat diet displayed glucose intolerance, which was more prominent in FoxM1$^{\Delta panc}$ mice, but all mice on the chow diet remained glucose tolerant. FoxM1$^{\Delta panc}$ mice on the high-fat diet displayed reduced insulin secretion in response to glucose. Part of this impairment was explained by reduced β cell mass in FoxM1$^{\Delta panc}$ mice, which was also observed in chow-fed mice. However, no expansion of β cell mass was observed in Control mice in response to the high-fat diet, despite their ability to increase insulin secretion. Thus, the impaired insulin secretion observed in FoxM1$^{\Delta panc}$ mice may be due at least in part to β cell dysfunction rather than just reduced β cell number. Unfortunately, the failure of Control mice to under β cell mass expansion, and the lack of a significant increase in β cell proliferation, in response to the high-fat diet rendered this study inconclusive as to the role of FoxM1 in obesity-induced β cell mass compensation.

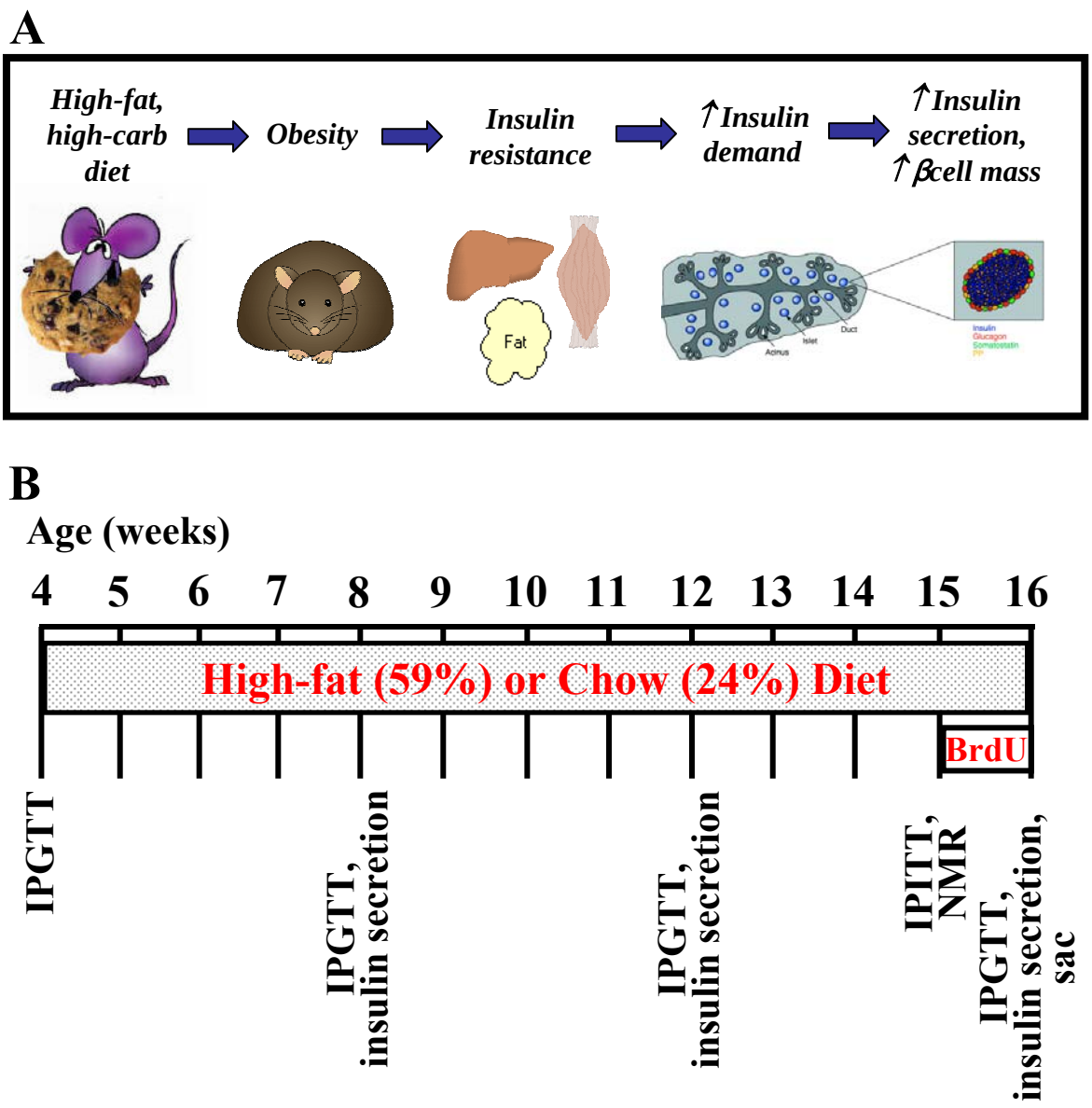

Figure 39. Diet-induced obesity. **(A)** High-fat/high-carbohydrate diets induce obesity, which causes insulin resistance in insulin target tissues such as liver, muscle, and fat. Insulin resistance results in an increased demand for insulin, which stimulates increased β cell insulin secretory function and β cell mass expansion. **(B)** Four week old mice were placed on either a high-fat/high-carbohydrate diet or a moderate-fat chow diet for 12 weeks. IPGTTs were performed at the start of the study and every 4 weeks thereafter. Insulin secretion was measured at 0 and 30 minutes during the IPGTT at 8, 12, and 16 weeks of age. At 15 weeks old, mice were subjected to IPITT and NMR body composition analysis and then given BrdU in the drinking water for 1 week. Mice were sacrificed at 16 weeks of age, after 12 weeks on the respective diets, and whole pancreas tissue was harvested.

The most likely reason this study failed was because the FoxM1$^{\Delta panc}$ and Control mice were on a mixed strain background. Therefore, a pilot study was performed to determine whether isogenic C57Bl/6 mice responded in the predicted ways to diet-induced obesity, and then FoxM1$^{\Delta panc}$ and Control mice were backcrossed to the C57Bl/6 background in order to repeat the study. These experiments verified that female mice on the C57Bl/6 strain background underwent β cell mass expansion in response to the high-fat diet.

Despite these setbacks, several interesting findings came from these studies that will be interesting to investigate further. First, a potential insulin secretory defect in FoxM1$^{\Delta panc}$ mice was identified by measuring plasma insulin levels before and after a glucose challenge. Preliminary results from islet perifusion and transcript expression analyses suggest that loss of FoxM1 may have other β cell effects in addition to regulating proliferation. Second, preliminary analysis of islet transcript expression suggested that *Foxm1* and some of its transcriptional targets were up-regulated within islets in response to the high-fat diet. Thus, follow-up of these studies is likely to yield interesting and important results regarding FoxM1's function in β cell adaptation.

Results

FoxM1$^{\Delta panc}$ and Control Mice on a Mixed Background

High-fat diet induced obesity in mixed background FoxM1$^{\Delta panc}$ and Control mice.

FoxM1$^{\Delta panc}$ and Control female littermates weighed the same amount at the outset of the study at 4 weeks of age (Figure 40A), prior to randomization into the two diet

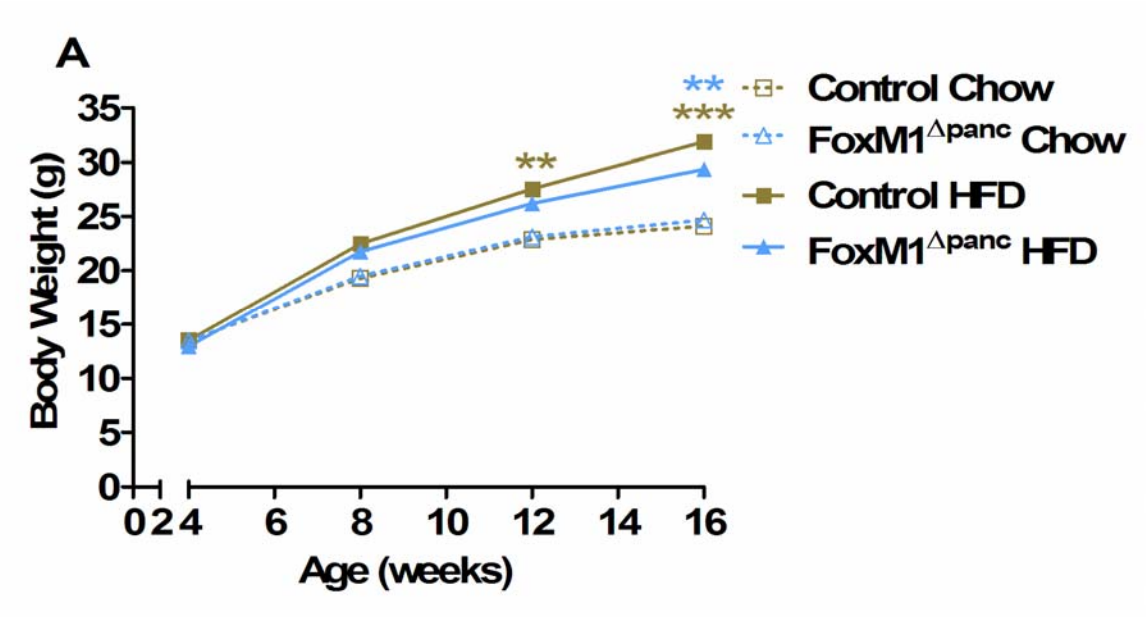

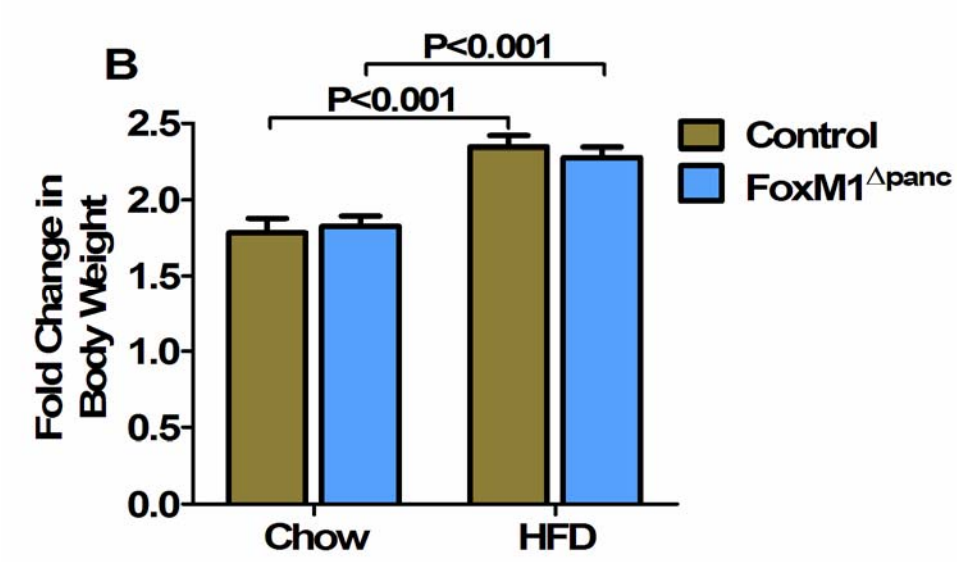

Figure 40. High-fat diet induced obesity in FoxM1$^{\Delta panc}$ and Control littermates. **(A)** Absolute body weight increased more dramatically in FoxM1$^{\Delta panc}$ and Control mice fed the high-fat diet versus the chow diet over the 12 week study period, from age 4 weeks (after weaning) to age 16 weeks. **(B)** Average fold-change in body weight over the 12 week study period was significantly greater in FoxM1$^{\Delta panc}$ and Control mice fed the high-fat diet versus the chow diet. Error bars represent SEM. Two-way ANOVA with Bonferroni's post-tests was used to measure significance. **P<0.01, ***P<0.001 HFD vs Chow. n=10-12 per group.

groups. However, feeding of the high-fat diet (HFD; 58.7% fat) induced obesity in both Control and FoxM1$^{\Delta panc}$ mice versus mice on a chow diet (mouse diet 5015, 25.3% fat), with body weights of the high-fat diet fed groups diverging from the chow-fed groups as early as 8 weeks of age, after being on the diet for 4 weeks. By the end of the study period, both Control and FoxM1$^{\Delta panc}$ mice on the high-fat diet exhibited significantly increased body weights versus chow-fed mice (Figure 40A), and total weight high-fat diet-fed mice was ~30% greater than that of mice fed the chow diet (Figure 40B). Importantly, no significant differences in weight gain were observed between Control and FoxM1$^{\Delta panc}$ mice, regardless of diet or gender.

To confirm that increased weight gain in mice on the high-fat diet versus chow was associated with increased adiposity, body composition analysis was performed at the end of the study period, after 12 weeks on the respective diets. In comparison to the chow diet, high-fat diet resulted in significantly increased body fat mass in both Control and FoxM1$^{\Delta panc}$ mice (Figure 41A). In addition, percent body weight composed of fat was also significantly increased by the high-fat diet, at the expense of lean muscle mass (Figure 41B). Again, these changes were similar between Control and FoxM1$^{\Delta panc}$ mice.

High-fat diet induced glucose intolerance in mixed background FoxM1$^{\Delta panc}$ and Control mice.

At four weeks of age, all mice were glucose tolerant (Figure 42A). However, after being fed the high-fat diet for only four weeks, both Control and FoxM1$^{\Delta panc}$ mice began to exhibit glucose intolerance, defined as significantly higher blood glucose levels during IPGTT compared to mice on the chow diet (Figure 42B). Additionally, FoxM1$^{\Delta panc}$ mice displayed significantly higher blood glucose levels at the later

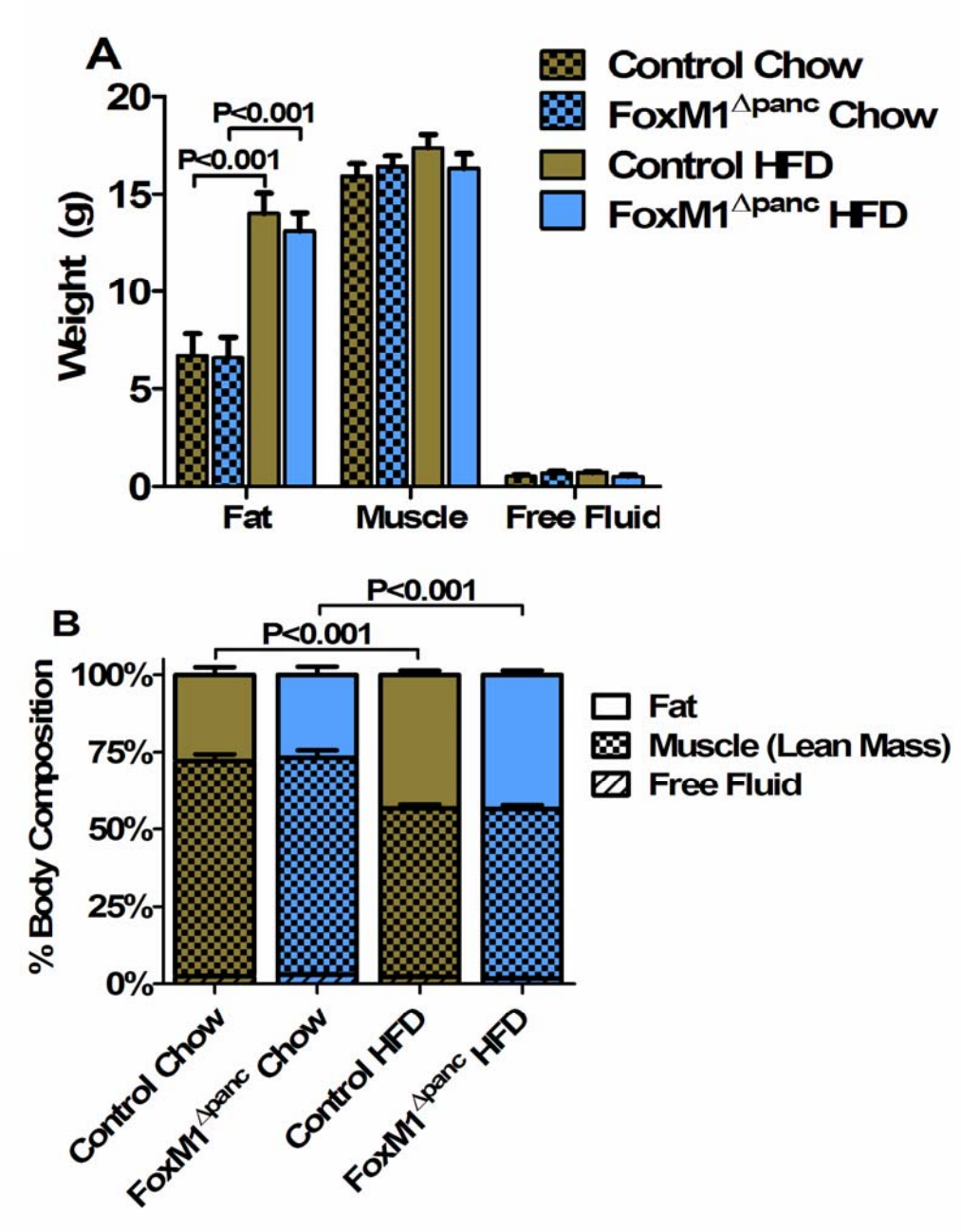

Figure 41. High-fat diet induced increased adiposity in FoxM1$^{\Delta panc}$ and Control littermates. (A) NMR spectroscopy reavealed that absolute weight of body fat was significantly greater in FoxM1$^{\Delta panc}$ and Control mice fed the high-fat diet versus the chow diet at the end of the 12 week study period. Lean mass (muscle) and weight of free fluid were not significantly altered. **(B)** Percent total body weight composed of fat was significantly increased in FoxM1$^{\Delta panc}$ and Control mice fed the high-fat diet versus the chow diet at the end of the 12 week study period, while percent body weight composed of lean mass was reduced. Error bars represent SEM. Two-way ANOVA with Bonferroni's post-tests was used to measure significance. n=8-9 per group.

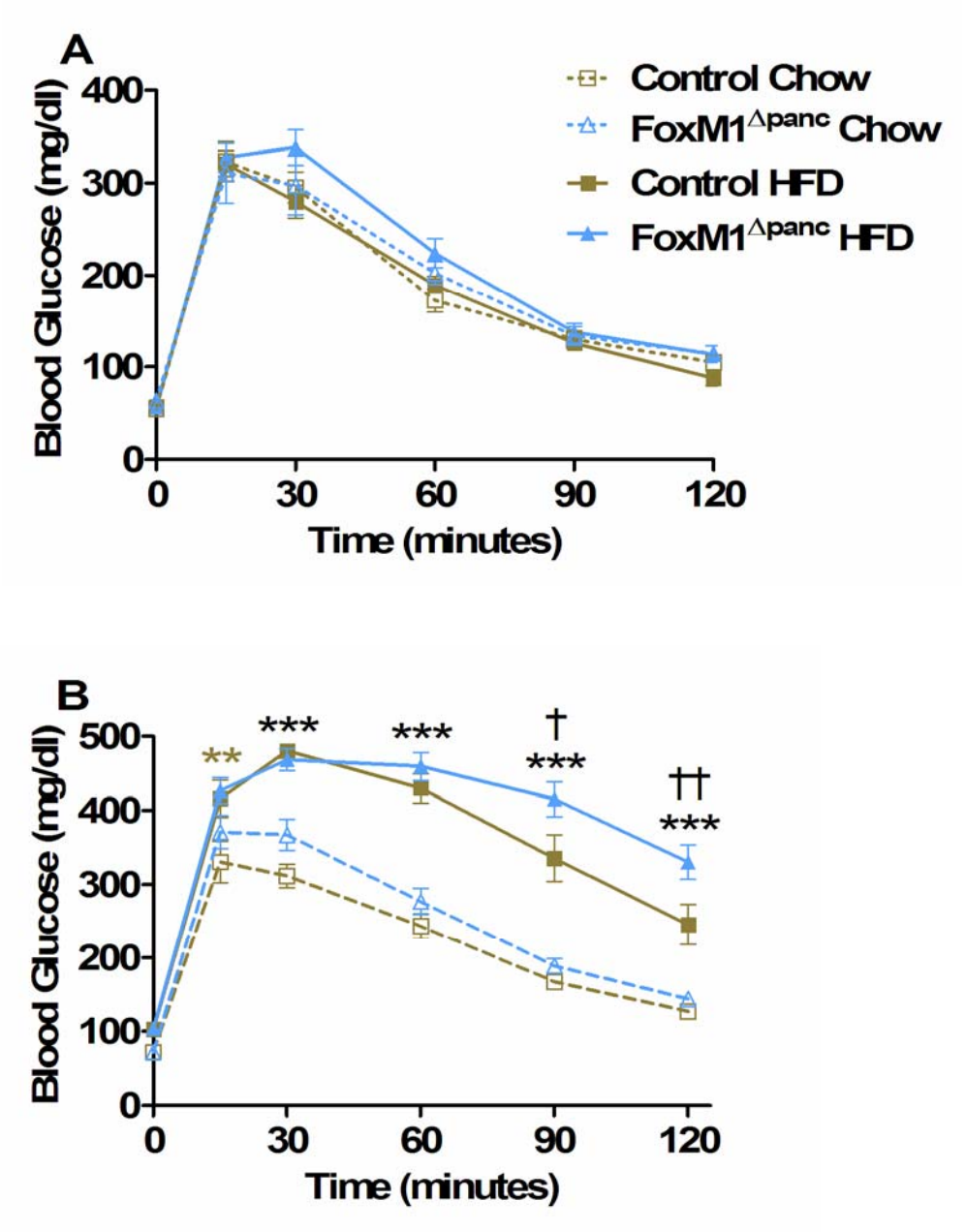

Figure 42. High-fat diet induced glucose intolerance in FoxM1$^{\Delta panc}$ and Control littermates. **(A)** IPGTT at 4 weeks of age showed that all mice at the beginning of the study displayed similar glucose tolerance. **(B)** IPGTT at 8 weeks of age, after being fed either the high-fat or chow diet for 4 weeks, showed that high-fat diet-fed mice displayed significant glucose intolerance, while mice fed the chow diet remained glucose tolerant. Error bars represent SEM. Two-way ANOVA with Bonferroni's post-tests was used to measure significance. **P<0.01, ***P<0.001 HFD vs Chow; †P<0.05, ††P<0.01 FoxM1$^{\Delta panc}$ HFD vs Control HFD. n=10-12 per group.

timepoints during IPGTT, indicating that loss of FoxM1 within the pancreas exacerbates high-fat diet-induced glucose intolerance. However, because glucose tolerance is determined by a combination of β cell function and peripheral insulin sensitivity, it was unclear what was affected by diet and what was affected by genotype.

High-fat diet induced insulin resistance in mixed background FoxM1$^{\Delta panc}$ and Control mice.

To assess peripheral insulin resistance, IPITTs were performed after 11 weeks on the respective diets. Surprisingly, no differences in insulin tolerance were observed between Control and FoxM1$^{\Delta panc}$ mice on either diet and high-fat diet did not significantly alter insulin tolerance in either group of mice (Figure 43A). However, use of the Homeostasis Model Assessment (HOMA) (fasting plasma insulin x fasting blood glucose / 22.5), an indirect measure of insulin sensitivity (Matthews *et al.*, 1985), revealed a trend for both Control and FoxM1$^{\Delta panc}$ mice to display insulin resistance as early as 4 weeks on the high-fat diet (Figure 43B). Importantly, no differences in IPITT or HOMA were observed between Control and FoxM1$^{\Delta panc}$ mice on either diet.

FoxM1$^{\Delta panc}$ mice on a mixed background exhibited impaired insulin secretion on the high-fat diet.

In order to better assess β cell function, insulin secretion was measured during IPGTTs at 0 and 30 minutes after glucose injection. In agreement with published results, Control mice displayed an approximate 2-fold increase in plasma insulin levels at 30 minutes versus 0 minutes after glucose injection after both 4 weeks (Figure 44A) and 12 weeks (Figure 44B) on the chow diet. At the 4 week timepoint, no significant differences

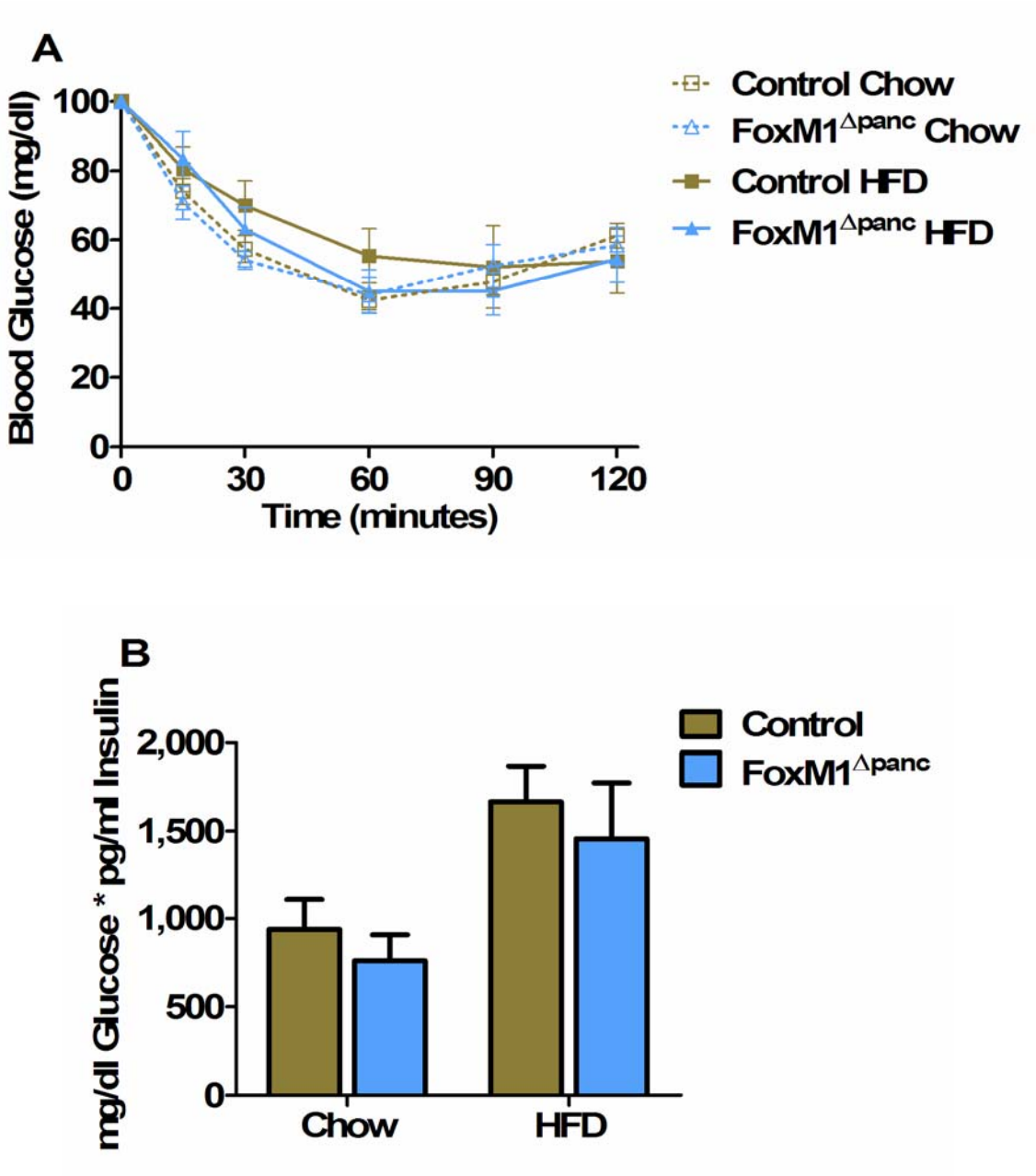

Figure 43. High-fat diet did not induce significant insulin resistance. (A) IPITT at 15 weeks of age showed no significant differences in insulin tolerance between Control or FoxM1$^{\Delta panc}$ mice fed the high-fat diet for 11 weeks versus those fed the chow diet. However, **(B)** HOMA calculation at 8 weeks of age, after being fed either a high-fat or chow diet for 4 weeks, revealed a trend for the high-fat diet-fed mice to display insulin resistance. Error bars represent SEM. Two-way ANOVA with Bonferroni's post-tests was used to measure significance. n=7-9 per group.

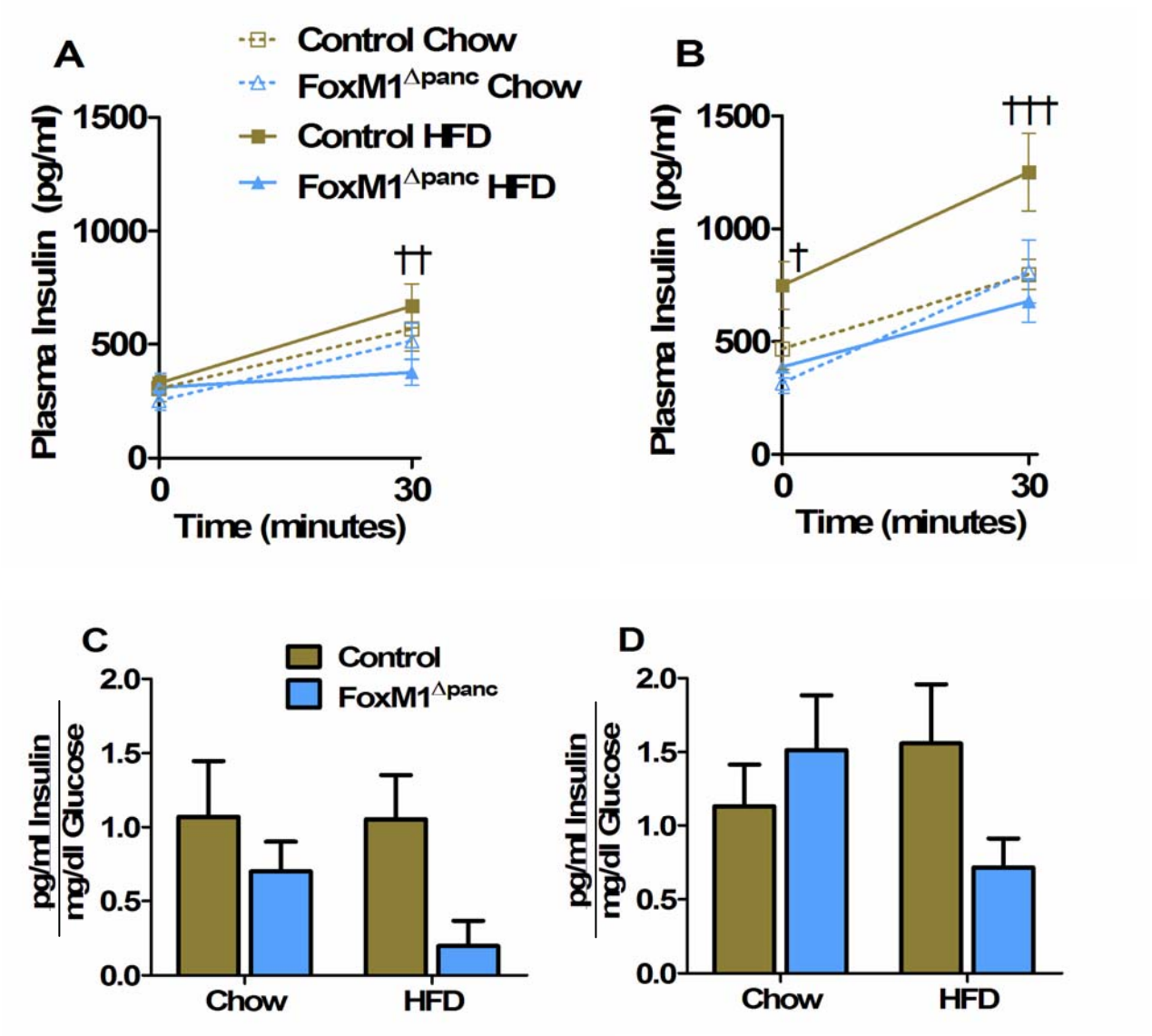

Figure 44. FoxM1$^{\Delta panc}$ mice fed the high-fat diet exhibited impaired insulin secretion. **(A)** Insulin secretion in Control mice on either diet and in FoxM1$^{\Delta panc}$ mice on the chow diet increased two-fold by 30 minutes after glucose injection during IPGTT at 8 weeks of age, after 4 weeks on the respective diets. However, FoxM1$^{\Delta panc}$ mice on the high-fat diet did not secrete more insulin at 30 minutes after glucose injection than at baseline. **(B)** After 12 weeks on the high-fat diet, Control mice exhibited increased fasting and 30-minute plasma insulin levels versus mice fed the chow diet, but no such increase was observed in FoxM1$^{\Delta panc}$ mice. **(C)** Calculation of the insulinogenic index revealed a trend for high-fat diet-fed FoxM1$^{\Delta panc}$ mice to display reduced β cell insulin secretory function after 4 weeks and **(D)** 8 weeks on the diet. Error bars represent SEM. Two-way ANOVA with Bonferroni's post-tests was used to measure significance. †P<0.05, ††P<0.01, †††P<0.001 FoxM1$^{\Delta panc}$ HFD vs Control HFD. n=10-12 per group.

were observed between Control and FoxM1$^{\Delta panc}$ mice on the chow diet at 0 or 30 minutes, nor on the high-fat diet at 0 minutes (Figure 44A). However, FoxM1$^{\Delta panc}$ mice, after 4 weeks on the high-fat diet, exhibited impaired insulin secretion in response to glucose, with no significant increase in plasma insulin levels at 30 minutes versus 0 minutes, resulting in the 30 minute plasma insulin level in these mice being significantly reduced compared to Control mice on the high-fat diet. This impairment in insulin secretion worsened by 12 weeks on the high-fat diet, as plasma insulin levels in FoxM1$^{\Delta panc}$ mice at this timepoint were only 50% of those of Control mice at both 0 and 30 minutes after glucose injection (Figure 44B). In comparison to mice on the chow diet, Control mice on the high-fat diet exhibited higher plasma insulin levels at both 0 and 30 minutes, whereas FoxM1$^{\Delta panc}$ mice did not secrete more insulin on the high-fat versus chow diet.

Comparing the results for blood glucose levels and plasma insulin levels at 0 and 30 minutes after glucose injection allowed for calculation of the insulinogenic index (change in plasma insulin / change in blood glucose), which is a measure of β cell secretory function (Wareham *et al.*, 1995). After both 4 weeks (Figure 44C) and 12 weeks (Figure 44D) on the high-fat diet, FoxM1$^{\Delta panc}$ mice displayed reduced insulinogenic indices compared to Control mice, although these differences were not statistically significant. Thus, based on insulin secretion and insulinogenic index calculations, FoxM1$^{\Delta panc}$ mice appear to exhibit defective insulin secretion when placed on the high-fat diet.

FoxM1$^{\Delta panc}$ mice on a mixed background exhibited reduced β cell mass compared to Controls, and high-fat diet did not stimulate β cell mass expansion.

As obesity-induced insulin resistance and hyperglycemia have been shown to stimulate β cell proliferation and expansion of β cell mass, it was of interest to determine whether FoxM1 was required for these processes. Additionally, it was possible that FoxM1$^{\Delta panc}$ mice displayed reduced insulin secretion on the high-fat diet because of impaired β cell mass compensation. At 16 weeks of age, although pancreas weight was similar to that of Control mice (Figure 45A), FoxM1$^{\Delta panc}$ mice displayed an approximate 40% reduction in β cell mass on both the chow and high-fat diets (Figure 45B). Surprisingly, high-fat diet did not significantly alter pancreas weight or β cell mass in either genotype.

As a corollary to β cell mass, pancreatic insulin content was assessed in Control and FoxM1$^{\Delta panc}$ mice after 12 weeks on the chow and high-fat diet. Indeed, pancreatic insulin content results were similar to those of β cell mass, with FoxM1$^{\Delta panc}$ mice exhibiting a 40% reduction versus Control mice when on the chow diet (Figure 45C). Additionally, high-fat diet had no effect on pancreatic insulin content in either group of mice.

High-fat diet did not stimulate significant β cell proliferation or apoptosis.

To determine whether high-fat diet had any effects on β cell proliferation that were not appreciated by analysis of β cell mass, BrdU incorporation into β cells was assessed during the 12th week on the diet. No significant differences in β cell proliferation were observed between Control and FoxM1$^{\Delta panc}$ mice fed the chow diet, but β cell proliferation was significantly reduced in FoxM1$^{\Delta panc}$ mice compared to Controls

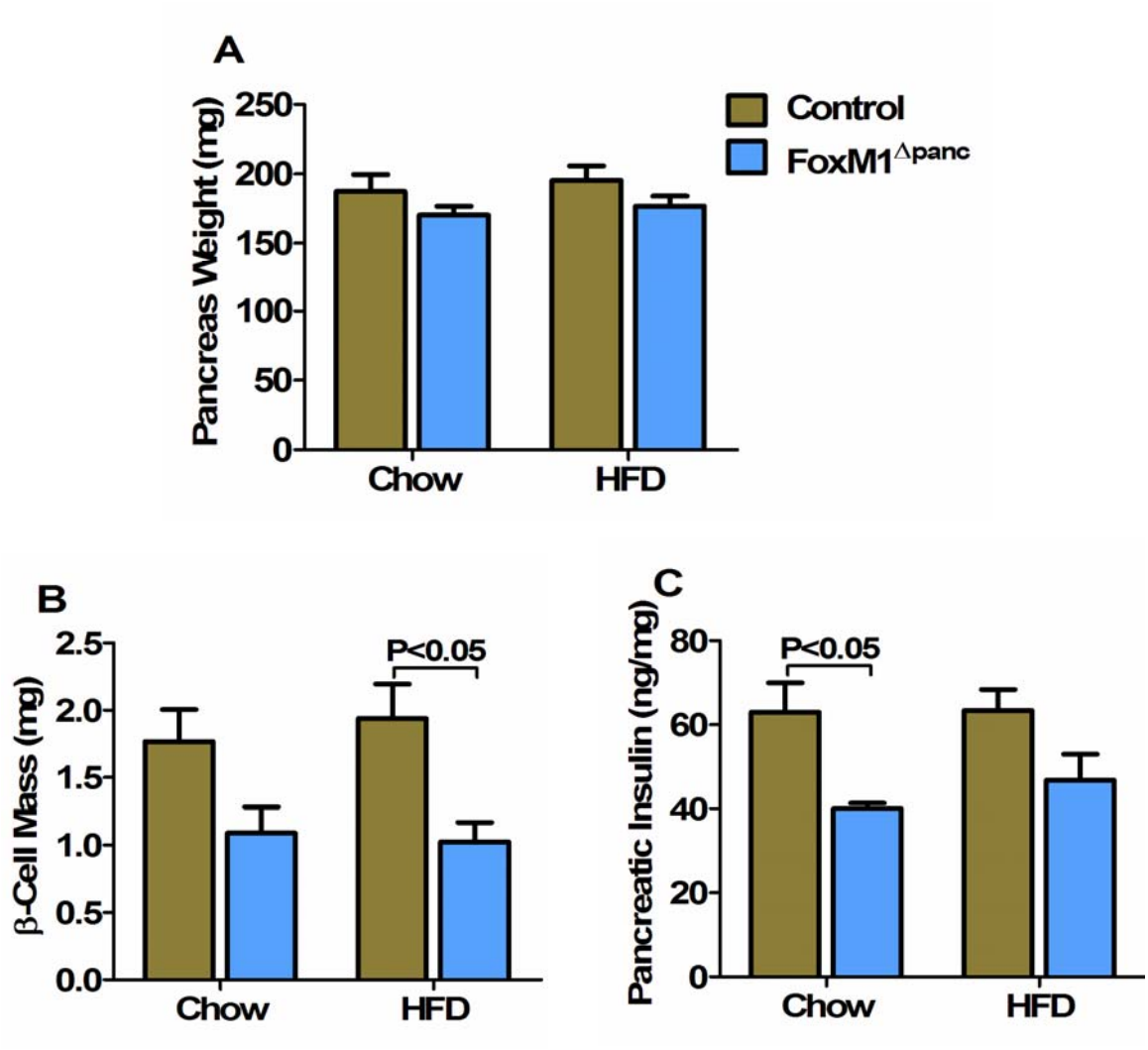

Figure 45. FoxM1$^{\Delta panc}$ mice exhibited reduced β cell mass and pancreatic insulin content compared to Controls, and neither was altered by high-fat diet. (A) Pancreas weight did not significantly differ between Control and FoxM1$^{\Delta panc}$ mice on either diet. However, **(B)** β cell mass and **(C)** pancreatic insulin content in FoxM1$^{\Delta panc}$ mice at 16 weeks of age were reduced by ~40% compared to Control mice on either diet. High-fat diet did not cause any changes in β cell mass or pancreatic insulin content in either genotype. Error bars represent SEM. Two-way ANOVA with Bonferroni's post-tests was used to measure significance. n=10-12 per group for A, n=5-6 per group for B and C.

when fed the high-fat diet (Figure 46A). Additionally, there was a trend for Control mice on the high-fat diet to exhibit increased β cell proliferation, whereas no such trend was observed for FoxM1$^{\Delta panc}$ mice on the high-fat versus chow diet.

It was surprising that high-fat diet did not stimulate significant β cell proliferation in Control mice, but it was possible that such stimulation occurred at an earlier timepoint, and that by 12 weeks on the diet, significant β cell compensation could no longer be observed. Therefore, BrdU incorporation into β cells was assessed during the 5th week on the diet, but again no differences in β cell proliferation between Control mice fed the high-fat diet versus the chow diet were apparent (Figure 46B). Additionally, it was possible that the high-fat diet stimulated β cell apoptosis that counter-balanced any hyperplasia or expansion that occurred. To this end, TUNEL labeling of β cells after 12 weeks on the diets was measured, but very few TUNEL^{+} β cells were observed in any group of mice (Figure 46C). Thus, high-fat diet did not appear to increase β cell apoptosis.

Together, these results suggested that mice on a mixed C57Bl/6 strain background do not exhibit β cell hyperplasia or β cell mass expansion in response to diet-induced obesity.

FoxM1$^{\Delta panc}$ mice on a mixed background displayed enlarged β cell size but reduced islet size.

Although this set of experiments did not allow for assessment of FoxM1's involvement in β cell hyperplasia and β cell mass expansion in response to diet-induced obesity, several interesting results were observed when comparing Control and FoxM1$^{\Delta panc}$ mice on either diet. Similar to what was reported in Chapter III, FoxM1$^{\Delta panc}$

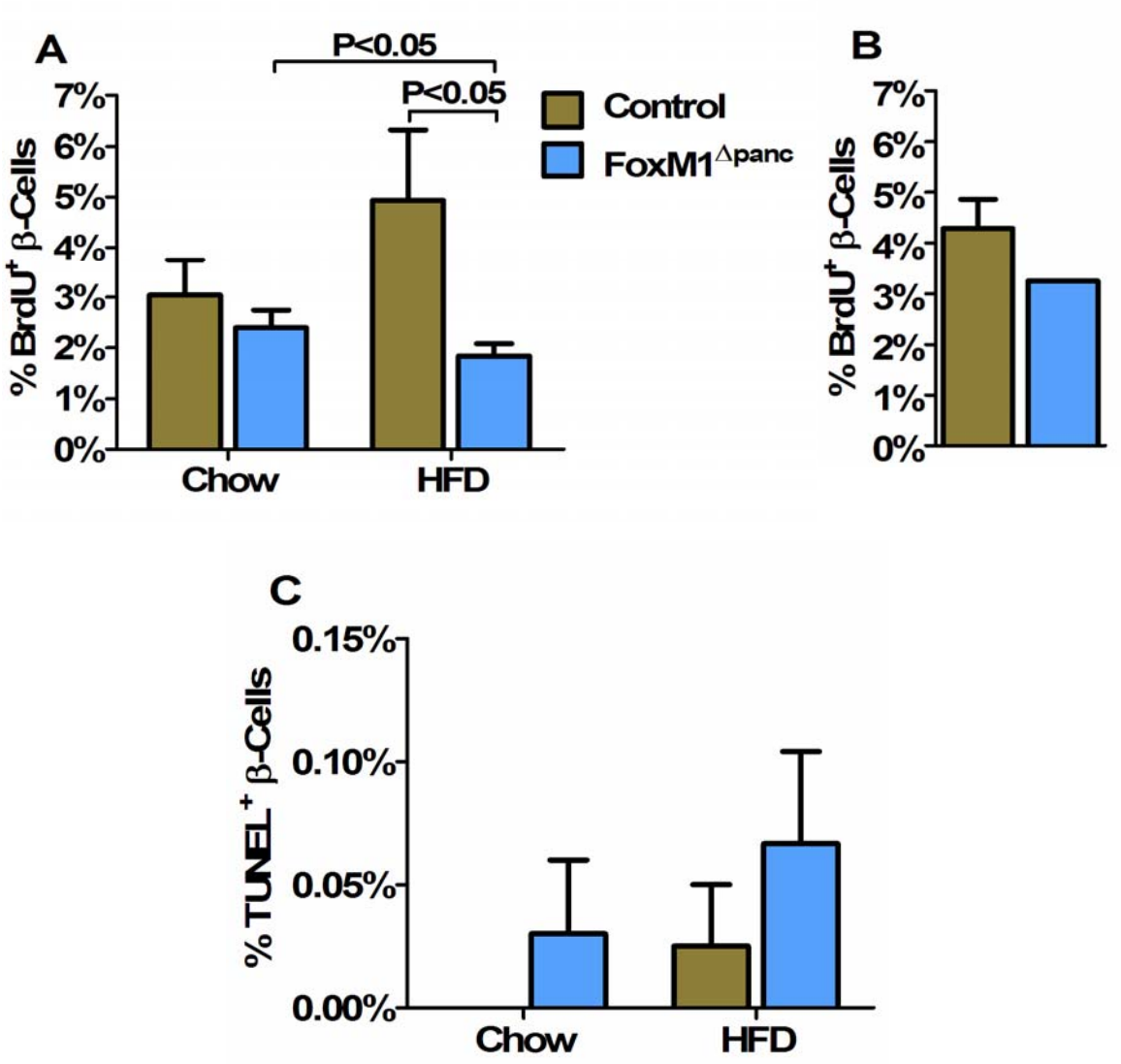

Figure 46. FoxM1$^{\Delta panc}$ mice exhibited reduced β cell proliferation after 12 weeks on the high-fat diet, but high-fat diet did not significantly stimulate β cell proliferation in Control mice. (A) BrdU incorporation into β cells was significantly reduced in FoxM1$^{\Delta panc}$ mice compared to Control mice after 12 weeks on the high-fat, but not chow, diet. High-fat diet did not significantly stimulate β cell proliferation in Control mice compared to chow diet, but did result in decreased β cell proliferation in FoxM1$^{\Delta panc}$ mice. **(B)** BrdU incorporation into β cells of Control and FoxM1$^{\Delta panc}$ mice after 5 weeks on the high-fat diet was similar to results observed after 12 weeks. **(C)** TUNEL labeling identified only a small number of β cells undergoing apoptosis in either Control or FoxM1$^{\Delta panc}$ mice after 12 weeks on either the high-fat or chow diet. Error bars represent SEM. Two-way ANOVA with Bonferroni's post-tests was used to measure significance for A and C. n=5-6 per group for A, n=3 Controls and 1 FoxM1$^{\Delta panc}$ for B, n=2-3 per group for C.

mice exhibited enlarged β cell size compared to Control mice on both the chow and high-fat diets (Figure 47A). Interestingly, high-fat diet did not result in significant increases in β cell size in either genotype. As discussed in Chapter III, FoxM1$^{\Delta panc}$ mice on the chow diet display enlarged nuclei due to endoreduplication, which partially accounts for the observed increase in cell size. Although β cell nucleus size was not directly measured in this study, it is likely that similar results would be obtained.

Despite having larger β cells, however, average islet size in FoxM1$^{\Delta panc}$ mice was reduced compared to Controls on both diets, and high-fat diet did not cause any changes in islet size versus chow diet (Figure 47B). The reduction in average islet size observed in FoxM1$^{\Delta panc}$ mice could in part be attributed to an increased proportion of small endocrine cell clusters versus definitive islets in these mice compared to Controls (Figure 47C). Additionally, islet density was significantly reduced in FoxM1$^{\Delta panc}$ mice compared to Controls after being fed the high-fat diet (Figure 47D).

Isogenic C57Bl/6 Mice Pilot Study

To confirm that isogenic C57Bl/6 female mice would undergo β cell hyperplasia and β cell mass expansion in response to the high-fat diet used in the above studies, and to determine whether a chow diet with reduced fat content would serve as a better control, pilot studies were performed using C57Bl/6JBom mice fed three different diets for 12 weeks: rodent diet 5001 (13.5% fat), mouse diet 5015 (25.3% fat), or high-fat/high-carbohydrate mouse diet F3282 (58.7% fat).

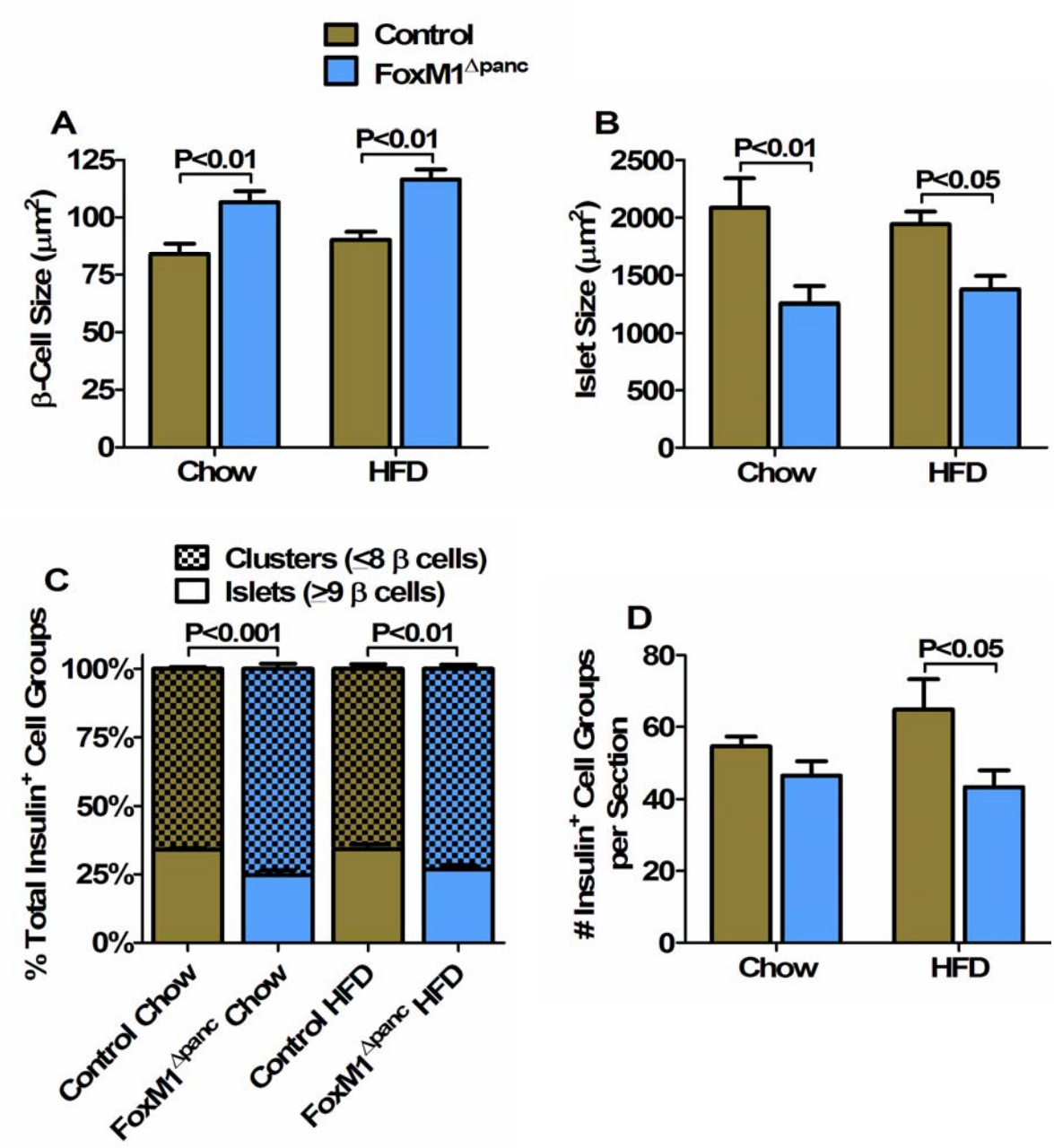

Figure 47. FoxM1$^{\Delta panc}$ mice exhibited enlarged β cell size but reduced islet size and density compared to Control littermates. **(A)** β cell size was significantly larger, while **(B)** islet size was significantly smaller, in FoxM1$^{\Delta panc}$ mice compared to Control mice after 12 weeks on either the chow or high-fat diet. High-fat diet did not significantly alter β cell or islet size versus chow diet. **(C)** The proportion of small endocrine cell clusters versus definitive islets was greater in FoxM1$^{\Delta panc}$ mice than Controls after 12 weeks on either the high-fat or chow diet and was not significantly altered by high-fat diet. **(D)** Islet density was significantly reduced in FoxM1$^{\Delta panc}$ mice compared to Controls after 12 weeks on the high-fat, but not chow diet. Error bars represent SEM. Two-way ANOVA with Bonferroni's post-tests was used to measure significance. n=5-6 per group.

High-fat diet induced obesity and glucose intolerance in C57Bl/6 mice.

Female C57Bl/6JBom littermates were weaned at four weeks of age, at which time their weights were similar (Figure 48A), prior to being placed on one of the three study diets. As early as four weeks after being fed the high-fat diet, the mice began to diverge in weight, which was exacerbated with age. While no significant differences in weight gain were observed between mice on the two chow diets, mice on the low-fat 5001 chow diet displayed a consistent trend towards less weight gain than mice on the moderate-fat 5015 chow diet.

In accordance with body weight, mice on the high-fat diet exhibited glucose intolerance as early as eight weeks of age, after only four weeks on the diet. Area under the curve (AUC) calculations, utilizing blood glucose levels during IPGTT, revealed that, despite all mice initially being normoglycemic, mice fed the high-fat diet displayed significantly higher blood glucose levels during IPGG than mice in either chow diet group at later timepoints (Figure 48B). Again, no significant differences were observed in AUC measurements between mice on the two chow diets.

High-fat diet stimulated β cell mass expansion in C57Bl/6 mice.

Mice fed the high-fat diet had larger pancreata than mice on either chow diet (Figure 49A), and these pancreata contained an increased percentage of insulin$^+$ tissue (Figure 49B). Together, these two phenomena resulted in mice on the high-fat diet exhibiting increased β cell mass versus mice on the chow diets (Figure 49C). Again, no differences in these parameters were apparent between mice on the two chow diets, although they did follow the body weight results, with mice on the low-fat 5001 chow

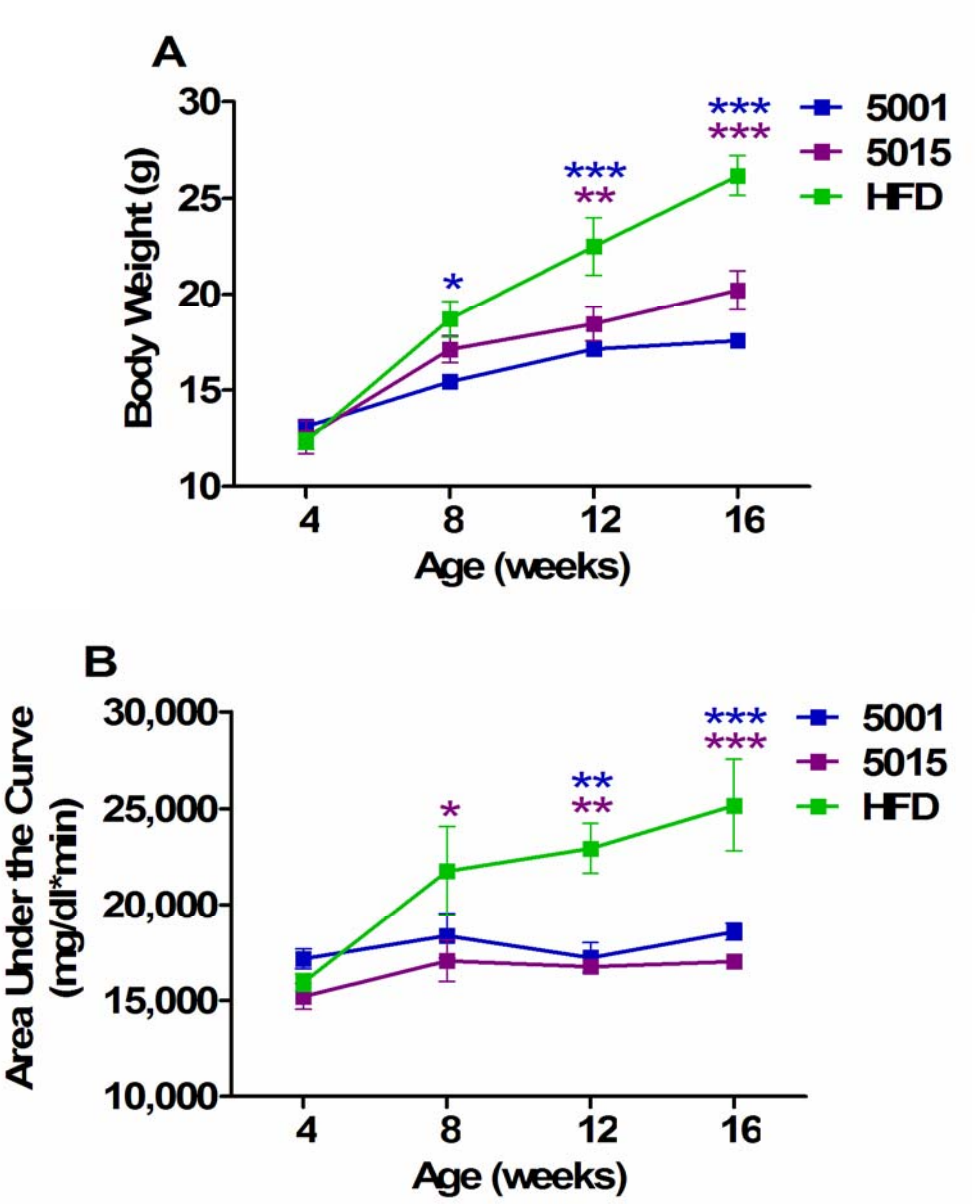

Figure 48. High-fat diet induced obesity and glucose intolerance in C57Bl/6 female mice. **(A)** Fasting body weight was measured every four weeks during the study, beginning at 4 weeks of age after weaning. All mice weighed approximately the same amount at 4 weeks of age, and subsequently the high-fat diet-fed group gained weight more rapidly and to a greater extent than either of the chow diet-fed groups. **(B)** Area under the curve (AUC) for glucose during IPGTT was calculated every four weeks during the study. While mice fed either chow diet maintained a stable AUC at all timepoints, high-fat diet-fed mice displayed glucose intolerance at 8, 12, and 16 weeks of age. Error bars represent SEM. Two-way ANOVA with Bonferroni's post-tests was used to measure significance. *P<0.05, **P<0.01, ***P<0.001 vs HFD. n=4-5 per group.

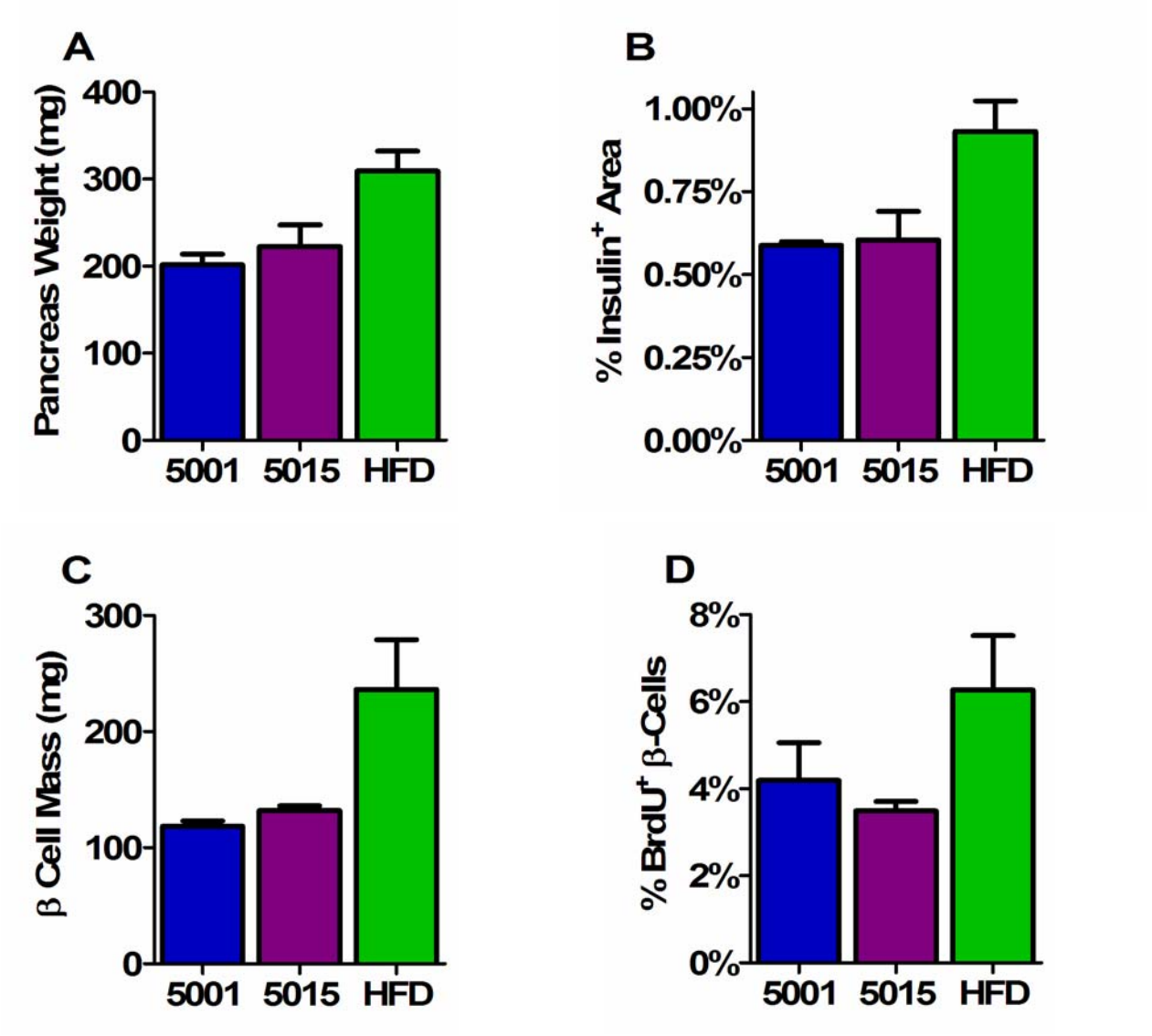

Figure 49. High-fat diet stimulated pancreas growth and β cell mass expansion in C57Bl/6 female mice. Although sample size was too small to reach significance, mice fed the high-fat diet exhibited a consistent trend towards increased **(A)** pancreas weight, **(B)** percent insulin$^+$ area within the pancreas, **(C)** β cell mass, and **(D)** BrdU incorporation into β cells. Error bars represent SEM. One-way ANOVA with Bonferroni's post-tests was used to measure significance. n=2 per group.

diet demonstrating the lowest values for pancreas weight, insulin$^+$ area, and β cell mass. A similar trend was observed for β cell proliferation, with mice on the high-fat diet displaying increased BrdU incorporation into β cells than mice on either chow diet (Figure 49D).

High-fat diet stimulated Foxm1 expression in C57Bl/6 islets.

qRT-PCR was used to assess whether diet-induced obesity altered *Foxm1* expression within islets. Indeed, *Foxm1* transcript levels mirrored the changes observed in β cell mass and proliferation, with mice fed the high-fat diet expressing a higher level of *Foxm1* transcripts compared to mice fed either of the chow diets (Figure 50). Additionally, enhanced expression of the FoxM1 targets *Plk1* and *Aurkb* was also observed, while there was no change in *Ccnd2*, which is not a known FoxM1 target.

Despite the small sample size for some of the analyses performed in this pilot study, it demonstrated that the high-fat diet used in the previous studies could elicit changes in β cell mass, β cell proliferation, and islet *Foxm1* expression in isogenic C57Bl/6 female mice. Additionally, this study suggested that the low-fat 5001 chow diet may be a better control diet to use in future studies. Thus, it was deemed worthwhile to pursue investigating FoxM1's role in β cell hyperplasia in response to diet-induced obesity, using mice on a congenic C57Bl/6 background.

Foxm1$^{flox/flox}$ Mice on a C57Bl/6 Background

Based on the results of the two aforementioned studies, *Foxm1*^{flox} and *Pdx1*$^{5.5kb}$-*Cre* mice were backcrossed eight generations to the C57Bl/6JBom strain, and

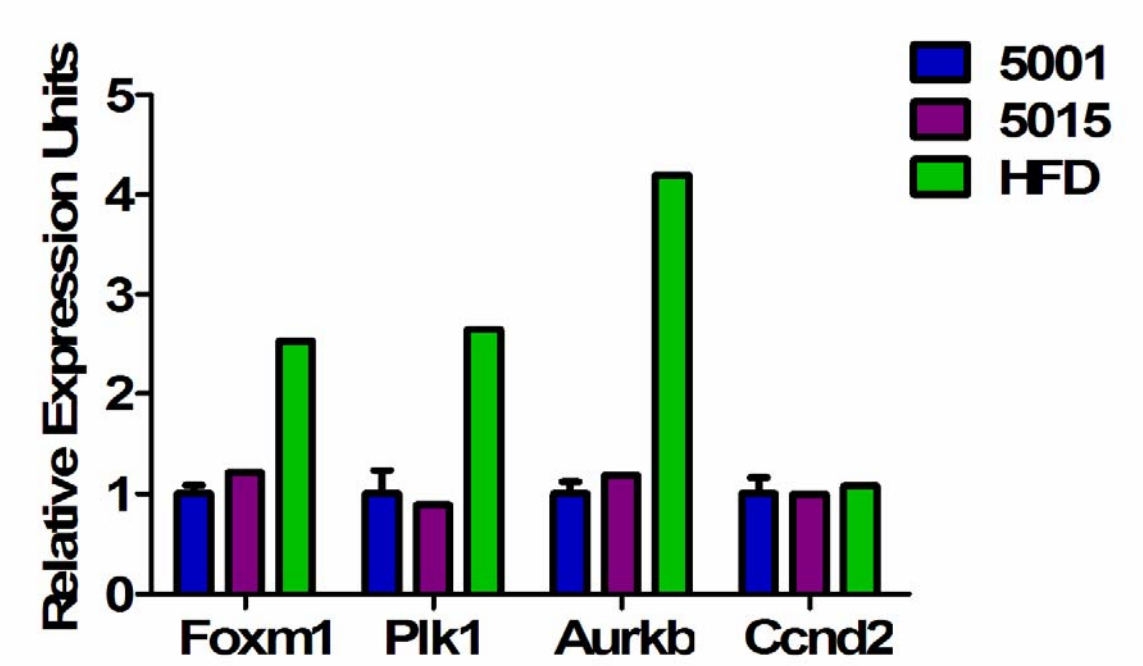

Figure 50. High-fat diet up-regulated *Foxm1* and some of its targets in C57Bl/6 female mice. *Foxm1*, *Plk1*, and *Aurkb*, but not *Ccnd2*, transcripts were up-regulated in mice fed the high-fat diet compared to mice fed either of the control diets. Error bars represent SEM. n=1-2 per group.

the original study of FoxM1's role in β cell adaptation to diet-induced obesity was repeated with a shorter end-point of eight weeks, as prior studies had demonstrated that many parameters were altered by high-fat diet feeding within this time period.

Unfortunately, during the course of the study, it was discovered that the *Pdx1*$^{5.5kb}$-*Cre* transgene had been silenced in the mouse colony prior to the beginning of the study. This was confirmed for the mice in this study, which had genotyped positive for the *Cre* transgene (Figure 51A) but still had the full-length floxed *Foxm1* allele and no null allele upon genotyping pancreas tissue from sections (Figure 51B). Additionally, Cre expression was undetectable in islet nuclei (Figure 51C). Thus, FoxM1$^{\Delta panc}$ mice were actually not included in the experiment, and all results reported here represent *Foxm1*$^{flox/flox}$ mice on either the high-fat diet or the low-fat 5001 chow diet.

High-fat diet induced obesity and glucose intolerance in Foxm1$^{flox/flox}$ mice on the C57Bl/6 background.

At four weeks of age, after weaning, *Foxm1*$^{flox/flox}$ female mice on the C57Bl/6 background were randomized into either the high-fat diet or low-fat chow diet groups. All mice has similar body weights at the beginning of the study, but within eight weeks mice fed the high-fat diet gained significantly more weight than did mice fed the chow diet (Figure 52A). Similarly, all mice exhibited similar glucose tolerance at four weeks of age (Figure 52B,C), but eight weeks of high-fat diet feeding resulted in glucose intolerance compared to mice fed the chow diet, evidenced by increased blood glucose levels after glucose injection during IPGTT (Figure 52B,D).

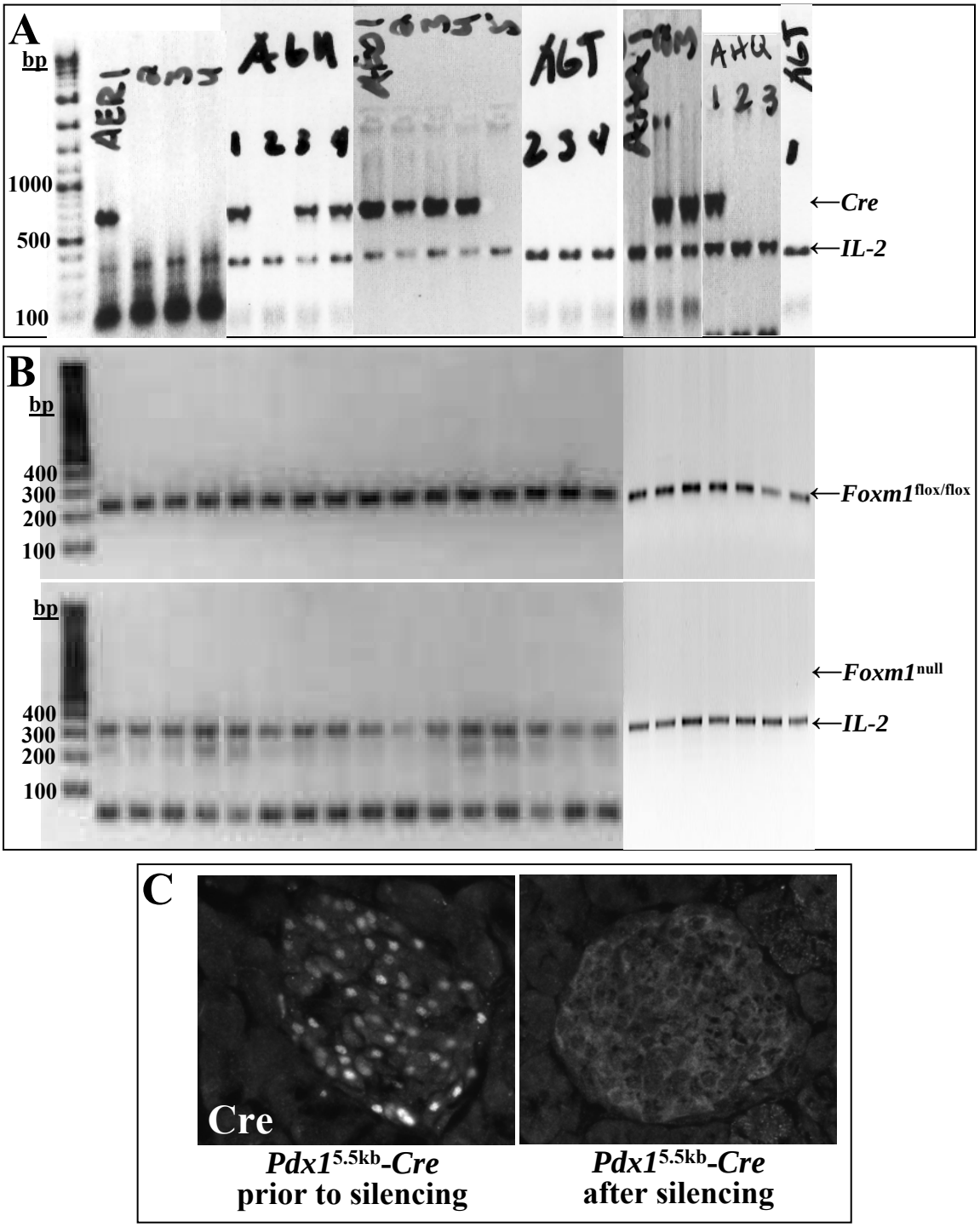

Figure 51. *Foxm1*$^{flox/flox}$;*Pdx1*$^{5.5kb}$-*Cre* mice on the C57Bl/6 background did not undergo Cre-mediated recombination of *Foxm1*. **(A)** Despite approximately half of the mice included in the study genotyping positive for the *Cre* transgene, **(B)** floxed *Foxm1* alleles were still present in pancreas tissue from all mice, while *Foxm1* null alleles were undetectable, and **(C)** Cre expression was undetectable in endocrine cell nuclei.

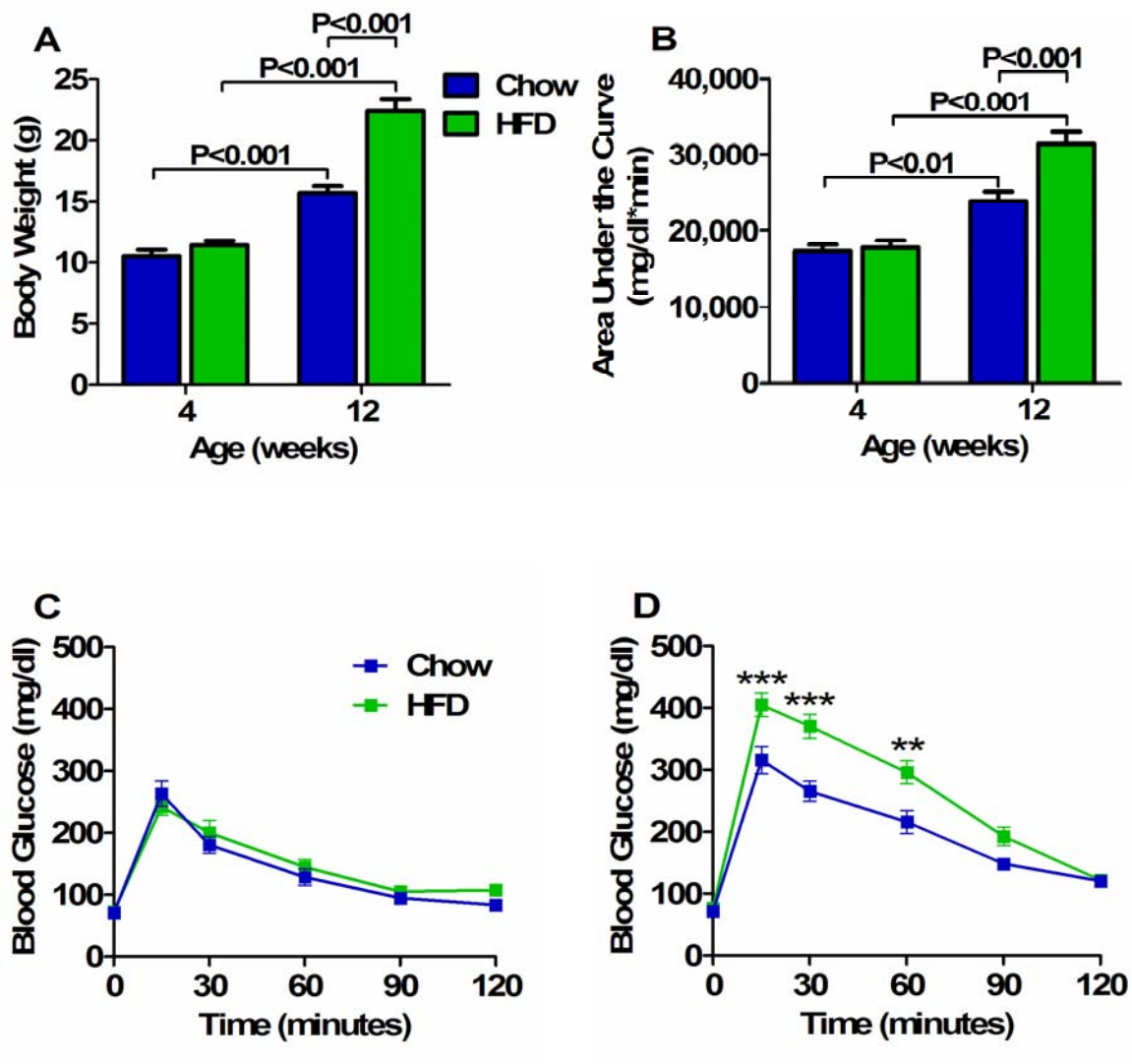

Figure 52. High-fat diet induced obesity and glucose intolerance in *Foxm1*$^{flox/flox}$ C57Bl/6 female mice. **(A)** Fasting body weight at 4 weeks of age was similar between all mice, but the high-fat diet-fed group subsequently gained more weight than the chow-fed group. **(B)** Area under the curve (AUC) for glucose during IPGTT increased over the 8 week study period to a greater extent in high-fat diet-fed mice versus chow-fed. **(B)** IPGTT at 4 weeks of age revealed no differences in glucose tolerance between the mice at the beginning of the study, **(C)** but after 8 weeks on the high-fat diet, *Foxm1*$^{flox/flox}$ C57Bl/6 mice exhibited hyperglycemia versus chow-fed mice. Error bars represent SEM. Two-way ANOVA with Bonferroni's post-tests was used to measure significance. **P<0.01, **P<0.001. n=11-12 per group.

High-fat diet stimulated β cell mass expansion in Foxm1$^{flox/flox}$ mice on the C57Bl/6 background.

Although pancreas weight was not significantly different in mice on the high-fat versus chow diet (Figure 53A), the percent of pancreas tissue composed of β cells was significantly increased in high-fat diet-fed mice versus chow diet-fed mice (Figure 53B). This resulted in an approximate 50% increase in β cell mass in *Foxm1*$^{flox/flox}$ female mice on the high-fat diet compared to chow diet within eight weeks (Figure 53C).

Investigating Insulin Secretory β Cell Function in FoxM1$^{\Delta panc}$ Mice on a Mixed Background

Because FoxM1$^{\Delta panc}$ mice fed a high-fat diet exhibited reduced plasma insulin levels after a glucose challenge, it was of interest to determine whether this was due to a primary β cell defect associated with loss of FoxM1. To this end, a preliminary islet perifusion study was performed on isolated islets from nine week old female FoxM1$^{\Delta panc}$ and Control littermates. Comparison of islet responses to various secretagogues (high glucose, tolbutamide, IBMX, and KCl) revealed an approximate 50% reduction in insulin secretion from FoxM1$^{\Delta panc}$ islets compared to Control islets (Figure 54). Of course, this study compared islets from only one FoxM1$^{\Delta panc}$ mouse and one Control littermate, necessitating the need for further study. Unfortunately, the aforementioned silencing of the *Pdx1*$^{5.5kb}$-*Cre* transgene has precluded such studies from being performed as of yet.

An additional approach used to determine whether FoxM1$^{\Delta panc}$ islets exhibited non-proliferative defects was islet transcript expression analysis. For these analyses, a combination of routine qRT-PCR and higher-throughput arrays were utilized. Again, islet RNA was isolated from nine week old female FoxM1$^{\Delta panc}$ and Control littermates.

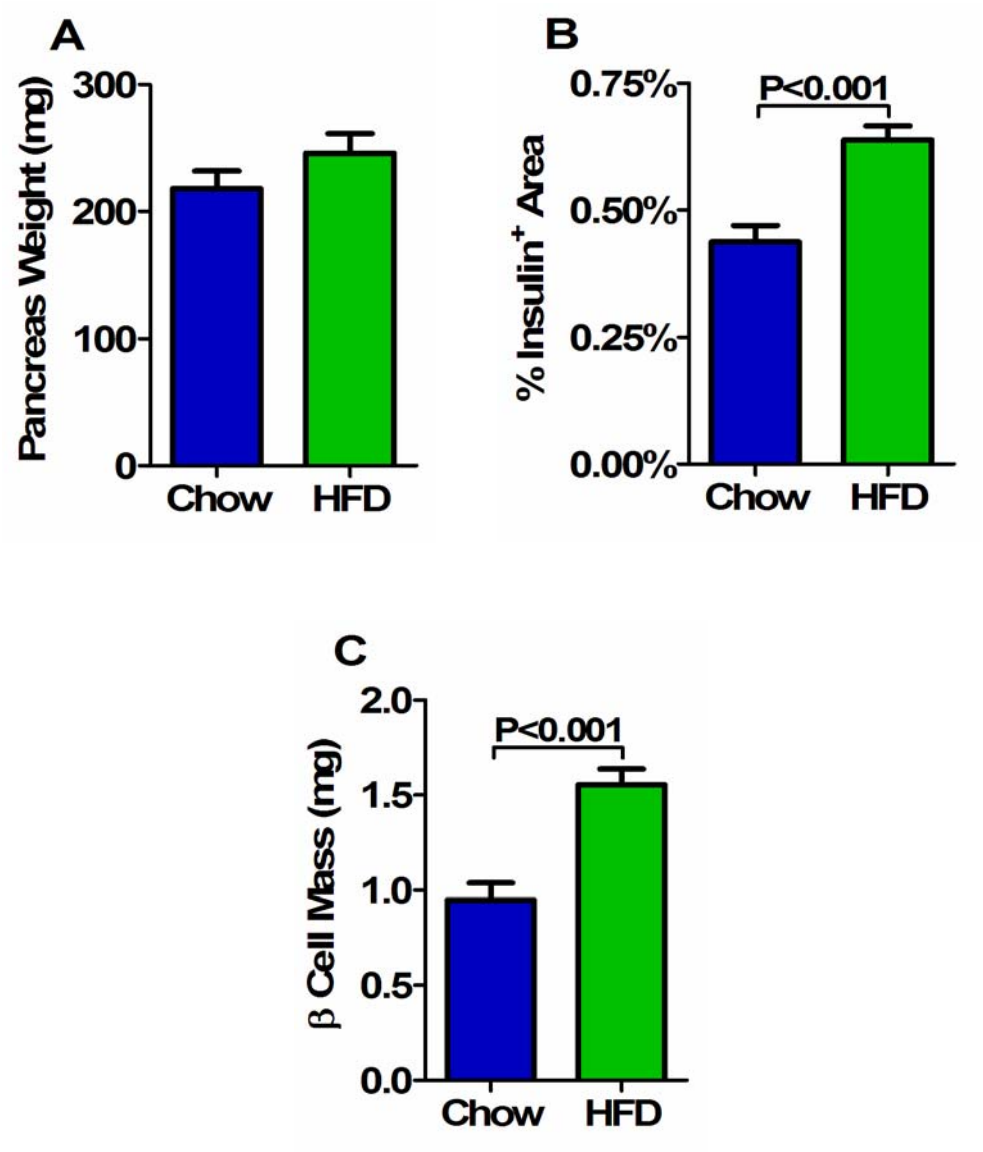

Figure 53. High-fat diet stimulated β cell mass expansion in *Foxm1*$^{flox/flox}$ C57Bl/6 female mice. **(A)** High-fat diet did not alter pancreas weight versus chow diet. However, **(B)** percent insulin^{+} area within the pancreas and **(C)** β cell mass were significantly increased in high-fat diet-fed mice versus chow-fed mice. Error bars represent SEM. Unpaired t-tests were used to measure significance. n=7-9 per group.

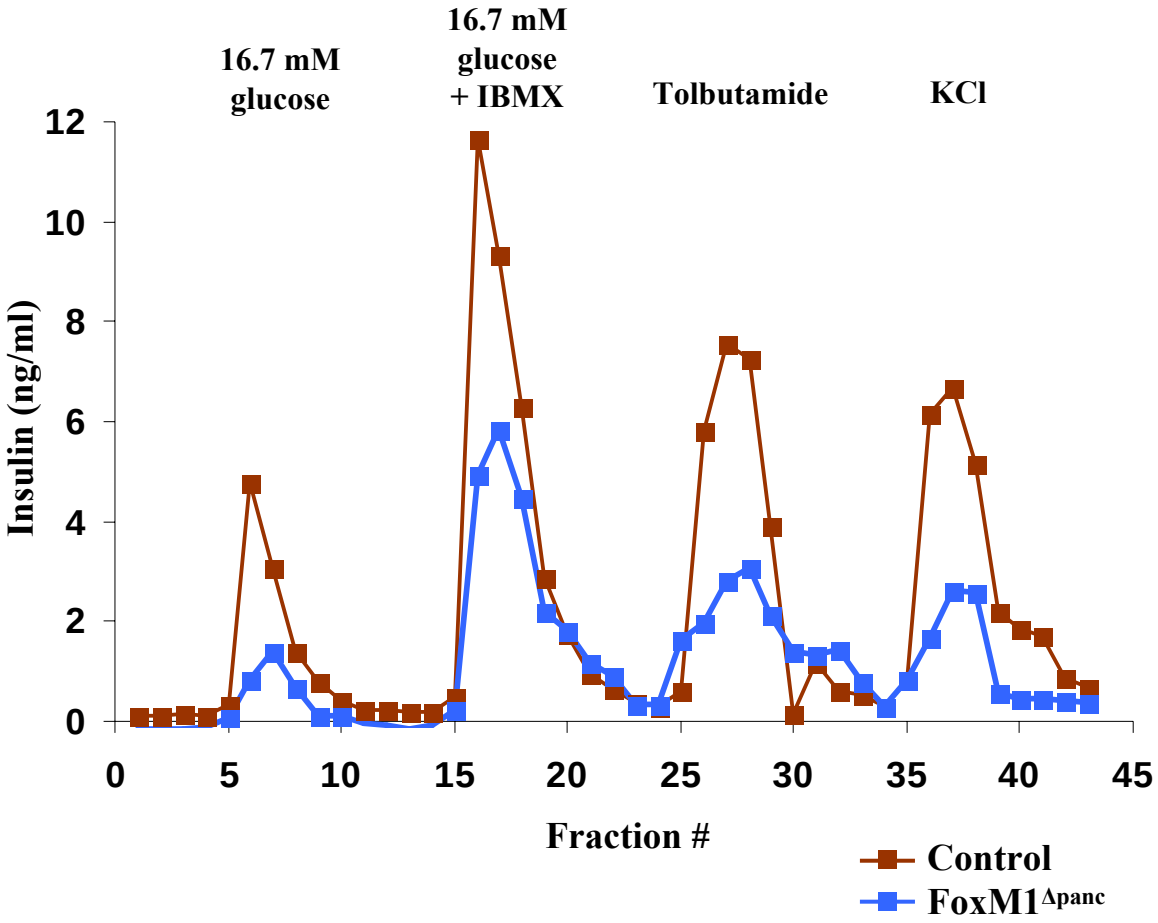

Figure 54. Preliminary analysis revealed a possible insulin secretory defect in FoxM1$^{\Delta panc}$ islets. 50.05 IEQ of each genotype were loaded onto perifusion columns and exposed to either 5.6 mM glucose (baseline) or one of four secretagogues (16.7 mM glucose, 16.7 mM glucose + IBMX, Tolbutamide, or KCl). Insulin concentration in the perifusate was measured by RIA. Insulin secretion in response to all secratagogues was reduced in FoxM1$^{\Delta panc}$ islets compared to Control islets. n=1 per group.

qRT-PCR revealed no significant differences in expression of the islet hormones *Insulin1*, *Insulin2*, or *Glucagon*, or of the mature islet transcription factors *Pdx1*, *MafA*, or *Arx* (Figure 55). However, FoxM1$^{\Delta panc}$ islets expressed reduced levels of the transcription factor *Pax4*. Additionally, the FoxM1 target *CenpA* was reduced in FoxM1$^{\Delta panc}$ islets, although other proliferation markers (*Plk1*, *Aurora B kinase*, and *Cyclin D2*) were not significantly altered. Thus, FoxM1$^{\Delta panc}$ islets do not express less insulin than Control islets, so the putative insulin secretory defect was likely due to downstream defects in insulin secretion.

To further investigate this hypothesis, Custom TaqMan Low Density Arrays were utilized to analyze expression of many targets, including islet hormones, transcription factors, cell cycle regulators (including some FoxM1 targets), and factors involved in insulin vesicle secretion. These analyses confirmed the reduced *CenpA* expression in FoxM1$^{\Delta panc}$ islets identified by qRT-PCR, but contradicted the *Pax4* results, with *Pax4* transcript levels being higher in FoxM1$^{\Delta panc}$ islets analyzed by the arrays (Figure 56). In fact, *CenpA* and *Pax4* were the most dramatically-altered transcripts using this technique. Additionally, the Cdk inhibitors *p16*^{INK4a} and *p21*^{Cip1} were up-regulated in FoxM1$^{\Delta panc}$ islets, concurring with a proliferative defect. The array data also suggested that some factors involved in insulin secretion (*Vamp2*, *Rab3a*, *Rab27a*, and *Myosin5a*) may be down-regulated in FoxM1$^{\Delta panc}$ islets, while *Munc13b* may be up-regulated. However, because of technical issues several RNA samples could not be analyzed, and thus, these studies need to be repeated before any conclusions can be drawn from the array data.

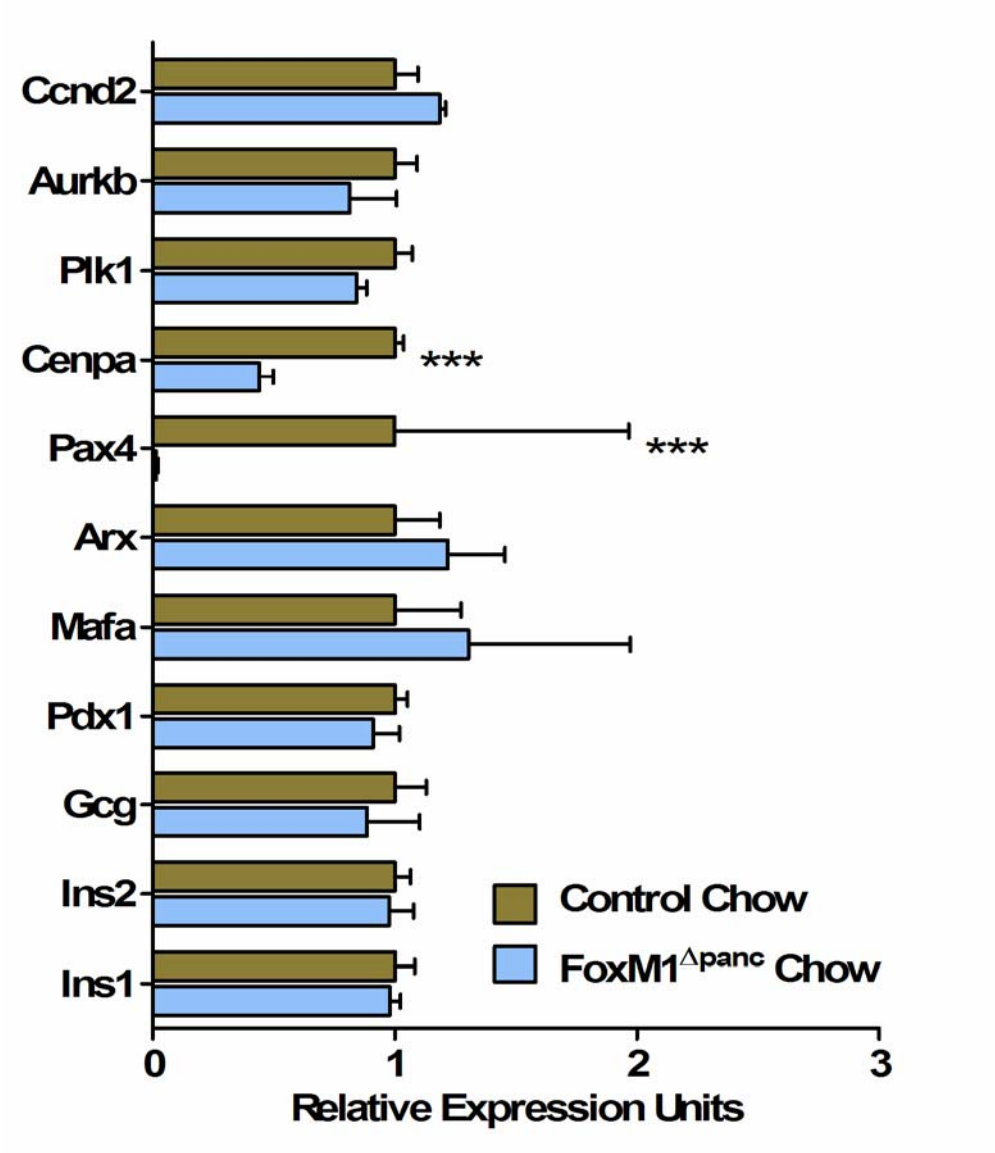

Figure 55. Real-time qRT-PCR analysis of transcript expression in FoxM1$^{\Delta panc}$ and Control islets. Error bars represent SEM. Unpaired t-tests were used to measure significance. ***P<0.001. n=4-5 per group.

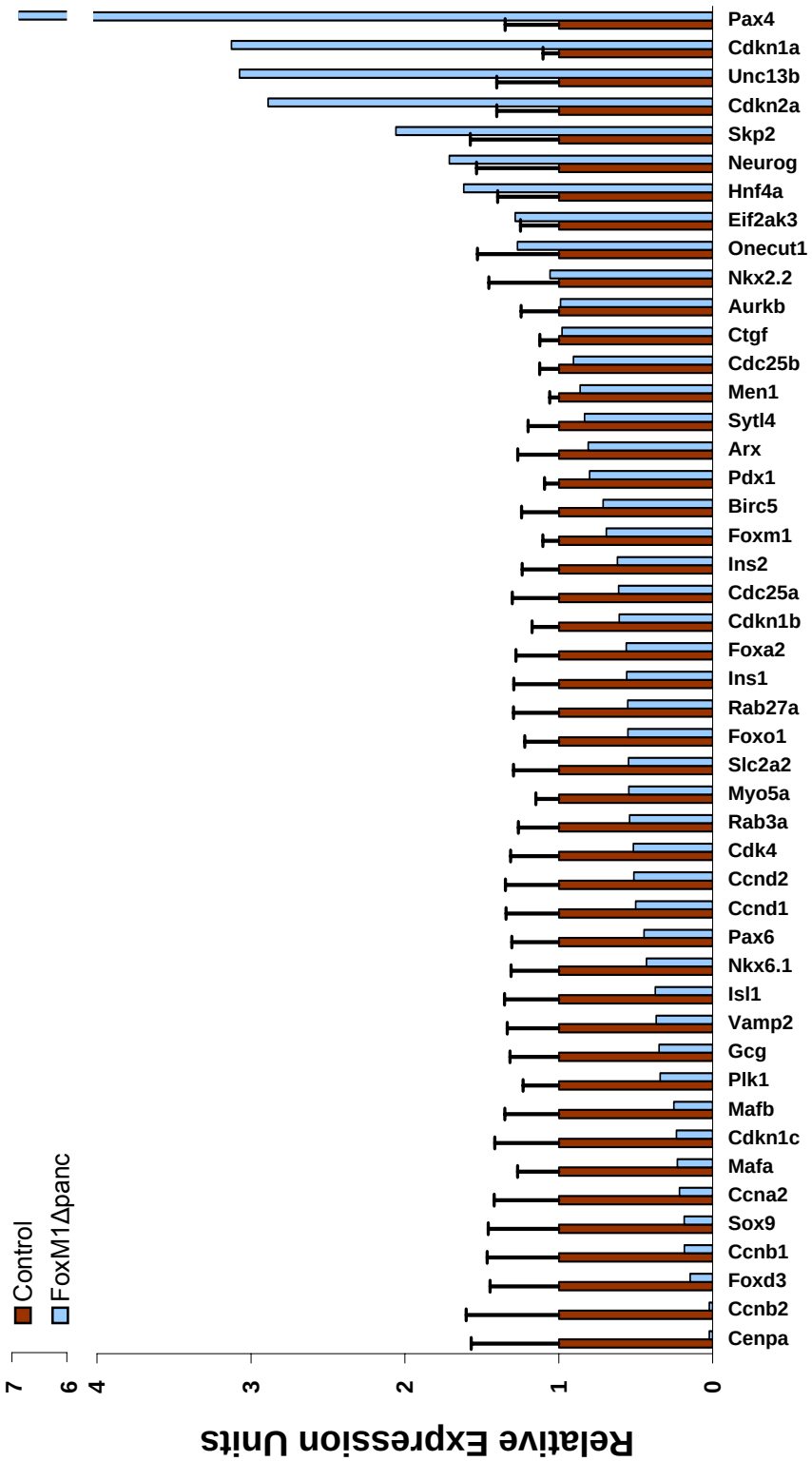

Figure 56. Analysis of transcript expression in FoxM1$^{\Delta panc}$ and Control islets using Custom TaqMan Low Density Arrays. Error bars represent SEM. n=3 Control, 1 FoxM1$^{\Delta panc}$.

Discussion

Diet-induced obesity has been utilized in many rodent studies as a means to stimulate β cell proliferation. However, not all mouse strains are affected in the same manner by a high-fat diet, and the C57Bl/6 strain is particularly susceptible to weight gain, glucose intolerance, and β cell compensation (Black *et al.*, 1998; Funkat *et al.*, 2004; Andrikopoulos *et al.*, 2005). Some of these distinctions may be due to significant differences in islet mass, number, and function that have been identified among various mouse strains (Bock *et al.*, 2005; Andrikopoulos *et al.*, 2005). Therefore, it is not entirely surprising that Control mice on a mixed background (129SvJ, ICR, CBA, C57Bl/6) did not undergo significant β cell mass expansion in response to the high-fat diet. However, these mice were outbred from the C57Bl/6 strain, and other groups have observed diet-induced β cell mass expansion in mouse strains other than C57Bl/6 (Gupta *et al.*, 2007).

In addition, different responses to high-fat diet are observed between male and female mice on the same genetic background. In general, male rodents are more susceptible to obesity and diabetes than are female rodents, due at least in part to estrogenic effects on body weight regulation, insulin sensitivity, and β cell mass and function (Geary *et al.*, 2001; Louet *et al.*, 2004; Choi *et al.*, 2005; Contreras *et al.*, 2002). Thus, many published studies regarding effects of high-fat diet utilized only male mice. However, the majority of FoxM1$^{\Delta panc}$ male mice develop glucose intolerance and diabetes under normal conditions by six to nine weeks of age, associated with islet necrosis and fatty infiltration of the pancreas (Zhang H *et al.*, 2006), which could mask any diet-induced effects. Despite these concerns, FoxM1$^{\Delta panc}$ and Control male mice

were included in the aforementioned high-fat studies. However, the majority of male mice, regardless of genotype, displayed glucose intolerance or diabetes when fed the high-fat diet, and FoxM1$^{\Delta panc}$ male mice consistently displayed impaired insulin secretion, regardless of diet. Therefore, only results from the female arm of the study were included here, as they are representative of both groups of data but lack the confounding effects of pre-existing hyperglycemia. Interestingly, Control male mice did undergo β cell mass expansion (2-fold) in response to the high-fat diet, revealing that β cell compensation occurred in male, but not female, mice on this particular mixed background.

To circumvent this conundrum, FoxM1$^{\Delta panc}$ mice were backcrossed onto the C57Bl/6 strain background before repeating the study. However, an alternative approach would be to use FoxM1$^{\Delta islet}$ male mice (*Foxm1*$^{flox/flox}$;*Pdx1*^{PB}-*CreER*^{TM}), in which *Foxm1* is specifically deleted within islet endocrine cells (primarily β cells) after injection of tamoxifen (Zhang H *et al.*, 2005). By delaying *Foxm1* deletion until just before the start of the study and restricting *Foxm1* deletion to islets, the confounding effects of pre-existing hyperglycemia and exocrine defects (Zhang H *et al.*, 2006) could be avoided, which may allow for better analysis of FoxM1's role in β cell mass expansion in response to diet-induced obesity. These studies have not yet been undertaken, but the necessary mice are readily available.

Another caveat to this study is that the high-fat and chow diets used were not matched for micronutrients. Thus, it is possible that some of the effects observed in response to the diets (or lack thereof) were due to differences in components of the diets other than fat. Additionally, it is becoming clearer that different types of fat sources have

different effects on body composition and insulin resistance (Rivellese *et al.*, 2002). Although the fat source in both the high-fat diet and mouse diet #5015 was lard, which is known to induce insulin resistance, it is possible that this fat source does not stimulate β cell compensation in the same manner as other fat sources. Future studies should aim to use matched diets with optimal fat sources in order to avoid these potential confounding factors, although the high-fat diet used in this study did stimulate β cell mass expansion in C57Bl/6 mice, and such effects would need to be verified for other diets.

When considering the use of other diets or other mouse models for diet-induced obesity studies, it will be important to verify that obesity actually correlates with insulin resistance, as the studies presented here have shown that obesity alone is not sufficient to stimulate β cell mass expansion. To this end, it may be worthwhile in future experiments to utilize hyperinsulinemic-euglycemic clamps to assess insulin resistance, rather than IPITTs or HOMA calculations. Although HOMA has been shown to correlate well with clamp-determined insulin sensitivity (Lee *et al.*, 2008), hyperinsulinemic-euglycemic clamps are considered the reference standard in humans and rodents (Ayala *et al.*, 2006). However, the clamps are technically difficult and would need to be an end-point analysis, as opposed to HOMA, which can be assessed repeatedly in the same mouse and relatively easily. Additionally, consideration should be given to administering glucose for IPGTTs based on lean body mass, rather than total body mass, as glucose levels in high-fat diet-fed mice were likely inflated in this study due to increased adiposity.

Although preliminary results presented here suggest that *Foxm1* transcript levels are up-regulated in mouse islets after exposure to a high-fat diet, these results will need to be confirmed, and ideally up-regulation within β cells specifically will need to be

assessed. Such studies have not yet been performed because of the lack of an acceptable anti-FoxM1 antibody. Once such an antibody is available, immunohistochemistry could be used to assess FoxM1 expression within particular cell types, both under normal and high-fat diet-fed conditions. Additionally, because nuclear localization of FoxM1 is essential for its transcriptional activity, and phosphorylation has been shown to regulate such localization and activity (Ma *et al.*, 2005), it will be important to determine whether sub-cellular localization of FoxM1 in different cell types is altered under various conditions. Importantly, mice fed diets with differing fat contents exhibit altered sub-cellular localization of another forkhead transcription factor, FoxD3 (Dr. Trish Labosky, Vanderbilt University; personal communication), and nuclear exclusion of FoxO is associated with insulin resistance (Okada *et al.*, 2007). Therefore, localization of FoxM1 may also change in response to a high-fat diet, and an antibody will be necessary in order to detect such a change. Chapter VI discusses the ongoing efforts to generate a monoclonal anti-FoxM1 antibody for use in western immunoblotting and/or immunohistochemistry in order to perform these experiments.

This study aimed to determine whether FoxM1 was required for β cell proliferation and β cell mass expansion in response to diet-induced obesity and insulin resistance, using mice with a pancreas-wide deletion of *Foxm1* (FoxM1$^{\Delta panc}$) fed a high-fat diet. However, Control mice failed to exhibit β cell mass expansion or increased β cell proliferation after being fed the high-fat diet, preventing any conclusions from being made regarding FoxM1's role in these processes. This series of studies revealed that female mice on a congenic C57Bl/6 strain background, but not those on a mixed background, responded to the high-fat diet as expected. Although FoxM1$^{\Delta panc}$ mice were

backcrossed to the C57Bl/6 background, the *Pdx1-Cre* transgene became silenced, and new mice will have to be backcrossed before the experiments can be repeated. The mechanism of gene silencing has not yet been determined, but it occurred in two different colonies of mice, on both the original and backcrossed strain backgrounds, during a similar timeframe. Thus, perhaps after a certain number of generations, the transgene underwent epigenetic modification, chromatin remodeling, and/or RNAi-mediated silencing.

Additionally, these studies indicated that FoxM1$^{\Delta panc}$ mice suffered from reduced insulin secretion when fed the high-fat diet, suggesting that FoxM1 may be important for the compensatory enhancement of β cell function that normally occurs in response to diet-induced obesity and insulin resistance. Importantly, the impairment in insulin secretion was not due to reduced *Insulin* gene transcription or reduced Insulin protein expression per β cell mass. Together with preliminary islet perifusion experiments that showed reduced insulin secretion in response to all secretagogues, these results suggest that loss of FoxM1 impairs general insulin secretion. These results are intriguing, particularly because mice with a global deletion of Skp2 (*Skp2*$^{-/-}$), which is a direct FoxM1 transcriptional target, also exhibited reduced insulin secretion in response to glucose without a reduction in insulin protein expression per β cell mass, as well as impaired β cell mass expansion in response to diet-induced obesity (Zhong *et al.*, 2007). Therefore, FoxM1 may regulate β cell mass expansion and β cell function through Skp2, although loss of FoxM1 may produce more dramatic effects than observed in *Skp2*$^{-/-}$ mice, as other transcriptional targets are likely affected as well. Thus, further study of FoxM1's role(s) in β cell compensation is justified.

CHAPTER V

UTILIZING *PDX1*^{PB}-*CRE-ER*^{TM} MICE FOR ISLET-SPECIFIC DELETION OF *FOXM1* AND LINEAGE TRACING

Introduction

There is much interest in generating new β cells both *in vivo* and *in vitro* in order to enhance or replace a patient's own β cell population. However, a definitive source of new β cells in the adult pancreas, and indeed whether new β cells can even be derived from adult human tissue, has not been conclusively determined. Several studies have shown that replication of pre-existing β cells is the primary mechanism by which β cell mass expansion and regeneration occurs during adulthood (Dor *et al.*, 2004; Teta *et al.*, 2007; Meier *et al.*, 2008) (Chapter III). However, because β cells differentiate from Ngn3^{+} precursors located within the ductal epithelium during development (Gradwohl *et al.*, 2000; Gu *et al.*, 2002), it is hypothesized that β cells may be able to be derived from duct cells in the adult. In support of this hypothesis, several groups have found that after pancreatic injury there are increased numbers of insulin^{+} cells within or directly adjacent to ducts (Bonner-Weir *et al.*, 1993; Hayashi *et al.*, 2003); the pancreatic progenitor and β cell marker, Pdx1, is up-regulated in duct cells (Sharma *et al.*, 1999); and Ngn3 is up-regulated (Xu *et al.*, 2008) (Chapter III). Furthermore, ductal epithelium isolated from mice and humans has been induced to differentiate into insulin-producing cells *in vitro* (Ramiya *et al.*, 2000; Heremans *et al.*, 2002).

In hopes of identifying a definitive β cell precursor population in the adult mouse, lineage tracing studies have been performed in which a particular cell population is

labeled with a heritable marker that will distinguish it and its progeny at a later timepoint upon histological analysis. Such studies have been performed using conditional Cre expression to recombine a marker, such as the Rosa26 reporter (Soriano, 1999) (Figure 18), in particular cell populations during development in order to determine into which cell types they differentiate. For adult lineage tracing, it is often necessary to use inducible, conditional Cre-mediated recombination to label a cell population at a specific timepoint. For this purpose, CreER^{TM}-expressing mouse lines are used, in which Cre recombinase is fused to a mutated form of the estrogen receptor ligand binding domain that renders it responsive to tamoxifen, but not endogenous estrogen (Littlewood *et al.*, 1995). Binding of CreER^{TM} to tamoxifen disrupts its interaction with heat shock proteins that sequester it in the cytoplasm, allowing for nuclear translocation of the fusion protein and Cre-mediated recombination of floxed target alleles (Figure 16B).

Several distinct CreER^{TM} mouse lines have been utilized for lineage tracing after pancreatic injury, although interpretation of the results are somewhat unclear. Most recently, adult duct cells were labeled by CreER^{TM}-mediated recombination of the *Rosa26* reporter locus, under the control of the *carbonic anhydrase II* (*CAII*) promoter, and labeled islet cells were observed following duct ligation (Bonner-Weir *et al.*, 2008). Thus, duct cells can contribute to formation of new islet cells, but the frequency of such occurrence was not reported, and no images were provided in the manuscript for interpretation. Interestingly, lineage tracing of acinar cells using the *elastase I* promoter driving expression of CreER^{TM} showed that acinar cells did not give rise to endocrine cells after 70-80% partial pancreatectomy (PPx), treatment with exendin-4, cerulein-induced pancreatitis, or duct ligation (Desai *et al.*, 2007). Finally, β cells themselves

have been lineage-labeled using the rat *insulin* promoter (RIP) to drive CreER^{TM}-mediated recombination of the Z/AP reporter (Dor *et al.*, 2004). In this study, a pulse-chase experiment was performed, in which β cells were labeled in adult mice by tamoxifen injection (pulse), and maintenance or dilution of this label within the β cell population over time and after 70% PPx (chase) was assessed (Figure 57A). In both cases, the percent of labeled β cells remained constant, indicating that non-β cells (unlabeled) do not give rise to β cells.

However, several caveats existed in the Dor *et al.* (2004) study that could have confounded the results. First, tamoxifen-induced recombination of the Z/AP reporter was significantly less than 100% (ranging from 30-60%, depending on the dose of tamoxifen administered), requiring extrapolation of the results to conclude that no new β cells are derived from non-β cells. Second, because the actual portion of the pancreas that undergoes regeneration is quite small in comparison to the remaining portion of the pancreas, which undergoes expansion of pre-existing tissue (see Chapter III), and because the regenerating portion was not analyzed separately, it is possible that the results were skewed by including only pre-existing islets and no new islets. Third, it was unclear whether tamoxifen was still present during the "chase" periods, as no phamacokinetic studies have been performed in rodents using doses as high as used in this study. Because the RIP would be activated in newly-differentiated β cells, regardless of their origin, these cells would express CreER^{TM}, and if tamoxifen had not yet been cleared from the bloodstream, the fusion protein would be translocated to the nucleus, recombination of the reporter allele would occur, and expression of the marker would have been interpreted as the cell being derived from a pre-existing β cell. Although the

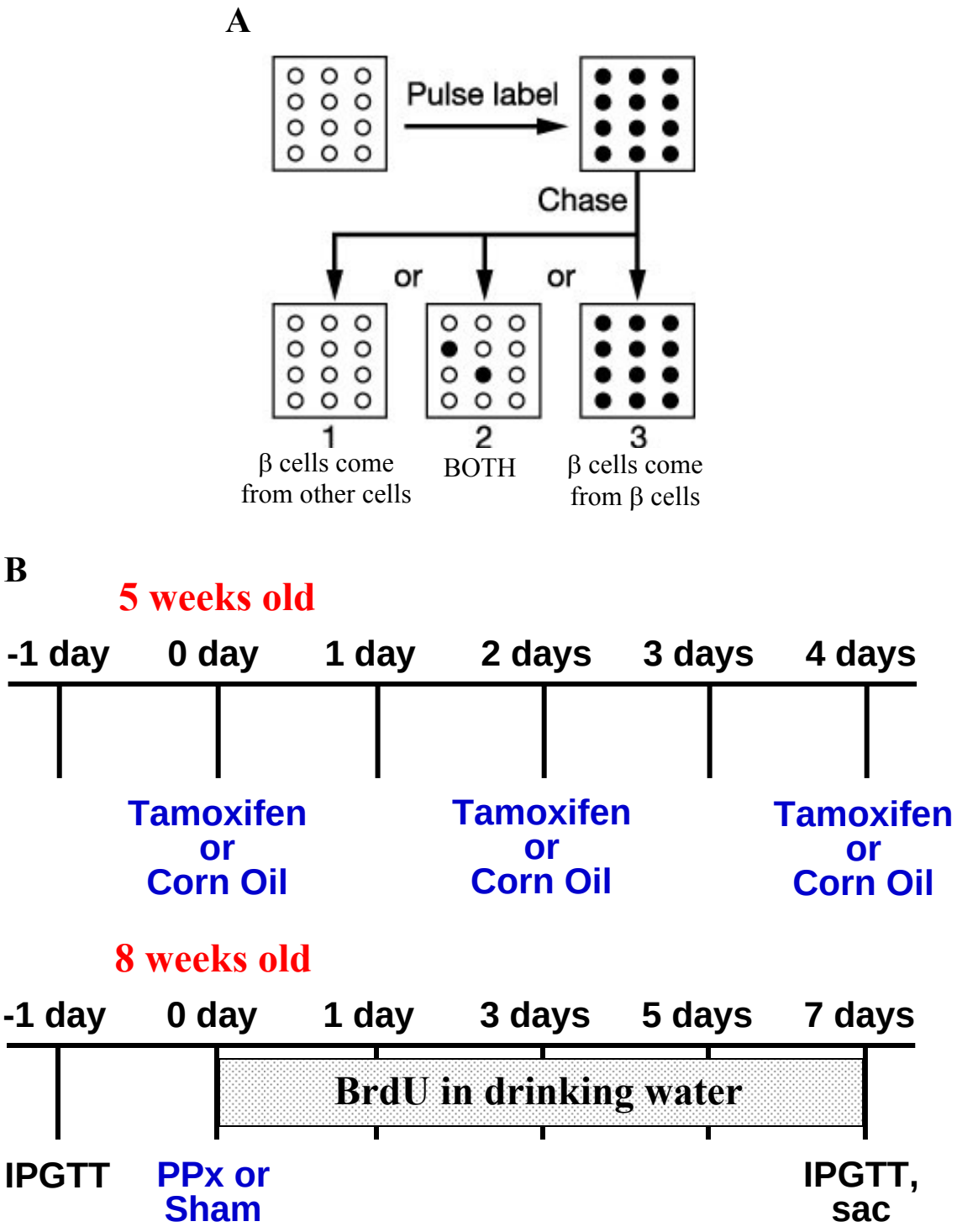

Figure 57. Pulse-chase lineage labeling of β cells. **(A)** Lineage labeling of β cells is accomplished by CreER-mediated recombination of a heritable reporter label (pulse) that can be assessed over a period of time (chase). **(B)** Experimental design of β cell lineage labeling experiments in *Pdx1*^{PB}-*CreER*^{TM};*R26*^{R} mice. Part A of figure is adapted from Dor *et al.* (2004).

contribution of neogenesis would most likely be small and would be restricted to or more prevalent in regenerating tissue, this study did not conclusively show that β cell neogenesis fails to occur after PPx or under normal conditions in the adult.

To address some of the above concerns, these studies were repeated with some modifications, seeking to determine whether β cell neogenesis occurred following 60% PPx, and, if so, to determine whether FoxM1 participated in this process. *Pdx1*^{PB}-*CreER*^{TM} mice were used rather than *RIP-CreER*^{TM} mice, as the *Pdx1*^{PB} promoter is also endocrine cell- (primarily β cell-) specific but is less leaky than the *RIP* (Jeanelle Kantz and Dr. Al Powers, Vanderbilt University; personal communication). 60% PPx was used as the method of pancreatic injury to induce regeneration, and the regenerating portion of the pancreas was separated from the remaining portion for analysis, as this portion is most likely to undergo neogenesis (see Chapter III). Five week old mice were injected subcutaneously with 3 injections of 8 mg tamoxifen each, and 60% PPx was performed 2 weeks after the final injections (Figure 57B), as it was hypothesized that tamoxifen would be cleared from the system within this time period.

Results

The original experimental design included *Foxm1*$^{floc/-}$;*Pdx1*^{PB}-*CreER*^{TM};*R26*^{R} and *Foxm1*$^{flox/+}$;*Pdx1*^{PB}-*CreER*^{TM};*R26*^{R} mice, in order to address both aims of this study with one set of experiments. However, despite multiple breeding schemes, there was no success in obtaining mice with a *Foxm1*^{fl} allele on the *R26*^{R} background, suggesting that the *Foxm1* and *Rosa26* loci were linked. In fact, both loci are located 13.3 centimorgans (cM) apart on mouse chromosome 6 (Figure 58A). Although this distance confers an

A

***Rosa26* locus**

Chrom 6; 48.7cM; 113,012,092-113,026,574bp

***Foxm1* locus**

Chrom 6; 62.0cM; 128,328,595-128,341,500bp

B

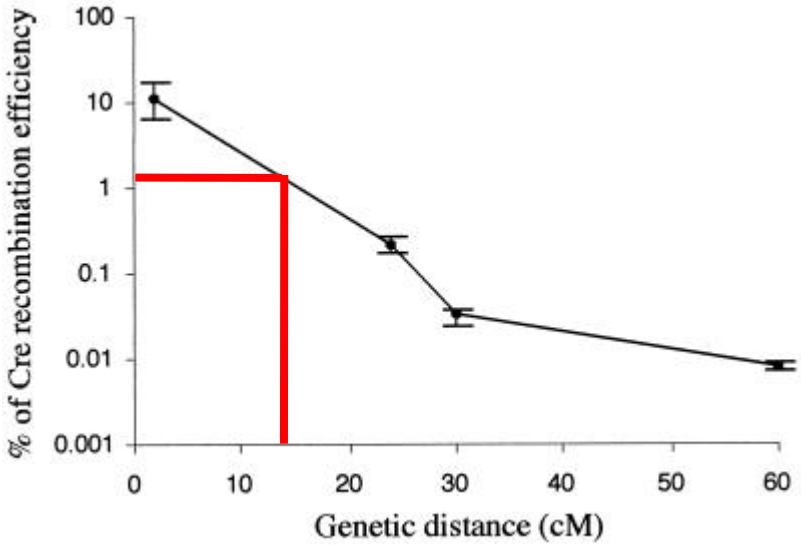

Figure 58. The *Foxm1* and *Rosa26* loci are closely located on mouse chromosome 6. (A) Chromosomal locations of *Rosa26* (*Thumpd3*) and *Foxm1* loci, provided by the University of California Santa Cruz (UCSC) Genome Browser. **(B)** Recombination efficiency of Cre recombinase diminishes with distance between loxP sites. The approximate distance and recombination efficiency between *Rosa26* and *Foxm1* are noted in red. Adapted from Zheng *et al*. (2000).

approximate 13% chance of recombination between the loci, no appropriate mice were generated after 6 litters and 47 pups. Even if these mice were generated, though, the presence of loxP sites within both the *Foxm1* and *Rosa26* loci presents the potential problem of Cre-mediated excision of the intervening sequence between the two loci, which includes multiple genes as well as the *LacZ* knock-in and could confound the results. Although rare, Cre-mediated recombination can occur between distant loxP sites (Zheng *et al.*, 2000) (Figure 58B).

To avert these concerns, $R26^{R}$ mice were replaced with Z/EG mice, which were generated by random transgenic insertion of a floxed *LacZ* coding sequence upstream of an *EGFP* coding sequence, driven by a ubiquitous CMV enhancer/chicken β-actin promoter (Novak *et al.*, 2000) (Figure 19). Unfortunately, Z/EG mice on the C57Bl/6 strain background, which was the background of the $Foxm1^{flox/-}$ and $Pdx1^{PB}$-$CreER^{TM}$ mice used in these studies, often displayed delayed growth and failure to thrive, which has also been observed by Jackson Laboratories, from which the mice were procured. This phenotype would have confounded assessment of physiological parameters and β cell mass, rendering these mice unusable for these experiments as well.

Finally, it was determined that $Pdx1^{PB}$-$CreER^{TM}$;$R26^{R}$ mice would be used for lineage tracing analysis to assess whether β cell neogenesis occurs following 60% PPx, while $Foxm1^{flox/-}$;$Pdx1^{PB}$-$CreER^{TM}$ and $Foxm1^{flox/+}$;$Pdx1^{PB}$-$CreER^{TM}$ mice would be used to assess FoxM1's role in β cell neogenesis following 60% PPx.

Efficiency of *Pdx1*^{PB}-*CreER*^{TM}-Mediated Recombination of *R26*^{R}

The protocol of 3 subcutaneous injections of 8 mg tamoxifen into 5 week old *Pdx1*^{PB}-*CreER*^{TM};*R26*^{R} female mice resulted in ~90% recombination of *R26*^{R} in β cells by 9 weeks of age, assessed by double-labeling with anti-insulin and anti-β-galactosidase antibodies. At 8 weeks old, mice were subjected to either 60% PPx or Sham, and one week later the percentage of total β cells that were β-galactosidase^{+} was compared. Preliminary analyses of the percentage of β-galactosidase^{+} β cells in the splenic pancreatic lobe of mice that underwent 60% PPx versus a Sham operation revealed no obvious difference in β cell labeling (Figure 59A-C). These results may indicate that non-β cells (unlabeled) did not give rise to new β cells after 60% PPx, although further analysis is necessary.

Longevity of Cre Nuclear Localization Following Tamoxifen Injection

Although tamoxifen injection is often used to perform "pulse-chase" experiments, the particular nature of this lineage labeling study requires that the "pulse" time frame be very well defined to ensure that any β cells that may differentiate from unlabeled precursors during the "chase" period do not undergo CreER-mediated recombination and express the lineage label. Because CreER nuclear localization correlates with recombination activity and is dependent on tamoxifen presence, anti-Cre antibody labeling was performed in order to assess Cre protein sub-cellular localization after tamoxifen injection, as an indirect assessment of tamoxifen presence. The PPx experiments were designed to account for slow clearing of tamoxifen, with *Pdx1*^{PB}-*CreER*^{TM};*R26*^{R} mice subjected to PPx or Sham two weeks after tamoxifen

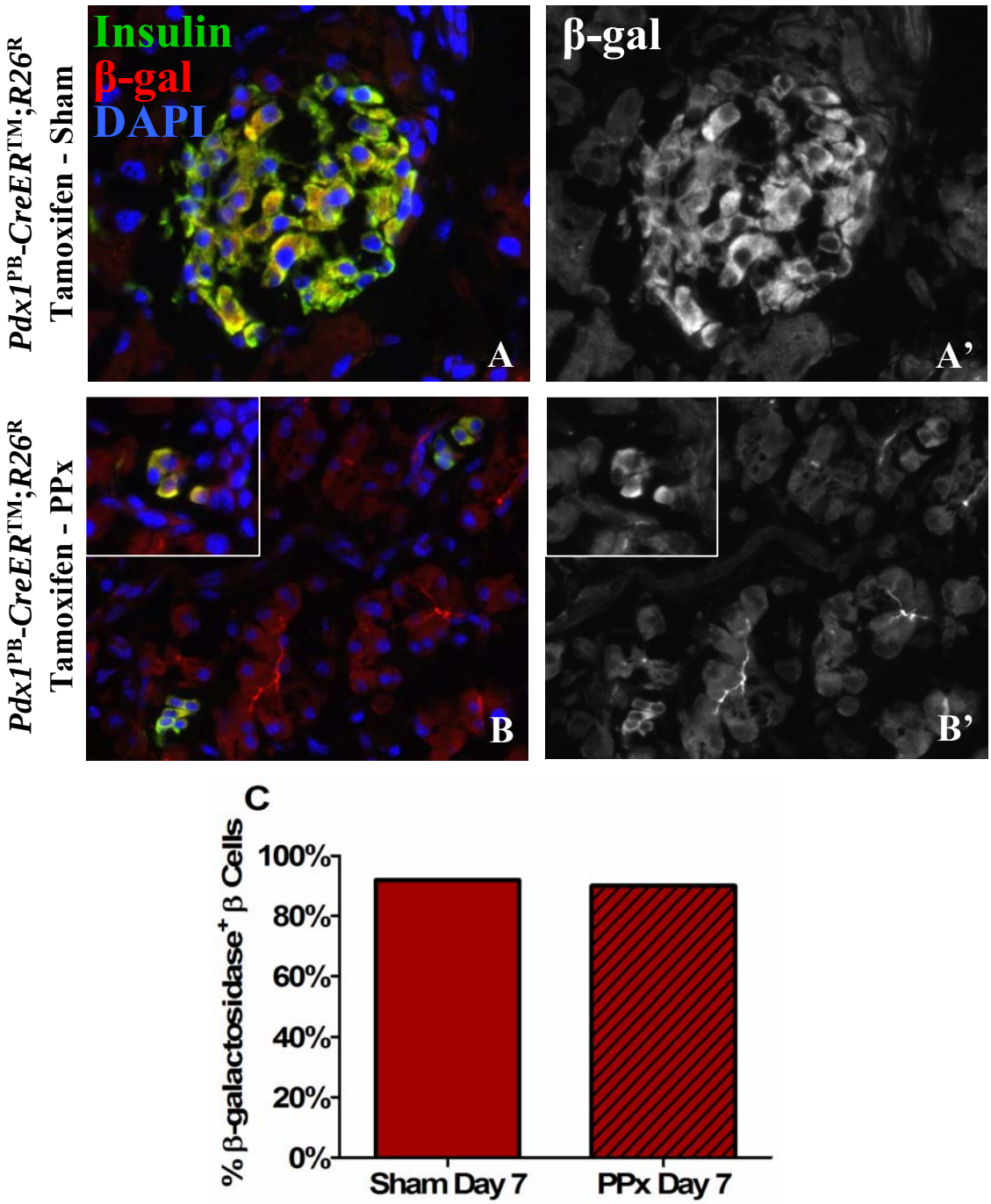

Figure 59. *Pdx1*^{PB}-*CreER*^{TM} mediated high levels of recombination of *R26*^{R} in β cells. *Pdx1*^{PB}-*CreER*^{TM};*R26*^{R} mice were injected 3 times with 8 mg tamoxifen and underwent a Sham operation or 60% PPx. **(A)** Cryosections of the splenic lobe of Sham and **(B)** PPx-operated mice were labeled for Insulin (green), β-galactosidase (red), and DAPI (blue). Inset shows an additional islet. **(C)** Approximately 90% of β cells were β-galactosidase^{+} at 7 days after either a Sham operation or 60% PPx. All images were captured at 400X magnification. n=1 per group.

injection and then sacrificed one week after the operation. Surprisingly, even after this three week "chase" period, Cre protein was localized primarily to the nuclei of the majority of β cells (Figure 60A,A'). In contrast, *Pdx1*^{PB}-*CreER*^{TM};*R26*^{R} mice injected with vehicle (corn oil) alone did not display any significant amount of nuclear-localized Cre (Figure 60B,B'). These findings suggested that tamoxifen was still present in injected animals for much longer than anticipated. Thus, lineage labeling experiments were postponed until the time frames of tamoxifen and Cre activity were better characterized.

To determine whether there was a time point by which Cre was no longer localized to the nucleus, time course experiments were performed in which *Pdx1*^{PB}-*CreER*^{TM};*R26*^{R} mice were administered 3 injections of 8 mg tamoxifen each, and the mice were sacrificed at various time points thereafter for Cre labeling of pancreatic sections. This analysis revealed that the intensity of Cre labeling in individual nuclei, tended to decline over time, although a significant number of β cell nuclei were labeled strongly for Cre even 8 weeks after tamoxifen injection (Figure 61A,A',B,B').

To determine whether the relatively high dose of tamoxifen was responsible for the persistent Cre nuclear localization, the number of tamoxifen injections was reduced to either two injections of 8 mg tamoxifen each or a single injection of 8 mg tamoxifen. At five weeks after two injections, *Pdx1*^{PB}-*CreER*^{TM};*R26*^{R} mice displayed similar results as observed at three or five weeks after three injections, with the majority of β cells exhibiting strong nuclear Cre labeling (Figure 62A,A'). However, five weeks after a single tamoxifen injection, there were very few β cell nuclei labeled with Cre (Figure 62B,B'), implying that the dose of tamoxifen administered correlated with nuclear

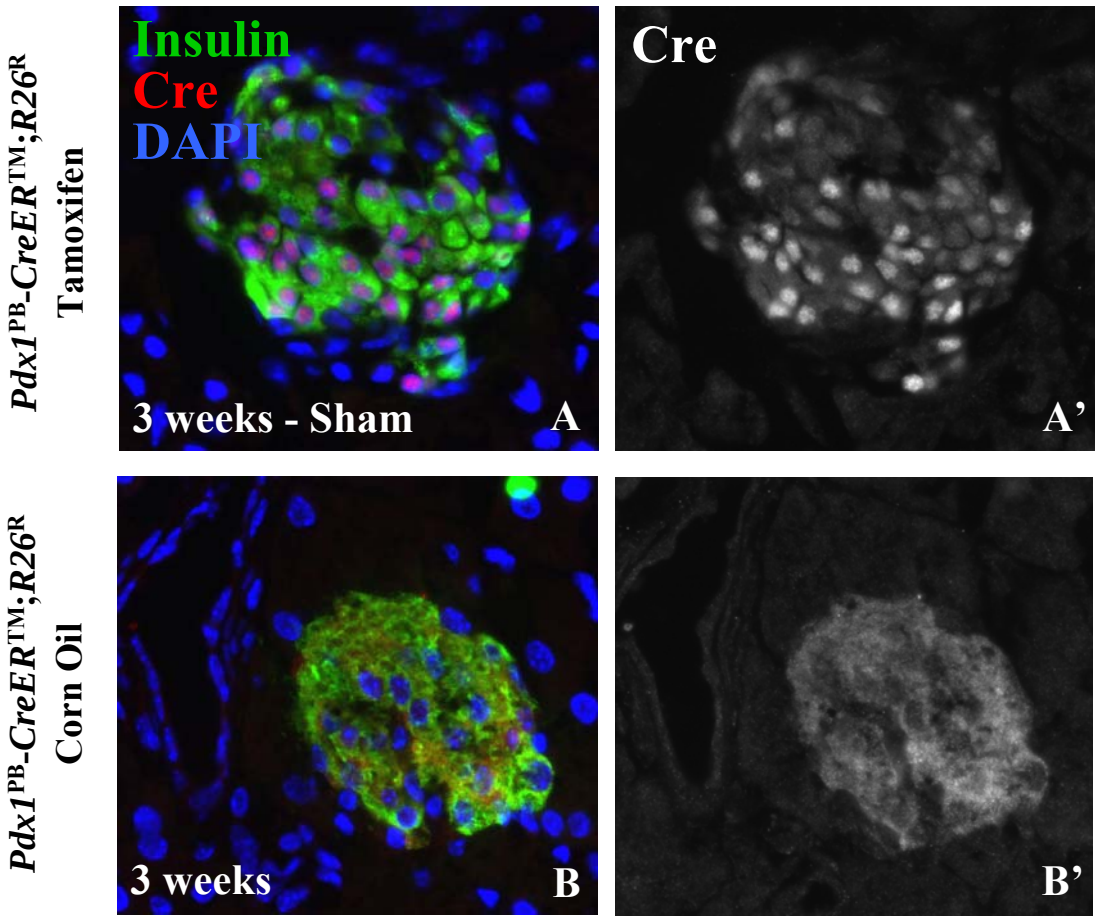

Figure 60. Cre was primarily localized to islet nuclei 3 weeks after *Pdx1*^{PB}-*CreER*^{TM};*R26*^{R} mice were injected 3 times with 8 mg tamoxifen. (A) Cryosections of the splenic lobe from Sham-operated mice previously injected with tamoxifen were labeled for Insulin (green), Cre (red), and DAPI (blue). The majority of β cells exhibited strong Cre labeling within the nucleus. **(B)** Pancreas cryosections from *Pdx1*^{PB}-*CreER*^{TM};*R26*^{R} mice injected three times with vehicle (corn oil) alone showed strong cytoplasmic, but not nuclear, Cre labeling. All images were captured at 400X magnification.

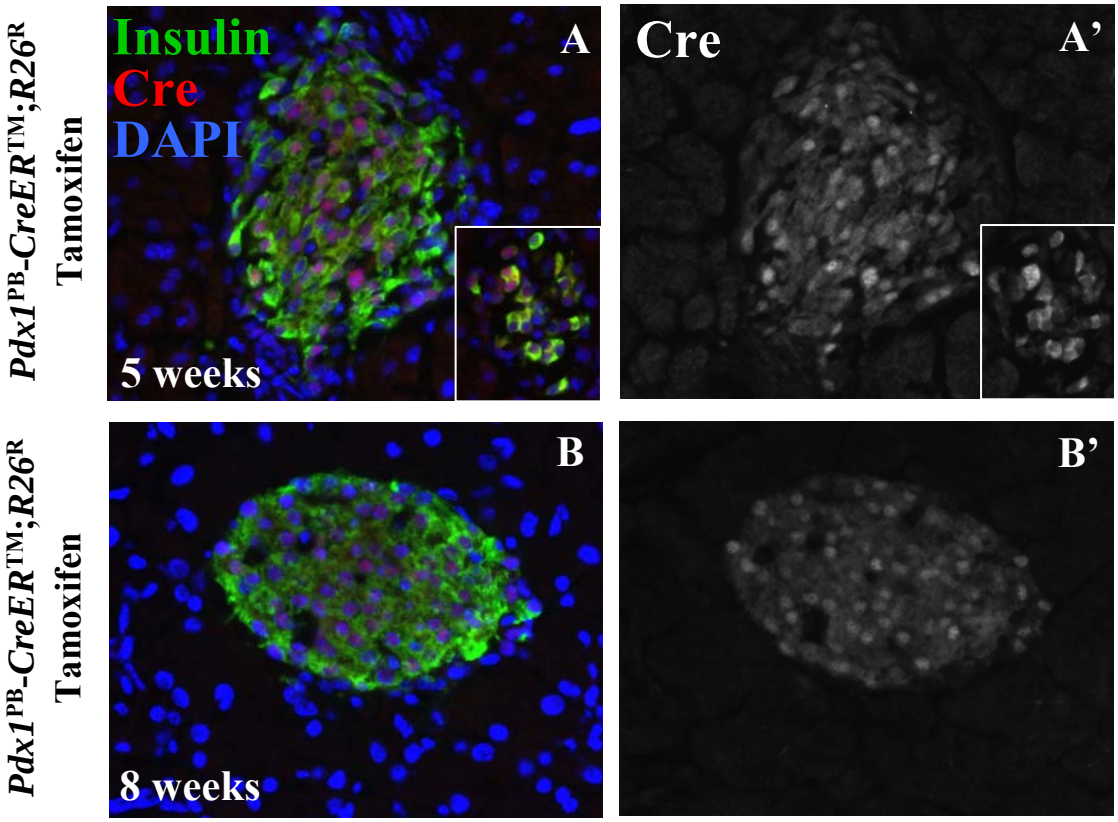

Figure 61. Nuclear localization of Cre persisted until at least 8 weeks after tamoxifen injection. *Pdx1*^{PB}-*CreER*^{TM};*R26*^{R} mice were injected 3 times with 8 mg tamoxifen, and pancreatic tissue was harvested either 5 weeks **(A)** or 8 weeks **(B)** following tamoxifen injection. Pancreatic cryosections were labeled for Insulin (green), Cre (red), and DAPI (blue). Inset shows an additional islet. The intensity of Cre labeling appeared to decrease with time, although the majority of β cells continued to exhibit Cre labeling within the nucleus. All images were captured at 400X magnification.

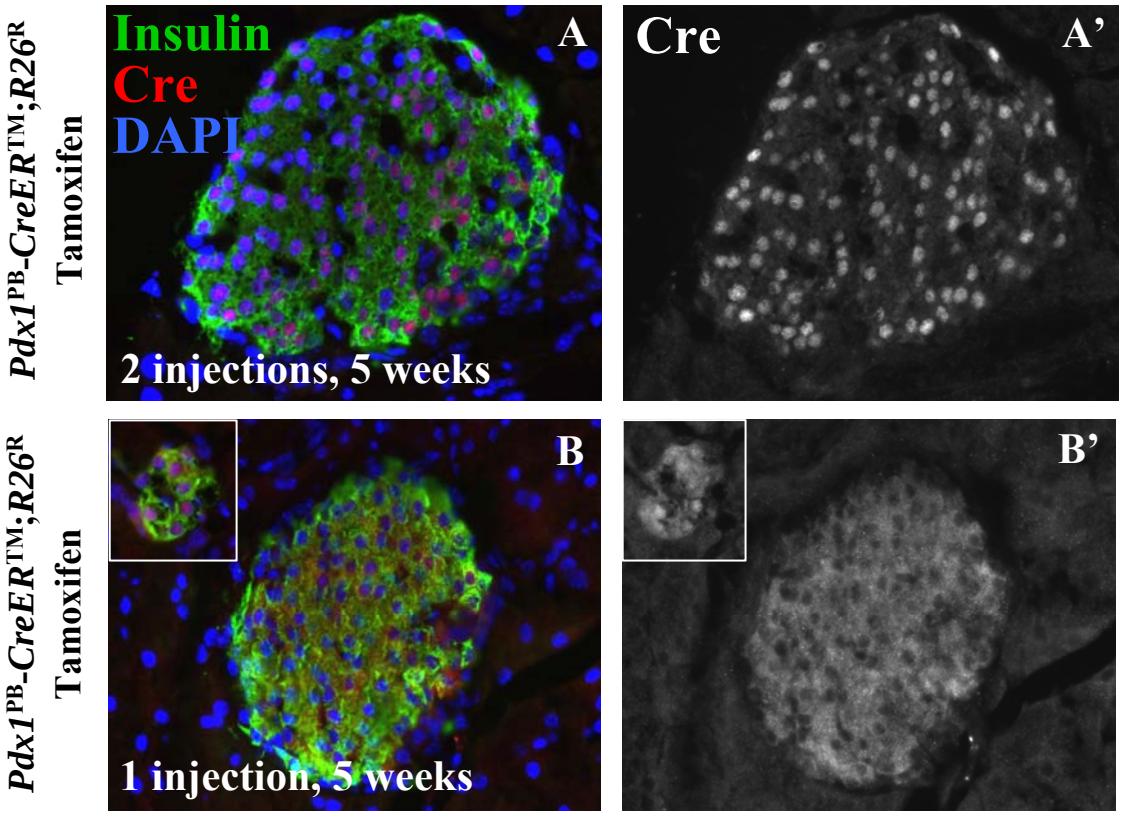

Figure 62. Tamoxifen dose correlated with nuclear localization of Cre protein in *Pdx1*^{PB}-*CreER*^{TM};*R26*^{R} mice. *Pdx1*^{PB}-*CreER*^{TM};*R26*^{R} mice were administered either **(A)** 2 injections of 8 mg tamoxifen each or **(B)** a single injection of 8 mg tamoxifen. Five weeks later, pancreatic cryosections were labeled for Insulin (green), Cre (red), and DAPI (blue). Inset shows an additional islet. Five weeks after 2 injections, the majority of β cells exhibited strong Cre labeling within the nucleus. However, after only a single injection, the majority of β cells showed strong cytoplasmic, but not nuclear, Cre labeling, although there was substantial variation among islets. All images were captured at 400X magnification.

localization of Cre. Similarly, tamoxifen dose directly correlated with *R26*^{R} recombination, assessed by β-galactosidase expression. *Pdx1*^{PB}-*CreER*^{TM};*R26*^{R} mice after only one or two tamoxifen injections displayed a reduced percentage of β-galactosidase^{+} β cells compared to that observed after three injections (Figure 63A,A',B,B').

The persistence of Cre nuclear localization suggested that perhaps tamoxifen is not readily metabolized and cleared from the body. To directly address this issue, our laboratory in collaboration with Rachel Reinert and Dr. Al Powers (Vanderbilt University) are planning experiments to determine the pharmacokinetic profile of tamoxifen in mice and to determine whether *Pdx1*^{PB}-*CreER*^{TM};*R26*^{R} islets will undergo recombination when transplanted into mice previously injected with tamoxifen.

FoxM1$^{\Delta islet}$ Mice Subjected to 60% PPx

Although lineage tracing experiments were inconclusive and were postponed due to possible confounding effects of tamoxifen longevity, data from studies performed on *Foxm1*$^{flox/flox}$;*Pdx1*$^{5.5kb}$-*Cre* (FoxM1$^{\Delta panc}$) and *Foxm1*$^{flox/flox}$ mice indicated that β cell neogenesis occurred following 60% PPx and was not impaired in the absence of FoxM1 (see Chapter III). Supporting experiments were designed to determine whether FoxM1 is required in non-endocrine cells for the generation of new β cells after 60% PPx, using *Foxm1*$^{flox/-}$;*Pdx1*^{PB}-*CreER*^{TM} (FoxM1$^{\Delta islet}$) and *Foxm1*$^{flox/+}$;*Pdx1*^{PB}-*CreER*^{TM} female littermates. These mice were subjected to 60% PPx or a Sham operation, and regeneration of β cell mass was evaluated. Additionally, the extent of β cell mass regeneration in these mice was compared to that of FoxM1$^{\Delta panc}$ mice to determine

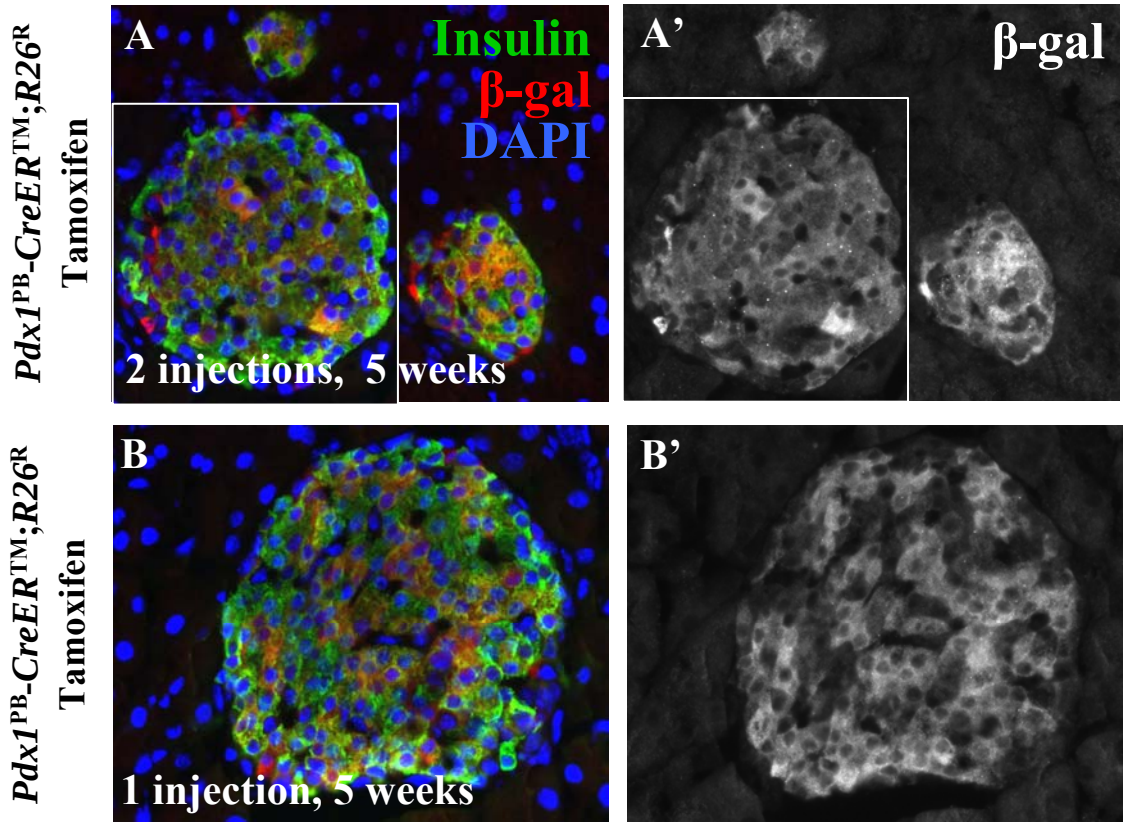

Figure 63. Tamoxifen dose directly correlated with β-galactosidase expression in *Pdx1*^{PB}-*CreER*^{TM};*R26*^{R} mice. *Pdx1*^{PB}-*CreER*^{TM};*R26*^{R} mice were administered either **(A)** 2 injections of 8 mg tamoxifen each or **(B)** a single injection of 8 mg tamoxifen. Five weeks later, pancreatic cryosections were labeled for Insulin (green), β-galactosidase (red), and DAPI (blue). In both cases, the percentage of β-galactosidase^{+} β cells was less than 90%. Inset shows an additional islet. All images were captured at 400X magnification.

whether loss of FoxM1 in all pancreatic cells was more detrimental than islet-specific loss of FoxM1. If at 7 days after PPx, β cell mass in FoxM1$^{\Delta islet}$ mice was reduced compared to Control littermates, and if this reduction was proportionate to the reduced β cell mass observed in FoxM1$^{\Delta panc}$ mice compared to their Control littermates (Chapter III), then these results would suggest that FoxM1 was only required islet cells for β cell mass regeneration. In contrast, if at 7 days after PPx, β cell mass in FoxM1$^{\Delta islet}$ versus Control littermates was reduced to a lesser extent than observed in FoxM1$^{\Delta panc}$ versus Control littermates, then these results would suggest that both islet and non-islet cells required FoxM1 for regeneration of β cell mass. Both interpretations are dependent on high CreER-mediated recombination efficiency of the *Foxm1*$^{flox/flox}$ locus.

Fourteen mice have thus far been included in the experiment, of which only six have been evaluated for β cell mass. Regardless of genotype or tamoxifen injection, all mice exhibited similar body weight (Figure 64A) and glucose tolerance 7 days after PPx (Figure 64B). Of the pancreata that have been analyzed to date, the weight of the splenic lobe 7 days after PPx was slightly reduced in FoxM1$^{\Delta islet}$ mice compared to Controls, whereas duodenal lobe weight was increased (Figure 65A). Furthermore, there appeared to be reduced regeneration of β cell mass in the splenic lobe of FoxM1$^{\Delta islet}$ mice compared to Controls (Figure 65C), which correlated with reduced percent insulin^{+} area on pancreatic sections (Figure 65B). In comparison to FoxM1$^{\Delta panc}$ female mice, however, FoxM1$^{\Delta islet}$ mice exhibited similar reductions in β cell mass regeneration compared to their respective Control littermates. One week after 60% PPx, β cell mass in FoxM1$^{\Delta panc}$ mice was ~50% that of Control littermates (0.057 mg versus 1.02 mg; Figure 27C), and FoxM1$^{\Delta islet}$ mice similar exhibited only ~50% the β cell mass of Control

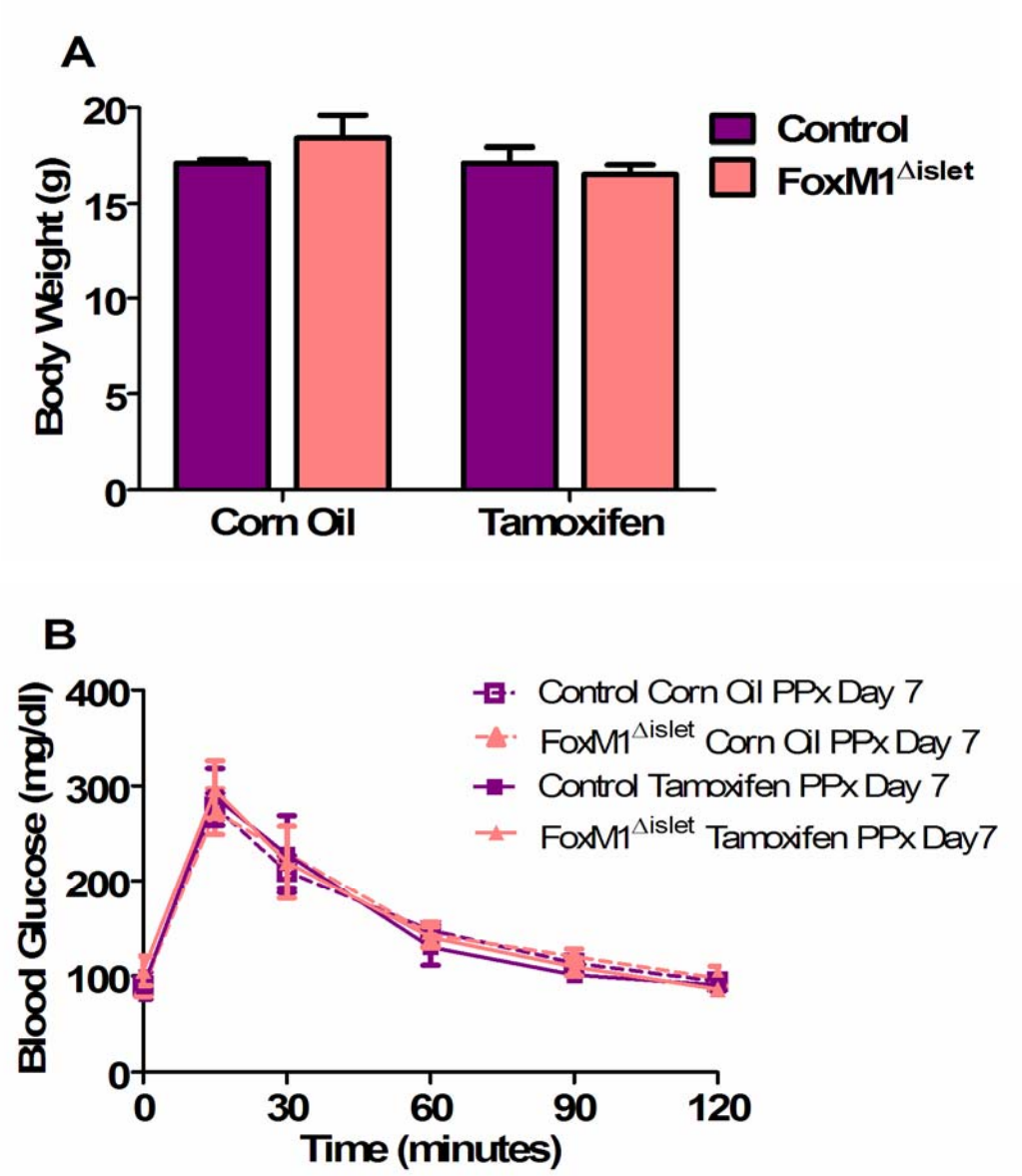

Figure 64. Foxm1$^{\Delta islet}$ and Control mice exhibited similar body weights and glucose tolerance. Mice were injected with either vehicle (corn oil) or tamoxifen and then subjected to 60% PPx. 7 days after PPx, **(A)** body weight was measured, and **(B)** IPGTT was performed. Error bars represent SEM. Two-way ANOVA with Bonferroni's post-tests was used to measure significance. n=2-3 per group for Corn Oil-injected, 4-5 per group for Tamoxifen-injected.

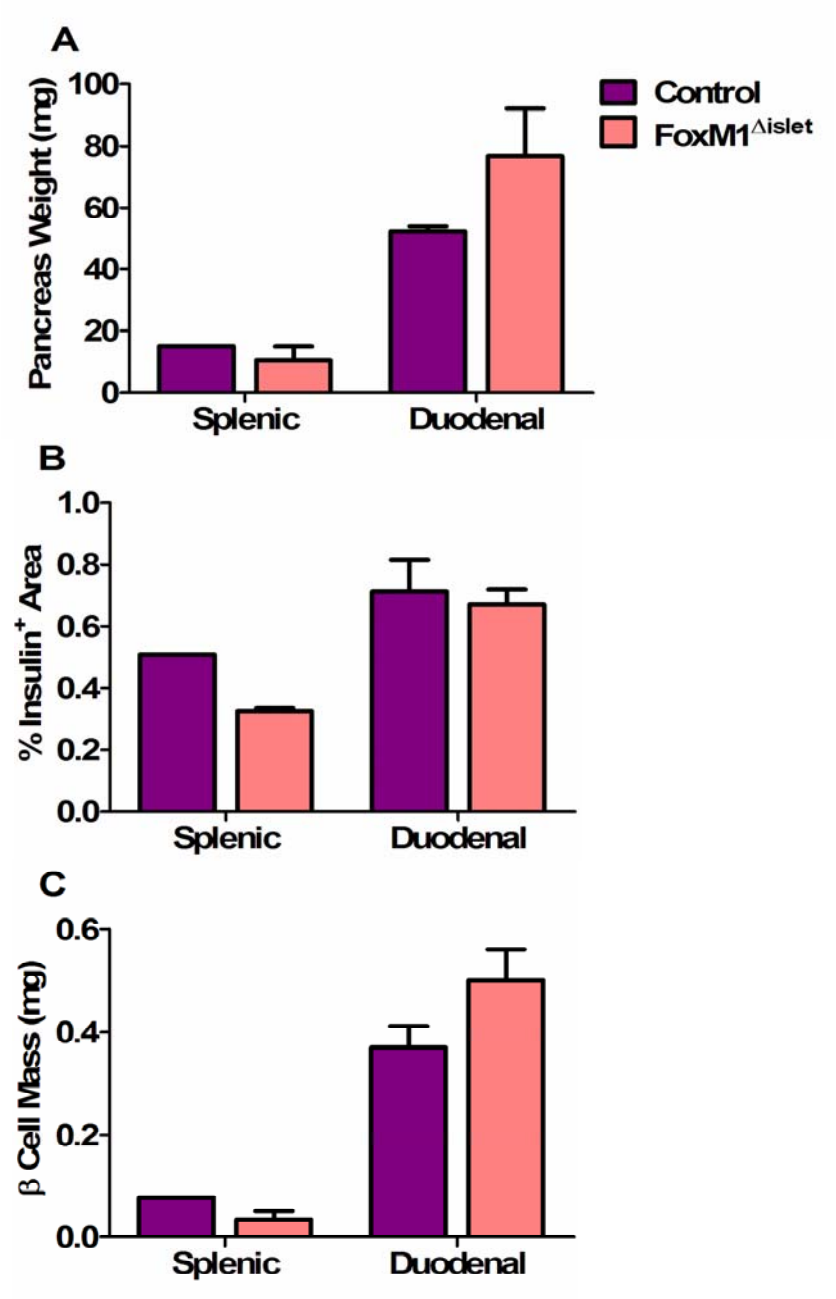

Figure 65. After 60% PPx, β cell mass in the regenerating splenic lobe of Foxm1$^{\Delta islet}$ mice was reduced compared to Control mice. Mice were injected with tamoxifen and then subjected to 60% PPx. **(A)** 7 days after PPx, splenic lobe weight was slightly reduced, while duodenal lobe weight was increased, in Foxm1$^{\Delta islet}$ mice versus Controls. **(B)** Percent insulin^{+} pancreatic area on sections was also reduced in the splenic, but not duodenal, lobe of Foxm1$^{\Delta islet}$ mice versus Controls. **(C)** Taking into account tissue weight and % insulin^{+} area, β cell mass in the splenic lobe was reduced, while that in the duodenal lobe was increased, in Foxm1$^{\Delta islet}$ mice versus Controls. Error bars represent SEM. Two-way ANOVA with Bonferroni's post-tests was used to measure significance. n=1-3 per group.

littermates at the same time point (0.035 mg versus 0.077 mg; Figure 65C). The different mixed strain backgrounds of the two Cre-expressing mouse lines likely accounted for the different β cell mass results in the respective Control mice. Of course, additional analyses need to be performed on the remaining tissue samples before any conclusions can be drawn from these experiments.

Discussion

The field of β cell regeneration has been debated for quite some time regarding not only the source(s) and mechanism(s) of such regeneration, but also whether β cell neogenesis in fact occurs. There is also debate over whether neogenesis refers solely to progression from an undifferentiated cell to a differentiated one, or whether it can encompass such processes as de-differentiation and re-differentiation, and transdifferentiation. Regardless, it is clear that the type of pancreatic injury induced is paramount to the interpretations of the results, as is the precision with which analyses are performed. It is also clear that neogenesis is not the primary mechanism by which the β cell population regenerates or grows. However, the there is great potential for β cell neogenesis to influence future therapy for diabetic patients.

This study was begun before Xu *et al.* (2008) and Bonner-Weir *et al*. (2008) reported direct mechanistic and lineage tracing evidence for β cell neogenesis, respectively. These reports and the data presented in Chapter III substantiate the histological findings that have been reported by many groups in support of the occurrence of neogenesis. However, additional lineage tracing studies, particularly using other injury models, are vital to the field. Thus, these studies still merit completion.

Although the lineage tracing study has not yet been completed, it raised the possibility of an important caveat to time-sensitive CreER^{TM}-mediated lineage labeling systems, as nuclear-localized CreER protein was evident for many weeks after tamoxifen injection. Prior studies utilizing CreER lineage labeling suggested a 48 hour window of tamoxifen-induced CreER activity (Gu *et al.*, 2002). However, these studies utilized intraperitoneal injections of pregnant moms and analyzed embryonic recombination, which may have produced different results than observed in this study using subcutaneous injections and adult analyses. In general, substances injected intraperitoneally are more readily introduced into the bloodstream than if injected subcutaneously.

Of course, maintenance of Cre nuclear localization does not necessarily correlate with tamoxifen presence. Although CreER is translocated to the nucleus by binding to tamoxifen, it is unclear whether CreER is shuttled out of the nucleus in the absence of tamoxifen, and if so, how quickly this occurs. The slow reduction in nuclear-localized Cre protein after tamoxifen injection observed in this study could be due to slow clearance of tamoxifen and/or to high perdurance of Cre protein in combination with slow nuclear exclusion. However, it would not be surprising if tamoxifen is cleared slowly from the body, as tamoxifen and its metabolites are extremely hydrophobic (Figure 66) and consequently are stored at relatively high concentrations in adipose tissue (Kisanga *et al.*, 2003; Kisanga *et al.*, 2005). Furthermore, tamoxifen metabolites in general exhibit greater activity than tamoxifen itself (Lim *et al.*, 2005), meaning that extensive metabolism is required to clear tamoxifen activity. Therefore, pharmacokinetic

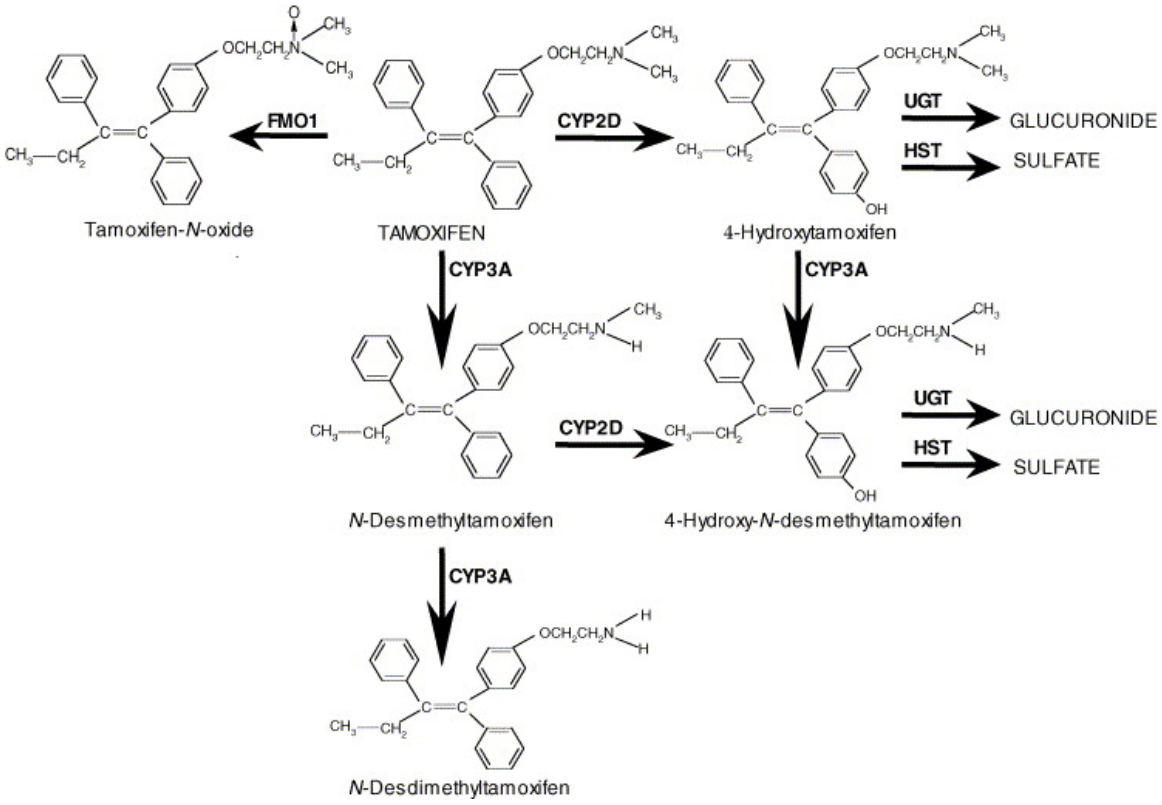

Figure 66. Tamoxifen metabolism pathways. Tamoxifen is extensively metabolized by the Cytochrome P450 (CYP) family in the liver. The metabolites 4-hydroxy-tamoxifen and N-desmethyltamoxifen have particularly high activity. Figure is from Kisanga *et al*. (2005).

profiling of tamoxifen, administered in the same manner (location and dose) used for lineage tracing studies is necessary for proper interpretation of results of such studies.

The study described in Chapter III suggested that FoxM1 is not required for β cell neogenesis following 60% PPx, utilizing FoxM1$^{\Delta panc}$ mice. The studies described here were designed to complement the original study, utilizing FoxM1$^{\Delta islet}$ mice and lineage labeling of β cells. Preliminary results suggested that regeneration of β cell mass was not improved in FoxM1$^{\Delta islet}$ versus FoxM1$^{\Delta panc}$ mice, indicating that FoxM1 was not required in non-endocrine cells for generation of new β cells. It is possible, however, that *Foxm1* was not actually deleted in FoxM1$^{\Delta islet}$ mice, as *Foxm1* transcript levels have not yet been measured in these mice by our laboratory. Interestingly, despite ~90% recombination of the *R26*^{R} reporter in β cells using the same method of CreER induction (Figure 59C), *Foxm1* transcript levels were only reduced by 27% in FoxM1$^{\Delta islet}$ islets compared to *Foxm1*$^{+/+}$;*Pdx1*^{PB}-*CreER*^{TM} Control islets sent to a collaborating lab (Jeremy Lavine and Dr. Alan Attie, University of Wisconsin – Madison, personal communication). These conflicting results could be due to differing efficiencies of CreER-mediated recombination at the *Rosa26* and *Foxm1* loci. To avoid the possibility of inefficient recombination, future experiments could use *Rip-Cre* mice to delete *Foxm1* in β cells. These mice may in fact provide a better comparison against FoxM1$^{\Delta panc}$ mice, as they would also undergo deletion of *Foxm1* during development. FoxM1$^{\Delta islet}$ mice were initially used in these experiments with the plan that they could be used for lineage tracing studies as well. However, combining these studies has been impossible, and the inherent difficulties and possible low efficiency of CreER-mediated recombination makes a constitutive Cre line preferable.

Another possible explanation for the lack of a difference in β cell mass regeneration between FoxM1$^{\Delta islet}$ and FoxM1$^{\Delta panc}$ mice is that, as Chapter III describes, the contribution of neogenesis to β cell mass recovery following 60% PPx is small in comparison to that of proliferation. Therefore, it may simply be difficult to detect a difference in neogenesis between FoxM1$^{\Delta islet}$ and FoxM1$^{\Delta panc}$ mice using the methods described here. However, direct lineage tracing using the recently-published duct-selective *CAII-CreER*^{TM} (Bonner-Weir *et al.*, 2008) or Cytokeratin (CK) 19-*CreER*^{TM} (Means *et al.*, 2008) mouse lines, in combination with *Foxm1* deletion, could potentially produce more precise data regarding FoxM1's role in β cell neogenesis.

CHAPTER VI

GENERATING A FOXM1 ANTIBODY

Introduction

FoxM1 was first identified in 1994 as an antigen for the MPM2 antibody, which recognizes a specific serine/threonine phosphorylation epitope in proteins phosphorylated during mitosis (Westendorf *et al.*, 1994). However, this antibody recognizes many other M-phase phosphorylated proteins (MPPs), meaning it is not selective for FoxM1. Since then, many anti-FoxM1 antibodies have been generated by various companies and laboratory groups. However, many of these antibodies specifically react with human FOXM1, but not mouse FoxM1. Furthermore, several of these antibodies were generated against a peptide and have not been verified. In order to perform analyses of FoxM1 expression, cellular and sub-cellular localization, and post-translational modification, it is necessary to have a specific antibody that can be used for these specific applications.

Our laboratory first utilized a polyclonal anti-FoxM1 antibody generated against the N-terminus by Dr. Robert H. Costa's laboratory (University of Illinois at Chicago) (Ye *et al.*, 1997) to detect FoxM1 protein in embryonic, perinatal, and adult pancreatic sections (Zhang H *et al.*, 2006). However, this antibody was only available for a short period of time, and results could not be replicated with other antibody preparations. Commercially-available antibodies from Santa Cruz Biotechnology that were generated against various fragments of the FoxM1 protein and have been used for immunocytochemistry on human cell lines (Ma *et al.*, 2005) have not been shown to

work on mouse tissue, and our laboratory was unable to detect a specific signal using these antibodies for immunohistochemistry on mouse tissue sections. Furthermore, commercially-available antibodies from AbCam that were generated against a FoxM1-specific peptide have not been verified by other groups, and indeed, our laboratory did not obtain positive results using such antibodies for immunohistochemistry.

Generally, it is difficult to detect protein on tissue sections due to the fixation process involved and the quarternary structure of the protein of interest, which can mask the epitope recognized by the antibody. Although many antigen retrieval methods exist to aid in exposing the epitope of interest, they are not always sufficient. Despite using protease digestion and heat-denaturing in both acidic and basic solutions with the anti-FoxM1 antibodies mentioned above, our laboratory has been unable to detect FoxM1 protein on mouse tissue.

Western immunoblotting avoids the concerns mentioned above with regard to immunohistochemistry because the proteins are denatured prior to incubation with the antibody and are separated based on mass. Thus, all epitopes should be exposed, and specificity is not a primary concern because the protein of interest can be identified by its size. A polyclonal anti-FoxM1 antibody generated against the C-terminus by Dr. Robert H. Costa's laboratory (University of Illinois at Chicago) (Wang *et al.*, 2005) was used for western immunoblotting of mouse protein. However, our laboratory found that the signal produced by this antibody was not specific for FoxM1, despite appearing at an appropriate mass, because signals were observed in lanes containing both WT and *Foxm1*$^{-/-}$ protein (Figure 67A). Similar results were observed using a commercially-available polyclonal anti-C-terminal-FoxM1 antibody from Santa Cruz Biotechnology

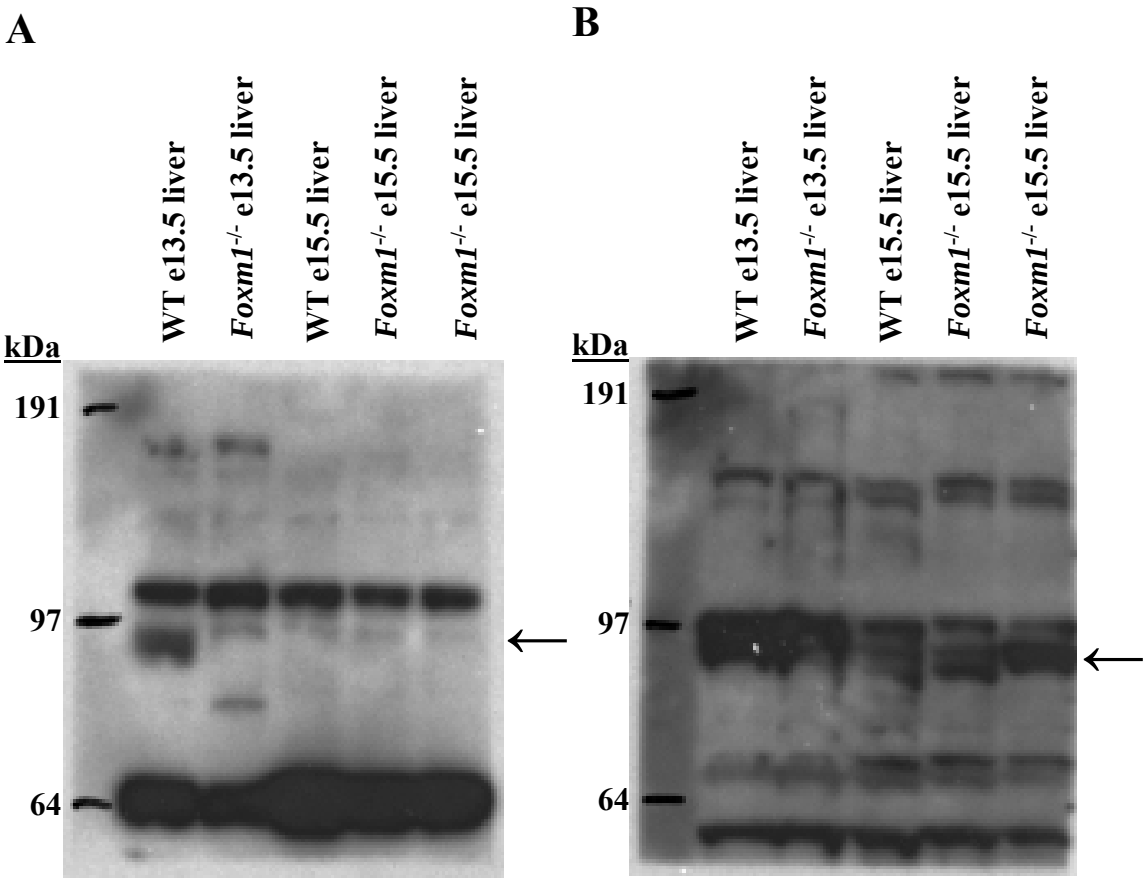

Figure 67. Available anti-FoxM1 antibodies are not specific. Western immunoblots were performed using protein extracted from embryonic liver from WT and *Foxm1*$^{-/-}$ littermates. **(A)** A polyclonal anti-C-terminal-FoxM1 antibody provided by Dr. Robert H. Costa's laboratory bound to a protein at slightly higher than 83 kDa (arrow), but bands at this size were also observed in *Foxm1*$^{-/-}$ protein extracts, and consistent results were not observed between different WT protein samples. **(B)** A polyclonal anti-C-terminal-FoxM1 antibody from Santa Cruz Biotechnology also bound to a protein at slightly higher than 83 kDa (arrow) in WT protein extracts, but no difference was observed between WT and *Foxm1*$^{-/-}$ extracts.

(Figure 67B), and no published studies using either of these antibodies had included protein from *Foxm1*$^{-/-}$ tissue. To determine whether *Foxm1* was actually deleted in *Foxm1*$^{-/-}$ mice, PCR was performed for the *Foxm1*^{WT} and *Foxm1*^{null} alleles (Figure 68A-D), and qRT-PCR was used to compare *Foxm1* transcript levels in embryonic liver samples between WT and *Foxm1*$^{-/-}$ littermates (Figure 68E). These results confirmed that *Foxm1*$^{-/-}$ mice indeed contained the truncated *Foxm1* gene but not the full-length gene, and that *Foxm1* transcripts were nearly undetectable. Thus, we are confident that *Foxm1*$^{-/-}$ extract and tissue can be used to identify specific anti-FoxM1 antibodies, and that the antibodies tested to date do not specifically recognize FoxM1.

As described in Chapters III and IV, qRT-PCR specifically detects mouse *Foxm1* or human *FOXM1* transcripts. However, as with western immunoblotting, expression cannot be assessed on a cellular basis. In an attempt to identify *Foxm1* transcript on tissue sections, *in situ* hybridization was performed. Radioactive *in situ* hybridization had previously shown widespread *Foxm1* expression on whole-embryo sections, including within the pancreas (Ye *et al.*, 1997). This finding was confirmed using non-radioactive *in situ* hybridization, which revealed that *Foxm1* was found to be expressed at relatively high levels in the embryonic cords, along the ductal epithelium, at e15.5 (Figure 69A) and in embryonic liver (Figure 69B). These results were similar to those observed in the pancreas using an anti-N-terminus FoxM1 antibody on embryonic mouse sections (Zhang H *et al.*, 2006) (Figure 14) and in the liver using radioactive *in situ* hybridization (Ye *et al.*, 1997). However, because of the high levels of RNase proteins within the pancreas after birth, *in situ* hybridization failed to detect *Foxm1* in adult tissues.

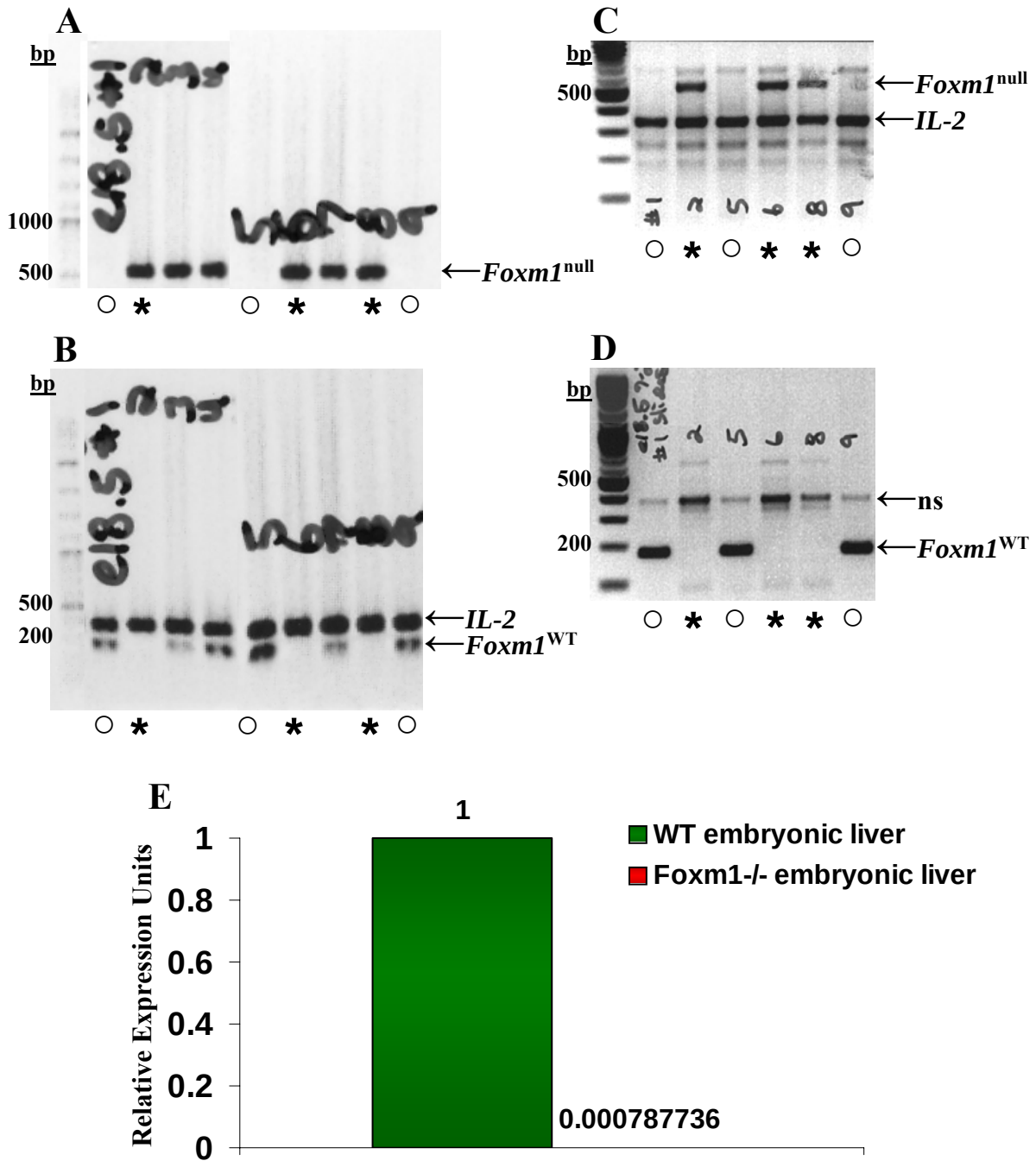

Figure 68. Confirmation of *Foxm1*$^{-/-}$ tissue. Embryos from *Foxm1*$^{+/-}$ inter-crosses were genotyped for *Foxm1* **(A)** null and **(B)** WT alleles using DNA from tail tissue. *Foxm1*$^{-/-}$ embryos (#2, 6, and 8, asterisks) and *Foxm1*$^{+/+}$ embryos (#1, 5, and 9, circles) were confirmed using DNA from pancreatic tissue sections by the presence of the **(C)** *Foxm1* null allele and the absence of the **(D)** *Foxm1* WT allele. Genotyping for *IL-2* was used as a control. ns=non-specific. **(E)** Real-time qRT-PCR was used to assess *Foxm1* transcripts in e15.5 liver samples in WT and *Foxm1*$^{+/-}$ littermates. n=1 per group.

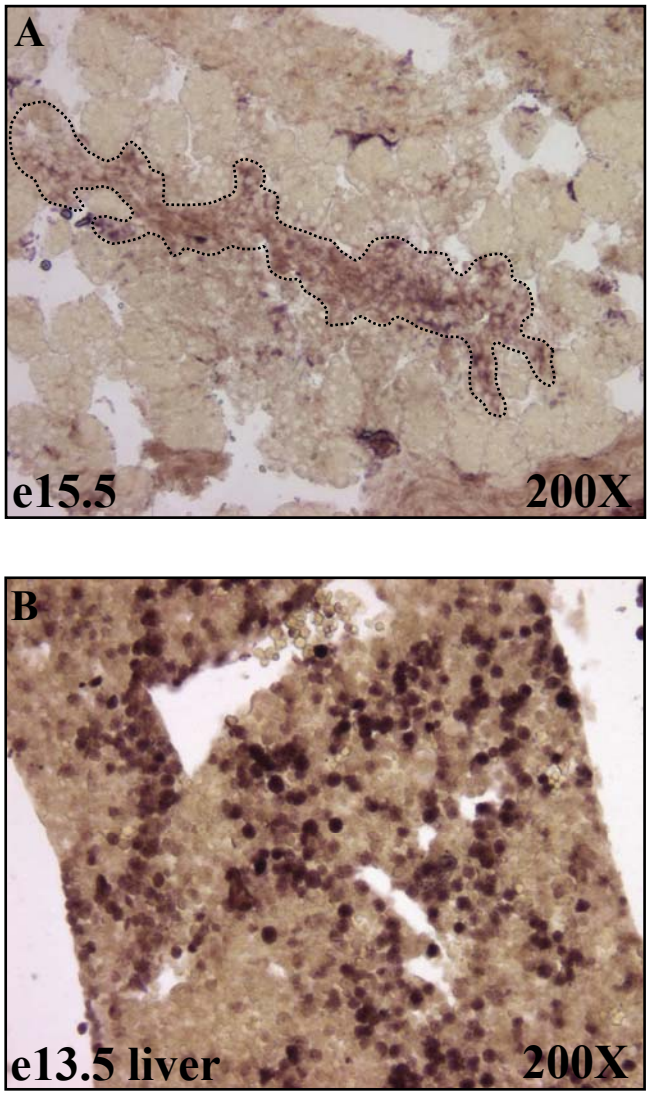

Figure 69. *In situ* hybridization for *Foxm1*. (A) *Foxm1* mRNA was detected in endocrine cords (outlined) of WT pancreas at e15.5 and in **(B)** WT liver at e13.5.

Currently, no antibody exists that can specifically detect mouse FoxM1 using immunohistochemistry or western immunoblotting. Such analyses would enhance the studies presented in Chapters III-V and could be used in future studies by our laboratory and others. To this end, our laboratory decided to generate an anti-FoxM1 antibody. This chapter describes the processes of generating and screening a monoclonal anti-FoxM1 antibody, which was done in collaboration with the Vanderbilt Monoclonal Antibody Core. However, some of the methods used and reagents generated in this project could be used for future production of other antibodies, such as phospho-specific or peptide antibodies.

The choice to generate a monoclonal versus polyclonal antibody was made based on the need for a highly-specific antibody for use primarily in immunohistochemistry. Because monoclonal antibodies recognize an individual epitope, they are more specific than are polyclonal antibodies, which can recognize multiple epitopes. Although in many cases, the multiple epitopes recognized by polyclonal antibodies are still specific to the protein of interest, there is a greater risk of cross-reaction with epitopes on other proteins. Because FoxM1 is part of a large family of proteins that all share homology in the DNA binding domain, cross-reactivity is concerning. Additionally, monoclonal antibodies can be produced in unlimited quantity, and all lots have similar characteristics because they are produced from a clonal population of hybridoma cells. Polyclonal antibodies are collected from animal sera, which can vary greatly. Therefore, a monoclonal antibody would be useful for many future experiments and for other laboratory groups.

Progress to Date and Future Directions

Because FoxM1 is a rather large protein with multiple domains, and its three-dimensional structure is not known, it was decided that a protein antigen would be preferable to a peptide antigen for generation of a monoclonal antibody. However, because of FoxM1's size and because of the concern regarding cross-reactivity with other Fox proteins mentioned above, it was decided that three fragments of the FoxM1 protein would be generated for immunization, none containing the DNA binding domain. These three fragments were generated from mouse *Foxm1* cDNA (NM_008021) using PCR, with Fragment 1 consisting of bp 172-870 (amino acids 1-233), Fragment 2 consisting of bp 1108-1938 (amino acids 313-589), and Fragment 3 consisting of bp 1939-2445 (amino acids 590-757) (Figure 70A). These fragments were designed to specifically exclude the forkhead DNA binding domain because BLAST search indicated that FoxM1 shares little sequence homology with other proteins outside of this domain (Figure 70B).

The coding sequence for each FoxM1 fragment was sub-cloned into the pAT107b vector that contains an N-terminal high-molecular weight (43.2 kDa) MBP tag, which can be cleaved by 3C protease, and a C-terminal small 8x polyhistidine tag, which cannot be cleaved. These tags not only allow for identification of fusion proteins, but the MBP tag confers enhanced solubility and immunogenicity to each fusion protein (Dr. Robert Carnahan, Vanderbilt University, personal communication) (Bannantine *et al.*, 2004). Additionally, this vector is a derivative of the pET vector, so expression of the fusion protein is driven by the T7 promoter, which is induced by IPTG but repressed in the absence of T7 RNA polymerase (Figure 71A).

A

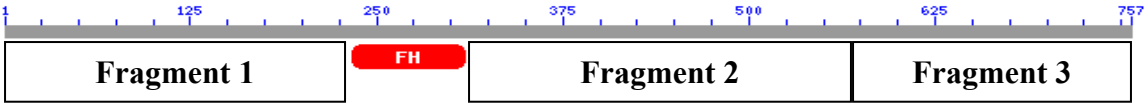

B

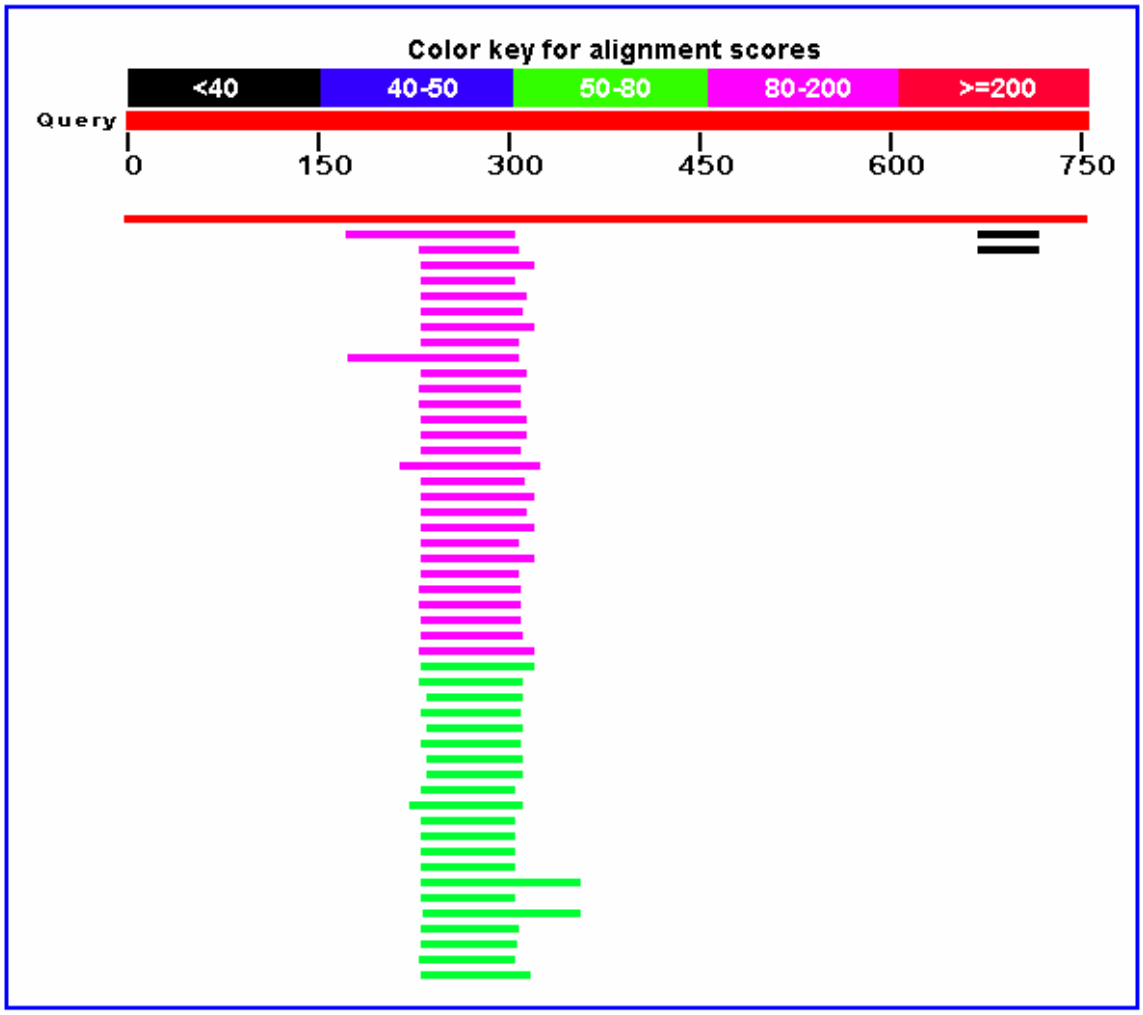

Figure 70. Generation of FoxM1 fragments. **(A)** Three fragments of mouse FoxM1 were generated, corresponding to the N-terminal, middle, and C-terminal regions (Fragment 1, 2, and 3, respectively). The forkhead (FH) DNA binding domain was excluded from these fragments because **(B)** FoxM1 shares high sequence homology with other Fox proteins within this domain. B was obtained from NCBI BLAST search of mouse FoxM1 protein sequence (NP_032047) against mouse reference proteins (refseq_protein). Search was performed on August 12, 2008.

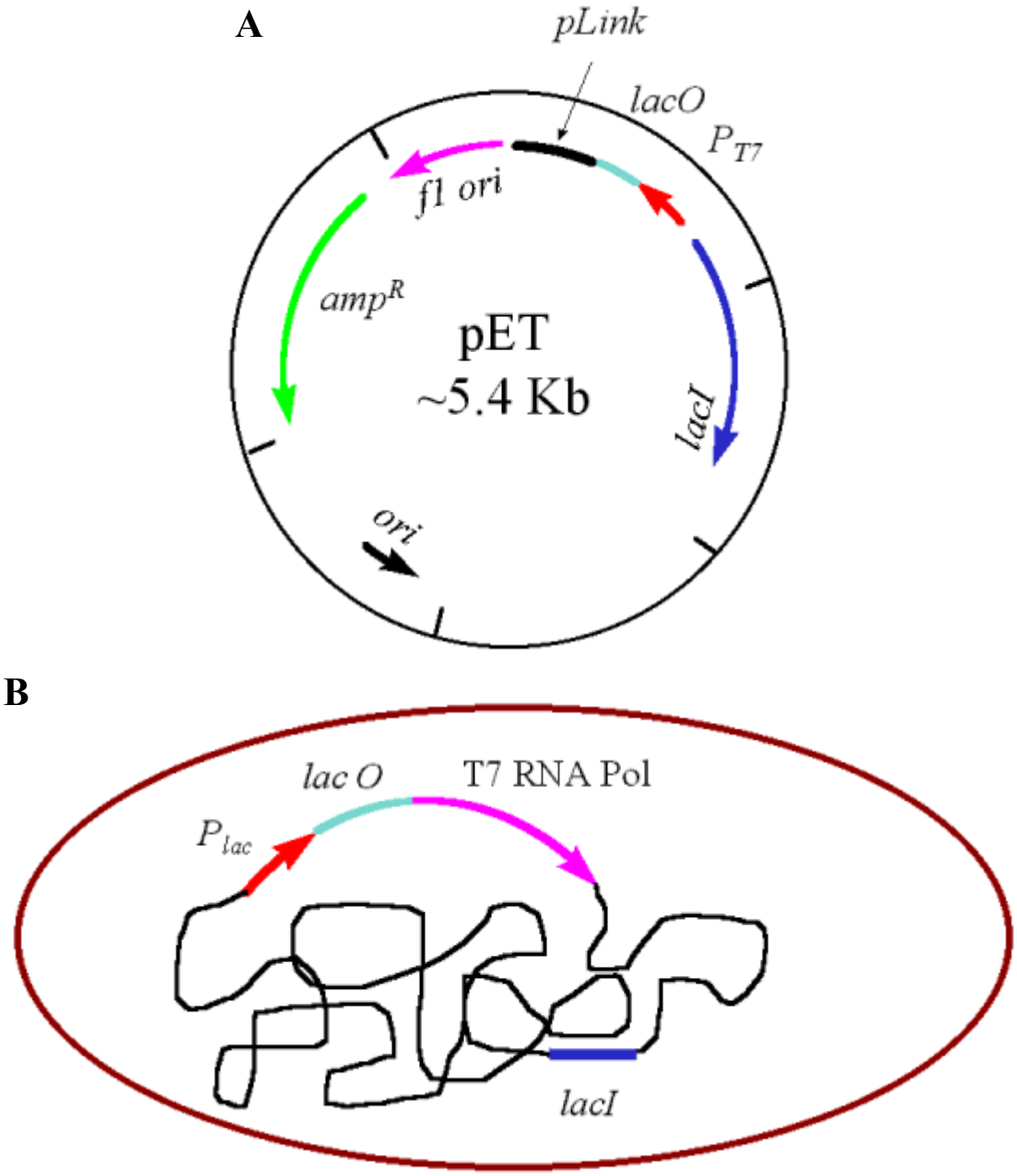

Figure 71. T7 expression system. (A) The pET vector and its derivatives, such as pAT107b, consist of a T7 RNA polymerase-responsive promoter (P_{T7}) upstream of a *lac* operon (*lacO*), a polylinker site (*pLink*) into which a sequence of interest can be inserted, and a *lac* repressor gene (*lacI*). In the absence of T7 polymerase and lactose (or IPTG), expression of the gene of interest is repressed. **(B)** The host chromosome of BL(DE3) *E. coli* contains the coding sequence for T7 RNA polymerase under control of the *lac* operator system. Presence of lactose or IPTG de-represses expression of T7 RNA polymerase, and the combined presence of these factors promotes expression of the gene of interest.

Each FoxM1 fragment-MBP fusion protein was expressed in BL21-CodonPlus (DE3)-RIPL *E. coli* (Stratagene), which contain the coding sequence for T7 RNA polymerase, driven by an IPTG-inducible promoter (Figure 71B). These bacteria also contain plasmids that carry genes encoding the *argU*, *ileY*, *leuW*, and *proL* tRNAs, which are normally rarely expressed in *E. coli* and can limit translation of heterologous proteins.

Small-scale inductions were used to assess and optimize culture, induction, and purification conditions. Cultures were induced with IPTG for 2, 4, or 6 hours at 37°C, 32°C, 29°C, or 25°C. Initial analyses of bacterial lysates indicated that the Fragment 1-MBP fusion protein was efficiently induced at 37°C after 2 hours, while Fragments 2- and 3-MBP were recovered at much lower levels (bands at 68, 73, and 61, respectively; Figure 72). These results suggested that the Fragment 2-MBP and Fragment 3-MBP fusion proteins were relatively insoluble. Induction for longer periods of time at lower temperatures, which can improve solubility, did not produce dramatically different results for Fragment 2-MBP compared to induction at 37°C (Figure 73). However, a slight improvement in recovery was observed for Fragment 3-MBP after induction at 32°C for 2 hours. Comparison of insoluble (pelleted) and soluble (supernatant) fractions of the lysate confirmed that the majority of the Fragment 2- and 3-MBP fusion proteins were insoluble, and that Fragment 2-MBP was less soluble than Fragment 3-MBP (Figure 74).

Large-scale cultures were then induced with IPTG for 2 hours at 32°C, and lysate was purified under denaturing conditions using amylose resin, which bound to the MBP tag on each FoxM1 fragment and was then competed away by maltose. All three fragment-MBP fusion proteins were efficiently induced (crude lysate, Figure 75). However, only Fragment 1-MBP was efficiently purified, while the majority of Fragment

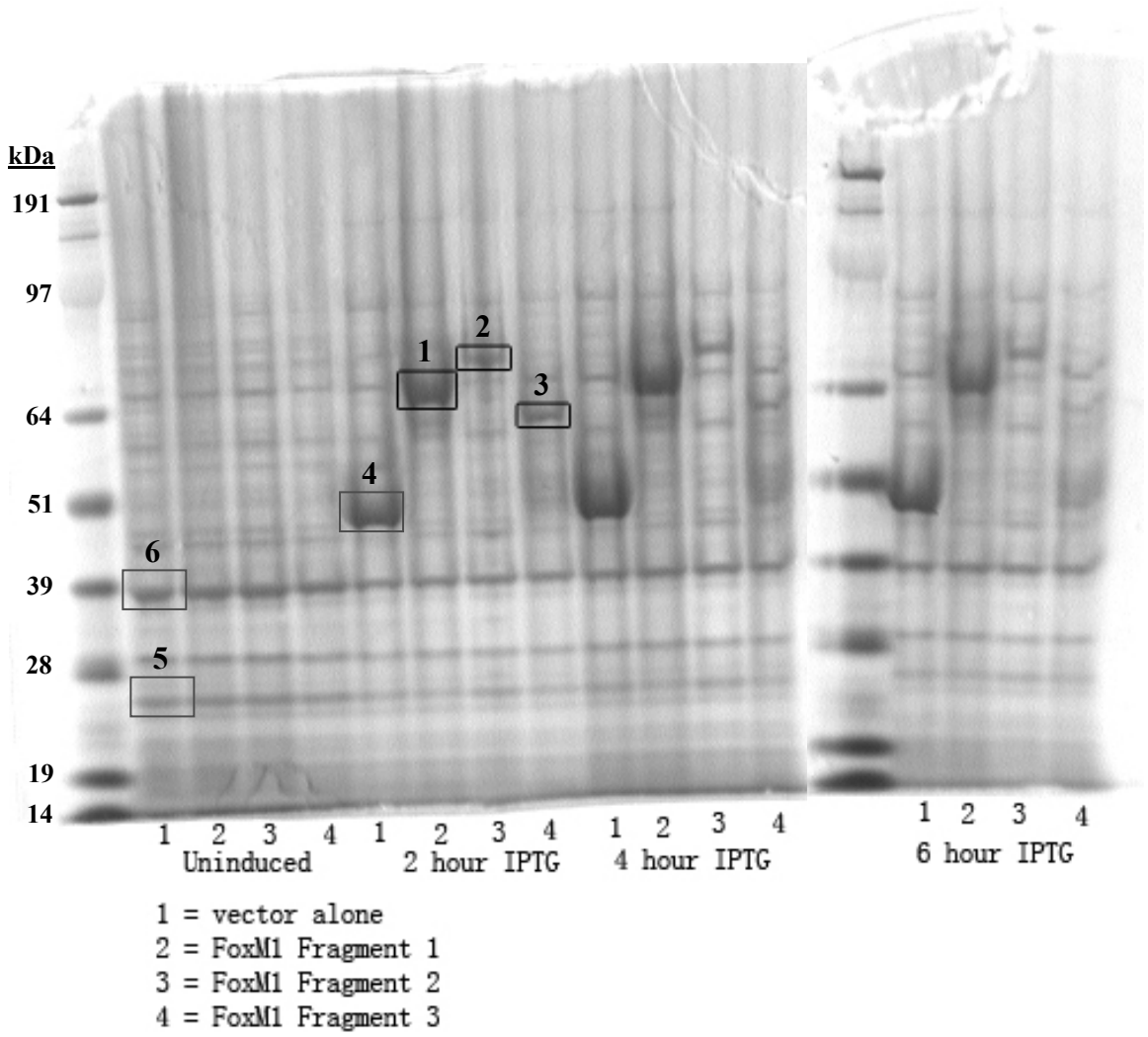

Figure 72. IPTG induced expression of FoxM1 Fragment 1-, 2-, and 3-MBP fusion proteins. Crude cell lysates were collected from transformed BL21-CodonPlus (DE3)-RIPL *E. coli* prior to or 2, 4, or 6 hours after induction with IPTG. Band at 43 kDa represents MBP (vector, 4), band at 68 kDa represents FoxM1 Fragment 1-MBP (1), band at 73 kDa represents FoxM1 Fragment 2-MBP (2), and band at 61 kDa represents FoxM1 Fragment 3-MBP (3). Bands at 26 and 38 kDa represent chloramphenicol acetyl transferase (5) and the streptomycin resistance gene product (6), respectively, which are inherent to BL21-CodonPlus (DE3)-RIPL *E. coli*.

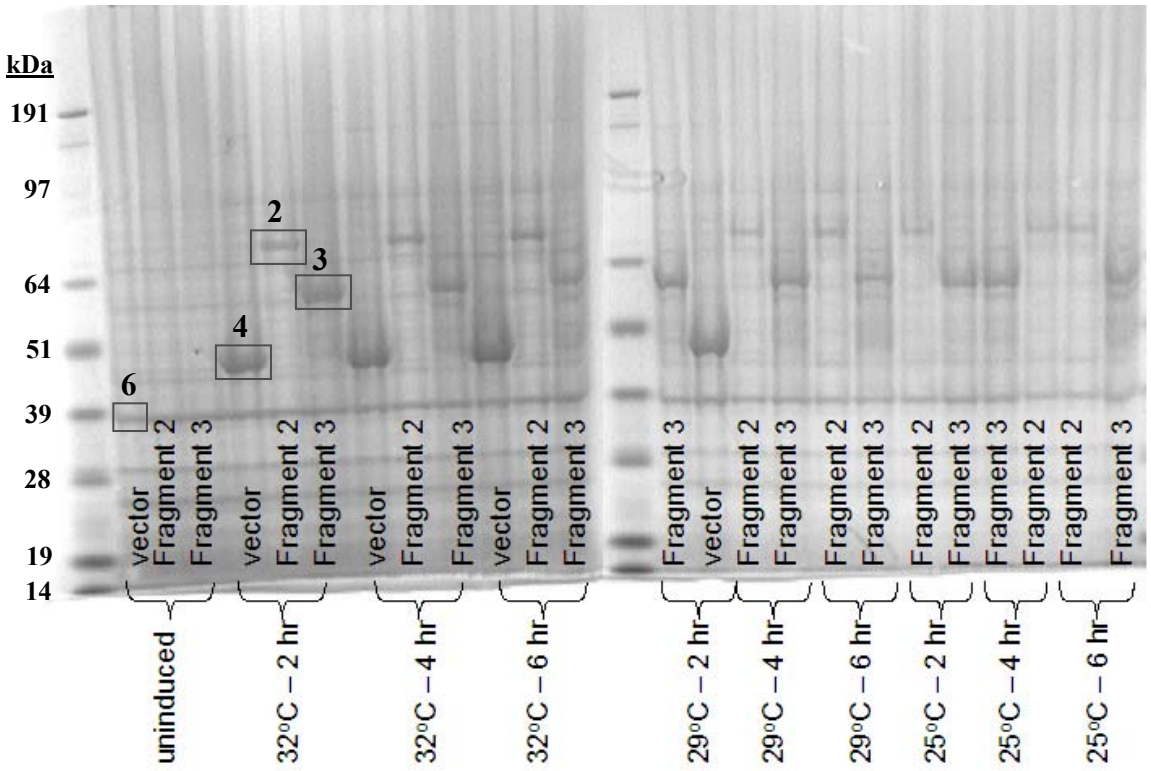

Figure 73. Lower induction temperatures modestly improved FoxM1 Fragment 3-MBP solubility. Crude cell lysates from BL21-CodonPlus (DE3)-RIPL *E. coli* were collected either prior to or 2, 4, or 6 hours after induction at 32, 29, or 25°C. Band at 43 kDa represents MBP (vector, 4), band at 73 kDa represents FoxM1 Fragment 2-MBP (2), and band at 61 kDa represents FoxM1 Fragment 3-MBP (3). Band at 38 kDa represents the streptomycin resistance gene product (6), which is inherent to BL21-CodonPlus (DE3)-RIPL *E. coli*.

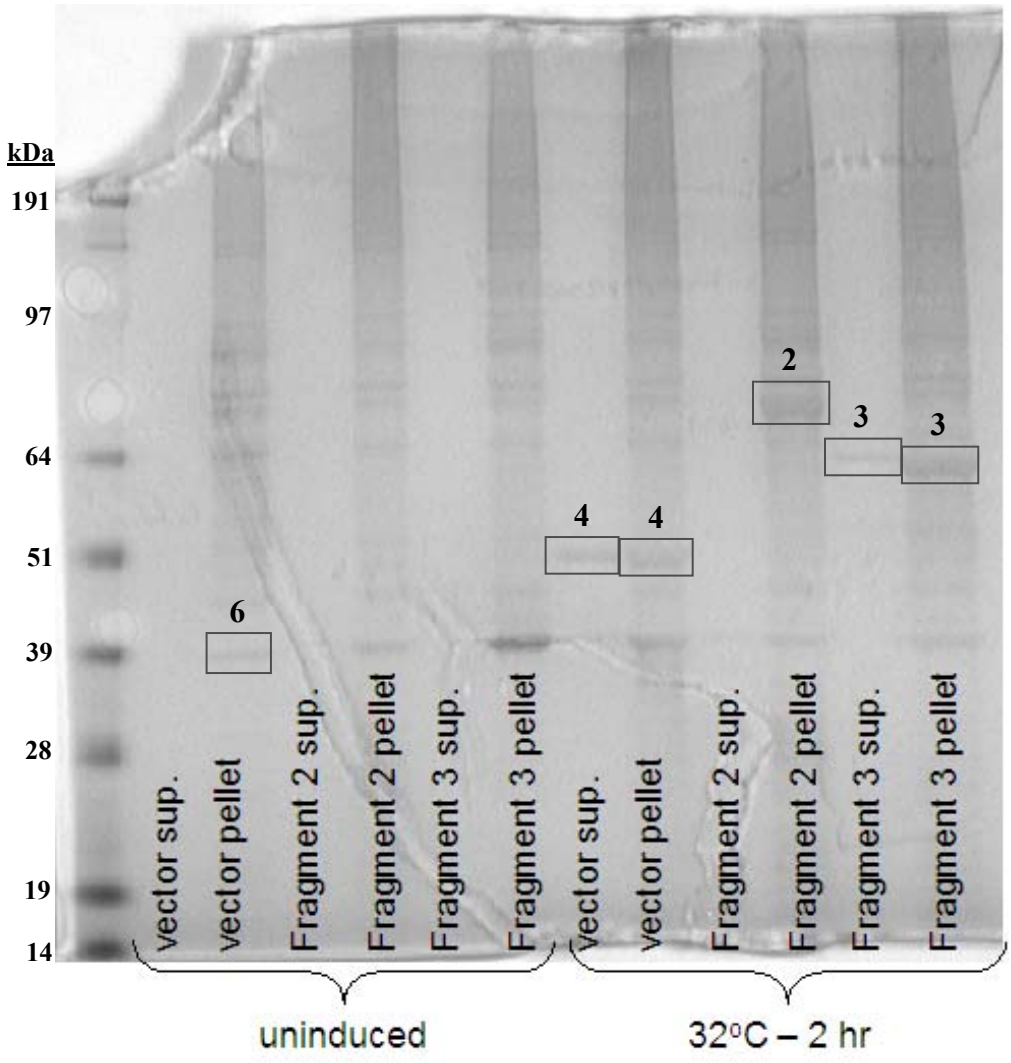

Figure 74. FoxM1 Fragment 2- and 3-MBP fusion proteins were highly insoluble. Crude cell lysates from BL21-CodonPlus (DE3)-RIPL *E. coli* were collected either prior to or 2 hours after induction with IPTG at 32°C, and then centrifuged to separate soluble (supernatant; sup.) and insoluble (pellet) fractions. Band at 43 kDa represents MBP (vector, 4), band at 73 kDa represents FoxM1 Fragment 2-MBP (2), and band at 61 kDa represents FoxM1 Fragment 3-MBP (3). Band at 38 kDa represents the streptomycin resistance gene product (6), which is inherent to BL21-CodonPlus (DE3)-RIPL *E. coli*.

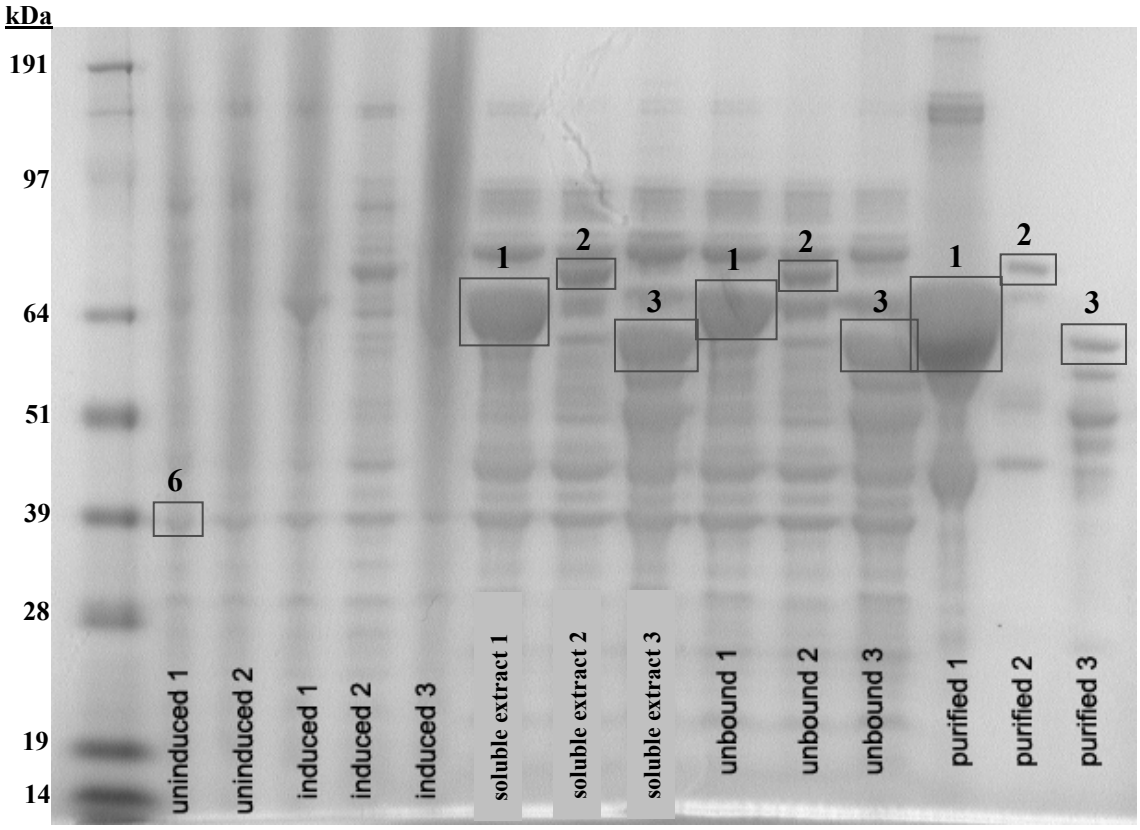

Figure 75. Final purification of FoxM1 Fragment 1-, 2-, and 3-MBP fusion proteins. Small samples of crude cell lysates were collected from BL21-CodonPlus (DE3)-RIPL *E. coli* transformed with either FoxM1 Fragment 1-MBP, Fragment 2-MBP, or Fragment 3-MBP prior to induction (uninduced) or 2 hours after induction with IPTG at 32^{o}C (induced). The remainder of the large-scale culture was then collected, and the lysate supernatant (soluble extract) was incubated with amylose resin. After pelleting of the resin and bound proteins, the supernatant (unbound) was collected. Bound proteins were then eluted from the resin (purified). Band at 68 kDa represents FoxM1 Fragment 1-MBP (1), band at 73 kDa represents FoxM1 Fragment 2-MBP (2), and band at 61 kDa represents FoxM1 Fragment 3-MBP (3). Band at 38 kDa represents the streptomycin resistance gene product (6), which is inherent to BL21-CodonPlus (DE3)-RIPL *E. coli*.

2- and 3-MBP were not bound or purified by the amylose resin. Additionally, none of the fragments were completely purified, as a number of contaminating proteins remained in each preparation after eluting from the amylose resin. Despite these difficulties, a sufficient amount of Fragment 1-MBP and Fragment 3-MBP were recovered for injection into recipient mice in the Vanderbilt Monoclonal Antibody Core.

Mice were injected with both Fragment 1- and Fragment 3-MBP fusion proteins simultaneously. Pre-immune and post-immune sera were collected from mice and screened for reactivity against mouse FoxM1 protein on embryonic mouse liver sections and protein extracted from mouse embryos. Specificity was analyzed by comparing tissue or protein from WT and *Foxm1*$^{-/-}$ embryos. Sera collected after three total injections of Fragment 1-MBP and Fragment 3-MBP showed no specific reactions against FoxM1 using either screening method. However, after a fourth injection, sera from two mice reacted with protein at ~83 kDa, the predicted molecular weight of mouse FoxM1 (Figure 76). These bands were only observed in extracts from WT, but not *Foxm1*$^{-/-}$, embryos, suggesting that these mice are producing antibodies specific to FoxM1. To confirm that this band likely represented FoxM1, HeLa cells were transfected with full-length mouse *Foxm1* cDNA, and protein extracts were subjected to western immunoblotting with sera from mice injected with Fragment 1-MBP and Fragment 3-MBP. This screen showed that all injected mice were producing antibodies that reacted against a protein at ~83 kDa in transfected cells (Figure 77). This band was very weak in extracts from HeLa cells transfected with a negative control, likely representing relatively low levels of endogenous human FOXM1 expression. The fact that all serum samples reacted with FoxM1 in transfected HeLa cell extracts but only two

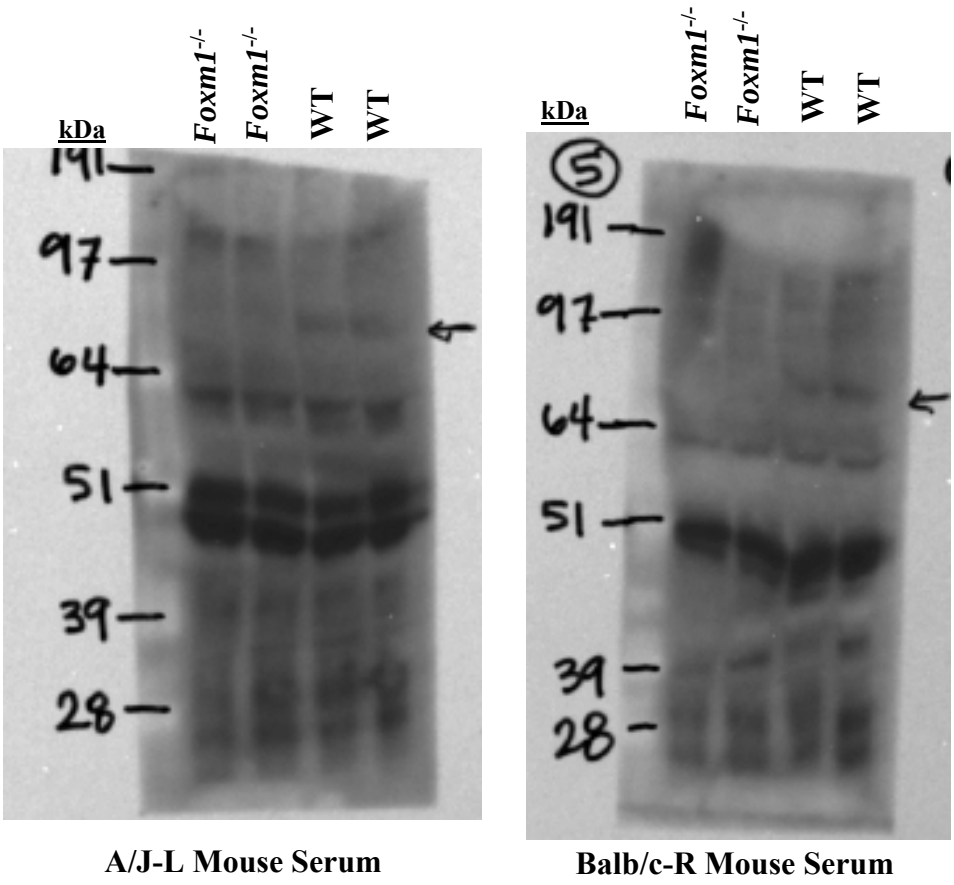

Figure 76. Endogenous mouse FoxM1 was detected by sera from two antigen-injected mice. Total protein extracts were collected from WT and *Foxm1*$^{-/-}$ embryos and used for western immunoblotting with sera from antigen-injected A/J and Balb/c mice. Sera from two mice produced bands at ~83 kDa (arrows) specifically in WT, but not *Foxm1*$^{-/-}$ extracts (arrows).

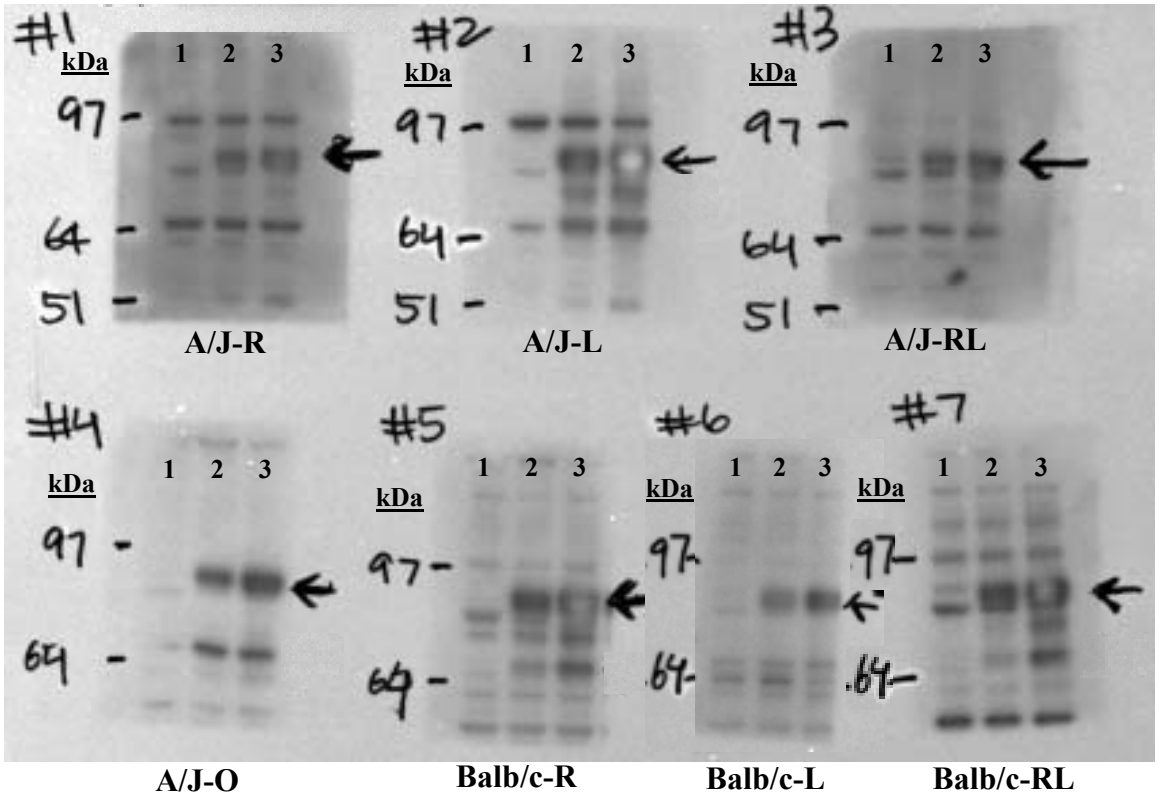

Figure 77. Recombinant FoxM1 was detected by sera from all antigen-injected mice. HeLa cells were transfected with no DNA (lane 1) or mouse *Foxm1* cDNA in pcDNA3.1 (lanes 2 and 3). Nuclear proteins were then extracted and used for western immunoblotting with sera from seven different antigen-injected A/J or Balb/c mice (#1-7). All sera samples produced bands at ~83 kDa that were predominant in the transfected HeLa cell extracts (arrows).

serum samples reacted with endogenous FoxM1 in mouse embryo extracts was likely due to the relatively higher amount of FoxM1 being produced by the transfected HeLa cells in comparison to embryonic tissue, along with differences in antibody affinity. Based on these results, it is highly probable that the endogenous mouse protein bound by the sera from the two mice was indeed FoxM1. No specific reactions were observed using these sera for immunohistochemistry on mouse embryonic liver paraffin sections. Instead, several of the serum samples reacted with both WT and *Foxm1*$^{-/-}$ tissue. However, there was not enough sera available to test using various antigen retrieval methods, on cryosections, or to otherwise optimize these experiments.

Because mice were injected with N-terminal (Fragment 1) and C-terminal (Fragment 3) regions of the FoxM1 protein, it is possible that some antibodies produced by these mice bind to the N-terminal portion of FoxM1, for which the coding sequence is not deleted by recombination of *Foxm1*$^{flox/flox}$ alleles. qRT-PCR primers used to detect *Foxm1* transcripts bind to sequences in exons 4-7, which are not present in the *Foxm1*^{null} allele. Therefore, it is currently unknown whether truncated FoxM1 mRNA or protein is produced after Cre-mediated recombination. The presence of an N-terminal truncated FoxM1 protein could yield false-positive results upon screening of *Foxm1*$^{-/-}$ tissue. Thus, it is possible that some of the serum samples contain FoxM1-specific antibodies even though they react with *Foxm1*$^{-/-}$ tissue, which may be why no specific reactivity was observed on tissue sections but was observed on western immunoblots.

Based on the positive western immunoblot results, the next step in generating a monoclonal antibody will involve isolating the antibody-producing B cells from a chosen mouse and fusing these cells with an immortal myeloma cell line to form hybridomas.

Hybridoma clones will then be identified and screened for anti-FoxM1 antibody production. Because conditioned media from these cells will be readily available, several screening techniques will likely be employed to detect one or more antibodies that can be used for western immunoblotting and/or immunohistochemistry, as these will be the primary uses for such an antibody in our laboratory. It is expected that an antibody will be identified that yields a positive result upon western immunoblotting, because crude sera produced such a result. However, it cannot be predicted whether or not any antibody generated will be able to be used for immunohistochemistry. Thorough screening using multiple antigen retrieval and signal amplification methods will likely be necessary. If after such screening a useful antibody has still not been identified, then efforts should be diverted to generating a polyclonal antibody against either a FoxM1 fragment or peptide. Because of the potential utility of a specific anti-FoxM1 antibody, this project remains a worthwhile endeavor.

CHAPTER VII

SUMMARY AND FUTURE DIRECTIONS

Previous to this work, FoxM1 was known to activate transcription of multiple cell cycle regulators in several cell types outside of the pancreas. Its importance in cell cycle control was evident from global deletion studies, which resulted in late embryonic lethality (Krupczak-Hollis *et al.*, 2004). Additionally, FoxM1 had been shown to play an important role in liver regeneration, using both deletion and over-expression experiments (Ye *et al.*, 1999; Wang *et al.*, 2002a; Wang *et al.*, 2002b). Pancreas-selective deletion studies performed in our laboratory revealed that absence of FoxM1 resulted in reduced postnatal β cell mass and proliferation, associated with progressive diabetes (Zhang H *et al.*, 2006). It was just becoming clear at this time that β cells exhibited several unique cell cycle characteristics: requirements for particular cell cycle regulators (Rane *et al.*, 1999; Georgia and Bhushan, 2004; Kushner *et al.*, 2005b), different requirements during embryogenesis versus neonatal versus adult timepoints (Krishnamurthy *et al.*, 2006; Georgia and Bhushan, 2006; Rachdi *et al.*, 2006; Zhang W *et al.*, 2006), and altered expression of different cell cycle regulators in response to different proliferative stimuli (Uchida *et al.*, 2005; Cozar-Castellano *et al.*, 2006c; Friedrichsen *et al.*, 2006). Thus, it was of great interest to determine whether FoxM1 is required for proper β cell proliferation at different ages and under different circumstances (Figure 78A). Additionally, we wanted to determine whether FoxM1 is involved in any of the other processes that regulate β cell mass (Figure 78B).

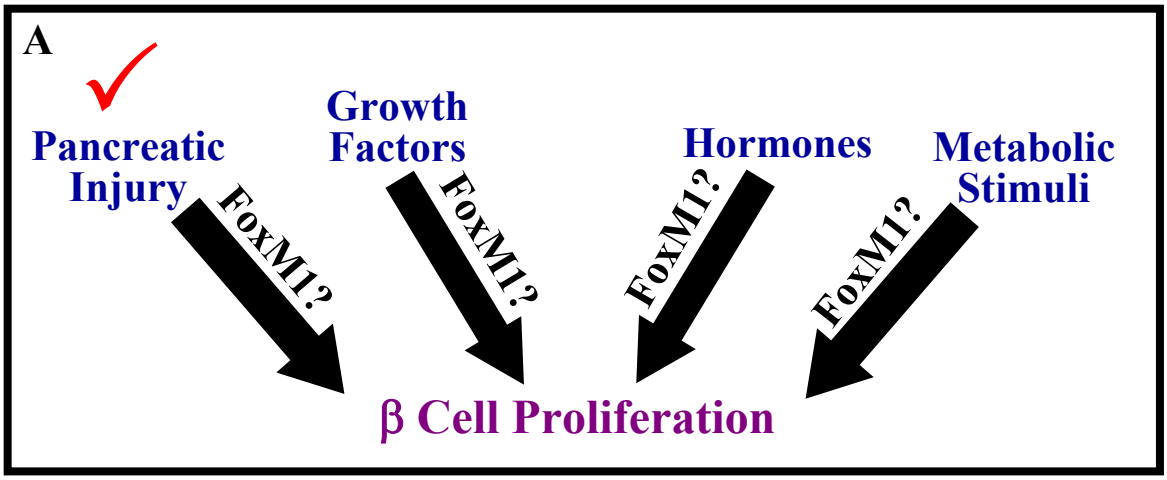

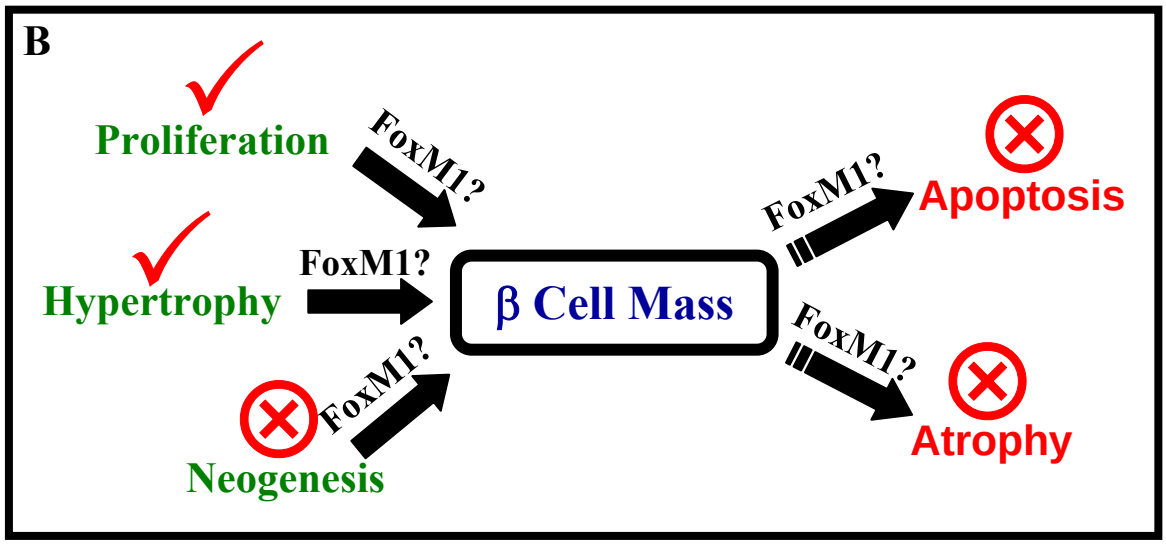

Figure 78. Summary of FoxM1's role in β cell mass regeneration and expansion. **(A)** β cells are known to proliferate in response to pancreatic injury, growth factors, hormones, and metabolic stimuli. Our laboratory seeks to define FoxM1's role in such stimulation of β cell proliferation. This dissertation revealed a role for FoxM1 down-stream of 60% PPx. **(B)** Proliferation of pre-existing β cells was impaired in the absence of FoxM1, whereas proliferation of newly-differentiated (neogenic) β cells did not require FoxM1. β cell neogenesis and apoptosis were not affected by loss of FoxM1, but β cell hypertrophy was observed in FoxM1$^{\Delta panc}$ mice. Check-marks indicate FoxM1's involvement. X-marks indicate FoxM1 is not involved.

Mice with a pancreas-wide deletion of *Foxm1* (FoxM1$^{\Delta panc}$) previously were shown to exhibit normal β cell mass at birth and relatively normal growth of β cell mass during the neonatal period (Zhang H *et al.*, 2006). However, at 4 weeks of age and older, further growth of β cell mass was inhibited, and β cell proliferation was reduced in FoxM1$^{\Delta panc}$ mice compared to Control littermates. Findings presented in this dissertation revealed that β cell proliferation was not reduced in late-stage FoxM1$^{\Delta panc}$ embryos (Chapter III), indicating that FoxM1 is differentially required for β cell proliferation at different ages. An interesting follow-up experiment would be to analyze β cell proliferation during the neonatal period to determine whether, despite normal growth of β cell mass, there is defective β cell proliferation that is compensated for by enhanced β cell neogenesis, as neogenesis is known to normally occur during this period (Scaglia *et al.*, 1997).

In an effort to determine whether FoxM1 is required for enhanced β cell proliferation in response to pancreatic injury or insulin resistance, euglycemic FoxM1$^{\Delta panc}$ female mice were subjected to 60% PPx or diet-induced obesity, respectively. Other members of our laboratory are investigating FoxM1's role in β cell proliferation stimulated during pregnancy and in response to various growth factors. Unfortunately, experimental obstacles beyond our control precluded analysis of high-fat diet-induced β cell proliferation in FoxM1$^{\Delta panc}$ mice at this time, although these experiments are ready to be repeated in the future. With regard to injury-induced β cell proliferation, however, it was determined that FoxM1 did indeed play an important role.

60% PPx stimulated *Foxm1* up-regulation within islets and β cell proliferation in Control mice. Proliferation was enhanced in both the splenic (regenerating) and

duodenal (expanding) lobes of the pancreas, indicating that β cells were responding to general cues, such as growth factors, initiated by injury of only the splenic portion of the pancreas. However, in FoxM1$^{\Delta panc}$ mice β cell proliferation was only significantly stimulated within the splenic/regenerating lobe, although to a lesser extent than in Control mice. Furthermore, β cell proliferation in the splenic lobe was significantly blunted by loss of FoxM1 specifically within definitive islets of 9 or more β cells, but not within small clusters of 8 or fewer β cells. As small endocrine cell clusters likely formed via neogenesis, while larger islets were likely pre-existing, these results once again suggested that β cells have different requirements for FoxM1 at different developmental stages (Figure 79).

Other studies from our laboratory indicated that *Foxm1* transcripts were up-regulated in islets during pregnancy and that FoxM1$^{\Delta panc}$ female mice exhibited a failure of β cell mass expansion and β cell hyperplasia during pregnancy that ultimately resulted in gestational diabetes (Hongie Zhang and Jia Zhang *et al*., manuscript in preparation). In contrast to the results observed following 60% PPx, no increase in β cell proliferation was observed in FoxM1$^{\Delta panc}$ female mice in response to pregnancy, further supporting the conclusion that FoxM1 is absolutely required for proliferation of pre-existing β cells in the adult.

Because of the interest in stimulating β cell proliferation as a therapeutic method for diabetic patients, understanding the proliferative cues to which β cells respond and the pathways activated by such cues could greatly improve this endeavor. Currently, the growth factors HGF and IGF-1 and the pregnancy hormone PL are being investigated in our laboratory to determine whether they act upstream of FoxM1. Additionally, it could

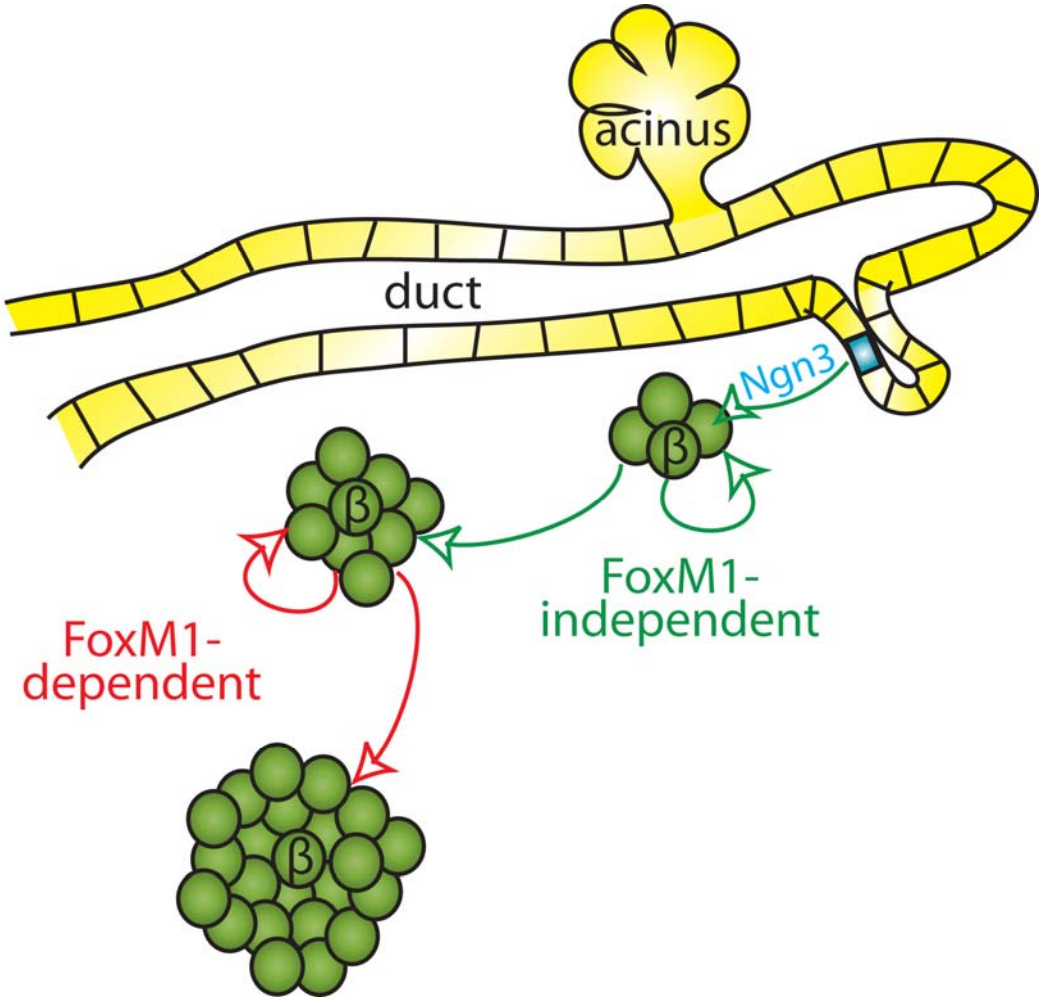

Figure 79. Working model of FoxM1's role in β cell proliferation. β cells differentiate from $Ngn3^{+}$ precursor cells in the ductal epithelium, both during development and during regeneration after 60% PPx. Initially, these newly-formed β cells can replicate in a FoxM1-independent manner. However, after a certain point, which has not yet been clearly determined, β cells become dependent on FoxM1 for continued proliferation.

prove useful to determine which growth factors are up-regulated and/or released in response to 60% PPx, as these are likely to act through FoxM1 to stimulate β cell proliferation.

These and other signaling pathways may act through FoxM1 by enhancing its transcription or its activity, both of which should be evaluated in future studies. As discussed in Chapter I, little is known regarding which factors and which regions of the *Foxm1* promoter are responsible for controlling FoxM1 expression. Furthermore, based on the over-expression studies presented in Chapter III, in which *Rosa26-FOXM1c* Tg mice did not exhibit any effects of ubiquitous FoxM1 over-expression on β cells or glucose homeostasis after 60% PPx, it is possible that expression of FoxM1 does not always correlate with activity. Thus, there is also need for further study of FoxM1's post-translational modifications and their influence on FoxM1 activity. It is known that FoxM1 is phosphorylated on multiple residues, some of which are necessary for FoxM1's sub-cellular localization and/or transcriptional activity (Major *et al.*, 2004; Ma *et al.*, 2005), and it will be important to evaluate FoxM1 phosphorylation status as well as its expression in future studies. Additionally, with regard to manipulating β cell proliferation, it may be necessary to specifically activate FoxM1 or over-express a constitutively active form of FoxM1 in order to achieve the desired effect(s). This could be accomplished by activation of specific signaling pathways or kinases, or by phospho-mimetic mutation of specific FoxM1 amino acids.

Our laboratory is currently developing a monoclonal antibody for analysis of FoxM1 expression levels and sub-cellular localization (Chapter VI). However, phospho-specific antibodies may also be useful to better evaluate FoxM1 activity. Anti-FoxM1

antibodies could also be used in chromatin immunoprecipitation (ChIP) experiments to examine down-stream targets of FoxM1, both to verify putative targets in β cells, including those up-regulated after PPx along with FoxM1, and to identify new targets. Other laboratories have shown that FoxM1 directly activates transcription of genes, such as *Lama4*, *ERα*, and *Jnk1*, which have functions not exclusive to proliferation (Kim *et al.*, 2005; Madureira *et al.*, 2006; Wang *et al.*, 2008a). Because we have identified a potential role for FoxM1 in β cell insulin secretory function, it is likely that other targets remain to be discovered in the β cell. ChIP on chip and ChIP-Seq techniques, in addition to microarray data comparing FoxM1$^{\Delta panc}$ and Control islets, could be used to elucidate such targets.

Although insulin secretion may be impaired in FoxM1$^{\Delta panc}$ mice, β cell differentiation does not seem to be impaired, as neither insulin expression per β cell nor β cell neogenesis, during either development or regeneration, are affected by loss of FoxM1. Thus, FoxM1 may regulate targets that are involved in the mechanics of insulin exocytosis, as observed in *Foxa2*$^{flox/flox}$;*Pdx1-CreER*^{T2} mice, which displayed insulin secretory defects associated with changes in expression of genes involved in insulin granule synthesis, vesicular trafficking, and exocytosis (Gao *et al.*, 2007). Because impaired insulin secretion was only observed in FoxM1$^{\Delta panc}$ mice fed a high-fat diet, FoxM1 may regulate genes that are involved in β cell compensation. It is known that enhanced insulin secretory function and β cell hypertrophy occur in response to diet-induced obesity and insulin resistance (Lingohr *et al.*, 2002; Kahn *et al.*, 2006), and it is hypothesized that these two responses are related. It is clear from the studies presented in Chapters III and IV that FoxM1$^{\Delta panc}$ mice exhibit β cell hypertrophy under normal

conditions, and this basal state may impede adaptation to cellular stressors. Thus, further investigation of FoxM1's role in β cell function may lend some insight into how β cells compensate for increased insulin demand.

Because Type II diabetes results from a relative insufficiency of β cell mass and function, it is possible that altered FoxM1 expression or activity may be related to susceptibility to this disease. Thus far, no direct link between diabetes and FoxM1 has been described in human studies. However, genome-wide association studies are in their infancy, and the fact that polymorphisms in only a handful of genes have thus far been linked to Type II diabetes, which is an admittedly complex and multigenic disease, suggests that more susceptibility loci remain to be identified. Additionally, FoxM1 may be indirectly implicated by its association with pathways that regulate its expression and/or activity. Again, further characterization of FoxM1's transcriptional regulation and post-translational modification may lend insight into potential defects associated with diabetes.

This dissertation described the effects of loss of FoxM1 on β cell mass regeneration and expansion, which are summarized in Figure 78A,B. These experiments demonstrated that FoxM1 played an important role in proliferation of pre-existing β cells but not newly-differentiated β cells, and that β cell hypertrophy occurred in the absence of FoxM1. However, neither β cell neogenesis nor apoptosis were affected by loss of FoxM1. Therefore, FoxM1 does play a role in β cell mass regeneration following 60% PPx, but its role in β cell mass expansion in response to diet-induced obesity or other stimuli of β cell proliferation has yet to be determined.

REFERENCES

Ackermann, AM and Gannon, M. (2007) Molecular regulation of pancreatic beta-cell mass development, maintenance, and expansion. *J Mol Endocrinol*. **38** (2): 193-206.

Ahlgren, U, Pfaff, SL, Jessell, TM, Edlund, T and Edlund, H. (1997) Independent requirement for ISL1 in formation of pancreatic mesenchyme and islet cells. *Nature*. **385** (6613): 257-260.

Ahlgren, U, Jonsson, J, Jonsson, L, Simu, K and Edlund, H. (1998) Beta-cell-specific inactivation of the mouse Ipf1/Pdx1 gene results in loss of the beta-cell phenotype and maturity onset diabetes. *Genes Dev*. **12** (12): 1763-1768.

Andrikopoulos, S, Massa, CM, Aston-Mourney, K, Funkat, A, Fam, BC, Hull, RL, Kahn, SE and Proietto, J. (2005) Differential effect of inbred mouse strain (C57BL/6, DBA/2, 129T2) on insulin secretory function in response to a high fat diet. *J Endocrinol*. **187** (1): 45-53.

Apelqvist, A, Li, H, Sommer, L, Beatus, P, Anderson, DJ, Honjo, T, Hrabe de Angelis, M, Lendahl, U and Edlund, H. (1999) Notch signalling controls pancreatic cell differentiation. *Nature*. **400** (6747): 877-881.

Araki, E, Lipes, MA, Patti, M-E, Bruning, JC, Haag Iii, B, Johnson, RS and Kahn, CR. (1994) Alternative pathway of insulin signalling in mice with targeted disruption of the IRS-1 gene. *Nature*. **372** (6502): 186-190.

Artner, I, Le Lay, J, Hang, Y, Elghazi, L, Schisler, JC, Henderson, E, Sosa-Pineda, B and Stein, R. (2006) MafB: An Activator of the Glucagon Gene Expressed in Developing Islet alpha- and beta-Cells. *Diabetes*. **55** (2): 297-304.

Artner, I, Blanchi, B, Raum, JC, Guo, M, Kaneko, T, Cordes, S, Sieweke, M and Stein, R. (2007) MafB is required for islet beta cell maturation. *Proc Natl Acad Sci U S A*. **104** (10): 3853-3858.

Artner, I, Hang, Y, Guo, M, Gu, G and Stein, R. (2008) MafA is a dedicated activator of the insulin gene in vivo. *J Endocrinol*. **198** (2): 271-279.

Ayala, JE, Bracy, DP, McGuinness, OP and Wasserman, DH. (2006) Considerations in the design of hyperinsulinemic-euglycemic clamps in the conscious mouse. *Diabetes*. **55** (2): 390-397.

Bannantine, JP, Hansen, JK, Paustian, ML, Amonsin, A, Li, L-L, Stabel, JR and Kapur, V. (2004) Expression and immunogenicity of proteins encoded by sequences specific to *Mycobacterium avium* subsp. *paratuberculosis*. *J Clin Microbiol*. **42** (1): 106-114.

Barr, FA, Sillje, HHW and Nigg, EA. (2004) Polo-like kinases and the orchestration of cell division. *Nat Rev Mol Cell Biol*. **5** (6): 429-441.

Bernal-Mizrachi, E, Wen, W, Stahlhut, S, Welling, CM and Permutt, MA. (2001) Islet beta cell expression of constitutively active Akt1/PKBalpha induces striking hypertrophy, hyperplasia, and hyperinsulinemia. *J. Clin. Invest.* **108** (11): 1631-1638.

Bernal-Mizrachi, E, Fatrai, S, Johnson, JD, Ohsugi, M, Otani, K, Han, Z, Polonsky, KS and Permutt, MA. (2004) Defective insulin secretion and increased susceptibility to experimental diabetes are induced by reduced Akt activity in pancreatic islet beta cells. *J. Clin. Invest.* **114** (7): 928-936.

Bernard-Kargar, C and Ktorza, A. (2001) Endocrine pancreas plasticity under physiological and pathological conditions. *Diabetes*. **50** (Suppl 1): S30-35.

Bhushan, A, Itoh, N, Kato, S, Thiery, JP, Czernichow, P, Bellusci, S and Scharfmann, R. (2001) Fgf10 is essential for maintaining the proliferative capacity of epithelial progenitor cells during early pancreatic organogenesis. *Development*. **128** (24): 5109-5117.

Black, BL, Croom, J, Eisen, EJ, Petro, AE, Edwards, CL and Surwit, RS. (1998) Differential effects of fat and sucrose on body composition in A/J and C57BL/6 mice. *Metabolism*. **47** (11): 1354-1359.

Blyszczuk, P, Czyz, J, Kania, G, Wagner, M, Roll, U, St-Onge, L and Wobus, AM. (2003) Expression of Pax4 in embryonic stem cells promotes differentiation of nestin-positive progenitor and insulin-producing cells. *Proc Natl Acad Sci U S A*. **100** (3): 998-1003.

Bock, T, Pakkenberg, B and Buschard, K. (2005) Genetic Background Determines the Size and Structure of the Endocrine Pancreas. *Diabetes*. **54** (1): 133-137.

Bonner-Weir, S, Trent, D and Weir, GC. (1983) Partial pancreatectomy in the rat and subsequent defect in glucose-induced insulin release. *J Clin Invest*. **71** (6): 1544-1553.

Bonner-Weir, S, Deery, D, Leahy, JL and Weir, GC. (1989) Compensatory growth of pancreatic beta-cells in adult rats after short-term glucose infusion. *Diabetes*. **38** (1): 49-53.

Bonner-Weir, S, Baxter, LA, Schuppin, GT and Smith, FE. (1993) A second pathway for regeneration of adult exocrine and endocrine pancreas. A possible recapitulation of embryonic development. *Diabetes*. **42** (12): 1715-1720.

Bonner-Weir, S and Weir, GC. (2005) New sources of pancreatic beta-cells. *Nat Biotech*. **23** (7): 857-861.

Bonner-Weir, S, Inada, A, Yatoh, S, Li, WC, Aye, T, Toschi, E and Sharma, A. (2008) Transdifferentiation of pancreatic ductal cells to endocrine beta-cells. *Biochem Soc Trans*. **36** (Pt 3): 353-356.

Bornstein, G, Bloom, J, Sitry-Shevah, D, Nakayama, K, Pagano, M and Hershko, A. (2003) Role of the SCFSkp2 ubiquitin ligase in the degradation of p21Cip1 in S phase. *J Biol Chem*. **278** (28): 25752-25757.

Boushey, RP, Abadir, A, Flamez, D, Baggio, LL, Li, Y, Berger, V, Marshall, BA, Finegood, D, Wang, TC, Schuit, F and Drucker, DJ. (2003) Hypoglycemia, defective islet glucagon secretion, but normal islet mass in mice with a disruption of the gastrin gene. *Gastroenterology*. **125** (4): 1164-1174.

Breant, B, Gesina, E and Blondeau, B. (2006) Nutrition, glucocorticoids and pancreas development. *Horm Res*. **65** (suppl 3): 98-104.

Brissova, M, Shiota, M, Nicholson, WE, Gannon, M, Knobel, SM, Piston, DW, Wright, CV and Powers, AC. (2002) Reduction in pancreatic transcription factor PDX-1 impairs glucose-stimulated insulin secretion. *J Biol Chem*. **277** (13): 11225-11232.

Butler, AE, Janson, J, Bonner-Weir, S, Ritzel, R, Rizza, RA and Butler, PC. (2003) Beta-Cell Deficit and Increased Beta-Cell Apoptosis in Humans With Type 2 Diabetes. *Diabetes*. **52** (1): 102-110.

Butler, PC, Meier, JJ, Butler, AE and Bhushan, A. (2007) The replication of beta-cells in normal physiology, in disease and for therapy. *Nat Clin Pract Endocrinol Metab*. **3** (11): 758-768.

Cao Minh, L, Galasso, R, Gurlo, T, Basu, R, Rizza, RA and Butler, PC. (2008) Three fold increase in beta cell mass in twenty weeks in human pregnancy. *Diabetes*. **57** (Supplement 1): A1.

Carrano, AC, Eytan, E, Hershko, A and Pagano, M. (1999) SKP2 is required for ubiquitin-mediated degradation of the CDK inhibitor p27. *Nat Cell Biol*. **1** (4): 193-199.

Chen, H, Charlat, O, Tartaglia, LA, Woolf, EA, Weng, X, Ellis, SJ, Lakey, ND, Culpepper, J, More, KJ, Breitbart, RE, Duyk, GM, Tepper, RI and Morgenstern, JP. (1996) Evidence That the Diabetes Gene Encodes the Leptin Receptor: Identification of a Mutation in the Leptin Receptor Gene in db/db Mice. *Cell*. **84** (3): 491-495.

Choi, SB, Jang, JS and Park, S. (2005) Estrogen and Exercise May Enhance beta-Cell Function and Mass via Insulin Receptor Substrate 2 Induction in Ovariectomized Diabetic Rats. *Endocrinology*. **146** (11): 4786-4794.

Clark, KL, Halay, ED, Lai, E and Burley, SK. (1993) Co-crystal structure of the HNF-3/fork head DNA-recognition motif resembles histone H5. *Nature*. **364** (6436): 412-420.

Cohen, SE, Kokkotou, E, Biddinger, SB, Kondo, T, Gebhardt, R, Kratzsch, J, Mantzoros, CS and Kahn, CR. (2007) High Circulating Leptin Receptors with Normal Leptin Sensitivity in Liver-specific Insulin Receptor Knock-out (LIRKO) Mice. *J Biol Chem*. **282** (32): 23672-23678.

Collins, S, Martin, TL, Surwit, RS and Robidoux, J. (2004) Genetic vulnerability to diet-induced obesity in the C57BL/6J mouse: physiological and molecular characteristics. *Physiology & Behavior*. **81** (2): 243-248.

Collombat, P, Mansouri, A, Hecksher-Sorensen, J, Serup, P, Krull, J, Gradwohl, G and Gruss, P. (2003) Opposing actions of Arx and Pax4 in endocrine pancreas development. *Genes Dev*. **17** (20): 2591-2603.

Contreras, JL, Smyth, CA, Bilbao, G, Young, C, Thompson, JA and Eckhoff, DE. (2002) 17beta-estradiol protects isolated human pancreatic islets against proinflammatory cytokine-induced cell death: molecular mechanisms and islet functionality. *Transplantation*. **74** (9): 1252-1259.

Costa, RH, Grayson, DR and Darnell, JE, Jr. (1989) Multiple hepatocyte-enriched nuclear factors function in the regulation of transthyretin and alpha 1-antitrypsin genes. *Mol Cell Biol*. **9** (4): 1415-1425.

Costa, RH. (2005) FoxM1 dances with mitosis. *Nat Cell Biol*. **7** (2): 108-110.

Costa, RH, Kalinichenko, VV, Major, ML and Raychaudhuri, P. (2005) New and unexpected: forkhead meets ARF. *Current Opinion in Genetics & Development*. **15** (1): 42-48.

Cozar-Castellano, I, Fiaschi-Taesch, N, Bigatel, TA, Takane, KK, Garcia-Ocana, A, Vasavada, R and Stewart, AF. (2006a) Molecular control of cell cycle progression in the pancreatic beta-cell. *Endocr Rev*. **27** (4): 356-370.

Cozar-Castellano, I, Haught, M and Stewart, AF. (2006b) The cell cycle inhibitory protein p21cip is not essential for maintaining beta-cell cycle arrest or beta-cell function in vivo. *Diabetes*. **55** (12): 3271-3278.

Cozar-Castellano, I, Weinstock, M, Haught, M, Velazquez-Garcia, S, Sipula, D and Stewart, AF. (2006c) Evaluation of beta-cell replication in mice transgenic for hepatocyte growth factor and placental lactogen: comprehensive characterization of the G1/S regulatory proteins reveals unique involvement of p21cip. *Diabetes*. **55** (1): 70-77.

Crabtree, JS, Scacheri, PC, Ward, JM, McNally, SR, Swain, GP, Montagna, C, Hager, JH, Hanahan, D, Edlund, H, Magnuson, MA, Garrett-Beal, L, Burns, AL, Ried, T, Chandrasekharappa, SC, Marx, SJ, Spiegel, AM and Collins, FS. (2003) Of mice and MEN1: insulinomas in a conditional mouse knockout. *Mol. Cell. Biol.* **23** (17): 6075-6085.

D'Amour, KA, Bang, AG, Eliazer, S, Kelly, OG, Agulnick, AD, Smart, NG, Moorman, MA, Kroon, E, Carpenter, MK and Baetge, EE. (2006) Production of pancreatic hormone-expressing endocrine cells from human embryonic stem cells. *Nat Biotech*. **24** (11): 1392-1401.

Dai, J, Sultan, S, Taylor, SS and Higgins, JM. (2005) The kinase haspin is required for mitotic histone H3 Thr 3 phosphorylation and normal metaphase chromosome alignment. *Genes Dev*. **19** (4): 472-488.

De Leon, DD, Deng, S, Madani, R, Ahima, RS, Drucker, DJ and Stoffers, DA. (2003) Role of Endogenous Glucagon-Like Peptide-1 in Islet Regeneration After Partial Pancreatectomy. *Diabetes*. **52** (2): 365-371.

Desai, BM, Oliver-Krasinski, J, De Leon, DD, Farzad, C, Hong, N, Leach, SD and Stoffers, DA. (2007) Preexisting pancreatic acinar cells contribute to acinar cell, but not islet beta cell, regeneration. *J Clin Invest*. **117** (4): 971-977.

Devedjian, J-C, George, M, Casellas, A, Pujol, A, Visa, J, Pelegrin, M, Gros, L and Bosch, F. (2000) Transgenic mice overexpressing insulin-like growth factor-II in beta cells develop type 2 diabetes. *J. Clin. Invest.* **105** (6): 731-740.

Dor, Y, Brown, J, Martinez, OI and Melton, DA. (2004) Adult pancreatic beta-cells are formed by self-duplication rather than stem-cell differentiation. *Nature*. **429** (6987): 41-46.

Douard, R, Moutereau, S, Pernet, P, Chimingqi, M, Allory, Y, Manivet, P, Conti, M, Vaubourdolle, M, Cugnenc, P-H and Loric, S. (2006) Sonic Hedgehog-dependent proliferation in a series of patients with colorectal cancer. *Surgery*. **139** (5): 665-670.

Drucker, DJ. (2006) The biology of incretin hormones. *Cell Metab*. **3** (3): 153-165.

Dzau, VJ, Braun-Dullaeus, RC and Sedding, DG. (2002) Vascular proliferation and atherosclerosis: New perspectives and therapeutic strategies. *Nat Med*. **8** (11): 1249-1256.

Edlund, H. (2001) Developmental biology of the pancreas. *Diabetes*. **50** (Suppl 1): S5-9.

Fajas, L, Annicotte, J-S, Miard, S, Sarruf, D, Watanabe, M and Auwerx, J. (2004) Impaired pancreatic growth, beta cell mass, and beta cell function in E2F1-/- mice. *J. Clin. Invest.* **113** (9): 1288-1295.

Fatrai, S, Elghazi, L, Balcazar, N, Cras-Meneur, C, Krits, I, Kiyokawa, H and Bernal-Mizrachi, E. (2006) Akt Induces beta-cell proliferation by regulating cyclin D1, cyclin D2, and p21 levels and cyclin-dependent kinase-4 activity. *Diabetes*. **55** (2): 318-325.

Fiaschi-Taesch, NM, Bigatel, T, Sicari, B, Takane, K and Stewart, A. (2008) Overexpression of *cdk6*, a human specific beta cell Cdk, induces human beta cell proliferation and promotes engraftment and function of human islets. *Diabetes*. **57** (Supplement 1): A1.

Finegood, DT, Scaglia, L and Bonner-Weir, S. (1995) Dynamics of beta-cell mass in the growing rat pancreas: estimation with a simple mathematical model. *Diabetes*. **44** (3): 249-256.

Franklin, DS, Godfrey, VL, O'Brien, DA, Deng, C and Xiong, Y. (2000) Functional collaboration between different cyclin-dependent kinase inhibitors suppresses tumor growth with distinct tissue specificity. *Mol. Cell. Biol.* **20** (16): 6147-6158.

Freemark, M, Avril, I, Fleenor, D, Driscoll, P, Petro, A, Opara, E, Kendall, W, Oden, J, Bridges, S, Binart, N, Breant, B and Kelly, PA. (2002) Targeted deletion of the PRL receptor: effects on islet development, insulin production, and glucose tolerance. *Endocrinology*. **143** (4): 1378-1385.

Friedrichsen, BN, Neubauer, N, Lee, YC, Gram, VK, Blume, N, Petersen, JS, Nielsen, JH and Moldrup, A. (2006) Stimulation of pancreatic beta-cell replication by incretins involves transcriptional induction of cyclin D1 via multiple signalling pathways. *J Endocrinol*. **188** (3): 481-492.

Fujikawa, T, Oh, SH, Pi, L, Hatch, HM, Shupe, T and Petersen, BE. (2005) Teratoma formation leads to failure of treatment for type I diabetes using embryonic stem cell-derived insulin-producing cells. *Am J Pathol*. **166** (6): 1781-1791.

Fung, TK and Poon, RYC. (2005) A roller coaster ride with the mitotic cyclins. *Seminars in Cell & Developmental Biology*. **16** (3): 335-342.

Funkat, A, Massa, CM, Jovanovska, V, Proietto, J and Andrikopoulos, S. (2004) Metabolic Adaptations of Three Inbred Strains of Mice (C57BL/6, DBA/2, and 129T2) in Response to a High-Fat Diet. *J Nutrition*. **134** (12): 3264-3269.

Gannon, G, Mandriota, SJ, Cui, L, Baetens, D, Pepper, MS and Christofori, G. (2002) Overexpression of vascular endothelial growth factor-A165 enhances tumor angiogenesis but not metastasis during beta-cell carcinogenesis. *Cancer Res*. **62** (2): 603-608.

Gannon, M, Ray, MK, Van Zee, K, Rausa, F, Costa, RH and Wright, CV. (2000) Persistent expression of HNF6 in islet endocrine cells causes disrupted islet architecture and loss of beta cell function. *Development*. **127** (13): 2883-2895.

Gannon, M, Gamer, LW and Wright, CV. (2001) Regulatory regions driving developmental and tissue-specific expression of the essential pancreatic gene pdx1. *Dev Biol*. **238** (1): 185-201.

Gannon, M, Tweedie Ables, E, Crawford, L, Lowe, D, Offield, MF, Magnuson, MA and Wright, CVE. (2008) *pdx-1* function is specifically required in embryonic beta cells to generate appropriate numbers of endocrine cell types and maintain glucose homeostasis. *Developmental Biology*. **314** (2): 406-417.

Gao, N, White, P, Doliba, N, Golson, ML, Matschinsky, FM and Kaestner, KH. (2007) Foxa2 controls vesicle docking and insulin secretion in mature Beta cells. *Cell Metab*. **6** (4): 267-279.

Garcia-Ocana, A, Takane, KK, Syed, MA, Philbrick, WM, Vasavada, RC and Stewart, AF. (2000) Hepatocyte growth factor overexpression in the islet of transgenic mice increases beta cell proliferation, enhances islet mass, and induces mild hypoglycemia. *J. Biol. Chem.* **275** (2): 1226-1232.

Garcia-Ocana, A, Vasavada, RC, Cebrian, A, Reddy, V, Takane, KK, Lopez-Talavera, J-C and Stewart, AF. (2001) Transgenic overexpression of hepatocyte growth factor in the beta-cell markedly improves islet function and islet transplant outcomes in mice. *Diabetes*. **50** (12): 2752-2762.

Gartel, AL. (2007) FoxM1 inhibitors as potential anticancer drugs. *Expert Opin Ther Targets*. **12** (6): 663-665.

Gasa, R, Mrejen, C, Leachman, N, Otten, M, Barnes, M, Wang, J, Chakrabarti, S, Mirmira, R and German, M. (2004) Proendocrine genes coordinate the pancreatic islet differentiation program in vitro. *PNAS*. **101** (36): 13245-13250.

Geary, N, Asarian, L, Korach, KS, Pfaff, DW and Ogawa, S. (2001) Deficits in E2-Dependent Control of Feeding, Weight Gain, and Cholecystokinin Satiation in ER-alpha Null Mice. *Endocrinology*. **142** (11): 4751-4757.

George, M, Ayuso, E, Casellas, A, Costa, C, Devedjian, JC and Bosch, F. (2002) Beta cell expression of IGF-I leads to recovery from type 1 diabetes. *J Clin Invest*. **109** (9): 1153-1163.

Georgia, S and Bhushan, A. (2004) Beta cell replication is the primary mechanism for maintaining postnatal beta cell mass. *J. Clin. Invest.* **114** (7): 963-968.

Georgia, S and Bhushan, A. (2006) p27 Regulates the Transition of beta-Cells From Quiescence to Proliferation. *Diabetes*. **55** (11): 2950-2956.

Georgia, S, Soliz, R, Li, M, Zhang, P and Bhushan, A. (2006) p57 and Hes1 coordinate cell cycle exit with self-renewal of pancreatic progenitors. *Dev Biol*. **298** (1): 22-31.

Gerrish, K, Van Velkinburgh, JC and Stein, R. (2004) Conserved transcriptional regulatory domains of the pdx-1 gene. *Mol Endocrinol*. **18** (3): 533-548.

Gradwohl, G, Dierich, A, LeMeur, M and Guillemot, F. (2000) neurogenin3 is required for the development of the four endocrine cell lineages of the pancreas. *Proc Natl Acad Sci U S A*. **97** (4): 1607-1611.

Grapin-Botton, A, Majithia, AR and Melton, DA. (2001) Key events of pancreas formation are triggered in gut endoderm by ectopic expression of pancreatic regulatory genes. *Genes Dev*. **15** (4): 444-454.

Gu, G, Dubauskaite, J and Melton, DA. (2002) Direct evidence for the pancreatic lineage: NGN3+ cells are islet progenitors and are distinct from duct progenitors. *Development*. **129** (10): 2447-2457.

Gupta, RK, Gao, N, Gorski, RK, White, P, Hardy, OT, Rafiq, K, Brestelli, JE, Chen, G, Stoeckert, CJ, Jr. and Kaestner, KH. (2007) Expansion of adult beta-cell mass in response to increased metabolic demand is dependent on HNF-4alpha. *Genes & Development*. **21** (7): 756-769.

Gusarova, GA, Wang, I-C, Major, ML, Kalinichenko, VV, Ackerson, T, Petrovic, V and Costa, RH. (2007) A cell-penetrating ARF peptide inhibitor of FoxM1 in mouse hepatocellular carcinoma treatment. *J Clin Invest*. **117** (1): 99-111.

Guz, Y, Montminy, M, Stein, R, Leonard, J, Gamer, L, Wright, C and Teitelman, G. (1995) Expression of murine STF-1, a putative insulin gene transcription factor, in beta cells of pancreas, duodenal epithelium and pancreatic exocrine and endocrine progenitors during ontogeny. *Development*. **121** (1): 11-18.

Harding, HP, Zeng, H, Zhang, Y, Jungries, R, Chung, P, Plesken, H, Sabatini, DD and Ron, D. (2001) Diabetes mellitus and exocrine pancreatic dysfunction in Perk-/- mice reveals a role for translational control in secretory cell survival. *Molecular Cell*. **7** (6): 1153-1163.

Harrison, KA, Thaler, J, Pfaff, SL, Gu, H and Kehrl, JH. (1999) Pancreas dorsal lobe agenesis and abnormal islets of Langerhans in Hlxb9-deficient mice. *Nat Genet*. **23** (1): 71-75.

Hart, AW, Baeza, N, Apelqvist, A and Edlund, H. (2000) Attenuation of FGF signalling in mouse beta-cells leads to diabetes. *Nature*. **408** (6814): 864-868.

Hashimoto, N, Kido, Y, Uchida, T, Asahara, S-i, Shigeyama, Y, Matsuda, T, Takeda, A, Tsuchihashi, D, Nishizawa, A, Ogawa, W, Fujimoto, Y, Okamura, H, Arden, KC, Herrera, PL, Noda, T and Kasuga, M. (2006) Ablation of PDK1 in pancreatic beta cells induces diabetes as a result of loss of beta cell mass. *Nat Genet*. **38** (5): 589-593.

Hayashi, KY, Tamaki, H, Handa, K, Takahashi, T, Kakita, A and Yamashina, S. (2003) Differentiation and proliferation of endocrine cells in the regenerating rat pancreas after 90% pancreatectomy. *Arch Histol Cytol*. **66** (2): 163-174.

Heit, JJ, Apelqvist, AA, Gu, X, Winslow, MM, Neilson, JR, Crabtree, GR and Kim, SK. (2006a) Calcineurin/NFAT signalling regulates pancreatic beta-cell growth and function. *Nature*. **443** (7109): 345-349.

Heit, JJ, Karnik, SK and Kim, SK. (2006b) Intrinsic Regulators of Pancreatic beta-Cell Proliferation. *Annu Rev Cell Dev Biol*. **22** 311-338.

Hennige, AM, Burks, DJ, Ozcan, U, Kulkarni, RN, Ye, J, Park, S, Schubert, M, Fisher, TL, Dow, MA, Leshan, R, Zakaria, M, Mossa-Basha, M and White, MF. (2003) Upregulation of insulin receptor substrate-2 in pancreatic beta cells prevents diabetes. *J. Clin. Invest.* **112** (10): 1521-1532.

Heremans, Y, Van De Casteele, M, in't Veld, P, Gradwohl, G, Serup, P, Madsen, O, Pipeleers, D and Heimberg, H. (2002) Recapitulation of embryonic neuroendocrine differentiation in adult human pancreatic duct cells expressing neurogenin 3. *J. Cell Biol.* **159** (2): 303-312.

Herrera, PL. (2000) Adult insulin- and glucagon-producing cells differentiate from two independent cell lineages. *Development*. **127** (11): 2317-2322.

Howman, EV, Fowler, KJ, Newson, AJ, Redward, S, MacDonald, AC, Kalitsis, P and Choo, KHA. (2000) Early disruption of centromeric chromatin organization in centromere protein A (Cenpa) null mice. *PNAS*. **97** (3): 1148-1153.

Huang, H-P, Liu, M, El-Hodiri, HM, Chu, K, Jamrich, M and Tsai, M-J. (2000) Regulation of the Pancreatic Islet-Specific Gene BETA2 (neuroD) by Neurogenin 3. *Mol. Cell. Biol.* **20** (9): 3292-3307.

Hussain, MA, Porras, DL, Rowe, MH, West, JR, Song, WJ, Schreiber, WE and Wondisford, FE. (2006) Increased pancreatic beta-cell proliferation mediated by CREB binding protein gene activation. *Mol Cell Biol*. **26** (20): 7747-7759.

Iglesias, A, Murga, M, Laresgoiti, U, Skoudy, A, Bernales, I, Fullaondo, A, Moreno, B, Lloreta, J, Field, SJ, Real, FX and Zubiaga, AM. (2004) Diabetes and exocrine pancreatic insufficiency in E2F1/E2F2 double-mutant mice. *J. Clin. Invest.* **113** (10): 1398-1407.

Inada, A, Hamamoto, Y, Tsuura, Y, Miyazaki, J-i, Toyokuni, S, Ihara, Y, Nagai, K, Yamada, Y, Bonner-Weir, S and Seino, Y. (2004) Overexpression of inducible cyclic AMP early repressor inhibits transactivation of genes and cell proliferation in pancreatic beta cells. *Mol. Cell. Biol.* **24** (7): 2831-2841.

Inada, A, Weir, GC and Bonner-Weir, S. (2005) Induced ICER I-gamma down-regulates cyclin A expression and cell proliferation in insulin-producing beta cells. *Biochemical and Biophysical Research Communications*. **329** (3): 925-929.

Inoue, M, Hager, JH, Ferrara, N, Gerber, H-P and Hanahan, D. (2002) VEGF-A has a critical, nonredundant role in angiogenic switching and pancreatic beta cell carcinogenesis. *Cancer Cell*. **1** (2): 193-202.

Jacquemin, P, Durviaux, SM, Jensen, J, Godfraind, C, Gradwohl, G, Guillemot, F, Madsen, OD, Carmeliet, P, Dewerchin, M, Collen, D, Rousseau, GG and Lemaigre, FP. (2000) Transcription factor hepatocyte nuclear factor 6 regulates pancreatic endocrine cell differentiation and controls expression of the proendocrine gene ngn3. *Mol Cell Biol*. **20** (12): 4445-4454.

Jensen, J, Pedersen, EE, Galante, P, Hald, J, Heller, RS, Ishibashi, M, Kageyama, R, Guillemot, F, Serup, P and Madsen, OD. (2000) Control of endodermal endocrine development by Hes-1. *Nat Genet*. **24** (1): 36-44.

Jhala, US, Canettieri, G, Screaton, RA, Kulkarni, RN, Krajewski, S, Reed, J, Walker, J, Lin, X, White, M and Montminy, M. (2003) cAMP promotes pancreatic beta-cell survival via CREB-mediated induction of IRS2. *Genes Dev.* **17** (13): 1575-1580.

Joglekar, MV, Parekh, VS, Mehta, S, Bhonde, RR and Hardikar, AA. (2007) MicroRNA profiling of developing and regenerating pancreas reveal post-transcriptional regulation of neurogenin3. *Developmental Biology*. **311** (2): 603-612.

Johnson, JD, Ahmed, NT, Luciani, DS, Han, Z, Tran, H, Fujita, J, Misler, S, Edlund, H and Polonsky, KS. (2003) Increased islet apoptosis in Pdx1+/- mice. *J. Clin. Invest.* **111** (8): 1147-1160.

Jonsson, J, Carlsson, L, Edlund, T and Edlund, H. (1994) Insulin-promoter-factor 1 is required for pancreas development in mice. *Nature*. **371** (6498): 606-609.

Kaestner, KH, Knochel, W and Martinez, DE. (2000) Unified nomenclature for the winged helix/forkhead transcription factors. *Genes & Development*. **14** (2): 142-146.

Kahn, SE, Hull, RL and Utzschneider, KM. (2006) Mechanisms linking obesity to insulin resistance and type 2 diabetes. *Nature*. **444** (7121): 840-846.

Kalin, TV, Wang, IC, Ackerson, TJ, Major, ML, Detrisac, CJ, Kalinichenko, VV, Lyubimov, A and Costa, RH. (2006) Increased Levels of the FoxM1 Transcription Factor Accelerate Development and Progression of Prostate Carcinomas in both TRAMP and LADY Transgenic Mice. *Cancer Res*. **66** (3): 1712-1720.

Kalinichenko, VV, Gusarova, GA, Tan, Y, Wang, IC, Major, ML, Wang, X, Yoder, HM and Costa, RH. (2003) Ubiquitous Expression of the Forkhead Box M1B Transgene Accelerates Proliferation of Distinct Pulmonary Cell Types following Lung Injury. *J Biol Chem*. **278** (39): 37888-37894.

Kalinichenko, VV, Major, ML, Wang, X, Petrovic, V, Kuechle, J, Yoder, HM, Dennewitz, MB, Shin, B, Datta, A, Raychaudhuri, P and Costa, RH. (2004) Foxm1b transcription factor is essential for development of hepatocellular carcinomas and is negatively regulated by the p19ARF tumor suppressor. *Genes & Development*. **18** (7): 830-850.

Kalinina, OA, Kalinin, SA, Polack, EW, Mikaelian, I, Panda, S, Costa, RH and Adami, GR. (2003) Sustained hepatic expression of FoxM1B in transgenic mice has minimal effects on hepatocellular carcinoma development but increases cell proliferation rates in preneoplastic and early neoplastic lesions. *Oncogene*. **22** (40): 6266-6276.

Karnik, SK, Hughes, CM, Gu, X, Rozenblatt-Rosen, O, McLean, GW, Xiong, Y, Meyerson, M and Kim, SK. (2005) Menin regulates pancreatic islet growth by promoting histone methylation and expression of genes encoding p27Kip1 and p18INK4c. *PNAS*. **102** (41): 14659-14664.

Karnik, SK, Chen, H, McLean, GW, Heit, JJ, Gu, X, Zhang, AY, Fontaine, M, Yen, MH and Kim, SK. (2007) Menin Controls Growth of Pancreatic Beta-Cells in Pregnant Mice and Promotes Gestational Diabetes Mellitus. *Science*. **318** (5851): 806-809.

Kassem, SA, Ariel, I, Thornton, PS, Hussain, K, Smith, V, Lindley, KJ, Aynsley-Green, A and Glaser, B. (2001) p57KIP2 expression in normal islet cells and in hyperinsulinism of infancy. *Diabetes*. **50** (12): 2763-2769.

Kataoka, K, Han, SI, Shioda, S, Hirai, M, Nishizawa, M and Handa, H. (2002) MafA is a glucose-regulated and pancreatic beta-cell-specific transcriptional activator for the insulin gene. *J Biol Chem*. **277** (51): 49903-49910.

Kawaguchi, Y, Cooper, B, Gannon, M, Ray, M, MacDonald, RJ and Wright, CV. (2002) The role of the transcriptional regulator Ptf1a in converting intestinal to pancreatic progenitors. *Nat Genet*. **32** (1): 128-134.

Kim, I-M, Ramakrishna, S, Gusarova, GA, Yoder, HM, Costa, RH and Kalinichenko, VV. (2005) The forkhead box m1 transcription factor is essential for embryonic development of pulmonary vasculature. *J Biol Chem*. **280** (23): 22278-22286.

Kim, I-M, Ackerson, T, Ramakrishna, S, Tretiakova, M, Wang, IC, Kalin, TV, Major, ML, Gusarova, GA, Yoder, HM, Costa, RH and Kalinichenko, VV. (2006) The Forkhead Box m1 Transcription Factor Stimulates the Proliferation of Tumor Cells during Development of Lung Cancer. *Cancer Res*. **66** (4): 2153-2161.

Kim, SK and MacDonald, RJ. (2002) Signaling and transcriptional control of pancreatic organogenesis. *Curr Opin Genet Dev*. **12** (5): 540-547.

Kisanga, ER, Gjerde, J, Schjott, J, Mellgren, G and Lien, EA. (2003) Tamoxifen administration and metabolism in nude mice and nude rats. *J Steroid Biochem Mol Biol*. **84** (2-3): 361-367.

Kisanga, ER, Moi, LL, Gjerde, J, Mellgren, G and Lien, EA. (2005) Induction of hepatic drug-metabolising enzymes and tamoxifen metabolite profile in relation to administration route during low-dose treatment in nude rats. *J Steroid Biochem Mol Biol*. **94** (5): 489-498.

Kitamura, T, Nakae, J, Kitamura, Y, Kido, Y, Biggs, WH, III, Wright, CVE, White, MF, Arden, KC and Accili, D. (2002) The forkhead transcription factor Foxo1 links insulin signaling to Pdx1 regulation of pancreatic beta cell growth. *J. Clin. Invest.* **110** (12): 1839-1847.

Korver, W, Roose, J and Clevers, H. (1997a) The winged-helix transcription factor Trident is expressed in cycling cells. *Nucleic Acids Res*. **25** (9): 1715-1719.

Korver, W, Roose, J, Heinen, K, Weghuis, DO, de Bruijn, D, van Kessel, AG and Clevers, H. (1997b) The HumanTRIDENT/HFH-11/FKHL16Gene: Structure, Localization, and Promoter Characterization. *Genomics*. **46** (3): 435-442.

Korver, W, Schilham, MW, Moerer, P, van den Hoff, MJ, Dam, K, Lamers, WH, Medema, RH and Clevers, H. (1998) Uncoupling of S phase and mitosis in cardiomyocytes and hepatocytes lacking the winged-helix transcription factor Trident. *Curr Biol*. **8** (24): 1327-1330.

Krakowski, M, Kritzik, M, Jones, E, Krahl, T, Lee, J, Arnush, M, Gu, D, Mroczkowski, B and Sarvetnick, N. (1999) Transgenic expression of epidermal growth factor and keratinocyte growth factor in beta-cells results in substantial morphological changes. *J Endocrinol*. **162** (2): 167-175.

Krapp, A, Knofler, M, Ledermann, B, Burki, K, Berney, C, Zoerkler, N, Hagenbuchle, O and Wellauer, PK. (1998) The bHLH protein PTF1-p48 is essential for the formation of the exocrine and the correct spatial organization of the endocrine pancreas. *Genes Dev*. **12** (23): 3752-3763.

Krishnamurthy, J, Ramsey, MR, Ligon, KL, Torrice, C, Koh, A, Bonner-Weir, S and Sharpless, NE. (2006) p16INK4a induces an age-dependent decline in islet regenerative potential. *Nature*. **443** (7110): 453-457.

Kristinsson, SY, Thorolfsdottir, ET, Talseth, B, Steingrimsson, E, Thorsson, AB, Helgason, T, Hreidarsson, AB and Arngrimsson, R. (2001) MODY in Iceland is associated with mutations in HNF-1a and a novel mutation in NeuroD1. *Diabetologia*. **44** (11): 2098-2103.

Kroon, E, Martinson, LA, Kadoya, K, Bang, AG, Kelly, OG, Eliazer, S, Young, H, Richardson, M, Smart, NG, Cunningham, J, Agulnick, AD, D'Amour, KA, Carpenter, MK and Baetge, EE. (2008) Pancreatic endoderm derived from human embryonic stem cells generates glucose-responsive insulin-secreting cells in vivo. *Nat Biotech*. **26** (4): 443-452.

Krupczak-Hollis, K, Wang, X, Dennewitz, MB and Costa, RH. (2003) Growth hormone stimulates proliferation of old-aged regenerating liver through forkhead box m1b. *Hepatology*. **38** (6): 1552-1562.

Krupczak-Hollis, K, Wang, X, Kalinichenko, VV, Gusarova, GA, Wang, I-C, Dennewitz, MB, Yoder, HM, Kiyokawa, H, Kaestner, KH and Costa, RH. (2004) The mouse Forkhead Box m1 transcription factor is essential for hepatoblast mitosis and development of intrahepatic bile ducts and vessels during liver morphogenesis. *Developmental Biology*. **276** (1): 74-88.

Ku, HT, Zhang, N, Kubo, A, O'Connor, R, Mao, M, Keller, G and Bromberg, JS. (2004) Committing embryonic stem cells to early endocrine pancreas in vitro. *Stem Cells*. **22** (7): 1205-1217.

Kubota, N, Tobe, K, Terauchi, Y, Eto, K, Yamauchi, T, Suzuki, R, Tsubamoto, Y, Komeda, K, Nakano, R, Miki, H, Satoh, S, Sekihara, H, Sciacchitano, S, Lesniak, M, Aizawa, S, Nagai, R, Kimura, S, Akanuma, Y, Taylor, S and Kadowaki, T. (2000) Disruption of insulin receptor substrate 2 causes type 2 diabetes because of liver insulin resistance and lack of compensatory beta-cell hyperplasia. *Diabetes*. **49** (11): 1880-1889.

Kubota, N, Terauchi, Y, Tobe, K, Yano, W, Suzuki, R, Ueki, K, Takamoto, I, Satoh, H, Maki, T, Kubota, T, Moroi, M, Okada-Iwabu, M, Ezaki, O, Nagai, R, Ueta, Y, Kadowaki, T and Noda, T. (2004) Insulin receptor substrate 2 plays a crucial role in beta cells and the hypothalamus. *J. Clin. Invest.* **114** (7): 917-927.

Kulkarni, RN, Holzenberger, M, Shih, DQ, Ozcan, U, Stoffel, M, Magnuson, MA and Kahn, CR. (2002) Beta-cell-specific deletion of the Igf1 receptor leads to hyperinsulinemia and glucose intolerance but does not alter beta-cell mass. *Nat Genet*. **31** (1): 111-115.

Kushner, JA, Ciemerych, MA, Sicinska, E, Wartschow, LM, Teta, M, Long, SY, Sicinski, P and White, MF. (2005a) Cyclins D2 and D1 are essential for postnatal pancreatic beta-cell growth. *Mol. Cell. Biol.* **25** (9): 3752-3762.

Kushner, JA, Simpson, L, Wartschow, LM, Guo, S, Rankin, MM, Parsons, R and White, MF. (2005b) Phosphatase and tensin homolog regulation of islet growth and glucose homeostasis. *J Biol Chem*. **280** (47): 39388-39393.

Kwok, JMM, Myatt, SS, Marson, CM, Coombes, RC, Constantinidou, D and Lam, EWF. (2008) Thiostrepton selectively targets breast cancer cells through inhibition of forkhead box M1 expression. *Mol Cancer Ther*. **7** (7): 2022-2032.

Lai, E, Prezioso, VR, Smith, E, Litvin, O, Costa, RH and Darnell, JE. (1990) HNF-3A, a hepatocyte-enriched transcription factor of novel structure is regulated transcriptionally. *Genes & Development*. **4** (8): 1427-1436.

Lai, E, Prezioso, VR, Tao, WF, Chen, WS and Darnell, JE. (1991) Hepatocyte nuclear factor 3 alpha belongs to a gene family in mammals that is homologous to the Drosophila homeotic gene fork head. *Genes & Development*. **5** (3): 416-427.

Laoukili, J, Kooistra, MRH, Bras, A, Kauw, J, Kerkhoven, RM, Morrison, A, Clevers, H and Medema, RH. (2005) FoxM1 is required for execution of the mitotic programme and chromosome stability. *Nat Cell Biol*. **7** (2): 126-136.

Laoukili, J, Stahl, M and Medema, RH. (2007) FoxM1: At the crossroads of ageing and cancer. *Biochimica et Biophysica Acta (BBA) - Reviews on Cancer*. **1775** (1): 92-102.

Laoukili, J, Alvarez, M, Meijer, LAT, Stahl, M, Mohammed, S, Kleij, L, Heck, AJR and Medema, RH. (2008) Activation of FoxM1 during G2 Requires Cyclin A/Cdk-Dependent Relief of Autorepression by the FoxM1 N-Terminal Domain. *Mol Cell Biol*. **28** (9): 3076-3087.

Leahy, JL, Bonner-Weir, S and Weir, GC. (1988) Minimal chronic hyperglycemia is a critical determinant of impaired insulin secretion after an incomplete pancreatectomy. *J Clin Invest*. **81** (5): 1407-1414.

Lee, CS, De Leon, DD, Kaestner, KH and Stoffers, DA. (2006) Regeneration of Pancreatic Islets After Partial Pancreatectomy in Mice Does Not Involve the Reactivation of Neurogenin-3. *Diabetes*. **55** (2): 269-272.

Lee, S, Muniyappa, R, Yan, X, Chen, H, Yue, LQ, Hong, E-G, Kim, JK and Quon, MJ. (2008) Comparison between surrogate indexes of insulin sensitivity and resistance and hyperinsulinemic euglycemic clamp estimates in mice. *Am J Physiol Endocrinol Metab*. **294** (2): E261-270.

Leung, TWC, Lin, SSW, Tsang, ACC, Tong, CSW, Ching, JCY, Leung, WY, Gimlich, R, Wong, GG and Yao, KM. (2001) Over-expression of FoxM1 stimulates cyclin B1 expression. *FEBS letters*. **507** (1): 59-66.

Li, H, Arber, S, Jessell, TM and Edlund, H. (1999) Selective agenesis of the dorsal pancreas in mice lacking homeobox gene Hlxb9. *Nat Genet*. **23** (1): 67-70.

Lim, YC, Desta, Z, Flockhart, DA and Skaar, TC. (2005) Endoxifen (4-hydroxy-N-desmethyl-tamoxifen) has anti-estrogenic effects in breast cancer cells with potency similar to 4-hydroxy-tamoxifen. *Cancer Chemother Pharmacol*. **55** (5): 471-478.

Lindstrom, P. (2007) The Physiology of Obese-Hyperglycemic Mice [ob/ob Mice]. *The Scientific World Journal*. **7** 666-685.

Ling, Z, Wu, D, Zambre, Y, Flamez, D, Drucker, DJ, Pipeleers, DG and Schuit, FC. (2001) Glucagon-like peptide 1 receptor signaling influences topography of islet cells in mice. *Virchows Arch*. **438** (4): 382-387.

Lingohr, MK, Buettner, R and Rhodes, CJ. (2002) Pancreatic beta-cell growth and survival - a role in obesity-linked type 2 diabetes? *Trends in Molecular Medicine*. **8** (8): 375-384.

Linn, T, Strate, C and Schneider, K. (1999) Diet promotes beta-cell loss by apoptosis in prediabetic nonobese diabetic mice. *Endocrinology*. **140** (8): 3767-3773.

Littlewood, TD, Hancock, DC, Danielian, PS, Parker, MG and Evan, GI. (1995) A modified oestrogen receptor ligand-binding domain as an improved switch for the regulation of heterologous proteins. *Nucleic Acids Res*. **23** (10): 1686-1690.

Liu, J-L, Coschigano, KT, Robertson, K, Lipsett, M, Guo, Y, Kopchick, JJ, Kumar, U and Liu, YL. (2004) Disruption of growth hormone receptor gene causes diminished pancreatic islet size and increased insulin sensitivity in mice. *Am J Physiol Endocrinol Metab*. **287** (3): E405-413.

Liu, M, Dai, B, Kang, S-H, Ban, K, Huang, F-J, Lang, FF, Aldape, KD, Xie, T-x, Pelloski, CE, Xie, K, Sawaya, R and Huang, S. (2006) FoxM1B Is Overexpressed in Human Glioblastomas and Critically Regulates the Tumorigenicity of Glioma Cells. *Cancer Res*. **66** (7): 3593-3602.

Louet, JF, LeMay, C and Mauvais-Jarvis, F. (2004) Antidiabetic actions of estrogen: insight from human and genetic mouse models. *Curr Atheroscler Rep*. **6** (3): 180-185.

Lu, Y, Herrera, PL, Guo, Y, Sun, D, Tang, Z, LeRoith, D and Liu, JL. (2004) Pancreatic-specific inactivation of IGF-I gene causes enlarged pancreatic islets and significant resistance to diabetes. *Diabetes*. **53** (12): 3131-3141.

Luscher-Firzlaff, JM, Westendorf, JM, Zwicker, J, Burkhardt, H, Henriksson, M, Muller, R, Pirollet, F and Luscher, B. (1999) Interaction of the fork head domain transcription factor MPP2 with the human papilloma virus 16 E7 protein: enhancement of transformation and transactivation. *Oncogene*. **18** (41): 5620-5630.

Ly, DH, Lockhart, DJ, Lerner, RA and Schultz, PG. (2000) Mitotic Misregulation and Human Aging. *Science*. **287** (5462): 2486-2492.

Ma, RYM, Tong, THK, Cheung, AMS, Tsang, ACC, Leung, WY and Yao, K-M. (2005) Raf/MEK/MAPK signaling stimulates the nuclear translocation and transactivating activity of FOXM1c. *J Cell Sci*. **118** (4): 795-806.

Macfarlane, WM, Frayling, TM, Ellard, S, Evans, JC, Allen, LIS, Bulman, MP, Ayres, S, Shepherd, M, Clark, P, Millward, A, Demaine, A, Wilkin, T, Docherty, K and Hattersley, AT. (1999) Missense mutations in the insulin promoter factor-1 gene predispose to type 2 diabetes. *J. Clin. Invest.* **104** (9): R33-39.

Madureira, PA, Varshochi, R, Constantinidou, D, Francis, RE, Coombes, RC, Yao, K-M and Lam, EWF. (2006) The Forkhead Box M1 Protein Regulates the Transcription of the Estrogen Receptor alpha in Breast Cancer Cells. *J Biol Chem*. **281** (35): 25167-25176.

Major, ML, Lepe, R and Costa, RH. (2004) Forkhead box M1B transcriptional activity requires binding of Cdk-cyclin complexes for phosphorylation-dependent recruitment of p300/CBP coactivators. *Mol Cell Biol*. **24** (7): 2649-2661.

Martin, J, Hunt, SL, Dubus, P, Sotillo, R, Nehme-Pelluard, F, Magnuson, MA, Parlow, AF, Malumbres, M, Ortega, S and Barbacid, M. (2003) Genetic rescue of Cdk4 null mice restores pancreatic beta-cell proliferation but not homeostatic cell number. *Oncogene*. **22** (34): 5261-5269.

Massague, J. (2004) G1 cell-cycle control and cancer. *Nature*. **432** (7015): 298-306.

Matsuoka, TA, Artner, I, Henderson, E, Means, A, Sander, M and Stein, R. (2004) The MafA transcription factor appears to be responsible for tissue-specific expression of insulin. *Proc Natl Acad Sci U S A*. **101** (9): 2930-2933.

Matthews, DR, Hosker, JP, Rudenski, AS, Naylor, BA, Treacher, DF and Turner, RC. (1985) Homeostasis model assessment: insulin resistance and beta-cell function from fasting plasma glucose and insulin concentrations in man. *Diabetologia*. **28** (7): 412-419.

Mayo Clinic Staff, Mayo Foundation for Medical Education and Research. (2007) Type 2 diabetes: Risk factors. *MayoClinic.com*. July 30, 2008 <http://www.mayoclinic.com/health/type-2-diabetes/DS00585/DSECTION=risk-factors>

Means, AL, Xu, Y, Zhao, A, Ray, KC and Gu, G. (2008) A CK19(CreERT) knockin mouse line allows for conditional DNA recombination in epithelial cells in multiple endodermal organs. *Genesis*. **46** (6): 318-323.

Meier, JJ, Bhushan, A, Butler, AE, Rizza, RA and Butler, PC. (2005) Sustained beta cell apoptosis in patients with long-standing type 1 diabetes: indirect evidence for islet regeneration? *Diabetologia*. **48** (11): 2221-2228.

Meier, JJ, Lin, JC, Butler, AE, Galasso, R, Martinez, DS and Butler, PC. (2006) Direct evidence of attempted beta cell regeneration in an 89-year-old patient with recent-onset type 1 diabetes. *Diabetologia*. **49** (8): 1838-1844.

Meier, JJ, Butler, AE, Saisho, Y, Monchamp, T, Galasso, R, Bhushan, A, Rizza, RA and Butler, PC. (2008) Beta-cell replication is the primary mechanism subserving the postnatal expansion of beta-cell mass in humans. *Diabetes*. **57** (6): 1584-1594.

Melloul, D, Marshak, S and Cerasi, E. (2002) Regulation of pdx-1 gene expression. *Diabetes*. **51** (Suppl 3): S320-325.

Mettus, RV and Rane, SG. (2003) Characterization of the abnormal pancreatic development, reduced growth and infertility in Cdk4 mutant mice. *Oncogene*. **22** (52): 8413-8421.

Mokdad, AH, Bowman, BA, Ford, ES, Vinicor, F, Marks, JS and Koplan, JP. (2001) The Continuing Epidemics of Obesity and Diabetes in the United States. *JAMA*. **286** (10): 1195-1200.

Monaghan, AP, Kaestner, KH, Grau, E and Schutz, G. (1993) Postimplantation expression patterns indicate a role for the mouse forkhead/HNF-3 alpha, beta and gamma genes in determination of the definitive endoderm, chordamesoderm and neuroectoderm. *Development*. **119** (3): 567-578.

Montagnoli, A, Fiore, F, Eytan, E, Carrano, AC, Draetta, GF, Hershko, A and Pagano, M. (1999) Ubiquitination of p27 is regulated by Cdk-dependent phosphorylation and trimeric complex formation. *Genes Dev*. **13** (9): 1181-1189.

Montanya, E, Nacher, V, Biarnes, M and Soler, J. (2000) Linear correlation between beta-cell mass and body weight throughout the lifespan in Lewis rats: role of beta-cell hyperplasia and hypertrophy. *Diabetes*. **49** (8): 1341-1346.

Montelius, A, Marmigère, F, Baudet, C, Aquino, JB, Enerbäck, S and Ernfors, P. (2007) Emergence of the sensory nervous system as defined by Foxs1 expression. *Differentiation*. **75** (5): 404-417.

Naya, FJ, Stellrecht, CM and Tsai, M-J. (1995) Tissue-specific regulation of the insulin gene by a novel basic helix-loop-helix transcription factor. *Genes Dev.* **9** (8): 1009-1019.

Naya, FJ, Huang, H-P, Qiu, Y, Mutoh, H, DeMayo, FJ, Leiter, AB and Tsai, M-J. (1997) Diabetes, defective pancreatic morphogenesis, and abnormal enteroendocrine differentiation in BETA2/NeuroD-deficient mice. *Genes Dev.* **11** (18): 2323-2334.

Nishimura, W, Kondo, T, Salameh, T, El Khattabi, I, Dodge, R, Bonner-Weir, S and Sharma, A. (2006) A switch from MafB to MafA expression accompanies differentiation to pancreatic beta-cells. *Developmental Biology*. **293** (2): 526-539.

Novak, A, Guo, C, Yang, W, Nagy, A and Lobe, CG. (2000) Z/EG, a double reporter mouse line that expresses enhanced green fluorescent protein upon Cre-mediated excision. *Genesis*. **28** (3-4): 147-155.

Obama, K, Ura, K, Li, M, Katagiri, T, Tsunoda, T, Nomura, A, Satoh, S, Nakamura, Y and Furukawa, Y. (2005) Genome-wide analysis of gene expression in human intrahepatic cholangiocarcinoma. *Hepatology*. **41** (6): 1339-1348.

Offield, MF, Jetton, TL, Labosky, PA, Ray, M, Stein, RW, Magnuson, MA, Hogan, BL and Wright, CV. (1996) PDX-1 is required for pancreatic outgrowth and differentiation of the rostral duodenum. *Development*. **122** (3): 983-995.

Okabe, H, Satoh, S, Kato, T, Kitahara, O, Yanagawa, R, Yamaoka, Y, Tsunoda, T, Furukawa, Y and Nakamura, Y. (2001) Genome-wide Analysis of Gene Expression in Human Hepatocellular Carcinomas Using cDNA Microarray: Identification of Genes Involved in Viral Carcinogenesis and Tumor Progression. *Cancer Res*. **61** (5): 2129-2137.

Okada, T, Liew, CW, Hu, J, Hinault, C, Michael, MD, Krutzfeldt, J, Yin, C, Holzenberger, M, Stoffel, M and Kulkarni, RN. (2007) Insulin receptors in beta-cells are critical for islet compensatory growth response to insulin resistance. *PNAS*. **104** (21): 8977-8982.

Okamoto, H, Hribal, ML, Lin, HV, Bennett, WR, Ward, A and Accili, D. (2006) Role of the forkhead protein FoxO1 in beta cell compensation to insulin resistance. *J Clin Invest*. **116** (3): 775-782.

Olbrot, M, Rud, J, Moss, LG and Sharma, A. (2002) Identification of beta-cell-specific insulin gene transcription factor RIPE3b1 as mammalian MafA. *Proc Natl Acad Sci U S A*. **99** (10): 6737-6742.

Otani, K, Kulkarni, RN, Baldwin, AC, Krutzfeldt, J, Ueki, K, Stoffel, M, Kahn, CR and Polonsky, KS. (2004) Reduced beta-cell mass and altered glucose sensing impair insulin-secretory function in betaIRKO mice. *Am J Physiol Endocrinol Metab*. **286** (1): E41-49.

Pamir, N, Lynn, FC, Buchan, AMJ, Ehses, J, Hinke, SA, Pospisilik, JA, Miyawaki, K, Yamada, Y, Seino, Y, McIntosh, CHS and Pederson, RA. (2003) Glucose-dependent insulinotropic polypeptide receptor null mice exhibit compensatory changes in the enteroinsular axis. *Am J Physiol Endocrinol Metab*. **284** (5): E931-939.

Park, HJ, Costa, RH, Lau, LF, Tyner, AL and Raychaudhuri, P. (2008a) APC/C-Cdh1 Mediated Proteolysis of the Forkhead Box M1 Transcription Factor is Critical for Regulated Entry into S phase. *Mol Cell Biol*. **Epub ahead of print** 0038708.

Park, HJ, Wang, Z, Costa, RH, Tyner, A, Lau, LF and Raychaudhuri, P. (2008b) An N-terminal inhibitory domain modulates activity of FoxM1 during cell cycle. *Oncogene*. **27** (12): 1696-1704.

Park, JH, Stoffers, DA, Nicholls, RD and Simmons, RA. (2008) Development of type 2 diabetes following intrauterine growth retardation in rats is associated with progressive epigenetic silencing of *Pdx1*. *J Clin Invest*. **118** (6): 2316-2324.

Park, S, Hong, SM, Lee, JE and Sung, SR. (2007) Exercise improves glucose homeostasis that has been impaired by a high-fat diet by potentiating pancreatic beta-cell function and mass through IRS2 in diabetic rats. *J Appl Physiol*. **103** (5): 1764-1771.

Pei, X-H, Bai, F, Tsutsui, T, Kiyokawa, H and Xiong, Y. (2004) Genetic evidence for functional dependency of p18Ink4c on Cdk4. *Mol. Cell. Biol.* **24** (15): 6653-6664.

Pende, M, Kozma, SC, Jaquet, M, Oorschot, V, Burcelin, R, Le Marchand-Brustel, Y, Klumperman, J, Thorens, B and Thomas, G. (2000) Hypoinsulinaemia, glucose intolerance and diminished beta-cell size in S6K1-deficient mice. *Nature*. **408** (6815): 994-997.

Permutt, MA, Wasson, J and Cox, N. (2005) Genetic epidemiology of diabetes. *J Clin Invest*. **115** (6): 1431-1439.

Peshavaria, M, Larmie, BL, Lausier, J, Satish, B, Habibovic, A, Roskens, V, Larock, K, Everill, B, Leahy, JL and Jetton, TL. (2006) Regulation of pancreatic beta-cell regeneration in the normoglycemic 60% partial-pancreatectomy mouse. *Diabetes*. **55** (12): 3289-3298.

Petrik, J, Pell, JM, Arany, E, McDonald, TJ, Dean, WL, Reik, W and Hill, DJ. (1999) Overexpression of insulin-like growth factor-II in transgenic mice is associated with pancreatic islet cell hyperplasia. *Endocrinology*. **140** (5): 2353-2363.

Petrovic, V, Costa, RH, Lau, LF, Raychaudhuri, P and Tyner, AL. (2008) FoxM1 Regulates Growth Factor-induced Expression of Kinase-interacting Stathmin (KIS) to Promote Cell Cycle Progression. *J Biol Chem*. **283** (1): 453-460.

Pick, A, Clark, J, Kubstrup, C, Levisetti, M, Pugh, W, Bonner-Weir, S and Polonsky, K. (1998) Role of apoptosis in failure of beta-cell mass compensation for insulin resistance and beta-cell defects in the male Zucker diabetic fatty rat. *Diabetes*. **47** (3): 358-364.

Pictet, RL, Clark, WR, Williams, RH and Rutter, WJ. (1972) An ultrastructural analysis of the developing embryonic pancreas. *Developmental Biology*. **29** (4): 436-467.

Pilarsky, C, Wenzig, M, Specht, T, Saeger, HD and Grutzmann, R. (2004) Identification and Validation of Commonly Overexpressed Genes in Solid Tumors by Comparison of Microarray Data. *Neoplasia*. **6** (6): 744-750.

Porter, SE, Sorenson, RL, Dann, P, Garcia-Ocana, A, Stewart, AF and Vasavada, RC. (1998) Progressive pancreatic islet hyperplasia in the islet-targeted, parathyroid hormone-related protein-overexpressing mouse. *Endocrinology*. **139** (9): 3743-3751.

Prasadan, K, Daume, E, Preuett, B, Spilde, T, Bhatia, A, Kobayashi, H, Hembree, M, Manna, P and Gittes, GK. (2002) Glucagon is required for early insulin-positive differentiation in the developing mouse pancreas. *Diabetes*. **51** (11): 3229-3236.

Rachdi, L, Balcazar, N, Elghazi, L, Barker, DJ, Krits, I, Kiyokawa, H and Bernal-Mizrachi, E. (2006) Differential effects of p27 in regulation of beta-cell mass during development, neonatal period, and adult life. *Diabetes*. **55** (12): 3520-3528.

Radhakrishnan, SK, Bhat, UG, Hughes, DE, Wang, IC, Costa, RH and Gartel, AL. (2006) Identification of a Chemical Inhibitor of the Oncogenic Transcription Factor Forkhead Box M1. *Cancer Res*. **66** (19): 9731-9735.

Rajagopal, J, Anderson, WJ, Kume, S, Martinez, OI and Melton, DA. (2003) Insulin staining of ES cell progeny from insulin uptake. *Science*. **299** (5605): 363.

Ramiya, VK, Maraist, M, Arfors, KE, Schatz, DA, Peck, AB and Cornelius, JG. (2000) Reversal of insulin-dependent diabetes using islets generated in vitro from pancreatic stem cells. *Nat Med*. **6** (3): 278-282.

Rane, SG, Dubus, P, Mettus, RV, Galbreath, EJ, Boden, G, Reddy, EP and Barbacid, M. (1999) Loss of Cdk4 expression causes insulin-deficient diabetes and Cdk4 activation results in beta-islet cell hyperplasia. *Nat Genet*. **22** (1): 44-52.

Reusens, B and Remacle, C. (2006) Programming of the endocrine pancreas by the early nutritional environment. *Int J Biochem Cell Biol*. **38** (5-6): 913-922.

Rhodes, CJ. (2000) IGF-I and GH post-receptor signaling mechanisms for pancreatic beta-cell replication. *J Mol Endocrinol*. **24** (3): 303-311.

Rhodes, CJ. (2005) Type 2 diabetes-a matter of beta-cell life and death? *Science*. **307** (5708): 380-384.

Rivellese, AA, de Natale, C and Lilli, S. (2002) Type of dietary fat and insulin resistance. *Ann NY Acad Sci*. **967** 329-335.

Roccisana, J, Reddy, V, Vasavada, RC, Gonzalez-Pertusa, JA, Magnuson, MA and Garcia-Ocana, A. (2005) Targeted inactivation of hepatocyte growth factor receptor c-met in beta-cells leads to defective insulin secretion and GLUT-2 downregulation without alteration of beta-cell mass. *Diabetes*. **54** (7): 2090-2102.

Sander, M, Sussel, L, Conners, J, Scheel, D, Kalamaras, J, Dela Cruz, F, Schwitzgebel, V, Hayes-Jordan, A and German, M. (2000) Homeobox gene Nkx6.1 lies downstream of Nkx2.2 in the major pathway of beta-cell formation in the pancreas. *Development*. **127** (24): 5533-5540.

Scaglia, L, Smith, F and Bonner-Weir, S. (1995) Apoptosis contributes to the involution of beta cell mass in the post partum rat pancreas. *Endocrinology*. **136** (12): 5461-5468.

Scaglia, L, Cahill, CJ, Finegood, DT and Bonner-Weir, S. (1997) Apoptosis participates in the remodeling of the endocrine pancreas in the neonatal rat. *Endocrinology*. **138** (4): 1736-1741.

Schmittgen, TD and Livak, KJ. (2008) Analyzing real-time PCR data by the comparative C(T) method. *Nat Protoc*. **3** (6): 1101-1108.

Schwitzgebel, VM, Scheel, DW, Conners, JR, Kalamaras, J, Lee, JE, Anderson, DJ, Sussel, L, Johnson, JD and German, MS. (2000) Expression of neurogenin3 reveals an islet cell precursor population in the pancreas. *Development*. **127** (16): 3533-3542.

Shapiro, AMJ, Ricordi, C, Hering, BJ, Auchincloss, H, Lindblad, R, Robertson, RP, Secchi, A, Brendel, MD, Berney, T, Brennan, DC, Cagliero, E, Alejandro, R, Ryan, EA, DiMercurio, B, Morel, P, Polonsky, KS, Reems, J-A, Bretzel, RG, Bertuzzi, F, Froud, T, Kandaswamy, R, Sutherland, DER, Eisenbarth, G, Segal, M, Preiksaitis, J, Korbutt, GS, Barton, FB, Viviano, L, Seyfert-Margolis, V, Bluestone, J and Lakey, JRT. (2006) International Trial of the Edmonton Protocol for Islet Transplantation. *NEJM*. **355** (13): 1318-1330.

Sharma, A, Zangen, DH, Reitz, P, Taneja, M, Lissauer, ME, Miller, CP, Weir, GC, Habener, JF and Bonner-Weir, S. (1999) The homeodomain protein IDX-1 increases after an early burst of proliferation during pancreatic regeneration. *Diabetes*. **48** (3): 507-513.

Sheaff, RJ, Groudine, M, Gordon, M, Roberts, JM and Clurman, BE. (1997) Cyclin E-CDK2 is a regulator of p27Kip1. *Genes Dev*. **11** (11): 1464-1478.

Sladek, R, Rocheleau, G, Rung, J, Dina, C, Shen, L, Serre, D, Boutin, P, Vincent, D, Belisle, A, Hadjadj, S, Balkau, B, Heude, B, Charpentier, G, Hudson, TJ, Montpetit, A, Pshezhetsky, AV, Prentki, M, Posner, BI, Balding, DJ, Meyre, D, Polychronakos, C and Froguel, P. (2007) A genome-wide association study identifies novel risk loci for type 2 diabetes. *Nature*. **445** (7130): 881-885.

Smith, SB, Gasa, R, Watada, H, Wang, J, Griffen, SC and German, MS. (2003) Neurogenin3 and Hepatic Nuclear Factor 1 cooperate in activating pancreatic expression of Pax4. *J. Biol. Chem.* **278** (40): 38254-38259.

Sone, H and Kagawa, Y. (2005) Pancreatic beta cell senescence contributes to the pathogenesis of type 2 diabetes in high-fat diet-induced diabetic mice. *Diabetologia*. **48** (1): 58-67.

Soriano, P. (1999) Generalized lacZ expression with the ROSA26 Cre reporter strain. *Nat Genet*. **21** (1): 70-71.

Sosa-Pineda, B, Chowdhury, K, Torres, M, Oliver, G and Gruss, P. (1997) The Pax4 gene is essential for differentiation of insulin-producing beta cells in the mammalian pancreas. *Nature*. **386** (6623): 399-402.

Spooner, BS, Walther, BT and Rutter, WJ. (1970) The development of the dorsal and ventral mammalian pancreas in vivo and in vitro. *J. Cell Biol.* **47** (1): 235-246.

Steil, GM, Trivedi, N, Jonas, JC, Hasenkamp, WM, Sharma, A, Bonner-Weir, S and Weir, GC. (2001) Adaptation of beta-cell mass to substrate oversupply: enhanced function with normal gene expression. *Am J Physiol Endocrinol Metab*. **280** (5): E788-796.

Stiles, BL, Kuralwalla-Martinez, C, Guo, W, Gregorian, C, Wang, Y, Tian, J, Magnuson, MA and Wu, H. (2006) Selective deletion of Pten in pancreatic beta cells leads to increased islet mass and resistance to STZ-induced diabetes. *Mol. Cell. Biol.* **26** (7): 2772-2781.

Stoffers, DA, Ferrer, J, Clarke, WL and Habener, JF. (1997a) Early-onset type-ll diabetes mellitus (MODY4) linked to IPF1. *Nature*. **17** (2): 138-139.

Stoffers, DA, Zinkin, NT, Stanojevic, V, Clarke, WL and Habener, JF. (1997b) Pancreatic agenesis attributable to a single nucleotide deletion in the human IPF1 gene coding sequence. *Nat Genet*. **15** (1): 106-110.

Stoffers, DA, Heller, RS, Miller, CP and Habener, JF. (1999) Developmental expression of the homeodomain protein IDX-1 in mice transgenic for an IDX-1 promoter/lacZ transcriptional reporter. *Endocrinology*. **140** (11): 5374-5381.

Sussel, L, Kalamaras, J, Hartigan-O'Connor, DJ, Meneses, JJ, Pedersen, RA, Rubenstein, JL and German, MS. (1998) Mice lacking the homeodomain transcription factor Nkx2.2 have diabetes due to arrested differentiation of pancreatic beta cells. *Development*. **125** (12): 2213-2221.

Tamemoto, H, Kadowaki, T, Tobe, K, Yagi, T, Sakura, H, Hayakawa, T, Terauchi, Y, Ueki, K, Kaburagi, Y, Satoh, S, Sekihara, H, Yoshioka, S, Horikoshi, H, Furuta, Y, Ikawa, Y, Kasuga, M, Yazaki, Y and Aizawa, S. (1994) Insulin resistance and growth retardation in mice lacking insulin receptor substrate-1. *Nature*. **372** (6502): 182-186.

Teh, M-T, Wong, S-T, Neill, GW, Ghali, LR, Philpott, MP and Quinn, AG. (2002) FOXM1 Is a Downstream Target of Gli1 in Basal Cell Carcinomas. *Cancer Res*. **62** (16): 4773-4780.

Teta, M, Long, SY, Wartschow, LM, Rankin, MM and Kushner, JA. (2005) Very slow turnover of beta-cells in aged adult mice. *Diabetes*. **54** (9): 2557-2567.

Teta, M, Rankin, MM, Long, SY, Stein, GM and Kushner, JA. (2007) Growth and Regeneration of Adult Beta Cells Does Not Involve Specialized Progenitors. *Developmental Cell*. **12** (5): 817-826.

Tuteja, G and Kaestner, KH. (2007a) SnapShot: Forkhead Transcription Factors I. *Cell*. **130** (6): 1160.

Tuteja, G and Kaestner, KH. (2007b) SnapShot: Forkhead Transcription Factors II. *Cell*. **131** (1): 192.

Tuttle, RL, Gill, NS, Pugh, W, Lee, J-P, Koeberlein, B, Furth, EE, Polonsky, KS, Naji, A and Birnbaum, MJ. (2001) Regulation of pancreatic beta-cell growth and survival by the serine/threonine protein kinase Akt1/PKBalpha. *Nat Med*. **7** (10): 1133-1137.

Uchida, T, Nakamura, T, Hashimoto, N, Matsuda, T, Kotani, K, Sakaue, H, Kido, Y, Hayashi, Y, Nakayama, KI, White, MF and Kasuga, M. (2005) Deletion of Cdkn1b ameliorates hyperglycemia by maintaining compensatory hyperinsulinemia in diabetic mice. *Nat Med*. **11** (2): 175-182.

van den Boom, J, Wolter, M, Kuick, R, Misek, DE, Youkilis, AS, Wechsler, DS, Sommer, C, Reifenberger, G and Hanash, SM. (2003) Characterization of Gene Expression Profiles Associated with Glioma Progression Using Oligonucleotide-Based Microarray Analysis and Real-Time Reverse Transcription-Polymerase Chain Reaction. *Am J Pathol*. **163** (3): 1033-1043.

Vasavada, RC, Garcia-Ocana, A, Zawalich, WS, Sorenson, RL, Dann, P, Syed, M, Ogren, L, Talamantes, F and Stewart, AF. (2000) Targeted expression of placental lactogen in the beta cells of transgenic mice results in beta cell proliferation, islet mass augmentation, and hypoglycemia. *J. Biol. Chem.* **275** (20): 15399-15406.

Vasavada, RC, Cozar-Castellano, I, Sipula, D and Stewart, AF. (2007) Tissue-Specific Deletion of the Retinoblastoma Protein in the Pancreatic beta-Cell Has Limited Effects on beta-Cell Replication, Mass, and Function. *Diabetes*. **56** (1): 57-64.

Wang, I-C, Chen, Y-J, Hughes, D, Petrovic, V, Major, ML, Park, HJ, Tan, Y, Ackerson, T and Costa, RH. (2005) Forkhead box M1 regulates the transcriptional network of genes essential for mitotic progression and genes encoding the SCF (Skp2-Cks1) ubiquitin ligase. *Mol Cell Biol*. **25** (24): 10875-10894.

Wang, I-C, Chen, Y-J, Hughes, DE, Ackerson, T, Major, ML, Kalinichenko, VV, Costa, RH, Raychaudhuri, P, Tyner, AL and Lau, LF. (2008a) FOXM1 regulates transcription of JNK1 to promote the G1/S transition and tumor cell invasiveness. *J Biol Chem*. **Epub ahead of print** M709892200.

Wang, I-C, Meliton, L, Tretiakova, M, Costa, RH, Kalinichenko, VV and Kalin, TV. (2008b) Transgenic expression of the forkhead box M1 transcription factor induces formation of lung tumors. *Oncogene*. **27** (30): 4137-4149.

Wang, Q and Brubaker, PL. (2002) Glucagon-like peptide-1 treatment delays the onset of diabetes in 8 week-old db/db mice. *Diabetologia*. **45** (9): 1263-1273.

Wang, TC, Bonner-Weir, S, Oates, PS, Chulak, M, Simon, B, Merlino, GT, Schmidt, EV and Brand, SJ. (1993) Pancreatic gastrin stimulates islet differentiation of transforming growth factor alpha-induced ductular precursor cells. *J Clin Invest*. **92** (3): 1349-1356.

Wang, X, Quail, E, Hung, N-J, Tan, Y, Ye, H and Costa, RH. (2001) Increased levels of forkhead box M1B transcription factor in transgenic mouse hepatocytes prevent age-related proliferation defects in regenerating liver. *PNAS*. **98** (20): 11468-11473.

Wang, X, Kiyokawa, H, Dennewitz, MB and Costa, RH. (2002a) The Forkhead Box m1b transcription factor is essential for hepatocyte DNA replication and mitosis during mouse liver regeneration. *Proc Natl Acad Sci U S A*. **99** (26): 16881-16886.

Wang, X, Krupczak-Hollis, K, Tan, Y, Dennewitz, MB, Adami, GR and Costa, RH. (2002b) Increased hepatic Forkhead Box M1B (FoxM1B) levels in old-aged mice stimulated liver regeneration through diminished p27Kip1 protein levels and increased Cdc25B expression. *J Biol Chem*. **277** (46): 44310-44316.

Wareham, NJ, Phillips, DI, Byrne, CD and Hales, CN. (1995) The 30 minute insulin incremental response in an oral glucose tolerance test as a measure of insulin secretion. *Diabetes Medicine*. **12** (10): 931.

Weigel, D, Jürgens, G, Küttner, F, Seifert, E and Jäckle, H. (1989) The homeotic gene fork head encodes a nuclear protein and is expressed in the terminal regions of the Drosophila embryo. *Cell*. **57** (4): 645-658.

Weigel, D and Jäckle, H. (1990) The fork head domain: A novel DNA binding motif of eukaryotic transcription factors? *Cell*. **63** (3): 455-456.

The Wellcome Trust Case Control Consortium. (2007) Genome-wide association study of 14,000 cases of seven common diseases and 3,000 shared controls. *Nature*. **447** (7145): 661-678.

Westendorf, JM, Rao, PN and Gerace, L. (1994) Cloning of cDNAs for M-phase phosphoproteins recognized by the MPM2 monoclonal antibody and determination of the phosphorylated epitope. *PNAS*. **91** (2): 714-718.

Wierstra, I and Alves, J. (2006) FOXM1c transactivates the human c-myc promoter directly via the two TATA boxes P1 and P2. *FEBS Letters*. **273** (20): 4645-4667.

Wierstra, I and Alves, J. (2008) Cyclin E/Cdk2, P/CAF, and E1A regulate the transactivation of the c-myc promoter by FOXM1. *Biochemical and Biophysical Research Communications*. **368** (1): 107-115.

Williams, BO, Remington, L, Albert, DM, Mukai, S, Bronson, RT and Jacks, T. (1994) Cooperative tumorigenic effects of germline mutations in Rb and p53. *Nat Genet*. **7** (4): 480-484.

Withers, DJ, Gutierrez, JS, Towery, H, Burks, DJ, Ren, J-M, Previs, S, Zhang, Y, Bernal, D, Pons, S, Shulman, GI, Bonner-Weir, S and White, MF. (1998) Disruption of IRS-2 causes type 2 diabetes in mice. *Nature*. **391** (6670): 900-904.

Withers, DJ, Burks, DJ, Towery, HH, Altamuro, SL, Flint, CL and White, MF. (1999) Irs-2 coordinates Igf-1 receptor-mediated beta-cell development and peripheral insulin signalling. *Nat Genet*. **23** (1): 32-40.

Wonsey, DR and Follettie, MT. (2005) Loss of the Forkhead Transcription Factor FoxM1 Causes Centrosome Amplification and Mitotic Catastrophe. *Cancer Res*. **65** (12): 5181-5189.

Xu, X, D'Hoker, J, Stange, G, Bonne, S, De Leu, N, Xiao, X, Van De Casteele, M, Mellitzer, G, Ling, Z, Pipeleers, D, Bouwens, L, Scharfmann, R, Gradwohl, G and Heimberg, H. (2008) Beta Cells Can Be Generated from Endogenous Progenitors in Injured Adult Mouse Pancreas. *Cell*. **132** (2): 197-207.

Yao, KM, Sha, M, Lu, Z and Wong, GG. (1997) Molecular analysis of a novel winged helix protein, WIN. Expression pattern, DNA binding property, and alternative splicing within the DNA binding domain. *J Biol Chem*. **272** (32): 19827-19836.

Ye, H, Kelly, TF, Samadani, U, Lim, L, Rubio, S, Overdier, DG, Roebuck, KA and Costa, RH. (1997) Hepatocyte nuclear factor 3/fork head homolog 11 is expressed in proliferating epithelial and mesenchymal cells of embryonic and adult tissues. *Mol Cell Biol*. **17** (3): 1626-1641.

Ye, H, Holterman, AX, Yoo, KW, Franks, RR and Costa, RH. (1999) Premature Expression of the Winged Helix Transcription Factor HFH-11B in Regenerating Mouse Liver Accelerates Hepatocyte Entry into S Phase. *Mol Cell Biol*. **19** (12): 8570-8580.

Yoshida, Y, Wang, I-C, Yoder, HM, Davidson, NO and Costa, RH. (2007) The Forkhead Box M1 Transcription Factor Contributes to the Development and Growth of Mouse Colorectal Cancer. *Gastroenterology*. **132** (4): 1420-1431.

Zeggini, E, Scott, LJ, Saxena, R, Voight, BF and Consortium, DGRaM-aD. (2008) Meta-analysis of genome-wide association data and large-scale replication identifies additional susceptibility loci for type 2 diabetes. *Nat Genet*. **40** (5): 638-645.

Zhang, C, Moriguchi, T, Kajihara, M, Esaki, R, Harada, A, Shimohata, H, Oishi, H, Hamada, M, Morito, N, Hasegawa, K, Kudo, T, Engel, JD, Yamamoto, M and Takahashi, S. (2005) MafA is a key regulator of glucose-stimulated insulin secretion. *Mol. Cell. Biol.* **25** (12): 4969-4976.

Zhang, H, Fujitani, Y, Wright, CVE and Gannon, M. (2005) Efficient recombination in pancreatic islets by a tamoxifen-inducible Cre-recombinase. *Genesis*. **42** (3): 210-217.

Zhang, H, Ackermann, AM, Gusarova, GA, Lowe, D, Feng, X, Kopsombut, UG, Costa, RH and Gannon, M. (2006) The FoxM1 transcription factor is required to maintain pancreatic beta-cell mass. *Mol Endocrinol*. **20** (8): 1853-1866.

Zhang, P, McGrath, B, Li, S, Frank, A, Zambito, F, Reinert, J, Gannon, M, Ma, K, McNaughton, K and Cavener, DR. (2002) The PERK eukaryotic initiation factor 2 alpha kinase is required for the development of the skeletal system, postnatal growth, and the function and viability of the pancreas. *Mol Cell Biol*. **22** (11): 3864-3874.

Zhang, W, Feng, D, Li, Y, Iida, K, McGrath, B and Cavener, DR. (2006) PERK EIF2AK3 control of pancreatic beta cell differentiation and proliferation is required for postnatal glucose homeostasis. *Cell Metab*. **4** (6): 491-497.

Zhang, X, Gaspard, JP, Mizukami, Y, Li, J, Graeme-Cook, F and Chung, DC. (2005) Overexpression of Cyclin D1 in pancreatic beta-cells in vivo results in islet hyperplasia without hypoglycemia. *Diabetes*. **54** (3): 712-719.

Zhao, Y-Y, Gao, X-P, Zhao, YD, Mirza, MK, Frey, RS, Kalinichenko, VV, Wang, I-C, Costa, RH and Malik, AB. (2006) Endothelial cell-restricted disruption of FoxM1 impairs endothelial repair following LPS-induced vascular injury. *J Clin Invest*. **116** (9): 2333-2343.

Zheng, B, Sage, M, Sheppeard, EA, Jurecic, V and Bradley, A. (2000) Engineering mouse chromosomes with Cre-loxP: range, efficiency, and somatic applications. *Mol Cell Biol*. **20** (2): 648-655.

Zhong, L, Georgia, S, Tschen, S-i, Nakayama, K, Nakayama, KI and Bhushan, A. (2007) Essential role of Skp2-mediated p27 degradation in growth and adaptive expansion of pancreatic beta-cells. *J Clin Invest*. **117** (10): 2869-2876.